

CORROSION OF STEEL BRIDGE GIRDER ANCHOR BOLTS

A Thesis
Presented to
The Academic Faculty

By

Lisa Lindquist

In Partial Fulfillment
Of the Requirements for the Degree
Master of Science in Civil Engineering
Georgia Institute of Technology

August 2008

CORROSION OF STEEL BRIDGE GIRDER ANCHOR BOLTS

Approved by:

Dr. Lawrence F. Kahn, Advisor
School of Civil and Environmental Engineering
Georgia Institute of Technology

Dr. Preet Singh
School of Materials Science and Engineering
Georgia Institute of Technology

Dr. Kimberly E. Kurtis
School of Civil and Environmental Engineering
Georgia Institute of Technology

Date Approved: May 8, 2008

ACKNOWLEDGEMENTS

The completion of this research and Master's thesis would not have been possible without the help of several people. First, I would like to thank fellow officemate and friend, Robert Moser, for being my partner in this research and contributing time, effort, and knowledge towards the understanding of anchor bolt corrosion. We are indebted to Dr. Preet Singh for providing expert advice and instruction on the corrosion process, and to the Institute of Paper Science and Technology for providing the facility for the experimental testing.

I would like to thank my advisor, Dr. Lawrence Kahn, for the guidance and support that he has provided throughout the year and for giving me the opportunity to complete this research. I also acknowledge the contribution of Dr. Kimberly Kurtis and her feedback throughout the process.

The Georgia Department of Transportation has provided the financial support for this project through Research Project No. 07-16, Task Order No. 02-42. The opinions and conclusions expressed herein are those of the author and do not represent the opinions, conclusions, policies, standards or specifications of the Georgia Department of Transportation or of other cooperating organizations.

Many GDOT employees were helpful by meeting with me and providing information regarding bearing design, maintenance, and inspection. I would specifically like to acknowledge Melissa Harper, Lyn Clements, Bill Duvall, Ben Rabun, David Crim, Kerry Wood, and Steve St. John.

Finally, I thank my fiancé, Erik Hoeke, for his unending support and patience.

TABLE OF CONTENTS

ACKNOWLEDGEMENTS.....	iii
LIST OF TABLES.....	iv
LIST OF FIGURES.....	vi
SUMMARY.....	xxi
CHAPTER 1: INTRODUCTION.....	1
1.1 Problem statement and research objectives.....	1
1.2 Research approach.....	1
1.3 Significance of research.....	1
CHAPTER 2: STEEL GIRDER BEARING DESIGN, MATERIALS, AND MAINTENANCE IN GEORGIA.....	4
2.1 Bridge bearings.....	4
2.2 Safety issues.....	8
2.3 Bearing materials.....	9
2.4 Maintenance procedures.....	11
CHAPTER 3: CORROSION BACKGROUND.....	14
3.1 Basics of corrosion.....	14
3.2 Corrosion mechanisms.....	29
3.3 Corrosion measurements.....	39
CHAPTER 4: LITERATURE REVIEW.....	47
4.1 Concepts in bearing design.....	47
4.2 Corrosion of bridge bearings.....	59
CHAPTER 5: GEORGIA STATEWIDE CONDITION ASSESSMENT.....	64
5.1 Inspection report survey process.....	64
5.2 Extent of anchor bolt corrosion in Georgia.....	65
5.3 Bridge age statistics.....	74
CHAPTER 6: FIELD INVESTIGATION REPORTS.....	83
6.1 Inspection methods.....	83
6.2 Bridges in Metro Atlanta area, Georgia DOT District 7.....	84
6.3 Bridges in south Georgia, GDOT Districts 4 and 5.....	93
6.4 Bridges in north Georgia, GDOT Districts 1 and 6.....	99

CHAPTER 7: FAILURE ANALYSIS OF FIELD SPECIMENS.....	101
7.1 Visual analysis.....	101
7.2 Microscopy of failure surface.....	106
7.3 Analysis of bolt scale.....	112
CHAPTER 8: LABORATORY EXPERIMENTAL TESTING.....	115
8.1 Experimental method.....	115
8.2 Experimental set-up	118
8.3 Experimental procedures.....	128
8.4 Results.....	130
CHAPTER 9: DISCUSSION.....	154
9.1 Causes of anchor bolt corrosion.....	154
9.2 Role of bearing design in corrosion.....	158
9.3 Role of maintenance procedures in corrosion.....	159
9.4 Correlation to inspection report data.....	160
CHAPTER 10: CONCLUSIONS AND RECOMMENDATIONS.....	162
10.1 Summary	162
10.2 Conclusions.....	164
10.3 Recommendations.....	165
APPENDIX A: BRIDGES FROM QUERY OF INSPECTION REPORT DATA.....	168
APPENDIX B: ADDITIONAL FIELD INVESTIGATION PICTURES.....	276
B.1 Old Dixie Highway over Central of Georgia Railroad, District 7.....	277
B.2 Lawrenceville Highway over I-285, District 7.....	294
B.3 Memorial Drive over I-285, District 7.....	301
B.4 State Route 92 over I-20, District 7.....	309
B.5 State Route 122 over Little River, District 4.....	316
B.6 US 1 over Satilla River, District 5.....	327
B.7 State Route 121 over Fishing Creek, District 5.....	331
B.8 State Route 144 over Watermelon Creek, District 5.....	338
B.9 Northern Georgia bridges.....	339
APPENDIX C: SPECIMENS OBTAINED FROM BRIDGE DEMOLITION.....	342
APPENDIX D: ADDITIONAL DATA FROM EXPERIMENTAL TESTING.....	352
REFERENCES.....	359

LIST OF TABLES

Table 2.1	Material composition of steel alloys used in bearings (ASTM 2006; ASTM 2007).....	10
Table 2.2	Mechanical properties of steel alloys used in bearings (ASTM 2006; ASTM 2007).....	10
Table 4.1	Material composition of steel alloys used in bearings (ASTM 2006; ASTM 2007).....	57
Table 4.2	Mechanical properties of steel alloys used in bearings (ASTM 2006; ASTM 2007).....	57
Table 5.1	Percentage of the total number of steel girder bridges in Georgia in metropolitan and rural regions, and percentage of bridges with anchor bolt corrosion in each region.....	73
Table 5.2	Percentage of the total number of steel girder bridges in Georgia that are Interstate bridges, Interstate underpasses, and other spans, and percentage of bridges of each span type with anchor bolt corrosion.....	74
Table 5.3	Characteristic statistics of the age distributions of reported anchor bolt corrosion for the state of Georgia and for the environmental regions.....	81
Table 8.1	Soil solution analysis from S.R. 92 bridge over I-20 in District 7 used as basis for solutions in laboratory experimental testing.....	117
Table 8.2	Corrosion rates calculated by polarization resistance and gravimetric methods for select corrosion coupons.....	137
Table 8.3	Comparison of equilibrium corrosion potentials of galvanically coupled coupons to corrosion potentials of non-coupled coupons in the same solution. When coupled, the materials polarized each other.....	149
Table 8.4	Qualitative comparison of corrosion rates of galvanically coupled coupons to corrosion rates of non-coupled coupons in the same solution. Corrosion rates increased for the carbon steel when coupled with the more noble stainless steel or bronze.....	150

Table 8.5	Comparison of equilibrium corrosion potentials of coupons coupled in concentration cells to corrosion potentials of non-coupled coupons in the same solution. When coupled, the materials polarized each other.....	152
Table 8.6	Qualitative comparison of corrosion rates of coupons coupled in concentration cells to corrosion rates of non-coupled coupons in the same solution. Corrosion rates increased for the carbon steel coupled coupons.....	153
Table A.1	State owned steel girder bridges in Georgia.....	169
Table A.2	Steel girder bridges with superstructure maintenance item request number.....	210
Table A.3	Steel girder bridges in Georgia experiencing anchor bolt corrosion.....	230
Table A.4	Steel girder bridges with anchor bolt corrosion in northern Georgia.....	241
Table A.5	Steel girder bridges with anchor bolt corrosion in southern Georgia.....	247
Table A.6	Steel girder bridges with anchor bolt corrosion in coastal Georgia.....	251
Table A.7	Steel girder bridges with anchor bolt corrosion in metropolitan areas....	252
Table A.8	Steel girder bridges with anchor bolt corrosion in rural areas.....	256
Table A.9	Steel girder bridges with anchor bolt corrosion in the Interstate system.....	263
Table A.10	Steel girder bridges with anchor bolt corrosion spanning an Interstate road.....	267
Table A.11	Steel girder bridges with anchor bolt corrosion not related to Interstates.....	270
Table D.1	Results of soil analyses from bridges in all regions.....	353
Table D.2	Corrosion rates of long term samples determined by gravimetric and polarization resistance methods.....	357

LIST OF FIGURES

Figure 2.1	Typical fixed bearing design.....	5
Figure 2.2	Typical expansion bearing design.....	6
Figure 2.3	Typical fixed bearing in good condition.....	6
Figure 2.4	Typical expansion bearing in good condition.....	7
Figure 2.5	Debris around bearing at deck joint.....	8
Figure 2.6	Corroded anchor bolt.....	9
Figure 2.7	A sleeved bearing, a repair process in which steel angles are bolted to both sides of the bearing to prevent lateral movement, which has been subjected to corrosion attack.....	12
Figure 3.1	A standard Electromotive Force Series with respect to the standard hydrogen electrode. Reactions with more negative potentials are considered active, while reactions with more positive potentials are noble (Jones 1996).....	17
Figure 3.2	Exchange-current densities for hydrogen evolution on lead, iron, copper, and platinum surfaces. The surface of the electrode affects the magnitude of the exchange current density (Davis 2000).....	20
Figure 3.3	Evan's diagram of hydrogen and zinc half-cell reactions at equilibrium. The curves with negative slopes are the cathodic half-cell reactions, and the curves with positive slopes are the anodic half-cell reactions.(Singh 2008).....	22
Figure 3.4	Evan's diagram demonstrating mixed potential theory. Zinc and hydrogen electrochemical reactions polarize to reach an intermediate equilibrium value (Singh 2008).....	23
Figure 3.5	The effect of exchange current density on corrosion behavior. Higher exchange current densities lead to higher corrosion rates (Jones 1996).....	24
Figure 3.6	The effect of added oxidizers on corrosion behavior. Additional oxidizers increase the potential and current density of the electrochemical reaction (Fontana 1986).....	25

Figure 3.7	General polarization curve for an active-passive material. Current densities decrease at a specific passivation potential, and the metal becomes resistant to active corrosion. (Revie 2000).....	27
Figure 3.8	The intersection of three possible cathodic curves with the anodic curve of a passive metal. Corrosion rates are dependent on the current density at the intersection of the curves.(Revie 2000).....	28
Figure 3.9	Anodes and cathodes occur on same metal surface in general corrosion. (Singh 2008).....	29
Figure 3.10	Generic Evan’s diagram for galvanic corrosion. Coupled metals polarize each other, and the equilibrium potential at the intersection of the total oxidation and total reduction curves falls in between the potentials of the uncoupled metals. (Jones 1996).....	31
Figure 3.11	Galvanic series for seawater. According to thermodynamic principles, metals which have a large difference in potentials in the same environment have a high risk of developing galvanic corrosion if electrically coupled. Dark boxes correlate with active behavior for active-passive alloys. (Jones 1996).....	32
Figure 3.12	Typical locations where differential aeration cells are formed in application.(Landolt unpublished work).....	34
Figure 3.13	Typical crevice geometry and basic crevice corrosion mechanism. (Davis 2000).....	35
Figure 3.14	Fretting corrosion. As two metal surfaces wear against each other, oxide layers on the surface are broken and reformed. (Davis 2000).....	39
Figure 3.15	Schematic of the standard hydrogen electrode (SHE) device. The SHE establishes a zero point from which all other reference electrodes and potential measurements are based (Jones 1996).....	40
Figure 3.16	Schematic of the saturated calomel electrode (SCE) device. The SCE is commonly used in the laboratory. (Jones 1996).....	41
Figure 3.17	Typical cyclic polarization curve demonstrating E_{pit} , above which pitting initiates, and E_{prot} , below which the material is protected from pit growth and initiation (Jones 1996).....	44
Figure 4.1	Graphic summary of bearing types. (Lee 1994).....	51
Figure 5.1	Georgia counties labeled by number of bridges with anchor bolt corrosion in the state.....	67

Figure 5.2	Georgia counties labeled by percentage of the total number of steel girder bridges affected by anchor bolt corrosion.....	68
Figure 5.3	Three geographic regions in Georgia with different environmental conditions, percentage of the total number of steel girder bridges in Georgia in each region, and percentage of bridges with anchor bolt corrosion in each region.....	71
Figure 5.4	Distribution of bridge ages when anchor bolt corrosion is first reported for the whole State of Georgia.....	75
Figure 5.5	Distribution of bridge ages when anchor bolt corrosion is first reported for northern Georgia.....	76
Figure 5.6	Distribution of bridge ages when anchor bolt corrosion is first reported for southern Georgia.....	76
Figure 5.7	Distribution of bridge ages when anchor bolt corrosion is first reported for coastal Georgia.....	77
Figure 5.8	Distribution of bridge ages when anchor bolt corrosion is first reported for metropolitan areas in Georgia.....	78
Figure 5.9	Distribution of bridge ages when anchor bolt corrosion is first reported for rural areas in Georgia.....	78
Figure 5.10	Distribution of bridge ages when anchor bolt corrosion is first reported for Interstate bridges in Georgia.....	80
Figure 5.11	Distribution of bridge ages when anchor bolt corrosion is first reported for Interstate underpass bridges in Georgia.....	80
Figure 5.12	Distribution of bridge ages when anchor bolt corrosion is first reported for bridges not associated with the Interstate system in Georgia.....	81
Figure 6.1	Typical fixed bearing at Bent 9. In general the anchor bolts and nuts at the abutments appeared to be in good condition.....	85
Figure 6.2	Rust stains on bearing plates, beam flanges, and washers at interior bents, despite the apparent sturdy condition of the anchor bolts.....	86
Figure 6.3	Expansion slot filled with dirt and oxides at interior Bent 7.....	86

Figure 6.4	Corrosion on bearing plates of edge beam bearing at Bent 1. The anchor bolts were not obviously visibly or physically damaged by corrosion.....	88
Figure 6.5	Bearing at abutment without debris. Base plate has a quarter sized spot of corrosion scale.....	89
Figure 6.6	Bearing at abutment with debris. The base plate, anchor bolt, and bottom of the rocker that are enveloped in corrosion scale demonstrate the detrimental effect of debris at bearings.....	89
Figure 6.7	Anchor bolt which was easily broken. The base of the nut is approximately 1 ½-in above the top of the flange indicating that the bolt has been pushed up that distance by corrosion products. A steel angle had been previously bolted to the abutment to restrain lateral movement.....	91
Figure 6.8	Anchor bolt diameter swelled with corrosion product inhibits bolt movement within the bearing and restricts the thermal movements of the bridge.....	92
Figure 6.9	Corrosion product accumulation breaks anchor bolt nut.....	92
Figure 6.10	Typical anchor bolt corrosion of S.R. 122 bridge. The diameter of the bolts decreased just below the washer as they passed through the flange, reaching their smallest diameter approximately one to 1 ½ inches lower at the concrete interface.....	94
Figure 6.11	Anchor bolt cross section loss that has not been painted.....	95
Figure 6.12	Complete section loss in anchor bolt The anchor bolt and washer appear corrosion free above the top of the flange.....	95
Figure 6.13	US Route 1 over Satilla River. Only the four middle spans were steel girders and inspection of the bearings was limited.....	96
Figure 6.14	General corrosion on anchor bolt nut at a fixed bearing. The anchor bolt and nut did not move and the paint did not chip when struck with a hammer.....	97
Figure 6.15	Anchor bolt reduction in diameter due to corrosion in expansion slot. Dirt was cleared away to allow visual inspection within the expansion slot.....	98

Figure 6.16	Anchor bolt corrosion below washer. Corrosion loss occurred in the area between the concrete interface and the top of the beam flange.....	98
Figure 6.17	General corrosion on the anchor bolt nut and base plate at the expansion bearing. Limited access prevented a thorough investigation of the bolt condition below the washer and beam flange.....	99
Figure 7.1	Bolt 1 from northern Georgia at the SR 92 bridge over I-20. When this bolt was found, it was already bent and broken.....	101
Figure 7.2	Bolt 2 from northern Georgia at the SR 92 bridge over I-20. When this bolt was found, it was very loose and was easily broken by hand.....	102
Figure 7.3	Bolt from southern Georgia at the SR 122 bridge over Little River. The image on the left is a view of the bolt from the side, and the image on the right is a view of the bolt from directly underneath the washer. This bolt was already broken when it was found.....	102
Figure 7.4	Bearing plate and anchor bolts from an interior girder expansion bearing. The expansion slots are not visible because they are completely filled with debris and corrosion products.....	104
Figure 7.5	Bearing plate and anchor bolts from a fixed bearing.....	104
Figure 7.6	Build up of corrosion products prevented the anchor bolts from dislodging from the bearing plate.....	105
Figure 7.7	Corrosion build-up visible at the interface of the bolt and bearing plate.....	106
Figure 7.8	Surface of bolt shown in Figure 7.2 at 6.3x magnification. The surface of the bolt is uniformly rough in the necked region.....	108
Figure 7.9	Localized corrosion at paint defects on the surface of the bolt in Figure 7.2 at 12.5 x magnification.....	108
Figure 7.10	Edge of washer hole on washer found with bolt in Figure 7.1 at 6.3 x magnification. The crack may have originated at a crevice and was propagated by mechanical means.....	109
Figure 7.11	Corrosion product build up in the crevice of the bolt shaft and washer hole of the bolt shown in Figure 7.3 at 6.3 x magnification. The corrosion product fused the remaining bolt shaft to the washer.....	109

Figure 7.12	Surface of bolt in Figure 7.2 at 100 x magnification. Wavy surface indicates general corrosion.....	111
Figure 7.13	Surface of bolt in Figure 7.2 at 300 x magnification. Ridges in the surface were created during ductile failure of the bolt.....	111
Figure 7.14	Surface of bolt in Figure 7.2 at 500 x magnification. Voids on surface, corresponding to dark spots in the image, were opened during ductile failure.....	112
Figure 7.15	X-ray diffraction pattern for the bolt scale taken from the specimen shown in Figure 7.3. The peaks in the pattern correlate with iron, iron oxides, iron carbides, and iron silicates.....	113
Figure 8.1	Saturated calomel reference electrode and salt bridge used in all experimental laboratory tests.....	121
Figure 8.2	Example of long term test set-up. One solution container with carbon steel and stainless steel general, crevice, and waterline corrosion coupons.....	122
Figure 8.3	A waterline rack assembly with plastic washers electrically separating the stainless steel (left) and carbon steel (right) corrosion coupons.....	123
Figure 8.4	Experimental set-up for electrochemical polarization and cyclic polarization. The coupon that is being tested is clamped to the spout of the beaker.....	125
Figure 8.5	Computer software collects data from the potentiostat, which is electrically connected to the electrodes in the electrochemical polarization cell.....	126
Figure 8.6	Concentration cell coupling of similar metals in solutions with differing pH values. Stainless steel in solution with pH 13 is coupled with stainless steel in solution with pH 7.5, and carbon steel in solution with pH 13 is coupled with carbon steel in solution with pH 7.5.....	127
Figure 8.7	Long term corrosion potential readings of galvanized carbon steel corrosion coupons in the concentrated solution at pH 7.5. The galvanized carbon steel displays unstable passivity with potentials undulating between active and passive values.....	131

Figure 8.8	Long term corrosion potential readings of stainless steel corrosion coupons in the concentrated solution at pH 7.5. The stainless steel coupons have passive corrosion potentials.....	132
Figure 8.9	Long term corrosion potential readings of carbon steel corrosion coupons without zinc in the concentrated solution at pH 7.5. The carbon steel coupons without zinc have active corrosion potentials.....	133
Figure 8.10	Long term corrosion potential readings of galvanized carbon steel corrosion coupons in the concentrated solution at pH 13. The carbon steel coupons achieve passive potentials.....	134
Figure 8.11	Long term corrosion potential readings of stainless steel corrosion coupons in the concentrated solution at pH 13. The stainless steel coupons have passive potentials.....	135
Figure 8.12	Electrochemical polarization curves for stainless steel and carbon steel in concentrated solution with pH 7.5. The stainless steel displayed passivity, while the carbon steel actively corroded at significantly higher current densities.....	138
Figure 8.13	Electrochemical polarization curves for stainless steel and carbon steel in normal solution with pH 7.5. The stainless steel displayed passivity similar to stainless steel in concentrated solution, while the carbon steel actively corroded at current densities lower than current densities for carbon steel in concentrated solution.....	139
Figure 8.14	Electrochemical polarization curves for stainless steel and carbon steel in concentrated solution with pH 13. The stainless steel and carbon steel displayed similar passive behavior.....	140
Figure 8.15	Electrochemical polarization curves for stainless steel and carbon steel in normal solution with pH 13. The stainless steel and carbon steel displayed similar passive behavior to each other and to the steels in concentrated solution at pH 13.....	140
Figure 8.16	Cyclic polarization curves for Type 304 stainless steel subjected to localized corrosion. The protection potential is higher than the potential readings taken during the long term test of the same material, indicating that this material is protected from localized corrosion in this environment.....	144
Figure 8.17	Crevice formed on stainless steel corrosion coupon during cyclic polarization at 32 x magnification. The O-ring sealing the coupon to the glass opening in the polarization set-up created the crevice. Anchor bolts are also exposed to crevice conditions in the bearing	145

Figure 8.18	Pitting on the surface of the stainless steel corrosion coupon during cyclic polarization at 32 x magnification. The typical environment at a bridge bearing will not induce pitting corrosion in Type 304 stainless steel anchor bolts.....	145
Figure 8.19	Cyclic polarization of candidate alloys which may be considered for anchor bolt use. Type 316, Type 2101, and 2205 stainless steel alloys are considered acceptable alternative materials to Type 304 stainless steel.....	147
Figure 8.20	Cyclic polarization of candidate alloys which may be considered for anchor bolt use. The materials in this test were subjected to crevice effects resulting in a decrease in the protection potentials.....	148
Figure B.1	Edge beam cover plate and bearing.....	277
Figure B.2	Typical bearing assembly at abutment.....	278
Figure B.3	Bearing at abutment.....	278
Figure B.4	Corrosion between bearing plate and flange.....	279
Figure B.5	Typical corrosion in flange (1).....	279
Figure B.6	Typical corrosion in flange (2).....	280
Figure B.7	Close up of crevice corrosion in flange (1).....	280
Figure B.8	Close up of crevice corrosion in flange (2).....	281
Figure B.9	Interior beams without crevice corrosion.....	281
Figure B.10	Corroded nut.....	282
Figure B.11	Close up of corroded nut.....	282
Figure B.12	View from above a typical bolt. Not a pure hexagonal shape.....	283
Figure B.13	Edge beam bearing assemblies at interior Bent 2.....	283
Figure B.14	Close up of bearing and bolt at Bent 2.....	284
Figure B.15	Crevice corrosion in edge beam at Bent 2.....	284
Figure B.16	Bearing assemblies of interior beams at Bent 2.....	285

Figure B.17	Crevice corrosion in flange of interior beam at Bent 2.....	285
Figure B.18	Interior Bent 3.....	286
Figure B.19	Spalling diaphragms at interior bent.....	286
Figure B.20	Debris from diaphragms surrounding bearing.....	287
Figure B.21	Bearing assemblies of exterior beam at interior bent (1).....	287
Figure B.22	Bearing assemblies of exterior beam at interior bent (2).....	288
Figure B.23	Close-up of expansion slot.....	288
Figure B.24	Corroded bearing at interior Bent 3.....	289
Figure B.25	Accessing the joint at interior Bent 4.....	289
Figure B.26	Joint at Bent 4.....	290
Figure B.27	Bearing at southside of Bent 4.....	290
Figure B.28	Corrosion underneath flange at Bent 4 (1).....	291
Figure B.29	Corrosion underneath flange at Bent 4 (2).....	291
Figure B.30	Corrosion of the flange at Bent 4.....	292
Figure B.31	Corrosion around joint material at Bent 4.....	292
Figure B.32	Abutment backwall in between interior beams.....	293
Figure B.33	Oxides underneath chipped paint.....	293
Figure B.34	Typical fixed bearing at abutment (1).....	294
Figure B.35	Typical fixed bearing at abutment (2).....	294
Figure B.36	Edge beam bearing at abutment (1).....	295
Figure B.37	Edge beam bearing at abutment (2).....	295
Figure B.38	Corrosion of edge beam bearing at abutment (1).....	396
Figure B.39	Corrosion of edge beam bearing at abutment (2).....	396

Figure B.40	Fixed bearing at interior bent.....	397
Figure B.41	Close-up of debris around anchor bolt at interior bent.....	397
Figure B.42	Expansion bearing at interior bent (1).....	398
Figure B.43	Expansion bearing at interior bent (2).....	398
Figure B.44	Expansion bearing at interior bent (3).....	399
Figure B.45	Edge beam bearing at opposite abutment. Corrosion on bearing plates.....	399
Figure B.46	Fixed bearing at abutment.....	300
Figure B.47	Degradation of material behind fixed bearing.....	300
Figure B.48	Typical rocker bearing at west abutment (1).....	301
Figure B.49	Typical rocker bearing at west abutment (2).....	301
Figure B.50	Side view of rocker bearing at west abutment (1).....	302
Figure B.51	Side view of rocker bearing at west abutment (2).....	302
Figure B.52	Interior bent.....	303
Figure B.53	Typical bearing at interior bent (1).....	303
Figure B.54	Typical bearing at interior bent (2).....	304
Figure B.55	Typical rocker bearing at east abutment.....	304
Figure B.56	Slight corrosion on bearing plate.....	305
Figure B.57	Bearing debris causing increased bearing corrosion (1).....	305
Figure B.58	Bearing debris causing increased bearing corrosion (2).....	306
Figure B.59	Bearing debris causing increased bearing corrosion (3).....	306
Figure B.60	Bearing debris causing increased bearing corrosion (4).....	307
Figure B.61	Corrosion between rocker and bearing plate (1).....	307
Figure B.62	Corrosion between rocker and bearing plate (2).....	308

Figure B.63	Corrosion between rocker and bearing plate (3).....	308
Figure B.64	Corrosion between rocker and bearing plate (4).....	309
Figure B.65	Joint at abutment (1).....	309
Figure B.66	Joint at abutment (2).....	310
Figure B.67	Example of anchor bolt corrosion (1).....	310
Figure B.68	Example of anchor bolt corrosion (2).....	311
Figure B.69	Example of anchor bolt corrosion (3).....	311
Figure B.70	Example of anchor bolt and bearing corrosion.....	312
Figure B.71	Anchor bolt nut swelled with corrosion products (1).....	312
Figure B.72	Anchor bolt nut swelled with corrosion products (2).....	313
Figure B.73	Anchor bolt nut swelled with corrosion products (3).....	313
Figure B.74	Bearing assembly missing anchor bolt (1).....	314
Figure B.75	Bearing assembly missing anchor bolt (2).....	314
Figure B.76	Corrosion of bearing and bearing retrofit angles (1).....	315
Figure B.77	Corrosion of bearing and bearing retrofit angles (2).....	315
Figure B.78	Corrosion of bearing and bearing retrofit angles (3).....	316
Figure B.79	State Route 122 bridge over Little River.....	316
Figure B.80	Fixed bearing at interior bent in good condition.....	317
Figure B.81	Fixed bearing at interior bent with corrosion on bearing plate. Chipped paint only reveals orange primer paint underneath.....	317
Figure B.82	Close up of corrosion on bearing plate and chipped paint.....	318
Figure B.83	Expansion bearing at interior bent with signs of corrosion between the bearing plate.....	318
Figure B.84	Typical interior bent with fixed and expansion bearings (1).....	319

Figure B.85	Typical interior bent with fixed and expansion bearings (2).....	319
Figure B.86	Expansion bearing appearing in acceptable condition.....	320
Figure B.87	Closer inspection of expansion bearing reveals total anchor bolt corrosion.....	320
Figure B.88	Investigation of anchor bolt shafts in the bearing slot, beneath the washer.....	321
Figure B.89	Anchor bolt corrosion inside the bearing, beneath the washer (1).....	321
Figure B.90	Anchor bolt corrosion inside the bearing, beneath the washer (2).....	322
Figure B.91	Anchor bolt corrosion inside the bearing, beneath the washer (3).....	322
Figure B.92	Anchor bolt corrosion inside the bearing, beneath the washer (4).....	323
Figure B.93	Anchor bolt corrosion inside the bearing, beneath the washer (5).....	323
Figure B.94	Anchor bolt corrosion inside the bearing, beneath the washer (6).....	324
Figure B.95	Anchor bolt corrosion inside the bearing, beneath the washer (7).....	324
Figure B.96	Anchor bolt corrosion inside the bearing, beneath the washer (8).....	325
Figure B.97	Anchor bolt corrosion inside the bearing, beneath the washer (9).....	325
Figure B.98	Staining on the concrete piers from moisture from the deck joints.....	326
Figure B.99	Faulty deck joint.....	326
Figure B.100	Fixed bearing at steel girder end (1).....	327
Figure B.101	Fixed bearing at steel girder end (2).....	327
Figure B102	Expansion bearing.....	328
Figure B.103	Close up of an anchor bolt entering the expansion bearing base plate...	328
Figure B.104	Fixed rocker.....	329
Figure B.105	Close up of corrosion between bearing plates in the fixed rocker.....	329
Figure B.106	Link cantilever bearing by river.....	330

Figure B.107	Close-up of corrosion at deck joint above link bearing.....	330
Figure B.108	Fixed bearing at abutment.....	331
Figure B.109	Fixed bearing at interior bent.....	331
Figure B.110	Expansion and fixed bearings at expansion joint in the deck.....	332
Figure B.111	Bearing corrosion at deck joint.....	332
Figure B.112	Close-up of bearing corrosion at deck joint.....	333
Figure B.113	Investigation of anchor bolt shaft within the bearing by clearing away dirt.....	333
Figure B.114	Anchor bolt corrosion within the bearing (1).....	334
Figure B.115	Anchor bolt corrosion within the bearing (2).....	334
Figure B.116	Anchor bolt corrosion within the bearing (3).....	335
Figure B.117	Anchor bolt corrosion within the bearing (4).....	335
Figure B.118	Anchor bolt corrosion within the bearing (5).....	336
Figure B.119	Anchor bolt corrosion within the bearing (6).....	336
Figure B.120	Anchor bolt corrosion within the bearing (7).....	337
Figure B.121	Fixed bearing at abutment.....	338
Figure B.122	Expansion bearing at deck joint with visible corrosion on bearing plates.....	338
Figure B.123	Clearing away dirt to inspect anchor bolt shaft within the bearing.....	339
Figure B.124	I-75 bridge over South Marietta Parkway, District 7.....	339
Figure B.125	US Route 76 over a creek in Blue Ridge, District 6.....	340
Figure B.126	State Route 515 over Georgia Northeast Railroad in Blue Ridge, District 6.....	340
Figure B.127	US Route 19 over US Route 76, District 1.....	341
Figure C.1	Fixed bearing with corroded anchor bolts.....	343

Figure C.2	Corrosion product build-up in the anchor bolt hole (1).....	344
Figure C.3	Corrosion product build-up in the anchor bolt hole (2).....	344
Figure C.4	Corrosion product build-up in the anchor bolt hole (3).....	345
Figure C.5	Bolt and bearing plate from expansion bearing.....	345
Figure C.6	View of a fixed bearing with corroded anchor bolts from the top.....	346
Figure C.7	Anchor bolts protruding from fixed bearing plate.....	346
Figure C.8	Corrosion product on the anchor bolt protruding from the bearing plate (1).....	347
Figure C.9	Corrosion product on the anchor bolt protruding from the bearing plate (2).....	347
Figure C.10	Underside of a fixed bearing.....	348
Figure C.11	Close-up of anchor bolt where it enters bearing plate from concrete (1).....	348
Figure C.12	Close-up of anchor bolt where it enters bearing plate from concrete (2).....	349
Figure C.13	Fixed bearing plate and anchor bolts.....	349
Figure C.14	Close-up of anchor bolts protruding from bearing plate.....	350
Figure C.15	Anchor bolt in bearing hole with severe necking.....	350
Figure C.16	Single anchor bolt showing necking.....	351
Figure C.17	Single anchor bolt, deformed during demolition, showing severe necking.....	351
Figure D.1	Long term potential readings for carbon steel in normal solution pH 7.5.....	354
Figure D.2	Long term potential readings for stainless steel in normal solution at pH 7.5.....	354
Figure D.3	Long term potential readings for carbon steel in normal solution at pH 13.....	355

Figure D.4	Long term potential readings for stainless steel in normal solution at pH 13.....	355
Figure D.5	Long term potential reading for carbon steel in pore solution.....	356
Figure D.6	Long term potential readings for stainless steel in pore solution.....	356
Figure D.7	Cyclic polarization curves for candidate alloys in normal solution at pH 7.5.....	358

SUMMARY

The research objectives for this project were to explicitly define the anchor bolt corrosion problem in the state of Georgia and recommend action to the Georgia Department of Transportation. The bearing assembly of concern is the plate bearing assembly, in which carbon steel and/or bronze plates are anchored by either carbon steel or stainless steel anchor bolts. Inspection report data revealed that anchor bolt corrosion was ubiquitous for all environments in Georgia; the problem was reported for 27% of the steel girder bridges throughout the state. Based on a synthesis of the field investigations, bolt failure analyses, laboratory experimental testing, and review of GDOT inspection report surveys, the corrosion of carbon steel anchor bolts is caused universally by concentration cell corrosion. Other corrosion mechanisms of concern are galvanic and crevice corrosion, which are both enhanced by the current bearing design.

Corrosion protection provided through zinc galvanization cannot sufficiently protect the carbon steel bolt for its entire service life. Corrosion potential and cyclic polarization data confirmed that ASTM Type 304, Type 316, Type 2101, and Type 2205 were protected from concentration cell and localized corrosion in the simulated bearing environment. Therefore, it is recommended that the stainless steel anchor bolts of these types be used in future designs and that the bolts should be electrically separated from all dissimilar metals using a Nylon or Teflon washer to prevent preferential corrosion of carbon steel. It is further recommended that the bronze lube plate should be eliminated entirely and that the bearing type should be a reinforced elastomeric bearing. Maintenance of existing sliding plate bearings should include regular cleaning by

brushing away debris from the bearing surfaces, and bridges with carbon steel anchor bolts should be retrofitted to provide additional lateral restraint according to current maintenance procedures.

CHAPTER 1: INTRODUCTION

1.1 Problem statement and research objectives

Inspections of steel girder bridges throughout the state of Georgia have revealed a widespread problem: corrosion in the steel superstructure's bearing areas that threaten the structural integrity of many bridges. The predominant component of the bearing assemblies found to be corroding is the anchor bolts fastening the steel girders to the concrete pier caps. The corrosion of these anchor bolts can result in two serious problems: reduction of lateral load bearing capacity of the bridge and increased stresses in bridge components due to immovable bearings. In both cases the safety of the structure is jeopardized under normal and seismic loading. While anchor bolt corrosion is known to exist in Georgia, the extent and specific cause of the problem is still unknown.

The research objectives for this project were to explicitly define the anchor bolt corrosion problem in the state of Georgia, research solutions to the problem, and recommend action to the Georgia Department of Transportation. Specifically, the research aimed to define the extent and cause of anchor bolt corrosion and to gain further knowledge from literature review. The final objective was to recommend bearing design procedure and maintenance actions to abate anchor bolt corrosion in Georgia.

1.2 Research approach

The first objective of this research was to explicitly define the nature of the anchor bolt corrosion problem in the state of Georgia. As a first step, the researcher interviewed key personnel within the state Department of Transportation to understand

the key bearing design principles, maintenance procedures, and the history of both. The researcher compiled and interpreted inspection data from throughout the state. An analysis of these data provides answers concerning the extent of the problem throughout the state.

To determine the cause of the corrosion, eight key bridges were inspected by the researcher and were used as case studies representing anchor bolt corrosion throughout the state. Metallurgical samples obtained from these bridges were analyzed in the laboratory. Corrosion products from the samples analyzed by x-ray diffraction provided information about the corrosive environment of the bolts, while bolt analysis performed with optical and scanning electron microscopes was used to determine the mode of corrosion per bolt

Additionally, laboratory experiments were conducted on metallurgical samples from new anchor bolts to analyze the corrosion behavior of the materials. Corrosion potential, cyclic polarization and polarization resistance data of samples in simulated environmental bearing conditions were used to evaluate the corrosion resistance of the current anchor bolt materials and several alternative alloys.

The second objective of this project was to research solutions to abate anchor bolt corrosion in Georgia. An in-depth literature review was performed to determine concepts of bearing design, maintenance, and corrosion. Additionally, the review covered the properties of alternative corrosion resistant alloys considered for use as bolt material.

Finally, the third objective was to recommend best practice solutions for bearing design and maintenance. The recommendations include alternatives in new anchor bolt construction which provide greater corrosion resistance, and include suggestions for

improved maintenance procedures to address corrosion in existing bridges. A synthesis of the results from the first two objectives was the basis of the recommendations.

1.3 Significance of research

The proposed research investigates the nature of anchor bolt corrosion in the state of Georgia. In the process of the investigation, specific causes and modes of corrosion in bearing assemblies were explored. As a result, specific corrosion mechanisms in anchor bolts of steel girders bridges were determined. The intellectual merit of this research is that in understanding the corrosion mechanisms, engineers will be able to make informed decisions regarding bridge bearing design and material specifications.

The advent of corrosion resistant anchor bolts in bridge bearing assemblies has broad impacts. First, bridges will become overall safer structures when corrosion is eliminated from bearings. Bearings will be able respond adequately to normal thermal stresses, protecting other bridge components from unnecessary high stresses. Additionally, bridges will maintain lateral load resisting capacity.

Second, corrosion resistant bearing assemblies will ultimately provide longer-lasting structures, which is an economic benefit to the state and its residents. As a result of this research, anchor bolts will be designed for a service life of over 100 years, reducing the need for costly repairs or reconstruction in the bridge's lifetime.

CHAPTER 2: STEEL GIRDER BEARING DESIGN, MATERIALS, AND MAINTENANCE IN GEORGIA

2.1 Bridge bearings

Bridge bearings assemblies function to anchor the bridge superstructure to the piers and to allow for normal expansion and contraction of the bridge superstructure. Accordingly, the bearing assembly provides resistance against lateral loading transverse to the structure, such as wind, earthquake or vehicle impact loads. At the expansion end of a bridge span, the bearing contains a mechanism for rotational and/or sliding motion to accommodate the thermal movements of the superstructure.

Various types of bearing assemblies are commonly used in Georgia. This research project focused on the corrosion of the anchor bolts in the plate bearing assemblies. A typical current design for a plate bearing is shown in Figures 2.1 and 2.2. The bearing assembly at the fixed end of the span typically consists of two plates: the base plate, which is positioned on top of the pier cap, and the sole plate, which is welded to the underside of the girder flange. An anchor bolt that is embedded in a three-inch diameter hole in the pier cap with non-shrink grout passes through a $1 \frac{7}{16}$ -inch hole in each plate in the bearing assembly and the flange of the girder, where it is fastened with a washer and nut. At the expansion end of the span, the bearing assembly contains three plates: the base plate and sole plate, and a self lubricating, or “lube” plate. In the expansion bearing the bolt passes through $1 \frac{7}{16}$ -inch by $2 \frac{1}{2}$ to 3-inch slotted holes in the lube and sole plates and flange. As the bridge superstructure undergoes thermal expansion or contraction, the girder and sole plate slide on the lube plate, and the anchor bolt’s

position in the slotted holes changes. Figures 2.3 and 2.4 show an expansion and a fixed bearing in good condition.

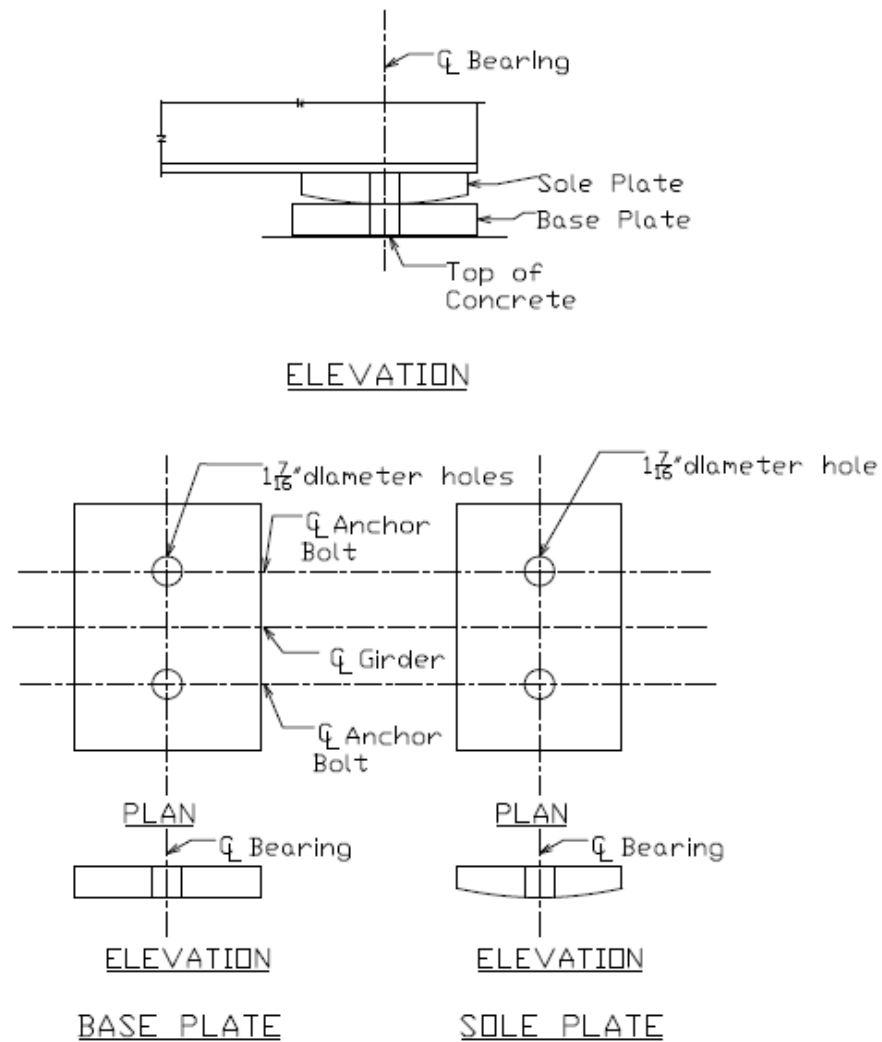


Figure 2.1: Typical fixed bearing design

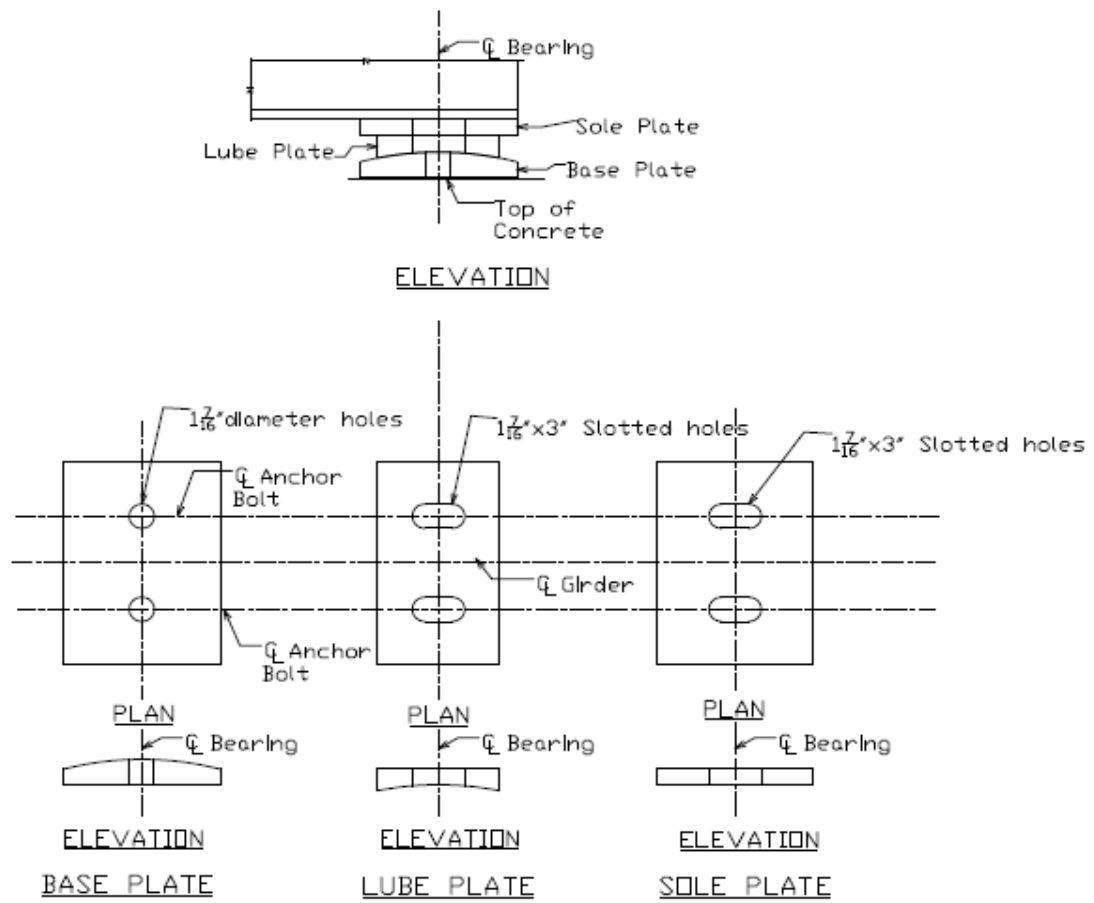


Figure 2.2: Typical expansion bearing design.



Figure 2.3: Typical fixed bearing in good condition



Figure 2.4: Typical expansion bearing in good condition

Under the bridge superstructure, the bridge bearing is exposed to unfavorable environmental conditions. In addition to the moisture in the atmosphere, bearings may be exposed to excess moisture that improperly drains from the bridge deck through deck joints. As moisture drains from the deck it carries aggressive agents, such as chlorides and sulfates, to the bearings. Dirt and debris that collect on the surface of the pier cap around the bearings provide a medium for the highly conductive solution. Often, the moist dirt is packed around the anchor bolt in the slotted hole of the expansion bearing. Figure 2.5 shows the environmental condition of a bearing under a deck joint. Under these conditions, the bearings and anchor bolts are prone to corrosive attack.



Figure 2.5: Debris around bearing at deck joint.

2.2 Safety issues

Products of corrosion can cause bearings to become fixed in one position. Bearings are designed to allow expansion and contraction of the bridge girders according to thermal conditions. When the girders are restrained from natural movement, high stresses form in the steel girder and the concrete pier cap, and failure in these bridge components may result.

Second, when anchor bolts corrode, the cross-sectional area of the bolt shaft is reduced. Consequently, the strength of the bolt is reduced. In severe cases of anchor bolt corrosion, the bolt may be easily broken off by hand. Figure 2.6 shows an example of an anchor bolt with significantly reduced cross sectional area due to corrosion. The lateral load resisting mechanism of a bridge structure depends on the strength of the anchor bolts; an unsafe structure results when the bolts are corroded. In the event of lateral

vehicular impact to the bridge, high wind load, or an earthquake, a bridge with a reduced lateral load capacity is more prone to failure.



Figure 2.6: Corroded anchor bolt

2.3 Bearing materials

In the bearing design an important factor contributing to the corrosion resistance of the bearing is the material used for all components. Eleven bridge plans provided by the Georgia Department of Transportation were representative of the construction of steel girder bridges in different eras ranging from the 1930s to present day. A review of these plans provided insight into the historical development of the materials used in the bearing design.

The material composition and mechanical properties of steels used in current plate bearing designs and steels considered for use in future designs are shown in Tables 2.1 and 2.2. Cells in the table in which “...” appears indicates that there are no requirements for that category; cells in which “xx” appears indicates that the category does not apply to the material. The material properties of the structural carbon steel (CS) conform to ASTM A709: “Standard Specification for Structural Steel for Bridges”, and the material

properties of the stainless steel (SS) alloys conform to ASTM 276: “Standard Specification for Stainless Steel Bars and Shapes”.

Table 2.1: Material composition of steel alloys used in bearings (ASTM 2006; ASTM 2007).

Steel Designation	Material composition in %								
	C	Mn	P	S	Si	Cr	Ni	Mo	N
CS: Grade 36	0.26	...	0.04	0.05	0.40	xx	xx	xx	xx
SS: 304	0.08	2.00	0.045	0.030	1.00	18.0-20.0	8.0-11.0
SS: 316	0.08	2.00	0.045	0.030	1.00	16.0-18.0	10.0-14.0	2.00-3.00	...
SS: 2101	0.040	4.0-6.0	0.040	0.030	1.00	21.0-22.0	1.35-1.70	0.10-0.80	0.20-0.25
SS: 2205	0.030	2.00	0.030	0.020	1.00	22.0-23.0	4.5-6.5	3.0-3.5	0.14-0.20

Table 2.2: Mechanical properties of steel alloys used in bearings (ASTM 2006; ASTM 2007).

Steel Designation	Mechanical properties			
	Yield Strength, ksi	Tensile Strength, ksi	Elongation, %	Brinell Hardness number
CS: Grade 36	36	58-80	23	...
SS: 304	30	75	40	...
SS: 316	30	75	40	...
SS: 2101	65	94	30	290
SS: 2205	65	95	25	290

Traditionally, the base plates and the sole plates of the bearing assembly conform to ASTM A709 Grade 36 carbon steel – a practice which has been continued in current design. Prior to 1960, the self-lubricating bronze plate was not a part of the plate bearing design. With a few exceptions, a cast bronze lube plate conforming to ASTM B 22 was introduced in bearing designs in the mid-1960s. In current practice lube plates are cast bronze with lubricating oil machined onto them.

In the design of the bearing, the anchor bolt material has undergone the most significant change. Before 1990, anchor bolts were ASTM Grade 36 carbon steel. Due to the high frequency of anchor bolt corrosion problems, the Georgia Department of Transportation started requiring the use of stainless steel conforming to ASTM A276 Type 304 anchor bolts in the early 1990s. Type 304 stainless steel was chosen because it was the most economical corrosion resistant material available at the time. Aside from the material specification, the other physical properties of the bolts remained the same. The bolts are generally 1 1/4-inch in diameter and 18 inches long. Both the previous carbon steel bolts and newer stainless steel bolts used are swaged, or dimpled, where they are grouted into the concrete, and are threaded at the top 4 1/4-inches, where they pass through the bearing plates. The mechanical properties of the stainless steel anchor bolt were determined to be acceptable by the Georgia Department of Transportation (GDOT). Since the switch to using stainless steel bolts, no attempt has been made to electrically separate the stainless steel nut and washer from the carbon steel girder flange.

Lastly, according to officials at the Georgia Department of Transportation, the majority of anchor bolt corrosion was observed to occur at the interface where the bolt protrudes from the concrete pier cap. In response to this observation the bearing design began to require a neoprene pad to be placed between the concrete and the base plate.

2.4 Maintenance procedures

The DOT maintenance department reports that deicers are rarely used, limiting the threat of chloride contamination of the bearings. However, the maintenance department admits that debris is not regularly cleaned out from around the bearing.

Debris which is left around the bearings can trap any chlorides and other ions at the site, creating a corrosive environment.

The previous State Bridge Maintenance Engineer, Ben Rabun, informed the researcher on May 22, 2007 that routine bridge inspections have revealed a high number of loose anchor bolts, which is a sign of anchor bolt corrosion. Bearings in which the anchor bolts are no longer functional are repaired by “sleeving”. Sleeving a bearing is a process in which steel angles or Z channels are bolted to either side of the bearing to prevent lateral movement. Stainless steel bolts are used for the repair. The durability of this repair has not been quantified by GDOT. Figure 2.7 shows a sleeved bearing in the field, which has been subject to corrosion attack.



Figure 2.7: A sleeved bearing, a repair process in which steel angles are bolted to both sides of the bearing to prevent lateral movement, which has been subjected to corrosion attack.

Other measures are also being taken to replace existing carbon steel anchor bolts with stainless steel bolts. For example, the Georgia DOT is now requiring that for any

bridge widening or jacking projects, the anchor bolts on the existing structure must be replaced with stainless steel bolts. Also, a bolt replacement method of coring out old anchor bolts through the flange and into the concrete has been proposed by one contractor, but has not yet been attempted.

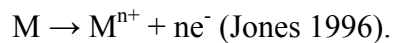
CHAPTER 3: CORROSION BACKGROUND

3.1 Basics of corrosion

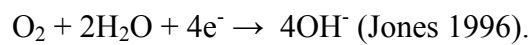
Corrosion is the degradation of material. For a majority of metals and metallic alloys, degradation is a result of electrochemical reactions between the material and the environment (Davis 2000). In this chapter, the concepts of electrochemical corrosion are presented along with a summary of several specific forms of corrosion and ways of measuring corrosion in metals.

Electrochemical corrosion is the reaction of metals in an aqueous environment involving the transfer of electrons. For this process to occur, a corrosion cell must have four components: an anode and a cathode, and an ionic current path and an electronic path between them (Singh 2008). Electrochemical corrosion proceeds when electrons are transferred from the anode to the cathode along the electronic path, enabling the dissolution of metal ions.

The anode of a corrosion cell is the location on the metal surface where the metal ions undergo dissolution. As the metal goes into solution, electrons are generated. This reaction is called the anodic or oxidation reaction, because the metal species is oxidized in the process according to the following general equation:



The electrons that are released in the oxidation reaction are consumed at the cathode by the cathodic, or reduction reaction. A typical cathodic reaction in neutral solutions involves the reduction of oxygen:



Separately, the anodic and cathodic reactions are called half-cell reactions.

The electronic path of the corrosion cell through which the electrons flow is within the metal itself, or through an electrical contact between metals. Meanwhile, the ionic current path of the corrosion cell is through the solution, or aqueous environment, with which the metal is in contact. Current flow between the anode and the cathode through the ionic path is created by the movement of charged ions in the solution; positive ions are attracted to the cathode, while negative ions move towards the anode. (Davis 2000). In laboratory settings a salt bridge connecting the anodic and cathodic half cells replicates the electrolytic solution that naturally connects the half cells in the field. The salt bridge allows the transfer of charged ions between the anode and the cathode.

When all four components of an electrochemical corrosion cell are present corrosion can occur. Yet, whether corrosion will occur or not is dependent on the thermodynamics of the cell.

3.1.1 Thermodynamics

The thermodynamics of a corrosion cell are the energy changes the cell experiences as it undergoes electrochemical corrosion. The free energy changes incurred during electrochemical reactions are the driving force of corrosion, because the cell reacts in order to achieve its lowest free energy state (Davis 2000). By reflecting the free energy changes available in electrochemical reactions, thermodynamics predicts whether corrosion occurs spontaneously and the direction of electrochemical reactions, which determines which half-cell reaction is anodic and which is cathodic. Any reaction which

produces a negative free energy change, ΔG , is thermodynamically favored (Jones 1996). However, kinetics of reaction may be controlled by other factors.

When the corrosion cell reaches its lowest free energy state and the reactions produce no net change in free energy, the system has reached equilibrium (Davis 2000). The equilibrium potential of a reaction, E° , is related to the free energy change of that reaction by

$$\Delta G^\circ = -nFE^\circ,$$

where F is Faraday's constant and n is the number of electrons participating in the reaction (Jones 1996). The equilibrium potential of a reaction is the characteristic thermodynamic measurement of a corrosion reaction, because it indicates the free energy and equilibrium conditions of the reaction (Singh 2008).

The equilibrium potential of an electrochemical reaction, E° , is the sum of the equilibrium potentials of each half-cell reaction, also known as the single electrode potentials or half-cell potentials. Half-cell electrode potentials, however, cannot be measured independently; potential values are in fact potential differences measured with respect to a specified reference electrode (Jones 1996). A listing of possible half cell reactions and their associated potentials at standard state with respect to a standard hydrogen electrode is called the Electromotive Force (emf) Series. A standard emf Series is presented in Figure 3.1 By convention, all the reactions listed in the emf series are written as reduction reactions (Jones 1996). Reactions with more negative potentials are considered active, while reactions with more positive potentials are noble.

	Reaction	Standard Potential, e° (volts vs. SHE)
Noble	$\text{Au}^{3+} + 3e^- = \text{Au}$	+1.498
	$\text{Cl}_2 + 2e^- = 2\text{Cl}^-$	+1.358
	$\text{O}_2 + 4\text{H}^+ + 4e^- = 2\text{H}_2\text{O}$ (pH 0)	+1.229
	$\text{Pt}^{2+} + 3e^- = \text{Pt}$	+1.118
	$\text{NO}_3^- + 4\text{H}^+ + 3e^- = \text{NO} + 2\text{H}_2\text{O}$	+0.957
	$\text{O}_2 + 2\text{H}_2\text{O} + 4e^- = 4\text{OH}^-$ (pH 7) ^a	+0.82
	$\text{Ag}^+ + e^- = \text{Ag}$	+0.799
	$\text{Hg}_2^{2+} + 2e^- = 2\text{Hg}$	+0.799
	$\text{Fe}^{3+} + e^- = \text{Fe}^{2+}$	+0.771
	$\text{O}_2 + 2\text{H}_2\text{O} + 4e^- = 4\text{OH}^-$ (pH 14)	+0.401
	$\text{Cu}^{2+} + 2e^- = \text{Cu}$	+0.342
	$\text{Sn}^{4+} + 2e^- = \text{Sn}^{2+}$	+0.15
	$2\text{H}^+ + 2e^- = \text{H}_2$	0.000
	$\text{Pb}^{2+} + 2e^- = \text{Pb}$	-0.126
	$\text{Sn}^{2+} + 2e^- = \text{Sn}$	-0.138
	$\text{Ni}^{2+} + 2e^- = \text{Ni}$	-0.250
	$\text{Co}^{2+} + 2e^- = \text{Co}$	-0.277
	$\text{Cd}^{2+} + 2e^- = \text{Cd}$	-0.403
	$2\text{H}_2\text{O} + 2e^- = \text{H}_2 + 2\text{OH}^-$ (pH 7) ^a	-0.413
	$\text{Fe}^{2+} + 2e^- = \text{Fe}$	-0.447
	$\text{Cr}^{3+} + 3e^- = \text{Cr}$	-0.744
	$\text{Zn}^{2+} + 2e^- = \text{Zn}$	-0.762
	$2\text{H}_2\text{O} + 2e^- = \text{H}_2 + 2\text{OH}^-$ (pH 14)	-0.828
	$\text{Al}^{3+} + 3e^- = \text{Al}$	-1.662
	$\text{Mg}^{2+} + 2e^- = \text{Mg}$	-2.372
	$\text{Na}^+ + e^- = \text{Na}$	-2.71
	$\text{K}^+ + e^- = \text{K}$	-2.931
Active		

Figure 3.1: A standard Electromotive Force Series with respect to the standard hydrogen electrode. Reactions with more negative potentials are considered active, while reactions with more positive potentials are noble (Jones 1996).

The emf Series is a tool that can be used to predict the direction of electrochemical reactions based on the half-cell electrode potentials. Since electrochemical reactions proceed spontaneously when the free energy is negative, it follows that corrosion occurs when the sum of the half-cell electrode potentials, E , is positive. Therefore, “[t]he half-cell reaction with the more active (negative) half-cell

potential always proceeds as an oxidation, and the one with the more noble half-cell potential always proceeds as a reduction in the spontaneous reaction produced by the pair.” (Jones 1996).

The emf Series lists the half-cell electrode potential measurements taken at a standard temperature and pressure. Since actual environments may not conform to the standard state, the half-cell potential may be adjusted for non-standard conditions using the Nernst equation:

$$E = E^o - \frac{RT}{nF} \ln \left(\frac{(B)^b (H_2O)^d}{(A)^a (H^+)^m} \right),$$

where R is the gas constant, T is the absolute temperature, F is Faraday’s constant, n is the number of electrons involved in the transfer, and the terms in the numerator of the natural log function represent the concentration of products of the reduction reaction, while the terms in the denominator represent the concentrations of the reactants (Jones 1996). From the Nernst equation, it is observed that if the concentration, or activity, of the metal ions in solution is higher, the measured half-cell potential is more noble. Also, as the concentration of the oxidizer, H^+ , increases, the potential increases. As a result, potential characterizes the oxidizing power of the solution of the corrosion cell.

Electrode potentials, as the characteristic thermodynamic property of electrochemical corrosion cells, provide insight into the driving force of corrosion, direction of electrochemical reactions, and the oxidizing power of the electrolytic solution. However, thermodynamics cannot predict the rate of corrosion, which is dependent on the kinetics of the electrochemical cells.

3.1.2 Kinetics

Thermodynamic properties of an electrochemical corrosion cell are useful in understanding the corrosion behavior of a material, but understanding the kinetic properties of the corrosion cell is more practical from an engineering standpoint. From the kinetics of the corrosion cell, the rate of corrosion and mass loss can be derived, the effects of polarization of a metal can be observed, and the active-passive behavior of metals can be examined.

As discussed previously, corrosion of metals often occurs electrochemically, meaning that electron flow is fundamental to the process. Therefore, a measure of the electron flow as current, I , in a corrosion cell is one measure of the corrosion rate. According to Faraday's Law for general or uniform corrosion, the amount of material dissolution or plating in solution is directly proportional to the electric current flowing through it (Jones 1996). Thus, a measure of the mass reacted is another measure of the corrosion rate. Faraday's Laws and uniform corrosion are discussed further in Sections 3.2 and 3.3.

3.1.2.1 Exchange current density

When the electrochemical cell is at equilibrium, the half-cell reactions thermodynamically produce zero net free energy. Similarly, zero net current is produced by the reactions. At equilibrium the rate of the oxidation reaction is equal to the rate of the reduction reaction. The current at which electrons are consumed at the same rate that they are generated is called the exchange current of the cell (Davis 2000). The magnitude of the exchange current density, or exchange current divided by the surface area, of a

corrosion cell is highly dependent on the surface on which the reactions are occurring, which in turn affects corrosion rates (Davis 2000).

Figure 3.2 illustrates the effect of electrode surface on exchange current density for hydrogen half-cell reactions. In Figure 3.2 three Evans's diagrams are shown; electrode potentials are plotted on the y-axis versus the log of the current density on the x-axis. Lines with negative slopes correspond to cathodic reactions – in this case the reaction of hydrogen ions to produce hydrogen gas. The lines with positive slopes correspond to anodic reaction – in this case the degradation of hydrogen gas into hydrogen ions and electrons. Equilibrium of the two half-cell reactions occurs where the two line intersect. From Figure 3.2 it can be observed that regardless of the metallic surface on which the electrochemical reaction of hydrogen evolution occurs, the point of intersection remains at the same equilibrium potential. In contrast, the exchange current density of the reaction varies by nine orders of magnitude depending on the electrode surface.

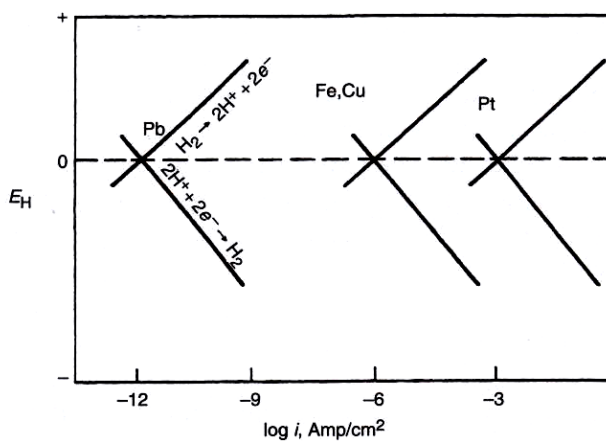


Figure 3.2: Exchange-current densities for hydrogen evolution on lead, iron, copper, and platinum surfaces. The surface of the electrode affects the magnitude of the exchange current density (Davis 2000).

3.1.2.2 Electrochemical polarization

Polarization of an electrochemical cell occurs when it is not at equilibrium. A corrosion cell is polarized when the potential is changed from the equilibrium potential by a net current at the material surface (Jones 1996). The net current induces energy changes of the electrode; electrons removed from the surface induce positive, or anodic, polarization, and electrons supplied to the surface induce negative, or cathodic, polarization (Singh 2008). Because polarization is a forced change in electrode potential, it is also referred to as overpotential. To study the corrosion behavior of a material, polarization may be induced in the laboratory by externally removing or supplying electrons at the electrode surface, as discussed in Section 3.3.

Net current at the electrode surface is induced naturally in corrosive environments in several ways. The first cause occurs when a limiting, or slow step, reaction rate affects the rate of charge transfer. Charge transfer may also be affected by a limited availability of reactants for a particular half-cell reaction at the surface of the electrode. Lastly, electrons may be supplied or consumed by a second electrochemical reaction, which eventually coexists with the first (Singh 2008).

3.1.3 Mixed potential theory

The coexistence of multiple electrochemical reactions is the basis for mixed potential theory. The Evans' diagrams in Figures 3.3 and 3.4 illustrate mixed potential theory with the dissolution of zinc in acid, where the anodic reaction is $\text{Zn} \rightarrow \text{Zn}^{2+} + 2\text{e}^-$ and the cathodic reaction is $2\text{H}^+ + 2\text{e}^- \rightarrow \text{H}_2$. As previously discussed, each half-cell reaction has its own equilibrium potential and exchange current density, as shown in

Figure 3.3. As the two reactions interact, they polarize each other to an intermediate value, as shown in Figure 3.4. The half-cell with the lower potential, zinc in this case, is polarized in the anodic direction, while the half-cell with the higher potential, hydrogen, is polarized cathodically (Singh 2008). The point where the polarized anodic and cathodic curves intersect defines the equilibrium of the electrochemical corrosion of zinc in hydrogen. The potential at the intersection is the corrosion potential, E_{corr} , of the electrochemical cell, and the current density is the corrosion current density, i_{corr} , of the cell. According to mixed potential theory, E_{corr} will always occur at an intermediate value between the half-cell equilibrium potentials (Singh 2008).

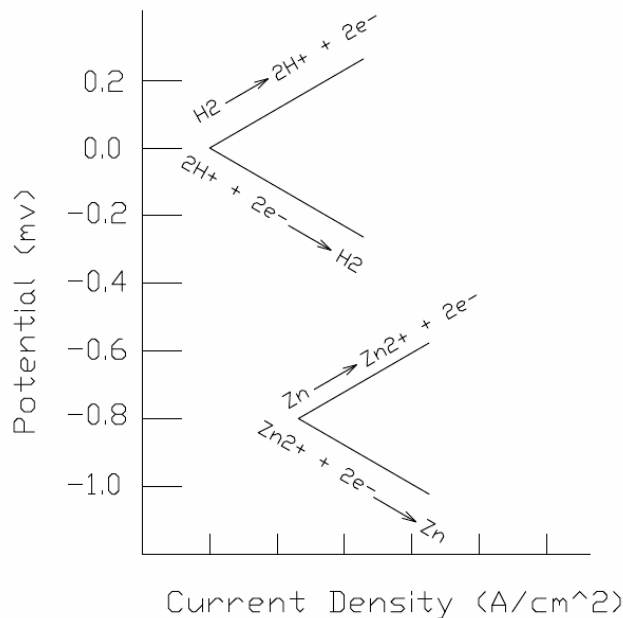


Figure 3.3: Evan's diagram of hydrogen and zinc half-cell reactions at equilibrium. The curves with negative slopes are the cathodic half-cell reactions, and the curves with positive slopes are the anodic half-cell reactions.(Singh 2008)

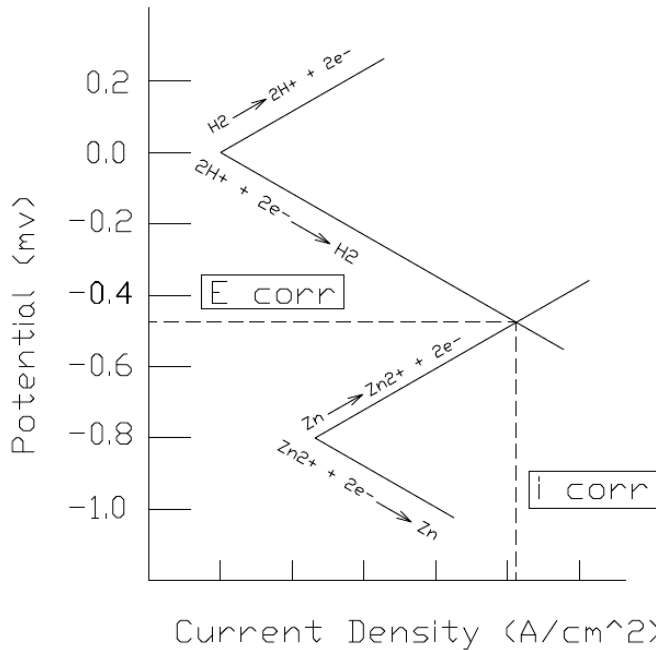


Figure 3.4: Evan's diagram demonstrating mixed potential theory. Zinc and hydrogen electrochemical reactions polarize to reach an intermediate equilibrium value (Singh 2008).

A few key factors that influence the location of the intersection of the anodic and cathodic curves, and thus influence the corrosion behavior, include the magnitude of the exchange current density and the addition of oxidizers to the solution. The effect of the exchange current density is illustrated in Figure 3.5 and the effect of an added oxidizer is shown in Figure 3.6.

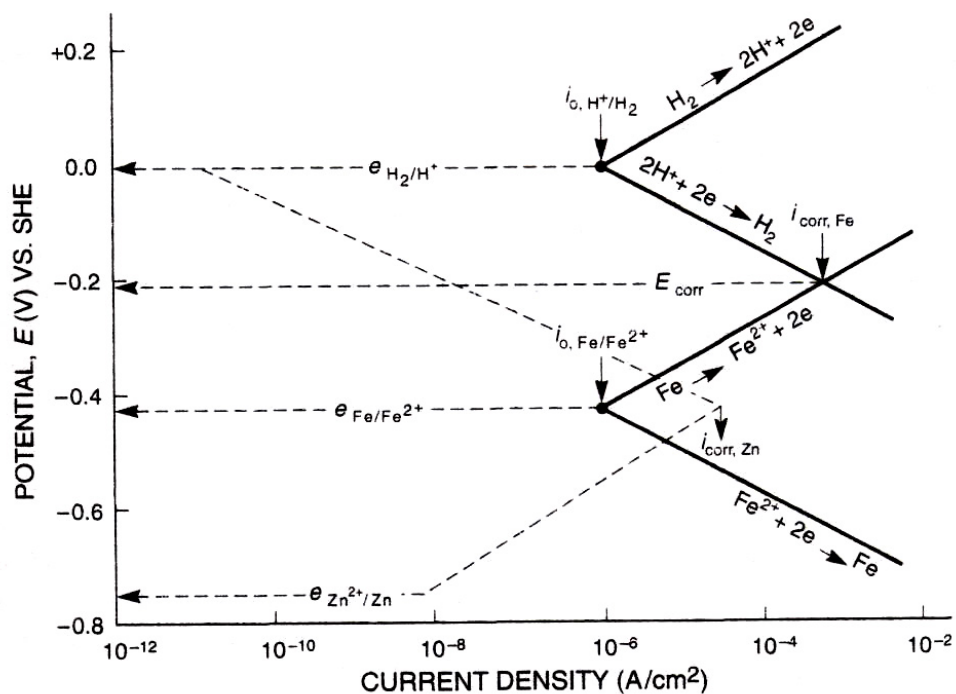


Figure 3.5: The effect of exchange current density on corrosion behavior. Higher exchange current densities lead to higher corrosion rates (Jones 1996).

Figure 3.5 compares the corrosion potential and corrosion current density of iron dissolution in acid with those for zinc dissolution in acid. The polarized anodic and cathodic curves for the corrosion of zinc are shown as dashed lines, and the behavior of the iron is shown with solid lines. For both reactions, the half-cell potential of the hydrogen reduction is the same. The half-cell reaction of the zinc is much more active (negative) than that for the iron, signifying a greater driving force for corrosion. However, the corrosion current density of iron dissolution is higher than that for zinc dissolution, because the exchange current density of the hydrogen half-cell is higher on the iron surface than on the zinc surface (Jones 1996). In this manner, mixed potential theory confirms that corrosion rate is dependent on the kinetics of the cell rather than the thermodynamics.

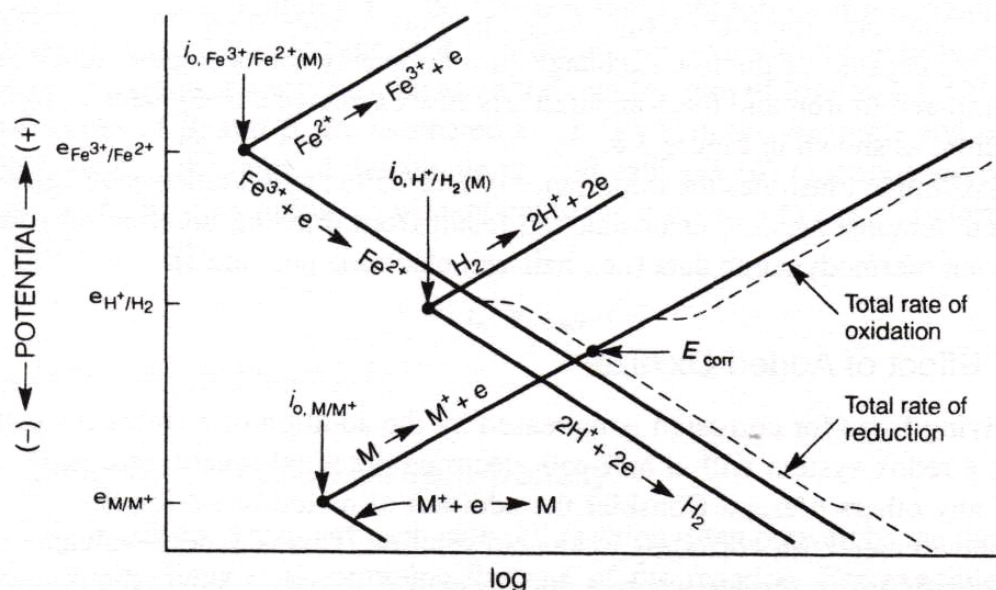


Figure 3.6: The effect of added oxidizers on corrosion behavior. Additional oxidizers increase the potential and current density of the electrochemical reaction (Fontana 1986).

The addition of oxidizers creates multiple cathodic reactions for a given anodic reaction. Figure 3.6 demonstrates the effect of the addition of the oxidizer Fe^{3+} on the corrosion potential and corrosion current density of the generic metal, M. Oxidation and reduction curves occurring at the same potentials added together to form the total rate are represented by the dashed lines in the figure. The intersection of the dashed line with the anodic curve for M occurs at a more noble potential and a higher corrosion current density than the intersection of the hydrogen cathodic curve with the anodic curve for M. Thus, it can be concluded that the addition of an oxidizer increases the driving force and the rate of the electrochemical reaction (Jones 1996).

3.1.4 Passivity

The thermodynamic and kinetic concepts presented in this chapter generally define the electrochemical corrosion behavior of metals. In some alloys, however, an additional property of corrosion, passivity, seemingly contradicts thermodynamics and alters the kinetics of a corrosion reaction. Passivity is “a condition of corrosion resistance due to formation of thin surface films under oxidizing conditions with high anodic polarization.” (Jones 1996).

Previously, it was assumed that as a material underwent anodic polarization, the current densities constantly increased and the material actively corroded. Materials that demonstrate passive behavior, on the other hand, experience a significant decrease in current density as the material is polarized in the anodic direction. Rather than the straight line representation of anodic polarization used in Figures 3.4 to 3.6, an anodic polarization curve for active-passive materials is generalized in Figure 3.7. The material initially exhibits active corrosion as it is polarized. The point at which current densities decrease occurs at the critical current density, i_c , and the passivation potential, E_p (Revie 2000).

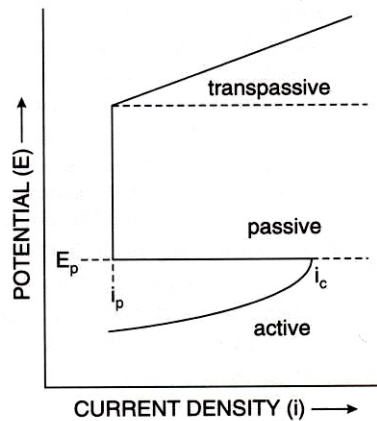


Figure 3.7: General polarization curve for an active-passive material. Current densities decrease at a specific passivation potential, and the metal becomes resistant to active corrosion. (Revie 2000)

Passivity is generally attributed to the formation of a film nanometers thick on the surface of the electrode that acts as a barrier to further oxidation of the metal. Several theories exist regarding the nature and properties of the passive film, and it is still an area of controversy among researchers (Revie 2000). It is accepted that high pH solutions aid passivation of iron based alloys (Landolt unpublished work). Typical materials that exhibit passive behavior are nickel, chromium, titanium, among others (Revie 2000). The passive behavior of stainless steels is attributed to the nickel and chromium alloying elements.

A material that forms a passive film is not guaranteed to resist all corrosion. At a sufficiently high enough potential, the passive film breaks down and the material may actively corrode again, in the transpassive region (Revie 2000). Regardless of the shape of the anodic polarization curve, corrosion of a material occurs where the anodic and cathodic curves intersect. Figure 3.8 demonstrates that the resistance of a metal to corrosion is also dependent on the cathodic reaction. Additionally, local breakdown of

passivity results in localized forms of corrosion, which are discussed further in Section 3.2.

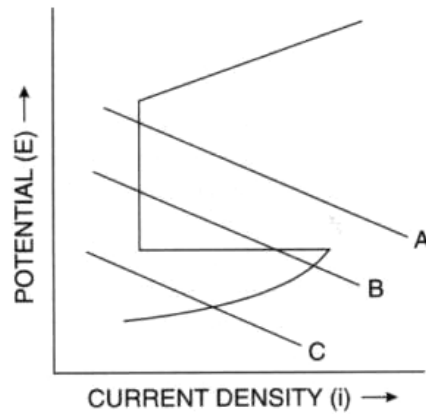


Figure 3.8: The intersection of three possible cathodic curves with the anodic curve of a passive metal. Corrosion rates are dependent on the current density at the intersection of the curves.(Revie 2000)

In Figure 3.8 three possible cathodic curves intersect the anodic curve with a passive region. In conditions where the cathodic curve intersects in the passive region of the anodic curve, such as curve A, the material is protected from corrosion. If the cathodic curve intersects in the active region, however, such as curve C, the material will actively corrode. When the cathodic curve intersects both the active and passive regions of the anodic curve, such as curve B, unstable passivity is formed, and corrosion rates fluctuate between high, active rates and low, passive rates (Revie 2000).

3.2 Corrosion mechanisms

The following section reviews several of the major corrosion mechanisms. In preference to a comprehensive discussion of all corrosion mechanisms, only the mechanisms pertinent to the GDOT steel bridge plate bearing assembly are presented.

3.2.1 General corrosion

Also known as uniform corrosion, general corrosion affects the entire exposed surface of a metal. Both the cathodic and anodic electrochemical reactions occur on the metal surface, in agreement with mixed potential theory. Due to microscopic non-homogeneities, such as grain boundaries or dislocations, the metal surface itself is divided into cathodic and anodic regions, as shown in Figure 3.9. Slight changes in the environment can induce cathodes to switch to anodes and vice versa, yielding a uniform metal dissolution along the metal surface (Singh 2008).

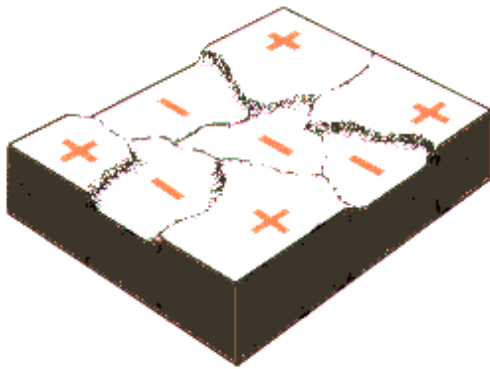


Figure 3.9: Anodes and cathodes occur on same metal surface in general corrosion. (Singh 2008).

Since the corrosion rates throughout the surface are similar and the metal loses mass uniformly along the part, Faraday's Laws relating mass loss to corrosion rates can be applied. Corrosion rate calculations from Faraday's Laws are discussed further in Section 3.3.

3.2.2 Galvanic corrosion

Electrical contact between dissimilar metals in the presence of electrolyte initiates galvanic corrosion. The potential difference between the two metals is the driving force for corrosion, and galvanic current flows between the two metals (Davis 2000). When coupled the metals polarize each other, and the most active metal becomes the anode. From mixed potential theory, shown graphically in Figure 3.10, the equilibrium potential of the couple occurs at the intersection of the total oxidation and total reduction curves, and is always in between the potentials of the uncoupled metals. Thus, the corrosion rate of the anodic metal increases, and the corrosion rate of the cathodic metal decreases (Jones 1996).

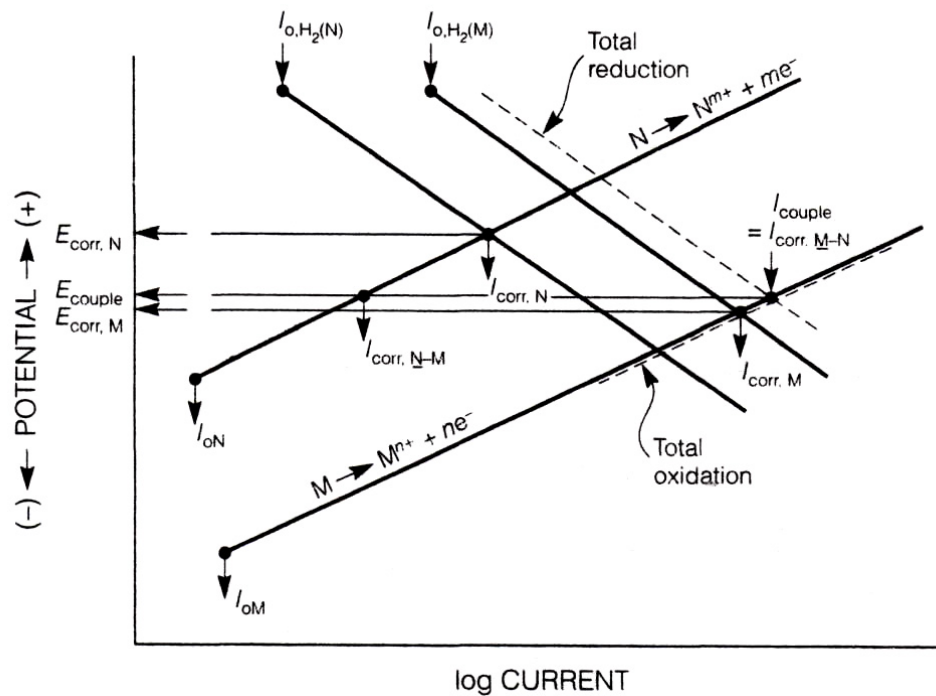


Figure 3.10: Generic Evan's diagram for galvanic corrosion. Coupled metals polarize each other, and the equilibrium potential at the intersection of the total oxidation and total reduction curves falls in between the potentials of the uncoupled metals. (Jones 1996).

Since the potential difference between the two metals is the driving force for galvanic corrosion, knowledge of the magnitude of the potential difference is necessary to determine whether galvanic corrosion will or will not occur. A comparison of the potentials of the uncoupled metals at equilibrium provides this knowledge. Keeping in mind that the equilibrium potentials of metals are dependent on environmental conditions, a galvanic series of metals can be created by measuring the potentials of several metals in a specific environment (Davis 2000). Figure 3.11 illustrates a galvanic series for typical construction materials in a seawater environment. The dark boxes in the figure correlate with active behavior for active-passive alloys. According to thermodynamic principles, metals which have a large difference in potentials in the same

environment have a high risk of developing galvanic corrosion if electrically coupled.

The potentials versus a saturated calomel reference electrode for Type 2101 and 2205

stainless steels are slightly higher than the potentials shown for stainless steel Type 316.

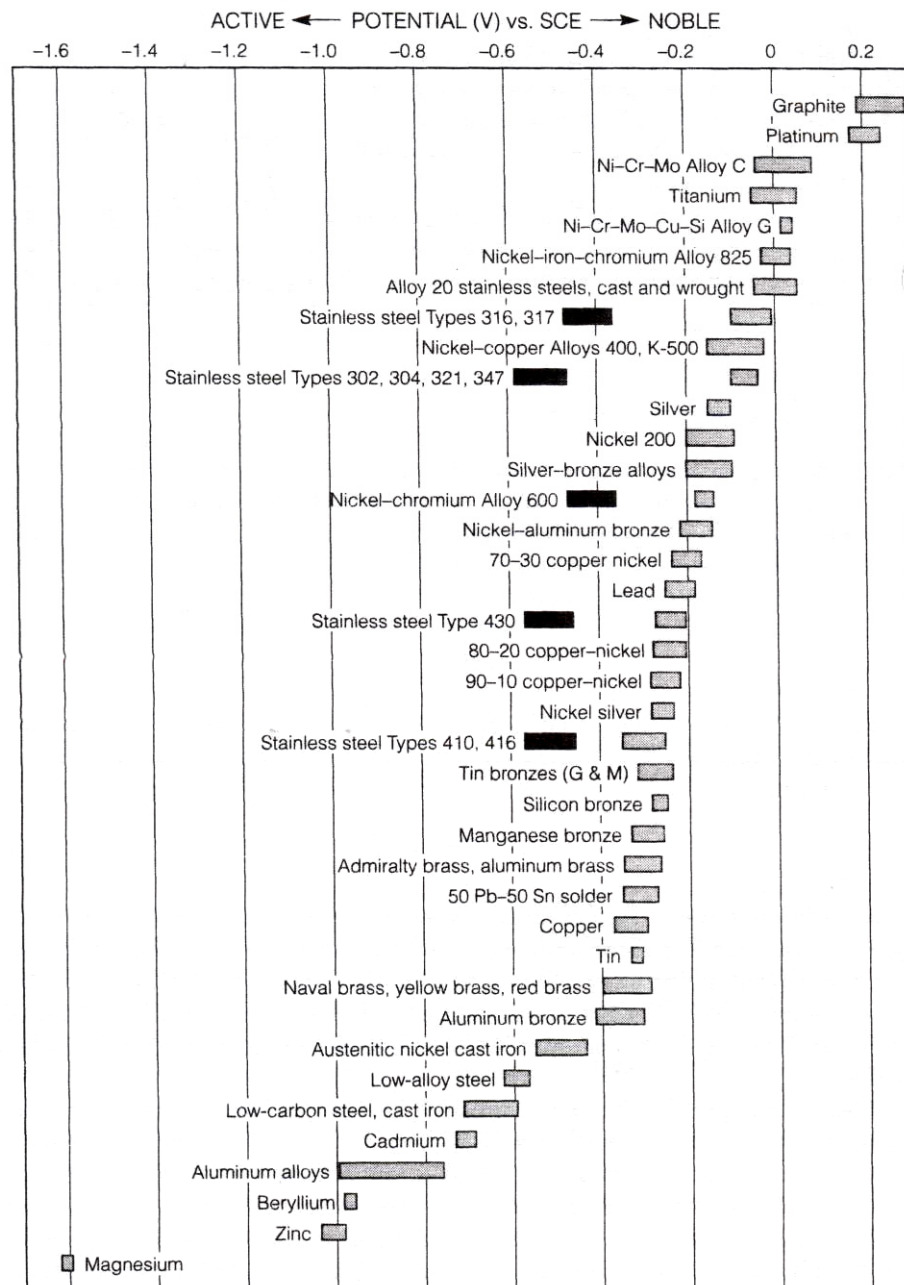


Figure 3.11: Galvanic series for seawater. According to thermodynamic principles, metals which have a large difference in potentials in the same environment have a high risk of developing galvanic corrosion if electrically coupled. Dark boxes correlate with active behavior for active-passive alloys. (Jones 1996).

A significant factor which affects the rate of galvanic corrosion is the ratio of the cathode area to the anode area. At equilibrium, the current flow at the anode and cathode is equal. When the area of the anode is decreased, the current density is increased, intensifying the corrosion at that area. Therefore a large cathode to anode area ratio creates severely accelerated corrosion on the anode (Davis 2000). On the other hand, a large anode to cathode area ratio is not detrimental because corrosion over a larger anodic surface reduces the rate of corrosion penetration (Jones 1996).

3.2.3 Concentration cell corrosion

The concentration cell corrosion mechanism is nearly the same as galvanic corrosion. Aspects of the two corrosion mechanisms that are the same are: (1) corrosion is initiated when materials at differing equilibrium potentials are electronically and ionically coupled; (2) polarization of the two materials yields an equilibrium potential in between the original uncoupled potentials; (3) the more active material becomes the anode and is preferentially corroded at an increased corrosion rate; and (4) cathode to anode area ratios affect the corrosion rate of the anode. The only difference of concentration cell corrosion from galvanic corrosion is that instead of a couple of two dissimilar metals with a potential difference, the couple exists between areas of differing potential for the same metal. Potential differences on the same material are caused by the exposure of the metal to dissimilar environments (Jones 1996).

A common example of concentration cell corrosion is the differential aeration cell. In differential aeration cells, or oxygen cells, varying concentrations of dissolved oxygen on a single metal surface creates the potential difference that drives corrosion

(Jones 1996). The electrochemical reactions at the anode and cathode of the metal then propagate the corrosion mechanism. At the cathode, the reduction of available dissolved oxygen increases the local pH, promoting greater passivity, while the oxidation of the metal at the anode produces M^+ (Landolt unpublished work). The local separation of the anode and the cathode in concentration cells allows the differential pH concentrations to build up (Landolt unpublished work). Typical places where differential aeration cells may form are illustrated in Figure 3.12.

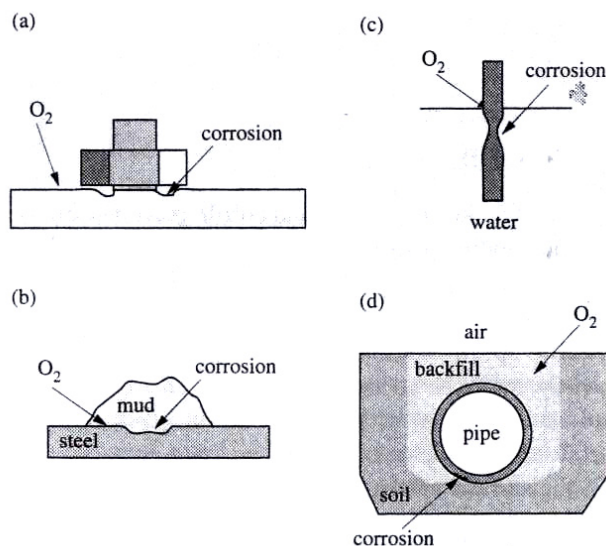


Figure 3.12: Typical locations where differential aeration cells are formed in application. (Landolt unpublished work).

3.2.4 Crevice corrosion

Concentration cells that form at localized areas on the material, such as at an opening between the material and another material, is known as crevice corrosion. The formation of the concentration cell is aided by the geometry of the crevice; small open

areas between two surfaces in which the opening width is smaller than the length of the open area creates areas of differential aeration (Jones 1996). Liquid electrolyte that is able to enter the crevice becomes trapped against the metal, because the crevice restricts the solution convection and the electrolyte does not wash out (Singh 2008). Figure 3.13 portrays a typical crevice geometry and illustrates the crevice corrosion mechanism.

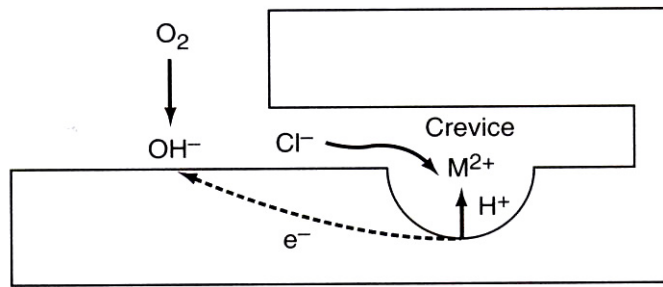


Figure 3.13: Typical crevice geometry and basic crevice corrosion mechanism. (Davis 2000)

In the shielded crevice area, the electrochemical reduction reactions deplete the dissolved oxygen, and an excess of positive metal ions collects. Halides, typically chlorides, migrate to the crevice to electrostatically neutralize the positive charge. The metal halides that form hydrolyze in water, producing hydrogen ions which lower the pH. The hydrogen and halide ions in the crevice accelerate metal dissolution, attracting more halides and increasing hydrolysis. In this manner, the propagation of crevice corrosion is autocatalytic in nature (Jones 1996). As the solution progresses to a lower pH, the metal within the crevice is the anode of the concentration cell, while outside the crevice, the oxygen rich solution on the metal surface acts as the cathode.

Passive materials may be protected from crevice corrosion, but as the metals are polarized to higher potentials, crevice corrosion initiates at a specific potential where passivity breaks down (Jones 1996). Crevice corrosion is dependent on many factors which are geometric, environmental, electrochemical, or metallurgical in nature (Davis 2000). Specifically, the variability in crevice geometry affects the individual breakdown potential for each application, and thus the initiation of crevice corrosion cannot be predicted for a particular alloy (Jones 1996). Once initiated, crevice corrosion attack is severe for passive alloys. The breakdown of the passive layer in the local area of the crevice yields a high cathode to anode ratio and corrosion penetration is intensified due to rapid metal loss in that small area (Davis 2000).

3.2.5 Pitting corrosion

Pitting corrosion is another form of localized corrosion that shares a similar corrosion mechanism as crevice corrosion. Inside actively corroding pits, oxygen is depleted and the same autocatalytic process of corrosion propagation exists as was described for crevice corrosion (Jones 1996). As with crevice corrosion, pitting corrosion is destructive because it can penetrate deeply into the metal at the anode, or pit.

Pits occur randomly along the surface of the metal, and thus, both active and passive areas exist simultaneously on the surface of the metal (Revie 2000). Generally, passive metals are more susceptible to pitting corrosion; active metals void of passive behavior typically corrode uniformly, instead. Additionally, among passive metals, some alloying elements in metals are more resistant to pitting than others. For example,

chromium and molybdenum have been found to strengthen passive layers of alloys and provide greater resistance to pitting (Revie 2000).

Several theories exist on the mechanism of pit initiation, and are still a controversial subject. The majority of pitting has been found to occur in the presence of halides, typically chloride (Revie 2000). As a metal surface is positively polarized, the negative chloride ions are electrostatically attracted and become more concentrated at the surface of the metal. Therefore, most theories attribute pit initiation to dissolution of metal halides that are formed when the passive layer is compromised (Singh 2008).

Pitting has been found to occur electrochemically when a metal reaches a critical polarization potential, E_{pit} . Above this potential, pitting initiates; below this potential existing pits may grow, but new pits do not initiate. Additionally, the potential at which existing pits repassivate is called the protection potential. Below the protection potential, pits do not grow or initiate (Jones 1996). The critical pitting potentials and protection potentials are dependent on the material, temperature, and chloride concentration.

The critical pitting potential for a particular alloy at a certain temperature and chloride concentration is typically higher than the break down potential required to initiate crevice corrosion. The geometry of the existing crevice at the metal surface provides an environment favorable to initiation of corrosion compared to pitting corrosion (Jones 1996). In crevice corrosion, the depletion of oxygen in the crevice initiates corrosion through a concentration cell effect, while pitting corrosion is initiated when passivity is broken and metal ions dissolve, under the aid of chloride attack (McCafferty 1974).

3.2.6 Stress corrosion cracking

The presence of corroding pits in a metallic member subject to tensile stresses can initiate cracking in the metal called stress corrosion cracking (Jones 1996). Stress corrosion cracking is a major concern because cracks cause brittle failure of otherwise ductile materials. Also, stress corrosion cracking affects materials in which corrosion is usually minimal in the absence of stress (Singh 2008). For a given set of environmental conditions and material composition, a threshold stress value can be found, only above which failure from cracking will occur (Revie 2000).

Once a crack has initiated, several mechanisms may be responsible for crack propagation. One theory proposes that cracks propagate as metal ions are preferentially dissolved at the crack tip; other crack propagation models follow theories of fracture mechanics (Jones 1996). A complete review of stress corrosion cracking mechanisms is omitted from this chapter, but the reader is directed to D.A. Jones' book, *Principles and Prevention of Corrosion*, for a more complete discussion.

3.2.7 Fretting corrosion

Fretting corrosion develops where movements between a metal and another solid occur when loaded (Jones 1996). As a form of mechanical and corrosive wear of a metal, fretting corrosion may be classified as either wear-oxidation or oxidation-wear. In wear-oxidation fretting, the two surfaces in contact with each other are not previously oxidized. An example of wear-oxidation fretting is an over-tightened bolt and nut which is subject to some form of mechanical vibration. As the surfaces wear on each other, small metallic particles break off, which then oxidize secondarily (Singh 2008).

In contrast, oxidation-wear fretting occurs where two previously oxidized surfaces contact each other. As the solids are subjected to movements, the oxidized layers of the solids are broken off, revealing clean material beneath. Depending on the environment, the clean metal surface may subsequently re-oxidize (Jones 1996). As shown in the schematic in Figure 3.14, the oxide film debris becomes trapped in between the solids, and functions as an abrasive agent during movement (Davis 2000).

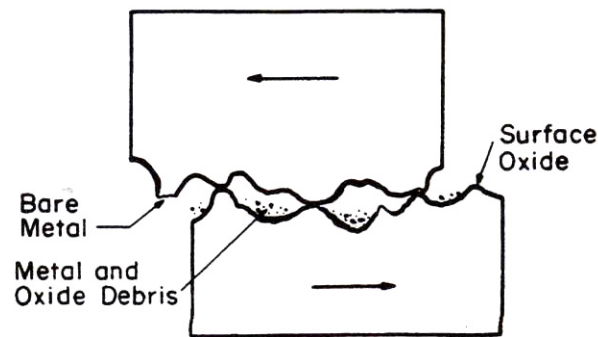


Figure 3.14: Fretting corrosion. As two metal surfaces wear against each other, oxide layers on the surface are broken and reformed. (Davis 2000).

3.3 Corrosion measurements

In this section, ways to quantify and interpret corrosion behavior are presented. The following methods are used in laboratory corrosion experiments. Specific application and results of each technique is presented in Chapter 8.

3.3.1 Corrosion potential readings

The first measurement that is useful in understanding the corrosion behavior of a material is the measurement of corrosion potential of a metal in oxidizing solution. As

discussed in Section 3.1, corrosion potential is the characteristic thermodynamic measurement of a corrosion reaction, because it indicates the free energy and equilibrium conditions of the reaction (Singh 2008).

The corrosion potential of a material cannot be measured directly, but must be measured as a potential difference with respect to a reference electrode. The most common reference electrode is the standard hydrogen electrode (SHE). A schematic representation of the SHE device is shown in Figure 3.15. The SHE establishes a zero point from which all other reference electrodes and potential measurements are based (Jones 1996). The zero point for half-cell electrode potentials is the hydrogen reduction reaction.

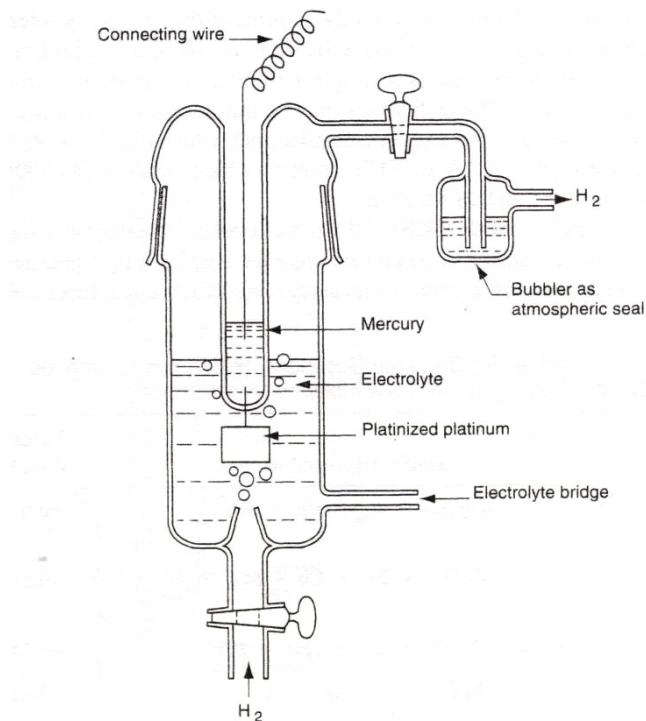


Figure 3.15: Schematic of the standard hydrogen electrode (SHE) device. The SHE establishes a zero point from which all other reference electrodes and potential measurements are based (Jones 1996).

A commonly used reference electrode in laboratory settings is the saturated calomel electrode (SCE). A schematic representation of the SCE device is shown in Figure 3.16. The SCE employs the reduction reaction of mercury in contact with a saturated potassium chloride solution. Potential differences measured with respect to the SCE are 0.241 volts more positive than those measured against the SHE (Jones 1996).

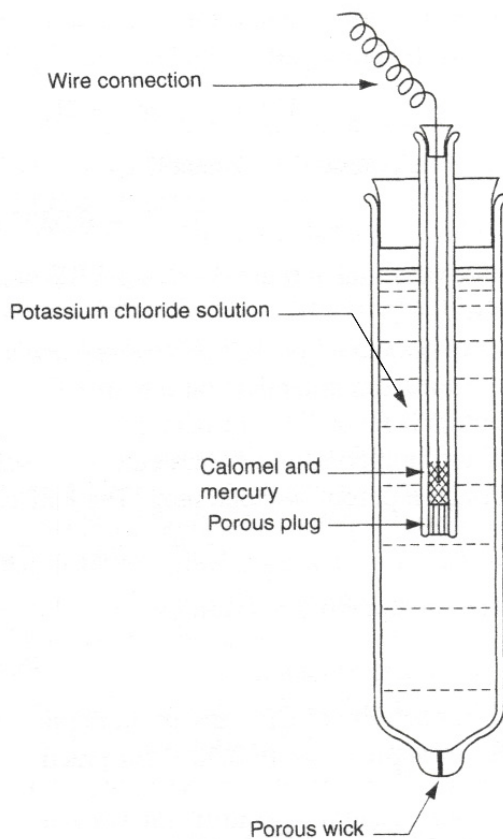


Figure 3.16: Schematic of the saturated calomel electrode (SCE) device. The SCE is commonly used in the laboratory. (Jones 1996)

Potential differences are measured by electrochemically connecting the reference electrode to the corroding metal. The electric connection is provided by wire leads and

includes a connection to a voltmeter, and the ionic connection is provided through a salt bridge between the reference and the metal. Because the half-cell potential of the reference is known, the corrosion potential of the metal is determined as the voltage generated between the two electrodes is read from the voltmeter.

3.3.2 Electrochemical polarization

Electrochemical polarization curves provide insight into the kinetics of corrosion for a particular material. To study the corrosion behavior of a material, polarization may be induced in the laboratory by externally removing or supplying electrons at the electrode surface by a potentiostat. A plot of the log of the current density versus the potential during the polarization reveals how a material will behave under real applications. For example, a steadily increasing current density with respect to potential indicates that the metal is actively corroding, while a drop in current density at a certain potential indicates the formation of a passive layer at the passivation potential, as shown in Figure 3.7.

The potential sweep applied to the metal can be either potentiostatic or potentiodynamic. In a potentiostatic sweep, the current density of the working electrode, or metal being tested, comes to a steady value before potential is forced to change. In a potentiodynamic sweep, the potential of the working electrode is continuously changed at a certain rate, regardless of the stability of the current density (Jones 1996). A potentiostatic sweep generally gives the most accurate polarization curve, but a potentiodynamic sweep is useful in the laboratory where curves can be generated and analyzed quickly.

3.3.3 Cyclic polarization

Cyclic polarization is a form of electrochemical polarization used to evaluate the pitting and protection potentials of metals. During cyclic polarization, the potential is raised into the transpassive region for the material and then reversed. The behavior of the material, determined by the current density, during the reverse sweep serves as evidence of whether pitting or localized corrosion has occurred. If the current densities for each potential are equivalent to those at the same potential on the forward scan, then the passive layer has not been affected. However, if the current densities for each potential are higher than those during the forward scan, then it is apparent that the passive layer has been compromised and localized corrosion has initiated.

Figure 3.17 illustrates a general curve generated by cyclic polarization in the presence of chlorides. The point at which the passivity is broken and local corrosion initiates in the transpassive region is the pitting potential, E_{pit} . The point where the curve of the reverse sweep returns to intersect the curve of the forward sweep is the protection potential, E_{prot} (Jones 1996). As discussed in Section 3.2, pitting is only initiated at potentials above E_{pit} , existing pits will grow at potentials in between E_{prot} and E_{pit} , and the metal is protected from pit growth and initiation at potentials below E_{prot} .

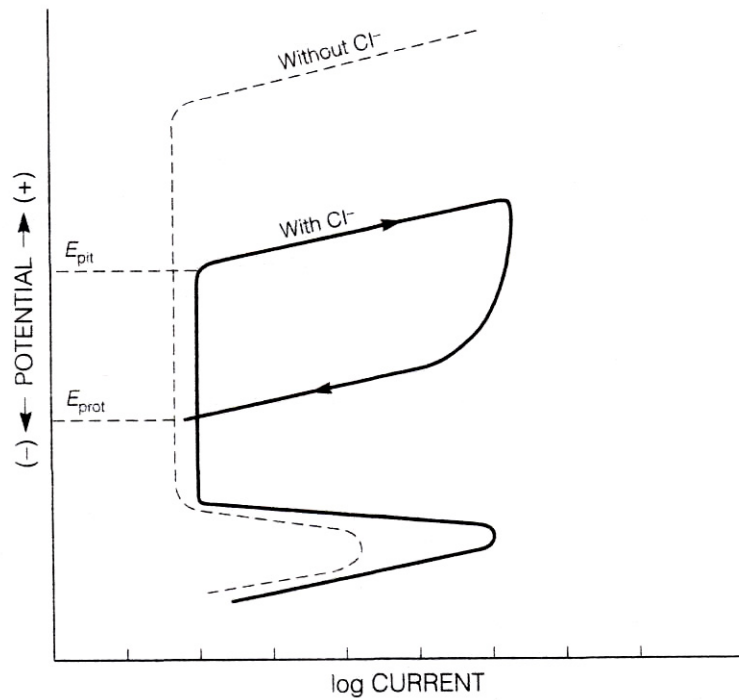


Figure 3.17: Typical cyclic polarization curve demonstrating E_{pit} , above which pitting initiates, and E_{prot} , below which the material is protected from pit growth and initiation (Jones 1996).

3.3.4 Gravimetric calculation of corrosion rate

Perhaps the simplest way to measure corrosion rate of a material is through the measure of weight loss over time. According to Faraday's Law for general or uniform corrosion, the amount of material reacting in solution is directly proportional to the electric current flowing through it (Jones 1996). The relation between weight lost, W , and corrosion rate is defined by:

$$W = \frac{A_n \cdot I \cdot t}{n_e \cdot F}$$

where A_n is the total atomic weight of the material, I is the current, t is time, n_e is the number of electrons involved in the reactions, and F is Faraday's constant (Jones 1996).

Rearranging for rate and dividing by density produces an equation for thickness lost, or

penetration. In a neater form accounting for constants and conversion factors, the corrosion rate in mils/year, or 0.001 inch per year, is

$$\text{Corrosion rate} = \frac{534 \cdot W}{D \cdot A \cdot T}$$

and the corrosion rate in mm/year is

$$\text{Corrosion rate} = \frac{87.6 \cdot W}{D \cdot A \cdot T}$$

where W is the weight change of the material in milligrams, D is the density of the material in grams/cm³, A is the area in in², and T is time in hours.

It is important to note that Faraday's Laws relating mass loss to corrosion rate only apply to calculations of uniform corrosion rates. Gravimetric calculations cannot be used to measure local corrosion rates, because crevice or pit penetration is not a function of total weight loss.

3.3.5 Polarization resistance

Polarization resistance has been proven to be inversely proportional to corrosion rate, and thus is commonly used to determine corrosion rates. The polarization resistance of a sample is the slope of the polarization curve for that sample at its origin (Jones 1996). To measure the polarization resistance of a metal, a potentiostat is used to apply overvoltages within a few millivolts of the materials' equilibrium potential and the change in overvoltage, ε , over the change in applied current, i_{app} , is measured as the overvoltage approaches zero, or

$$R_p = \left[\frac{d\varepsilon}{di_{app}} \right]_{\varepsilon \rightarrow 0} \quad (\text{Jones 1996}).$$

The polarization resistance slope is related to the current density, and thus, the corrosion rate in mpy by

$$R_p = \frac{\beta_a \cdot \beta_c}{2.3 \cdot i_{corr} \cdot (\beta_a + \beta_c)}$$

where β_a and β_c are Tafel constants, which define the linear slopes on a semi-log graph of the half-cell reactions (Jones 1996).

Thus, the corrosion rate of the metal can be calculated using appropriately selected values for Tafel constants and a plot of the overvoltages versus the current (Jones 1996). Polarization resistance is a common method of determining corrosion rates quickly in the laboratory.

CHAPTER 4: LITERATURE REVIEW

4.1 Concepts in bearing design

4.1.1 Bearing loads and movements

Bearings are designed to support superstructure loading and movement. The purpose of the bridge bearing is to transfer loads from the superstructure to the substructure, while accommodating the movement of the superstructure in relation to the supports (Lee 1994).

Bearings are subjected to both vertical and horizontal loads. Horizontal loads in the longitudinal and transverse planes originate from external sources or are induced by restrained movements at the bearing (Lee 1994). Bearing restraint exists at all bearings due to frictional effects, but in some cases bearing restraint is fundamental to the bridge design. For example, end rotations are free to occur in simply supported spans, but the redundancies in continuously supported spans limit motion at interior bents (Lee 1994). Also, restraint in the transverse horizontal direction may be provided to prevent the girders from sliding off the bearings. The moments produced by this restraint must be accounted for in the bridge and bearing design.

External horizontal loads include wind loads, traffic braking and impact loads, and earthquake loads; and vertical loads arise from the bridge dead and live loads. Generally, the vertical bridge loads are distributed among the bearings (AASHTO 2007). Overall, the distribution of the loads on the bearings is dependent on bridge members' stiffnesses and the range of fabrication and construction inaccuracies (AASHTO 2007).

Superstructure movements relative to the substructure are three dimensional translational and rotational movements. The movements are caused by loading, deformation, and displacement conditions, and may be internal or external to the bridge. Internal sources of movement arise from the bridge material's response to the environment and loading. Bridges physically deform in response to: variations in temperature and humidity; material tendencies of creep, shrinkage, and fatigue; axial and flexural strains due to bridge loads or prestressing; and dynamic traffic or braking loads, among others (Lee 1994). External sources of movement include displacements caused by: earthquakes; impact loads; foundation settlements; and the construction procedure and tolerances (Lee 1994). In bearing design rotational movement about two horizontal axes and a vertical axis must be addressed in addition to the longitudinal and transverse movements (AASHTO 2007).

To design an appropriate bearing system, one must predict the expected loading and movement at the bearings. Several aspects affect the estimation of these design factors: 1) for curved or skewed bridges, translational movement affects both the longitudinal and transverse directions, 2) misalignments during installation causes initial rotations that may exceed calculated rotations due to loading, 3) bearing restraints induce forces, 4) the “worst-case” combination of loads and movements must be used for bearing design, considering both initial and long-term conditions (AASHTO 2007). Specific load calculations for bearing design are determined according to the limit states and load factors prescribed in Section 3 of AASTHO LRFD Bridge Design Specifications.

Uniform thermal changes along the cross section of a girder induce translational movement, which can be calculated using the equations in Section 3 of the AASHTO specifications. However, temperature usually varies differentially through the cross section. These temperature gradients induce thermal bending of the girders, which in turn produces rotational movement in addition to translational movement (Lee 1994). Calculations to account for thermal gradients are provided in Section 4 of the AASHTO specifications.

Typically, factored displacements and rotations are used for bearing design. In some cases a tolerance as high as 0.005 radians is added to the calculated expected rotations to account for inaccuracies in construction, and an additional 0.005 radians is added to account for other uncertainties (AASHTO 2007). Improperly designed bearings can result in increased stresses in bridge members, damaging the structure. According to AASHTO specifications, “[n]o damage due to ... bearing movement shall be permitted at the service limit state, and no irreparable damage shall occur at the strength limit or extreme event states.” (AASHTO 2007).

Movements due to creep and shrinkage and elastic shortening due to prestressing are not addressed in this chapter because these issues apply primarily to concrete girder bridges, while the scope of this research focuses on steel girder bridges.

4.1.2 Bearing selection

The bearing system for a particular bridge design is selected from the types of bearing available for use that satisfy the design considerations for that bridge. While AASHTO provides guidance on design considerations for bearings, in-depth resources on

bridge bearing design are not readily available. David Lee provides an excellent discussion of bridge bearing types and specific design considerations in his book, *Bridge Bearings and Expansion Joints* (1994).

4.1.2.1 Bearing types

In this section, the examination of bearing types is limited to simple or continuous span bearings at concrete supports. A graphic summary of the bearing types presented in this section is shown in Figure 4.1 (Lee 1994).

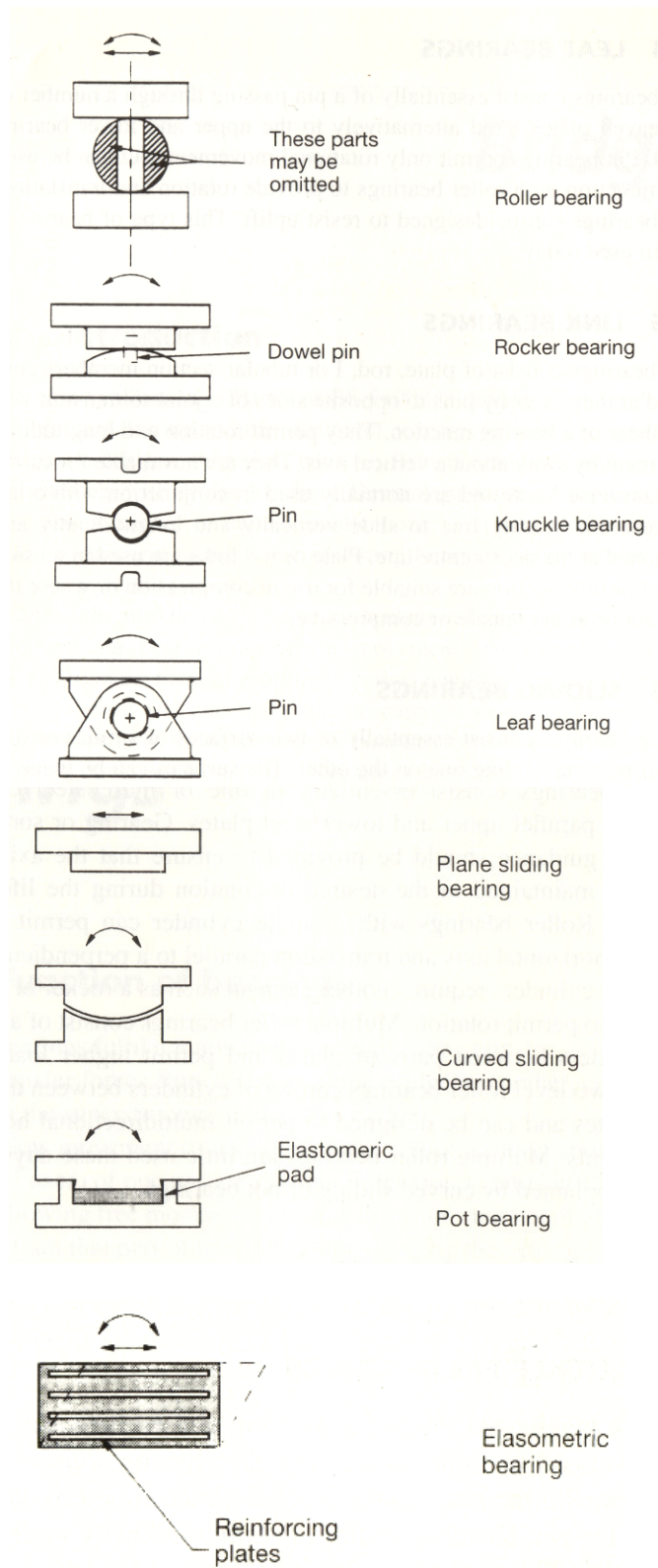


Figure 4.1: Graphic summary of bearing types. (Lee 1994).

Roller bearings that are comprised of one or more steel cylinders sandwiched between horizontal upper and lower steel plates allow longitudinal translation and rotation about the transverse horizontal axis. Guides are provided to maintain the positioning of the roller for its entire service life (Lee 1994). The curved surfaces at the bearing must have sufficient hardness to withstand deformation due to high bearing loads. Consequently, a single roller of a high tensile strength alloy may be used, or the load may be distributed among multiple mild steel rollers. In the application of multiple rollers, another bearing element, such as a knuckle or rocker, must be provided to accommodate for rotations (Lee 1994). For this reason, multiple roller bearings are no longer commonly used. Important design considerations specific to roller bearings are the selection of the radius and its effect on the stability of the bearing, and the mechanism employed to ensure proper alignment of the roller (Lee 1994).

In rocker bearings a curved surface is in contact with another surface that is either curved or flat. This type of bearing allows rotational but not translational movement (Lee 1994). For this reason, this bearing type is used at the fixed end of a span. A cylindrical curved surface permits rotation about the transverse horizontal axis, while a spherical curved surface enables rotation about multiple horizontal axes (Lee 1994). Similar to roller bearings, the curved surface of the rocker bearing must be hard enough to withstand deformation under bearing loads. A mechanism to prevent the horizontal movement of the two surfaces relative to each other is provided usually in the form of a dowel, or bolt connecting the two surfaces (Lee 1994).

In knuckle bearings an encapsulated pin provides rotational motion as the curved surfaces of the upper and lower support slide about the transverse axis. Translational

movement is restrained (Lee 1994). Knuckle bearings are difficult to maintain, and sliding surfaces tend to corrode, restraining all movement. Thus, knuckle bearings are seldom used anymore (Lee 1994).

Leaf bearings are a type of knuckle bearing where the pin passes through multiple plates which are alternately fixed to upper and lower steel plates. The same difficulties are present in leaf bearing designs as in traditional knuckle bearing design, and are also rarely used (Lee 1994).

Pot bearings are a type of bearing that are used in cases where the bearing is required to support large vertical load and a high degree of rotation. At the base of the bearing, a hollow metal cylinder contains an unreinforced elastomeric, neoprene pad. A piston fixed to the upper bearing plate transfers load from the bridge through the pad, which allows multidirectional rotation in the process (Lee 1994). The pot bearing itself does not allow translational motion. Present day pot bearings have replaced a heavy steel rocker bearing design and are typically used in long span or curved steel girder bridges.

Sliding bearings consist of two surfaces that are meant to slide against one another. The surfaces may be of either similar or dissimilar metals and may be either flat or curved. Flat surfaces allow translational but not rotational movements, while curved surfaces allow rotational but not translational movement (Lee 1994). Traditionally, one of the curved surfaces is a lubricated bronze plate. According to Lee, the metal plate sliding bearings are

“...very simple and cheap, but even when freshly and evenly lubricated the coefficient of friction is of the order of 20%. It was also found that, even with regular maintenance, the coefficient of friction increased to unacceptable limits. However, at a time when it appeared that sliding bearings were to become a historical curiosity, they were revitalized by the introduction of polytetrafluoroethylene (PTFE).” (Lee 1994).

PTFE is more commonly known as Teflon, and is well known for its chemical resistance and low coefficient of friction (AASHTO 2007). The application of PTFE to sliding mating surfaces improves the performance of sliding bearings. It is important, however, to protect the PTFE surface from debris, which could scratch the surface and increase the friction in the bearing. Equally important is that the PTFE is bonded to a corrosion resistant and hard metal plate, to prevent wearing of the Teflon surface. Such wearing would also increase the friction of the bearing. (Lee 1994). Thus, frequent maintenance is required for sliding bearings with or without the use of PTFE.

The final type of bearing is the elastomeric bearing. An elastomeric bearing is made of either natural or synthetic rubber that is stiff enough to support vertical loads and flexible enough to sustain translational and rotational movements. The bearing provides for multidirectional translation in the shearing capacity of the rubber as the surfaces of the rubber are able to move relative to each other. Rotational capacity is provided as the material exhibits a varying compressive strain across the cross section (Lee 1994). Stiffness is increased in some elastomeric bearings by incorporating steel plates within the rubber. Elastomeric bearings made with holes, to allow for anchorage and alignment, should be designed to be thicker, because the holes reduce the stiffness of the bearing and the ultimate load capacity (Lee 1994). An advantage of elastomeric bearings is that they require little maintenance because there are no mating surfaces to get filled with debris and no exposed metal to corrode (Lee 1994).

4.1.2.2 Other design considerations

When selecting a bearing system for a bridge, one must consider that the types of bearing elements discussed in the previous section can be combined to provide a mechanism for all necessary bridge movements. In addition to designing for bearing loads and movements, other factors can affect the selection of bearing type for a particular application.

First, the design life of the bearing may be an important factor in the selection of bearing type. Metallic bearings require constant maintenance to ensure proper functioning and a longer lifespan (Lee 1994). On the other hand, elastomeric bearings requiring no maintenance claim to have an equally long, or longer lifespan, as traditional bearings. While the lifetime of the alternate materials are promising, these claims have not yet been sufficiently proven in the field (Lee 1994). All bridge bearings suffer from material degradation eventually. To avoid premature bearing failure, Lee advises that “[b]earings should be detailed without crevices and recesses that can trap moisture and dirt. It is important to ensure that dissimilar materials that can give rise to corrosive currents are not used together” (1994).

Second, bearings should be selected that can be accurately installed in the available space. Accurate location of the bearings is important to avoid eccentric loadings or movements that were not accounted for in the design calculations (Lee 1994).

Third, the restraint provided by the bearing must be addressed. A bearing system may be selected according to the predicted frictional properties of the bearing. In many applications bearing restraints are necessary to prevent total or partial translational

movement. For example, the use of bolting or bedding adhesive may be required to prevent slipping of the bearing.

The use of “hold-down bolts”, or anchor bolts, is a common practice to provide stability in the transverse horizontal direction (Lee 1994). Over-tightening of the bolts should be avoided to prevent excessive compressive stresses from being introduced into the bearing. (Lee 1994). Also, “[s]ince bearing replacement may be required during the life of a structure, the provision of a restraint (e.g. dowels) through the bearings may cause difficulties, and an alternative location of the restraints should be considered.” (Lee 1994). A bearing system should be selected that can provide the necessary restraints in a convenient manner. In general, the base plate of most bearing types is anchored to the concrete pier cap, and thus the problem of anchor bolt corrosion is universal to all these bearings.

4.1.3 Bearing and anchor bolt materials

The following section provides an investigation into the compositions and properties of the metals typically used in metallic bearings. Table 4.1 and Table 4.2 show the material composition and mechanical properties of materials in use or considered for use in sliding plate bearings in Georgia. Cells in the table in which “...” appears indicates that there are no requirements for that category; cells in which “xx” appears indicates that the category does not apply to the material. The material properties of the structural carbon steel (CS) conform to ASTM A709: “Standard Specification for Structural Steel for Bridges”, and the material properties of the candidate stainless steel (SS) alloys conform to ASTM 276: “Standard Specification for Stainless Steel Bars and Shapes”.

Table 4.1: Material composition of steel alloys used in bearings (ASTM 2006; ASTM 2007).

Steel Designation	Material composition in %								
	C	Mn	P	S	Si	Cr	Ni	Mo	N
CS: Grade 36	0.26	...	0.04	0.05	0.40	xx	xx	xx	xx
SS: 304	0.08	2.00	0.045	0.030	1.00	18.0-20.0	8.0-11.0
SS: 316	0.08	2.00	0.045	0.030	1.00	16.0-18.0	10.0-14.0	2.00-3.00	...
SS: 2101	0.040	4.0-6.0	0.040	0.030	1.00	21.0-22.0	1.35-1.70	0.10-0.80	0.20-0.25
SS: 2205	0.030	2.00	0.030	0.020	1.00	22.0-23.0	4.5-6.5	3.0-3.5	0.14-0.20

Table 4.2: Mechanical properties of steel alloys used in bearings (ASTM 2006; ASTM 2007).

Steel Designation	Mechanical properties			
	Yield Strength, ksi	Tensile Strength, ksi	Elongation, %	Brinell Hardness number
CS: Grade 36	36	58-80	23	...
SS: 304	30	75	40	...
SS: 316	30	75	40	...
SS: 2101	65	94	30	290
SS: 2205	65	95	25	290

According to officials at GDOT, structural carbon steel is used for the base and sole bearing plates and was used for anchor bolts in construction prior to 1990 (Duvall et al. 2007). Currently, austenitic Type 304 stainless steel is specified by the Georgia Department of Transportation Bridge and Structures Design Policy Manual for use as anchor bolts (2007). This specification for anchor bolts was revised in the early 1990s, because stainless steel is known to be more corrosion resistant (Duvall et al. 2007). The mechanical properties of stainless steels have been found to be acceptable for anchor bolt application by GDOT.

Stainless steels are divided into categories by compositional type. Austenitic stainless steels are the most common, containing both chromium and nickel alloying elements in quantities that preserve the non-magnetic austenitic phase of the steel (SSINA 2005). Type 304 and Type 316 stainless steels are both austenitic stainless steels. Chromium is the main alloying element in the magnetic ferritic stainless steels, whose carbon content is low (SSINA 2005). Austenitic-ferritic grades of stainless steels, or duplex stainless steels, combine properties of both austenitic and ferritic grades, containing high amounts of both chromium and nickel. Duplex stainless steels are highly corrosion resistant and stronger than either austenitic or ferritic grades alone (SSINA 2005). Type 2101 and Type 2205 stainless steels are both duplex stainless steels. The last grade of stainless steels is martensitic stainless steel. Martensitic stainless steels are magnetic alloys that contain moderate to low levels of chromium, a moderate level of carbon, and a very low quantity of nickel (SSINA 2005). In general, martensitic stainless steels have a higher strength than austenitic stainless steels, but a lower toughness. Also, due to the lower levels of chromium in the martensitic stainless steel, it is more susceptible to corrosion in the presence of chlorides and low pH compared to austenitic or duplex grades of stainless steel. The stainless steel types included in Tables 4.1 and 4.2 are candidate alloys to be considered for anchor bolt use.

The metal specified for the self-lubricating plate in a Georgia plate bearing is bronze conforming to the ASTM B 22, Alloy UNS 91100 standard (GDOT 2007). According to bearing manufacturers, bronze lube plates are impressed with a mastic lubricant, which consists of graphite, a mix of metal oxides, and a binder (Dabkowski 2007) This lubricant is compressed into recesses and grooves in the bearing plate under

hydraulic pressure; the target-like recesses in the plate are approximately $\frac{1}{8}$ inch deep and cover 25 to 30 percent of the plate surface (Dabkowski 2007). The plate and lubricant is designed to survive the lifespan of the bearing.

4.2 Corrosion of bridge bearings

The following two sections provide a brief overview of the literature concerning corrosion of anchor bolt materials separately in the two environments to which concrete anchorages are exposed. The final section explores the combination of the environments, which is the realistic environment for anchor bolt application, and demonstrates the need for research in this area.

4.2.1 Steels embedded in concrete

4.2.1.1 Carbon steel reinforcements

The corrosion of carbon steel in concrete is an important issue concerning the durability of reinforced concrete structures and is well researched and documented phenomenon. In general, carbon steel is protected from corrosion when it is embedded in concrete because the high alkalinity of the concrete pore solution promotes steel passivation. The passive layer on the steel surface is broken by excess chloride ingress or carbonation of the concrete, which lowers the environmental pH. Once the passive layer is broken, corrosion of the reinforcing steel propagates according to the mechanisms discussed in Chapter 3. A detailed account of the corrosion of carbon reinforcing steel in concrete can be found in a number of textbooks, journal articles, and reports (ACI 2001;

Berke et al. 1993; Bohni 2005; Broomfield 2007; Hausmann 1967; Mehta and Monteiro 2006). Additionally, a significant quantity of research has been conducted concerning solely the initiation of corrosion, such as the chloride threshold level before passivity is broken, or the rate of concrete carbonation (Alonso et al. 2000; Glass and Buenfeld 1997; Gonzalez and Andrade 1982; Papadakis et al. 1991).

4.2.1.2 Stainless steel reinforcements

Due to the high number of incidences of carbon steel reinforcing bar corrosion, interest was generated in the use of stainless steel for concrete reinforcement. Therefore, numerous studies have been conducted on the corrosion behavior of stainless steels embedded in concrete. In general, it has been proven that the corrosion resistances of austenitic and duplex stainless steel grades are superior to that of carbon steel embedded in concrete in the presence of chlorides (Bertolini et al. 1996; Castro et al. 2003; Garcia-Alonso et al. 2007; Gu et al. 1996; Hartt et al. 2007).

4.2.1.3 Galvanic couplings of different steels in concrete

Since stainless steel reinforcements were introduced into reinforced concrete design, concern has arisen regarding the possibility of accelerated corrosion due to galvanic effects between the stainless and carbon steel reinforcements. According to theory presented in Chapter 3, both carbon and stainless steels are passivated in the alkaline concrete environment; thus, no significant potential difference exists between the two to thermodynamically trigger corrosion.

The results of several studies confirm that the corrosion rates of steel in concrete are not increased when passive stainless steel is electrically coupled with passive carbon steel (Abreu et al. 2002; Bertolini and Pedferri 2002; Qian et al. 2006). Additionally, when carbon steel is actively corroding in concrete, the galvanic effect of passive stainless steel bars coupled to the active carbon steel bars is not noticeably greater than the effect of passive carbon steel bars coupled to active carbon steel (Bertolini and Pedferri 2002; Qian et al. 2006). Thus, it can be concluded that “no significant risk of galvanic corrosion exists when carbon steel and stainless steel are electrically coupled in reinforced concrete structures.” (Abreu et al. 2002).

4.2.2 Bearing materials in atmospheric conditions

4.2.2.1 Corrosion of uncoupled steels

Carbon steel is known to corrode in general atmospheric conditions unless protected. For bridges and bearings, the traditional method of protection is by painting all exposed surfaces.

Stainless steel corrosion generally does not occur in normal atmospheric conditions, but localized corrosive attack may initiate depending on specific environmental conditions. For example, in the presence of chlorides, stainless steels may experience crevice or pitting corrosion. In one study, Johns and Shemwell explored the susceptibility of several stainless steel alloys to crevice corrosion when used as a fastener (Johns and Shemwell 1997). Crevice corrosion initiation is highly dependent on the crevice geometry, and thus specific investigations into this mechanism are not

particularly useful. However, a case can be made that the initiation of pitting corrosion can be measured as a critical pitting potential for each individual material and is a practical method for predicting the susceptibility of the material to pitting corrosion (Leckie 1970). Environmental factors that affect the pitting potential of a material are the temperature, chloride concentration, competitive anion concentrations, and the pH of the conductive solution (Frankel 1998; Leckie and Uhlig 1966).

4.2.2.2 Galvanic couplings of different materials

The mechanism of galvanic corrosion that was presented in Chapter 3 applies to cases in which carbon steel and stainless steels are in electrical contact in normal atmospheric conditions. A galvanic series for a typical marine environment shows that the potential for stainless steel is more noble than the potential for carbon steel, creating a thermodynamic drive for preferential corrosion of the carbon steel (Jones 1996). Similarly, most bronze alloys also have higher potentials than carbon steel (Jones 1996). Accordingly, the AISC Steel Construction Manual reports that the use of an austenitic stainless steel fastener on either carbon steel or bronze base materials will increase the corrosion rate of the base material (AISC 2005).

4.2.3 Corrosion behavior of anchorages in concrete

While an understanding of the corrosion behavior of anchor bolt materials both embedded in concrete and in atmospheric conditions is important, the environmental conditions cannot be addressed separately. As discussed in Chapter 3, the variation in

environmental conditions along a material can initiate corrosion, as well. This corrosion behavior of concrete anchorages is not widely studied.

In one study, Type 316 stainless steel rods were partially embedded in concrete specimens which were exposed to marine conditions (Flint and Cox 1988). Two exposure conditions were employed – full immersion and tidal immersion for up to twelve and a half years. The results of this study showed that the austenitic Type 316 stainless steel was remarkably resistant to corrosion, even at the interface where the rod protruded from the concrete block (Flint and Cox 1988). However, because this test stands alone, there is no repeatable evidence or corresponding studies with other candidate alloys to confirm the results.

CHAPTER 5: GEORGIA STATEWIDE CONDITION ASSESSMENT

5.1 Inspection report survey process

Access to the inspection reports for all state owned steel girder bridges were provided to the researcher by the Georgia Department of Transportation. Pertinent information queried from the inspection report database included the bridge serial and location code numbers, superstructure evaluation notes, year constructed, and superstructure condition code. The number of inspection reports reviewed was narrowed down by maintenance item request number. Only the inspection reports of bridges with a superstructure maintenance item request number were reviewed by the researcher, since corrosion of bearings falls under the superstructure maintenance category. Additionally, the dates at which the maintenance item was submitted and at which the request was completed was recorded. The earliest report with a superstructure maintenance item request was dated 1984.

In summary, a query of the inspection report database supplied the researcher with a list of state owned steel girder bridges in Georgia in which bearing and anchor bolt corrosion possibly existed. A thorough review of all the inspection reports from this list, covering 1984 to present day, provided the data presented in this chapter. The researcher read the superstructure evaluation notes to find reports indicative of bearing and anchor bolt corrosion.

In addition to specific reports of anchor bolt corrosion, reports of loose, pushed up, sheared off, or missing anchor bolts and reports of bearing corrosion implicitly denoted anchor bolt corrosion, as well. For example, loose, sheared, and missing anchor

bolts are symptoms of anchor bolt diameter reduction by corrosion losses. Anchor bolts that are pushed up imply that corrosion products have built up inside the bearing plates, forcing the bolt upwards. Considering these assumptions, a survey of the inspection reports allowed the researcher to quantify the extent of anchor bolt corrosion in Georgia.

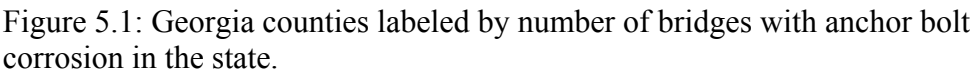
5.2 Extent of anchor bolt corrosion in Georgia

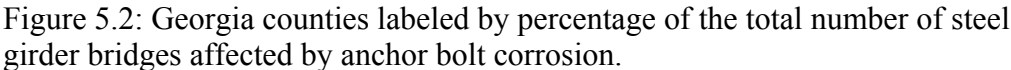
The query of the inspection report database revealed that there are 1500 steel girder bridges in Georgia. From the ensuing assessment of the inspection reports, 411 steel girder bridges, or 27% of the bridges, were judged to be experiencing anchor bolt corrosion. All of the bridges with reported anchor bolt corrosion were built before stainless steel anchor bolts were used in steel girder bridge bearings in Georgia, thus all reported anchor bolt corrosion pertains to carbon steel bolts. Possible trends relating anchor bolt corrosion to environmental conditions were examined by grouping bridges with anchor bolt corrosion by county, by region and by span type.

5.2.1 Bridges with anchor bolt corrosion grouped by county

Figures 5.1 and 5.2 illustrate the distribution of bridges experiencing anchor bolt corrosion throughout the state by county. In Figure 5.1 each county in the state is labeled with the number of bridges with corroding anchor bolts in that county. Counties with no labels do not contain any bridges with corroding anchor bolts. Subsequently, the percentages of the total number of steel girder bridges in each county that anchor bolt corrosion affects is shown by the county labels in Figure 5.2.

Counties in which a relatively high occurrence of anchor bolt corrosion was observed are highlighted. Counties in which the number of bridges with anchor bolt corrosion exceeded 10 are highlighted with yellow, whereas counties in which the percentage of bridges affected by anchor bolt corrosion exceeded 30% are highlighted with blue. Finally, counties in which the number of anchor bolt corrosion incidence exceeded 10 and the percentage exceeds 30% are highlighted in green.





From Figures 5.1 and 5.2 it is observed that anchor bolt corrosion occurs throughout the whole state. Areas of a high number and a high percentage of anchor bolt corrosion incidences, highlighted in green, were further examined for environmental or regional trends.

Four of the eight counties highlighted green correspond to metropolitan areas. The areas are Macon in Bibb County, Columbus in Muscogee County, Savannah in Chatham County, and Athens in Clarke County. In contrast, the counties within the metropolitan area of Atlanta, including Fulton, DeKalb, Gwinnett, Clayton, Douglas, and Cobb counties, do not have a high percentage of bridges with anchor bolt corrosion. Assuming that bridges in Atlanta are inspected and maintained the same way as bridges in other metropolitan areas, it cannot be concluded that an increased percentage of steel girder bridges in an urban environments develop anchor bolt corrosion.

The other four counties that are highlighted in green are Bartow, Forsyth, Hall, and Franklin counties. These counties are not densely populated, but are all geographically situated in the northern half of the state. A preliminary hypothesis may predict that a greater percentage of bridges located in the northern half of the state experience anchor bolt corrosion due to the effect that deicing chemicals have on the bearing environment. However, Figure 5.2 shows that counties in the southern half of Georgia, where chemical deicing agents are not used, experience similar amounts of anchor bolt corrosion. Therefore, it can be concluded from Figure 5.2 that the occurrence of anchor bolt corrosion is not proportional to the use of chemical deicers.

5.2.2 Bridges grouped by region

While grouping bridges with anchor bolt corrosion by county provided an illustration of the distribution of anchor bolt corrosion throughout the state, it could not provide conclusive evidence that anchor bolt corrosion could be related to certain environmental conditions. In the following sections the extent of anchor bolt corrosion is examined according to environmental regions to clearly investigate the effect of environment on the occurrence of anchor bolt corrosion. Regions were chosen that are either geographic or demographic in nature.

5.2.2.1 Geographic regions

The mutually exclusive geographic regions chosen were northern, southern, and coastal Georgia. In Figure 5.3 the three regions are separated by color; northern Georgia is in blue, southern Georgia in red, and coastal Georgia in green.

Differentiating northern Georgia from the other two regions is the use of chemical deicing agents on bridges. Chloride ions from the deicers, carried to the bearing by moisture leaking through deck joints, are aggressive agents known to initiate and accelerate corrosion. According to Ben Rabun, the previous State Bridge Maintenance Engineer, chemical deicers are used in GDOT Districts 1, 6, and 7, and in the northern counties of District 2. Thus, the northern Georgia region is loosely defined by Interstate 20, which passes through the southern edge of the Districts named.

Bridges in coastal Georgia are exposed to a constant moist environment, due to the high humidity in the region, and bridges spanning sea water may also have bearings

exposed to chloride ions. These conditions are favorable to the initiation and propagation of corrosion. Interstate 95 was selected as a simple boundary for the coastal region.

Unlike the northern and coastal Georgia regions, bridges in the southern Georgia region are not exposed to aggressively corrosive agents like chlorides. This region, south of Interstate 20 and west of Interstate 95, is subjected to higher temperatures year round, which may increase corrosion rates.

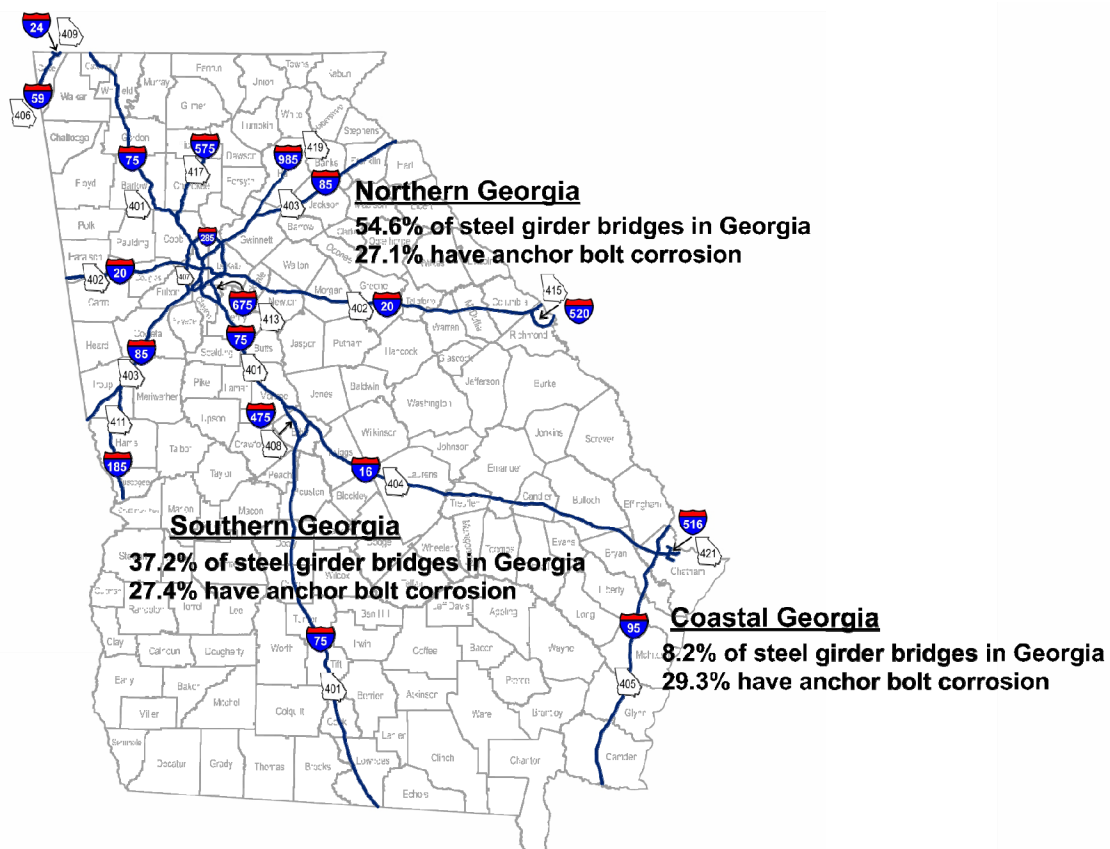


Figure 5.3: Three geographic regions in Georgia with different environmental conditions, percentage of the total number of steel girder bridges in Georgia in each region, and percentage of bridges with anchor bolt corrosion in each region.

Figure 5.3 shows the division of the three geographic regions along with the percentage of the total number steel girder bridges in Georgia contained in each region and the percentage of bridges with anchor bolt corrosion in each region. Despite the differences in environmental conditions in each region, Figure 5.3 shows that approximately 30% of the bridges in each region experienced anchor bolt corrosion. Since the percentage of bridges with anchor bolt corrosion in each region is nearly the same, it can be concluded that the differences in the geographic environments in Georgia do not significantly affect on the occurrence of anchor bolt corrosion.

5.2.2.2 Demographic regions

The demographic regions explored were metropolitan areas versus rural areas. Metropolitan areas were defined by the researcher as regions in which the population density was greater than or equal to 2,500 people per square mile. In these regions of higher population density, the daily traffic on the bridges is higher, subjecting the bridge and its bearings to increased fatigue loading. Also, the bridges in urban regions are environmentally exposed to a greater variety and quantity of pollutants, which may affect the corrosion process. By exploring the percentages of bridges with anchor bolt corrosion in metropolitan and rural regions, the effects of the urban environment on occurrence of anchor bolt corrosion were observed.

Table 5.1 shows that less than half of all the steel girder bridges in Georgia are located in metropolitan areas. Despite the number of bridges in each region, however, Table 5.1 also shows that nearly the same percentage of bridges in metropolitan and rural regions were found to experience anchor bolt corrosion. In both regions approximately 27% of the bridges exhibited anchor bolt corrosion – similar to the percentages of bridges

with anchor bolt corrosion in the geographic regions and the percentage calculated for the entire state. Therefore, it can be concluded that the differences in the environmental conditions throughout the state of Georgia do not affect the occurrence of anchor bolt corrosion in steel girder bridges.

Table 5.1: Percentage of the total number of steel girder bridges in Georgia in metropolitan and rural regions, and percentage of bridges with anchor bolt corrosion in each region.

Percentages	<u>Regional Areas</u>	
	Metro	Rural
% of steel girder bridges	37.1%	62.9%
% with anchor bolt corrosion	26.9%	27.7%

5.2.3 *Bridges grouped by span type*

The span types designated by the researcher were Interstate bridges, Interstate underpasses, or other spans. Bridges which are a part of the Interstate road system, or Interstate bridges, may span other roads as overpasses or may span water or lowlands. Interstate underpasses are bridges that carry other roads over the Interstate. Any bridges which are not a part of the Interstate system and do not span any Interstate roads fall under the classification of other spans. Other spans include bridges that span other roads, water, or low land. In general, Interstate bridges are subjected to heavier loads and more traffic compared to Interstate underpasses and other spans which are subjected to local traffic conditions.

In Table 5.2, the percentage of the total number of steel girder bridges for each span type is listed along with the percentage of bridges of each span type that are experiencing anchor bolt corrosion. From Table 5.2 it can be seen that slightly over one

quarter of the steel girder bridges in Georgia are part of Interstate roads, while over half of the steel girder bridges in Georgia are bridges that are not related to the Interstate system. Of those bridges away from Interstate traffic, approximately one quarter have reported anchor bolt corrosion, while reported anchor bolt corrosion for Interstate bridges approaches one third. The percentage of Interstate underpasses with anchor bolt corrosion falls in between one quarter and one third. These percentages suggest that the occurrence of anchor bolt corrosion may be related to loading conditions of the bridge.

Table 5.2: Percentage of the total number of steel girder bridges in Georgia that are Interstate bridges, Interstate underpasses, and other spans, and percentage of bridges of each span type with anchor bolt corrosion.

Percentages	Bridge Type		
	Interstate bridge	Interstate underpass	Other
% of steel girder bridges	26.5%	21.2%	52.3%
% with anchor bolt corrosion	32.7%	27.4%	24.7%

5.3 Bridge age statistics

To further assess the condition of anchor bolt corrosion in Georgia, the ages of the bridges with anchor bolt corrosion were examined. The age of each bridge at the time when anchor bolt corrosion was first reported was collected and a histogram was created to present the data, as shown in Figure 5.4. Each bar in the chart on the horizontal axis represents a ten year age range. The percentage of bridges with anchor bolt corrosion whose ages fit within a specific ten year age range is read from the vertical axis. The ages of the bridges are not representative of present day ages, but rather of the individual bridge ages when anchor bolt corrosion was first reported for each bridge.

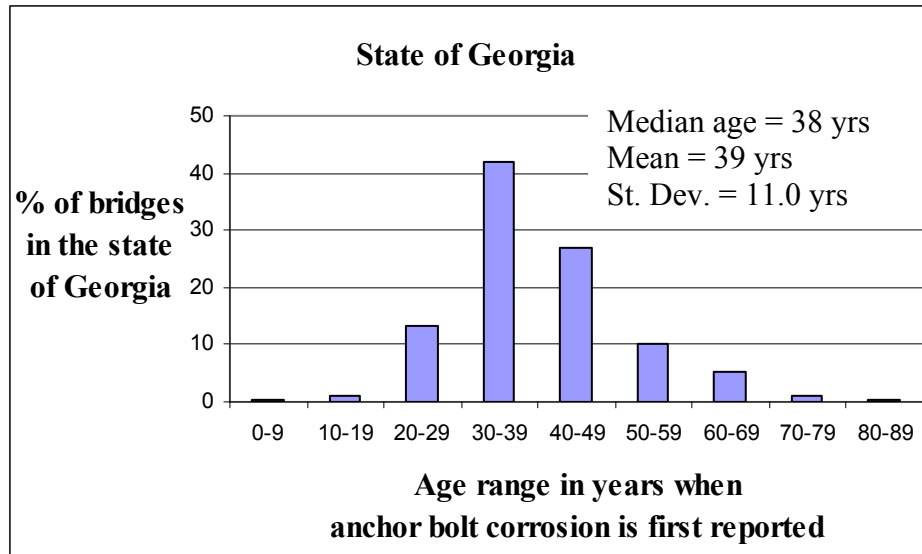


Figure 5.4: Distribution of bridge ages when anchor bolt corrosion is first reported for the whole State of Georgia.

From Figure 5.4 it can be seen that the greatest percentage of bridges with anchor bolt corrosion are first reported when they are between 30 and 40 years old. Overall, the age distribution is positively skewed, with more anchor bolt corrosion reported for bridges over 40 years old than reported for bridges less than 30 years old. The median and mean ages at which anchor bolt corrosion was reported in Georgia are 38 and 39 years, respectively.

In addition to the age distribution of bridges with anchor bolt corrosion for the entire state of Georgia, age distributions for each region defined in Section 5.2 are presented in Figures 5.5 through 5.12. By comparing the age distributions for each region the effect of environment on the initiation and/or propagation of anchor bolt corrosion can be observed.

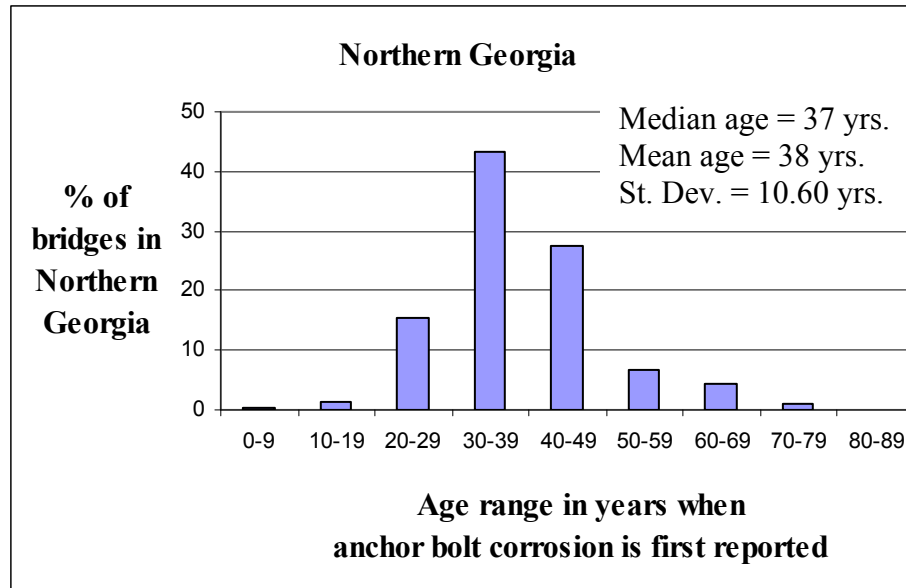


Figure 5.5: Distribution of bridge ages when anchor bolt corrosion is first reported for northern Georgia.

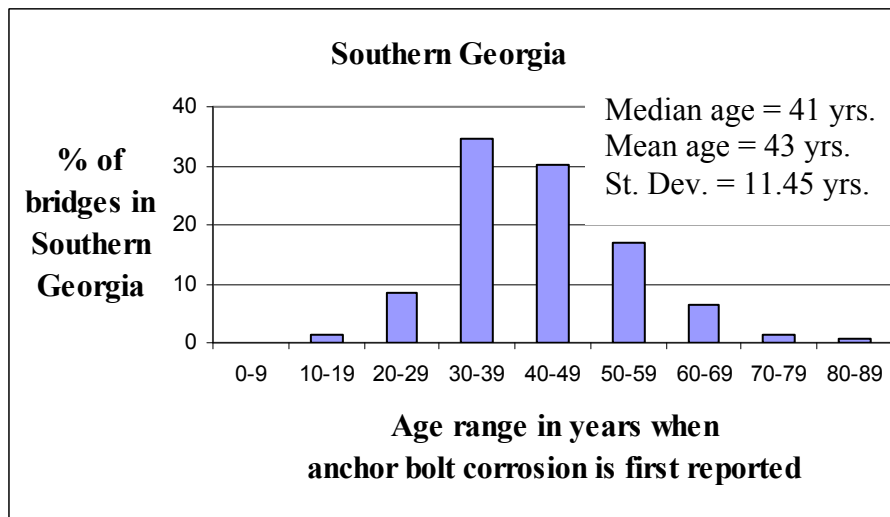


Figure 5.6: Distribution of bridge ages when anchor bolt corrosion is first reported for southern Georgia.

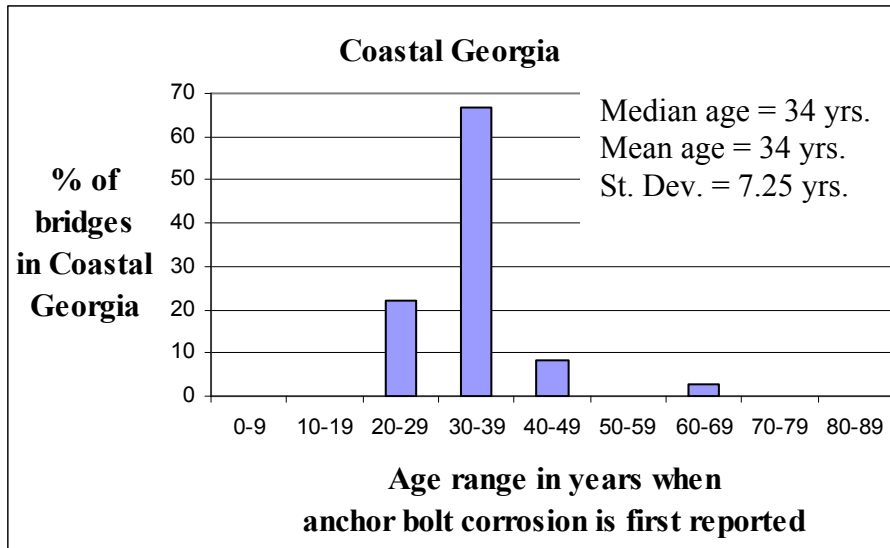


Figure 5.7: Distribution of bridge ages when anchor bolt corrosion is first reported for coastal Georgia.

Comparing Figure 5.5 to Figure 5.4, the age distribution for northern Georgia has a similar shape to the age distribution for the whole state. For all three geographic regions, the greatest percentage of anchor bolt corrosion is reported 30 to 39 years after the bridges are built. In the coastal Georgia region, shown in Figure 5.7, little variance in the distribution is observed, as approximately 65% of bridges with anchor bolt corrosion were reported in this 30-39 year age range. Conversely, in southern Georgia the age distribution is more positively skewed, and the mean and median ages for this region are 4 to 9 years higher than the other geographic regions.

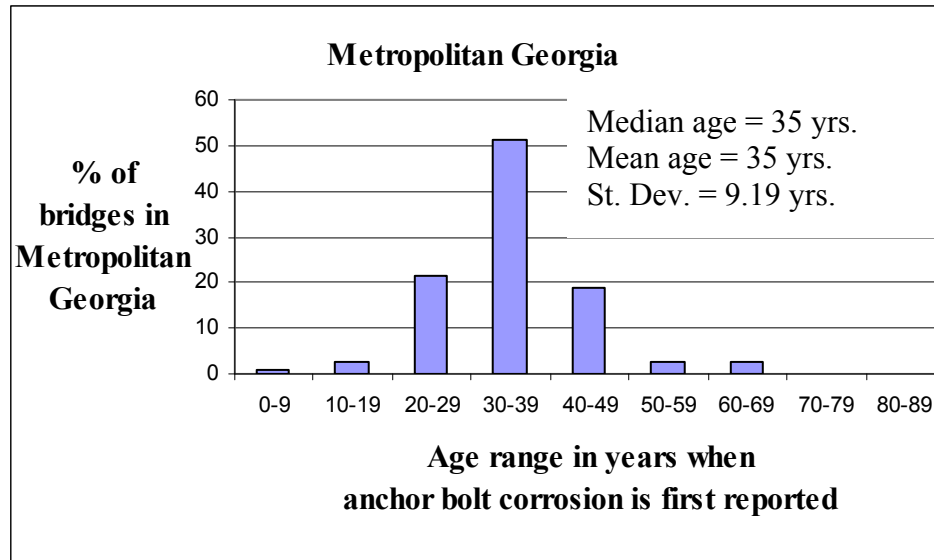


Figure 5.8: Distribution of bridge ages when anchor bolt corrosion is first reported for metropolitan areas in Georgia.

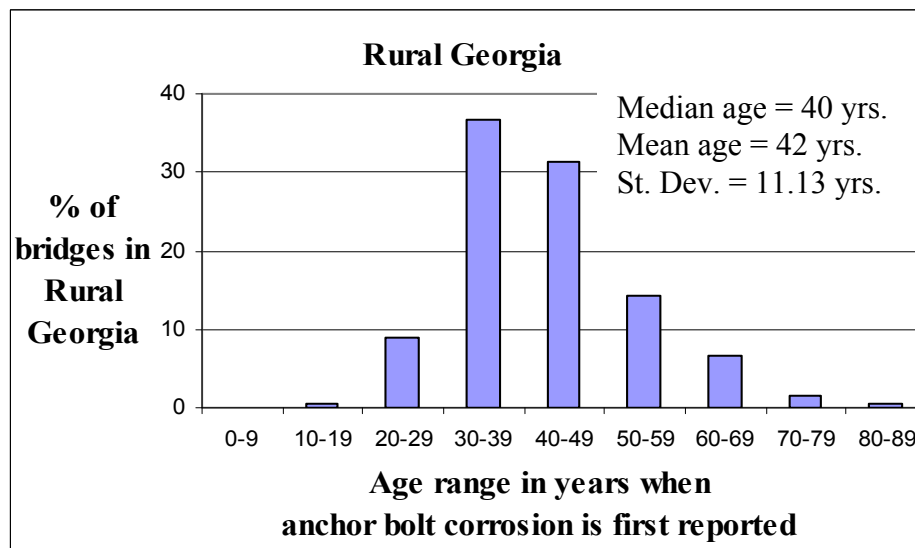


Figure 5.9: Distribution of bridge ages when anchor bolt corrosion is first reported for rural areas in Georgia.

The age distribution for bridges with anchor bolt corrosion in metropolitan areas of Georgia, shown in Figure 5.8, is symmetric about the 30 to 39 year age range; approximately 50% of the bridges with anchor bolt corrosion in the metropolitan areas

were reported in the 30 to 39 year age range. In contrast, the age distribution for bridges with anchor bolt corrosion in rural areas in Georgia is positively skewed and shifted toward higher ages. The 30 to 39 year age range contains 37% of the bridges in the region with anchor bolt corrosion; on either side of this range, the 40-49 year age range contains 31% while the 20 to 29 year age range contains just 9%. Additionally, the median and mean ages of bridges in rural areas are 5 to 7 years higher than those in metropolitan areas.

Anchor bolt corrosion in bridges associated with the Interstate system, either as a part of the Interstate roads or as an underpass, is most often reported three and a half decades after they are built. For both Interstate bridges and Interstate underpasses, the age distribution is symmetrically centered at the 30 to 39 year age range with narrow variance. However, the age distribution for the third span type shows that bridges that are not associated with the Interstate system tend to be older before anchor bolt corrosion is reported. Their age distribution is symmetrically centered at the 40 to 49 year age range, but has a wider variance.

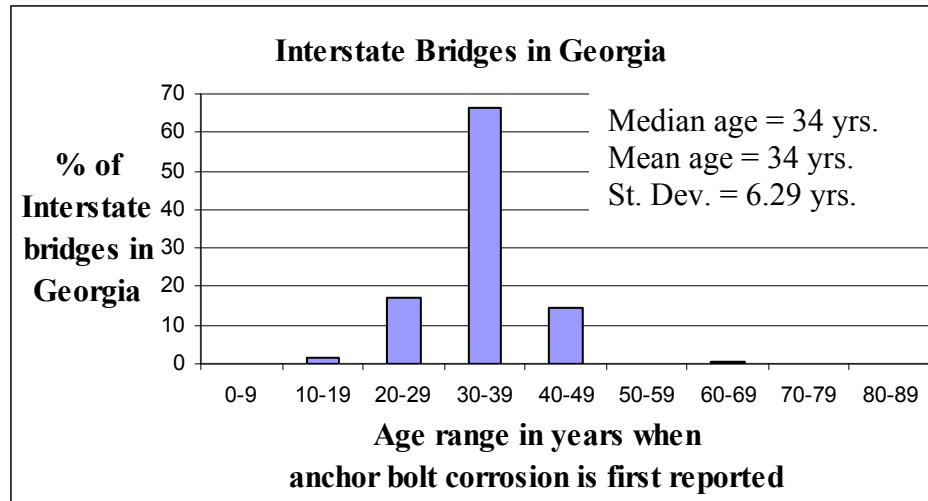


Figure 5.10: Distribution of bridge ages when anchor bolt corrosion is first reported for Interstate bridges in Georgia.

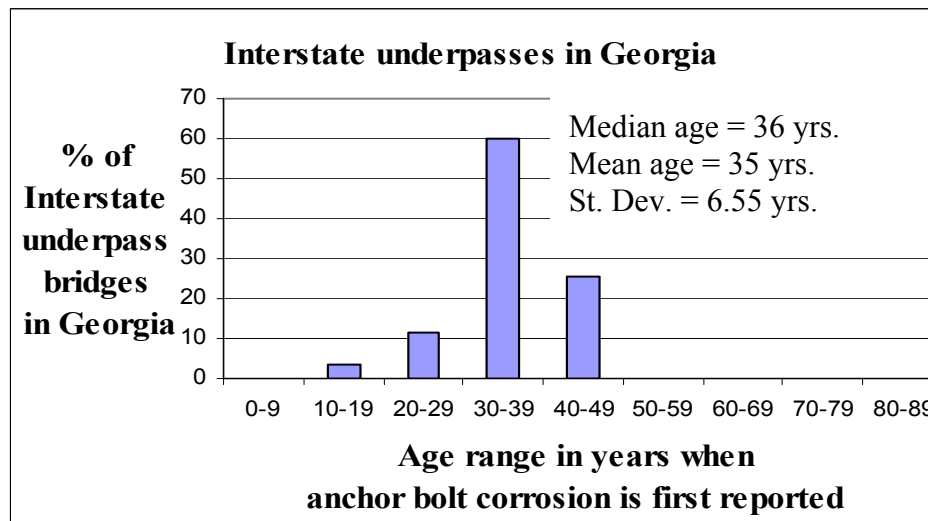


Figure 5.11: Distribution of bridge ages when anchor bolt corrosion is first reported for Interstate underpass bridges in Georgia.

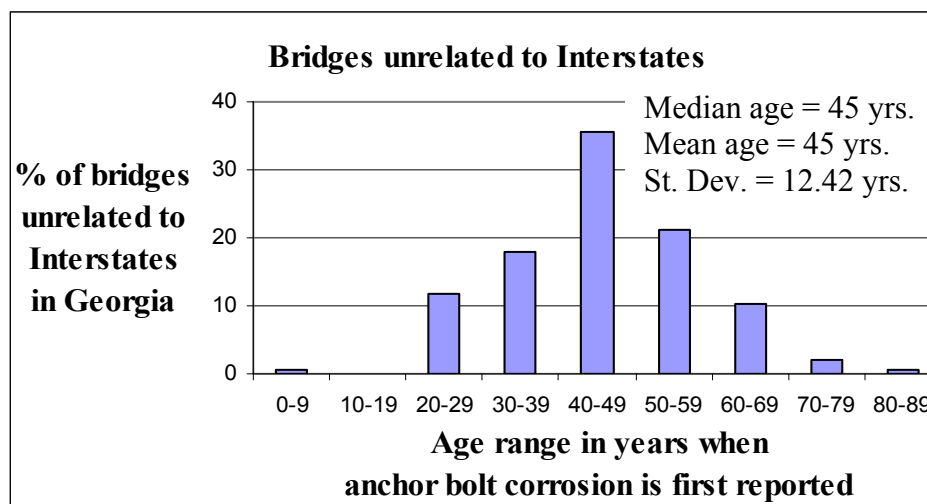


Figure 5.12: Distribution of bridge ages when anchor bolt corrosion is first reported for bridges not associated with the Interstate system in Georgia.

Table 5.3 concisely compares the age distributions of all the regions by reporting the median age, mean age, variance, and standard deviation of the age at which anchor bolt corrosion is first reported for each region.

Table 5.3: Characteristic statistics of the age distributions of reported anchor bolt corrosion for the state of Georgia and for the environmental regions.

Age distribution statistics	Regional areas								
	whole state	north GA	south GA	coast GA	City	Rural	Interstate bridge	Interstate underpass	Other
Median age (yrs)	38	37	41	34	35	40	34	36	45
Mean age (yrs)	39.4	38.1	42.5	33.9	34.9	42.0	34.1	35.0	44.9
Variance	121.1	113.2	131.1	52.6	84.5	123.9	39.6	42.9	154.3
Standard deviation	11.00	10.64	11.45	7.25	9.19	11.13	6.29	6.55	12.42

Key factors which may affect the age at which reported anchor bolt corrosion is first reported include the regularity and quality of inspections performed. For example,

anchor bolt corrosion may be detected at an earlier stage for bridges that are part of the Interstate system because these bridges may be more carefully or more regularly inspected compared to the non-Interstate bridges. If anchor bolt corrosion is not reported for non-Interstate bridges until the corrosion has progressed into later stages, then a higher age until anchor bolt corrosion incidence is misleading. A similar analogy may be drawn for bridges in metropolitan and rural regions.

Assuming equivalence in the inspection quality and regularity among all environmental regions, the differences in the age distributions imply that the environmental conditions do affect the rate at which corrosion initiates and/or propagates. It may be concluded that the rate of the incidence of anchor bolt corrosion is higher for bridges in coastal and northern Georgia compared to southern Georgia, is higher for bridges in metropolitan areas compared to rural areas, and is higher for bridges associated with the Interstate system compared to non-Interstate bridges. Further discussion of these results is provided in Chapter 9.

CHAPTER 6: FIELD INVESTIGATION REPORTS

6.1 Inspection Methods

Several bridges throughout the state of Georgia were selected to be inspected specifically for anchor bolt corrosion by the researcher. At each bridge attempts were made to inspect the anchor bolts at both fixed bearings and expansion bearings to evaluate the effect of bearing type on corrosion. However, for several of the highway bridges, access to the interior supports was not available, and in these cases only the bearings at the abutments were inspected.

The bearings were inspected by visual and physical methods. Visual signs of corrosion included rust staining, section loss in anchor bolts, and evidence of corrosion product by a “swelling” of bearing components. Physical methods of inspection included twisting or wiggling the bolt by hand, and hammering on the side of the bolt and nut. Corroded anchor bolts were found to be loose and would move upon contact, and paint would easily chip off a corroded anchor bolt or nut.

Additionally, soil samples from the bearings were collected from several bridges to further investigate the bearing environment in a laboratory analysis. The result of soil analysis is given in Chapter 8.

The following sections present the field inspection reports by region. Comparisons drawn from the reports for each region can be used to examine climate and local environmental effects on bearing corrosion.

6.2 Bridges in Metro Atlanta area, Georgia DOT District 7

The following four bridges in the Metro Atlanta area were chosen to be inspected because each one was in the process of being replaced at the time of the inspections. These bridges were not previously singled out by the Maintenance Department as bridges with reported anchor bolt corrosion.

6.2.1 Old Dixie Highway (State Route 3/US 19) over Central of Georgia Railroad.

The Old Dixie Highway bridge is located southeast of Atlanta in Clayton County, 0.35 miles south of I-285. Designed in 1937, the eight span steel girder bridge extends over the railroad tracks of the Central of Georgia Railroad. Numbering from west to east, spans one through three and six through eight consisted of ten simply supported steel girders. A new five span prestressed concrete girder bridge was built just to the south of the old bridge, and an embankment in place for the construction of the new bridge allowed inspection of the southernmost edge beam at Bent 7 and Bent 8, in addition to inspections at both abutments.

The bearings for the simple spans were one steel bearing plate approximately three inches thick placed between the concrete pier cap and steel flange. The anchor bolt passed through a slotted hole in the bearing plate and flange at the expansion end and a round hole at the fixed end. A typical fixed bearing at Bent 9 is shown in Figure 6.1.



Figure 6.1: Typical fixed bearing at Bent 9. In general the anchor bolts and nuts at the abutments appeared to be in good condition.

Upon general inspection the bolts and nuts in the bearing assemblies at Bents 1 and 9 appeared to be in good condition, with exception to a few anchor bolt nuts with flaking corrosion products. At the interior Bents 7 and 8, rust stains were noted on the bearing plates, beam flanges, and washers, despite the apparent sturdy condition of the anchor bolts, as shown in Figure 6.2. It was also noted that the interior bents collected more debris from spalling concrete diaphragms. Expansion slots were filled with dirt and oxides, as shown in Figure 6.3.



Figure 6.2: Rust stains on bearing plates, beam flanges, and washers at interior bents, despite the apparent sturdy condition of the anchor bolts.



Figure 6.3: Expansion slot filled with dirt and oxides at interior Bent 7.

In general, the anchor bolts of the Old Dixie Highway (State Route 3/US 19) bridge over Central of Georgia Railroad were not visibly damaged by corrosion. Instead, 95% of the corrosion observed at this site occurred in the girder flanges originating from crevice corrosion at the interface between the bearing plate and the girder flange. Before demolition of the bridge it was not apparent how this corrosion may have affected the

bolts inside the bearing assembly. No movements were observed when the nuts and bolts were twisted or struck with the hammer and the paint did not readily chip.

6.2.2 Lawrenceville Highway (State Route 10) over I-285

Lawrenceville Highway is located east of Atlanta, and the bridge that was inspected spanned eight lanes of I-285. An eight girder four span bridge, the middle two spans are continuous and the end spans are simply supported. This bridge was designed in 1967 and employed the typical plate bearing design presented in Chapter Two.

At the time of the inspection, the bridge appeared newly painted and cleaned. No obvious corrosion was visible and little debris was found at all of the bents. Slight crevice corrosion was found between the base and sole plate of the fixed bearing for the edge beam at Bent 1, which is shown in Figure 6.4. The anchor bolts of the Lawrenceville Highway (State Route 10) bridge over I-285 were not visibly or obviously physically damaged by corrosion. The bolts and nuts did not move and the paint did not chip when struck with the hammer.



Figure 6.4: Corrosion on bearing plates of edge beam bearing at Bent 1. The anchor bolts were not obviously visibly or physically damaged by corrosion.

6.2.3 Memorial Drive over I-285

Memorial Drive, just south of Lawrenceville Highway, is also east of Atlanta and spans six lanes of I-285. The Memorial Drive bridge was designed in 1965 – two years before the Lawrenceville Highway bridge. As a continuous four span bridge, rocker bearings are used at all of the supports except for the middle one.

Unlike the Lawrenceville Highway bridge, the Memorial Drive bridge had open deck joints above the abutments. For this reason, significantly more debris was found at the abutments of the Memorial Drive bridge compared to the Lawrenceville Highway bridge. The amount of debris notably affected the corrosion of the bearings.

Figures 6.5 and 6.6 show bearings from the Memorial Drive bridge without and with debris, respectively. At the bearing without significant debris, shown in Figure 6.5, a spot of corrosion scale approximately the size of a quarter was found on the base plate of the bearing and the other components appeared unaffected. In contrast, at the bearing surrounded by dirt and debris, shown in Figure 6.6, the entire base plate was enveloped in

corrosion scale along with the bottom of the rocker and the anchor bolt. While specific anchor bolt corrosion problems were not found, the inspection of the Memorial Drive bridge over I-285 clearly illustrated the detrimental effect that debris at bearings has on the corrosion behavior of those bearings.



Figure 6.5: Bearing at abutment without debris. Base plate has a quarter sized spot of corrosion scale.



Figure 6.6: Bearing at abutment with debris. The base plate, anchor bolt, and bottom of the rocker that are enveloped in corrosion scale demonstrate the detrimental effect of debris at bearings.

6.2.4 State Route 92 over I-20

State Route 92 crosses over six lanes of I-20 west of Atlanta in Douglas county. The nine girder four span bridge is simply supported at all spans. Designed in 1960, the bearing omits a lube plate and consists of a base plate and a sole plate, with slotted holes for the expansion bearing and round holes for the fixed bearing.

Due to limited access to the interior bents, only the abutment bearings were inspected for this bridge. Open joints at both abutments allowed the ingress of debris on the abutment pier caps. Significant bearing corrosion was observed for each of the nine girders, and anchor bolts were missing in 15 of 36 locations at the abutment bearings. At locations in which anchor bolts were present, the material and bolt strength were tested by striking the anchor bolt and nut with a hammer. At all bearings the paint on the bolts and nuts was found to chip easily when struck, revealing dark oxides beneath.

One third of the remaining bolts were found to be very loose when struck. Little force was needed to wiggle the bolts within the holes, and the diameters of the bolts were observed to have been reduced to less than $\frac{1}{2}$ inch. In two locations the anchor bolts broke off completely at the juncture of the beam flange and sole plate. Figure 6.7 shows one of these locations prior to the bolt breaking off. This figure reveals that the bolt had been pushed up approximately $1 \frac{1}{2}$ inches, presumably from the accumulation of oxides in the bearing hole. Although previous corrosion damage had been painted over, it can be seen that the diameter of the bolt started to decrease approximately one inch below the nut, indicating that the corrosion initiated within the bearing between the base and sole plate.



Figure 6.7: Anchor bolt which was easily broken. The base of the nut is approximately 1 ½-in above the top of the flange indicating that the bolt has been pushed up that distance by corrosion products. A steel angle had been previously bolted to the abutment to restrain lateral movement.

At four other locations bolts were also found to be pushed up, but remained tight within the bearing hole. In these instances the bolts' diameters appeared to be swelled with corrosion product which inhibited any bolt movement within the bearing, as shown in Figure 6.8. Similarly, at 80 percent of the anchor bolt locations, the anchor bolt nuts appeared swelled with oxides and painted over. At one site, the corrosion product accumulation grew so large that it cracked the nut apart, as shown in Figure 6.9.



Figure 6.8: Anchor bolt diameter swelled with corrosion product inhibits bolt movement within the bearing and restricts the thermal movements of the bridge.



Figure 6.9: Corrosion product accumulation breaks anchor bolt nut.

In summary, all of the existing anchor bolts and/or nuts at the abutment bearings of the State Route 92 bridge over I-20 were found to be significantly affected by anchor bolt corrosion.

6.3 Bridges in south Georgia, GDOT Districts 4 and 5

Four bridges scheduled for replacement were inspected in south Georgia. These bridges were near Valdosta and Waycross and were not near a coastal area.

6.3.1 State Route 122 over Little River, District 4

The State Route 122 bridge is approximately 40 simply supported spans extending over the Little River and surrounding lowlands for nearly ½ mile. Even after periods of heavy rain, only the middle quarter of the bridge spanned water. A new pre-stressed concrete girder bridge was in construction to the south of the existing bridge.

In this inspection, a random sample of the bearings on the west side of the river was examined using the bridge contractors bucket lift. The bearings consisted of a 1 inch base plate on the concrete pier cap and a ¼ inch flat sole plate beneath the girder flange. Expansion bearings had slotted holes and fixed bearings had round holes. Generally, the pier caps were clean of debris or bird droppings.

Of the anchor bolts inspected, approximately 40 percent displayed corrosion losses. Corrosion of the anchor bolts was observed most readily in the expansion bearings, as the slotted holes allowed greater access to the bolt shaft beneath the washer and girder flange. Signs of corrosion were most prevalent beneath leaking deck joints and in bearings closer to the river.

All corrosion losses observed were of a similar type. The anchor bolts appeared in good condition above the girder flange, but closer visual inspection of the bolt underneath the washer revealed gradual section loss of the bolt shaft. As shown in Figure 6.10, the diameter of the bolt began to decrease just below the washer as it passed through the

flange, reaching its smallest diameter approximately one to 1 ½ inches lower at the interface where the bolt protrudes from the concrete. In many instances the corrosion loss had been painted over. Figure 6.11 portrays the same type of corrosion loss that has not been painted over. In general, the diameter of the bolts at their smallest point was observed to be approximately ½ to ¾ inches, which was roughly 50 % of their original diameter and between 84% and 64% loss of cross section. Although in one case, shown in Figure 6.12, 100 percent section loss was observed.



Figure 6.10: Typical anchor bolt corrosion of S.R. 122 bridge. The diameter of the bolts decreased just below the washer as they passed through the flange, reaching their smallest diameter approximately one to 1 ½ inches lower at the concrete interface.



Figure 6.11: Anchor bolt cross section loss that has not been painted.



Figure 6.12: Complete section loss in anchor bolt The anchor bolt and washer appear corrosion free above the top of the flange.

6.3.2 US Route 1 over Satilla River, District 5

The US Route 1 bridge over the Satilla River was built in 1949 and is nearly one mile long. However, only the four spans over the river use steel girders, as shown in Figure 6.13. Access to the steel girder bearings was difficult, and the inspection was limited.



Figure 6.13: US Route 1 over Satilla River. Only the four middle spans were steel girders and inspection of the bearings was limited.

Aside from a few visible spots of general corrosion on the bearing plates and nuts, the bearings of the US Route 1 bridge appeared to be in good condition. Figure 6.14 shows general corrosion on the anchor bolt nut at the fixed end of the end span. Detailed investigation was not feasible to determine the condition of the bolts below the washer or flange at any of the bearings. The bolts and nuts did not move and the paint did not chip when struck with a hammer.



Figure 6.14: General corrosion on anchor bolt nut at a fixed bearing. The anchor bolt and nut did not move and the paint did not chip when struck with a hammer.

6.3.3 State Route 121 over Fishing Creek, District 5

Built in 1950, the State Route 121 bridge over Fishing Creek is a simply supported bridge. The bearing design employed a $\frac{1}{4}$ inch flat sole plate beneath the girder on top of a one inch flat base plate on the concrete pier. No debris was present around the bearings.

At the fixed ends of the spans, no anchor bolt corrosion was visible. However, at the bridge expansion joints, corrosion was observed under the bolt washers. Similar to the findings at the State Route 122 bridge, the bolts were discovered to be decreasing in diameter from where the bolt first passed through the flange to where they entered the concrete pier cap. Figures 6.15 and 6.16 provide two examples of this behavior, where dirt was cleared away from beneath the washer to allow visual inspection of the bolt shaft within the expansion slot.



Figure 6.15: Anchor bolt reduction in diameter due to corrosion in expansion slot. Dirt was cleared away to allow visual inspection within the expansion slot.



Figure 6.16: Anchor bolt corrosion below washer. Corrosion loss occurred in the area between the concrete interface and the top of the beam flange.

6.3.4 State Route 144 over Watermelon Creek, District 5

Spanning a small waterway, the State Route 144 bridge is a three span simply supported bridge that was built in 1948. Similar to the previous bridges inspected in the south Georgia region, the bearing design contained two flat plates. Also, no debris was near any of the bearings.

At the fixed end of the spans, no corrosion was observed by either visual or physical methods on the anchor bolts or bearing plates. Limited access to the expansion ends of the spans prevented a thorough investigation of the bolt condition below the washer and beam flange. However, general corrosion was observed on the anchor bolt nut and base plate, as shown in Figure 6.17. Additionally, corrosion product was scraped from the bottom of the washer.



Figure 6.17: General corrosion on the anchor bolt nut and base plate at the expansion bearing. Limited access prevented a thorough investigation of the bolt condition below the washer and beam flange.

6.4 Bridges in north Georgia, GDOT Districts 1 and 6

Three bridges in northern Georgia were visited to investigate the bearing and anchor bolt corrosion in this region. The bridges that were visited were: (1) US Route 76 over a creek in Blue Ridge, Fannin County, Georgia; (2) State Route 515 over Georgia Northeast Railroad in Blue Ridge, Fannin County, Georgia; and (3) US Route 19 over US Route 76 in Blairsville, Union County, Georgia. Access at each of these bridges was limited, preventing useful inspection of the bearing assemblies. Observations of bearing

corrosion could not be recorded. However, soil samples accessible near the bearings were collected and were analyzed to determine typical Georgia bearing environments, as described in Chapter 8.

CHAPTER 7: FAILURE ANALYSIS OF FIELD SPECIMENS

7.1 Visual analysis

7.1.1 Bolts broken in the field

During the field investigations, a few broken bolt specimens were obtained from corroding bearings. Two broken bolts, shown in Figures 7.1 and 7.2, were taken from the State Route 92 bridge over I-20 in Douglas County, constructed in 1962. One broken bolt, shown in Figure 7.3, was taken from the State Route 122 bridge over Little River in between Brooks and Lowndes counties, constructed in 1941.



Figure 7.1: Bolt 1 from northern Georgia at the SR 92 bridge over I-20. When this bolt was found, it was already bent and broken.



Figure 7.2: Bolt 2 from northern Georgia at the SR 92 bridge over I-20. When this bolt was found, it was very loose and was easily broken by hand.



Figure 7.3: Bolt from southern Georgia at the SR 122 bridge over Little River. The image on the left is a view of the bolt from the side, and the image on the right is a view of the bolt from directly underneath the washer. This bolt was already broken when it was found.

Both of the bolts in Figures 7.2 and 7.3 exhibit significant and rapid cross section loss. In areas where corrosion scale was present, it seemed to be uniform; the diameter of the bolt in Figure 7.3 was uniformly reduced. From the visual analysis of these two bolts,

it can be hypothesized that this uniform corrosion may be locally accelerated in the trapped solution in the surrounding cavity, forming a concentration cell.

The bolt in Figure 7.1 does not exhibit a rapid cross-sectional loss to the point where it is broken. Instead, it appears that the entire cross-section of the bolt beneath the washer is marginally decreased due to general, uniform corrosion and that the bolt was bent and broken by a mechanical force.

7.1.2 Bolts and bearing plates from bridge demolition

In addition to the broken specimens obtained during field investigations, whole anchor bolts and bearing plates were acquired from the demolition of the Old Dixie Highway bridge in Clayton county. A variety of bearing plates and anchor bolts were acquired from fixed and expansion bearings at edge and interior girders. Figures 7.4 and 7.5 show a typical fixed and expansion bearing.



Figure 7.4: Bearing plate and anchor bolts from an interior girder expansion bearing. The expansion slots are not visible because they are completely filled with debris and corrosion products.



Figure 7.5: Bearing plate and anchor bolts from a fixed bearing.

Originally, these samples were intended to be used for additional failure analysis. Unfortunately, difficulties in removing the anchor bolts from either expansion or fixed bearing plates prohibited further analysis. The anchor bolts had adhered to the bearing plates with corrosion products in the bearing holes acting as a weld. The shear strength of the adhesion is demonstrated in Figure 7.6. Even under the direct impact loads, the anchor bolt-bearing plate assembly would not dislodge.



Figure 7.6: Build up of corrosion products prevented the anchor bolts from dislodging from the bearing plate.

A commercially available corrosion debonding product was used in an attempt to disintegrate the corrosion scale. While the anchor bolts were still not freed from the bearing plate, enough corrosion scale was removed to allow the visual examination of the interface of the bolt and the bearing plate, as shown in Figure 7.7.



Figure 7.7: Corrosion build-up visible at the interface of the bolt and bearing plate.

From a visual analysis of these anchor bolts and bearing plates, it is clear that in most instances, the diameter of the anchor bolt is necked down near the bearing plate. The accumulation of corrosion product from the anchor bolt hides the extent of bolt cross-section loss. Accumulation of corrosion product in the bearing hole was so voluminous that it expanded outwards from the hole. In conclusion, these samples proved that corrosion of anchor bolts is not only detrimental to the bolt but the corrosion build up can be responsible for bearing seizure. Further failure analysis was subsequently performed on the broken bolts obtained during the field investigations.

7.2 Microscopy of failure surface

The bolts obtained during the field investigations were microscopically analyzed to gain insight into the mode of corrosion and bolt failure. Prior to microscopic analysis of the failure surface, the corrosion scale was cleaned from the bolt surface using

Clarke's solution, a hydrochloric acid solution with corrosion inhibitors conforming to ASTM G1: Standard Practice for Preparing, Cleaning and Evaluating Corrosion Test Specimens. To ensure that the cleaning solution would not induce corrosion, dummy samples of carbon steel were immersed in the solution. The solution was accepted when the dummy sample experienced no weight loss after immersion. The bolt samples were submerged in the solution in five-minute intervals, allowing the corrosion scale to dissolve in the acid without corroding the remaining carbon steel (ASTM 2003).

7.2.1 Optical microscopy

Optical microscopy of the bolt surfaces are shown in Figures 7.8 through 7.11. Since the corrosion morphology of galvanic and concentration cell corrosion is the same as general corrosion accelerated in a specific area, the surface appearance of areas exposed to these forms of corrosion appears similar to areas exposed to general corrosion. In a few of the following figures, an oxide film is shown to exist on the surface. Since the field specimens were cleaned of all corrosion scale prior to the surface analysis, any apparent oxides are due to general atmospheric corrosion during the analysis and are not related to the field conditions.

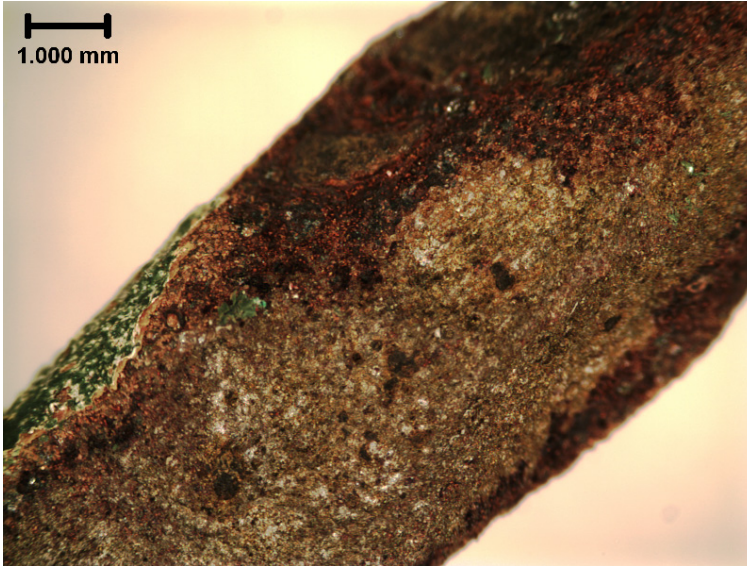


Figure 7.8: Surface of bolt shown in Figure 7.2 at 6.3x magnification. The surface of the bolt is uniformly rough in the necked region.

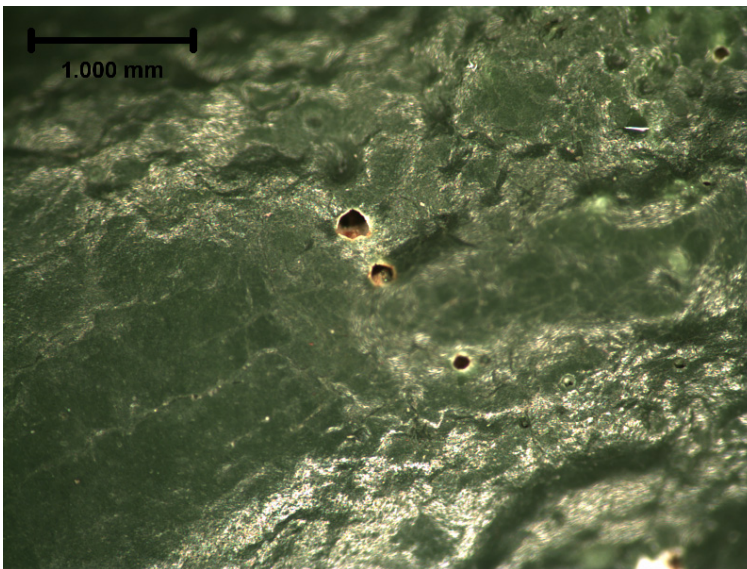


Figure 7.9: Localized corrosion at paint defects on the surface of the bolt in Figure 7.2 at 12.5 x magnification.



Figure 7.10: Edge of washer hole on washer found with bolt in Figure 7.1 at 6.3 x magnification. The crack may have originated at a crevice and was propagated by mechanical means.

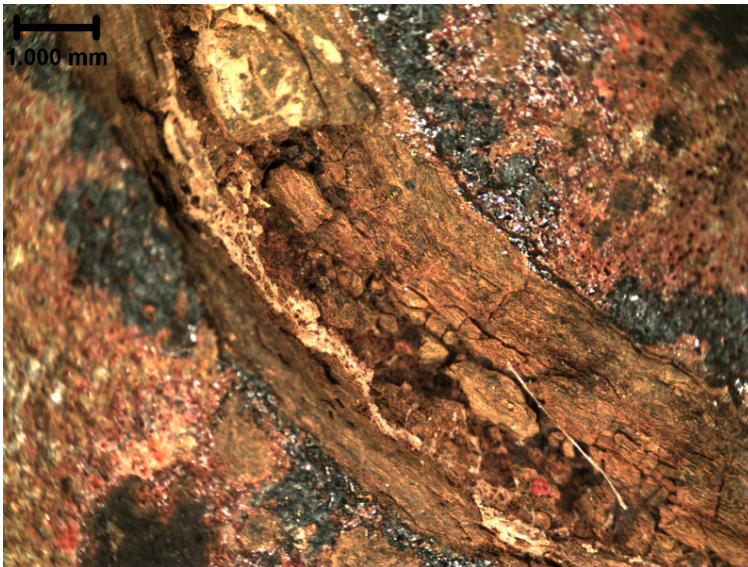


Figure 7.11: Corrosion product build up in the crevice of the bolt shaft and washer hole of the bolt shown in Figure 7.3 at 6.3 x magnification. The corrosion product fused the remaining bolt shaft to the washer.

In Figure 7.8, the surface of the bolt is analyzed at the region where the diameter of the bolt necks due to corrosion. The surface appears uniformly rough, indicating general

corrosion. No variation in the surface waves are evident that would indicate local pitting or crevice corrosion. Local corrosion is apparent, however, in Figure 7.9 where defects in the paint surface lead to pitting and crevice corrosion.

Figure 7.10 shows a surface with similar general corrosion characteristics to the surface in Figure 7.8, but with a noticeable crack. The image was taken from the washer found with the bolt in Figure 7.1. This crack may have been induced at a local pit or crevice at the edge of the washer hole, and was propagated by mechanical means and is not related to corrosion phenomenon.

In Figure 7.11 the crevice between the bolt and the washer hole is shown to be filled with layers of corrosion product, fusing what is left of the bolt shaft to the washer.

7.2.2 Scanning electron microscopy

Scanning electron microscopy was used to achieve a higher magnification at the bolt failure surfaces. Figures 7.12, 7.13, and 7.14 present the typical surface condition in the necked region of the field specimen shown in Figure 7.2 at 100, 300, and 500 times magnification.

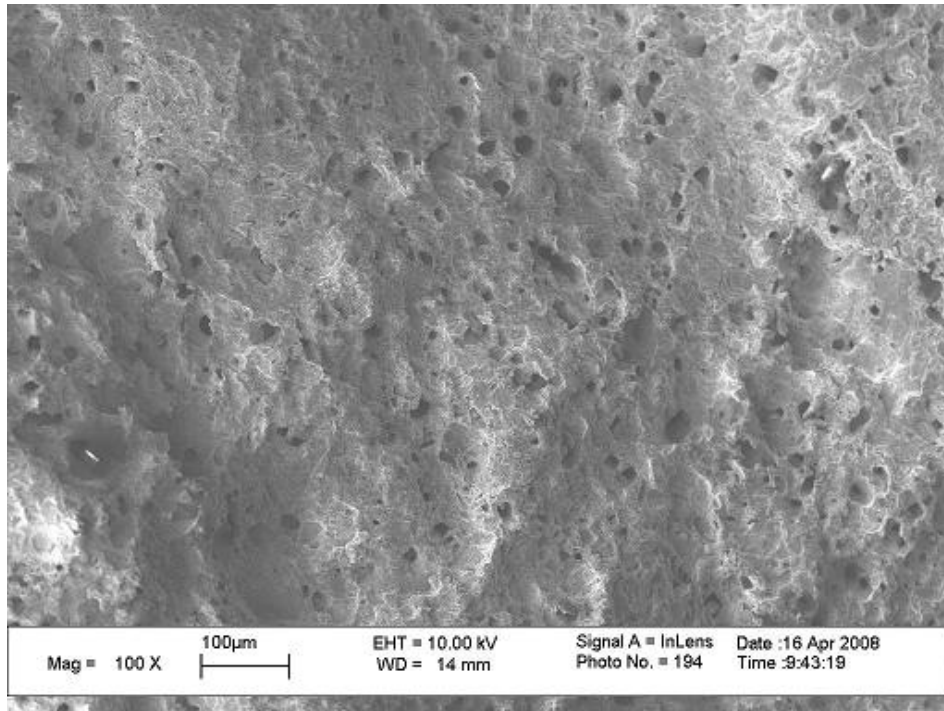


Figure 7.12: Surface of bolt in Figure 7.2 at 100 x magnification. Wavy surface indicates general corrosion.

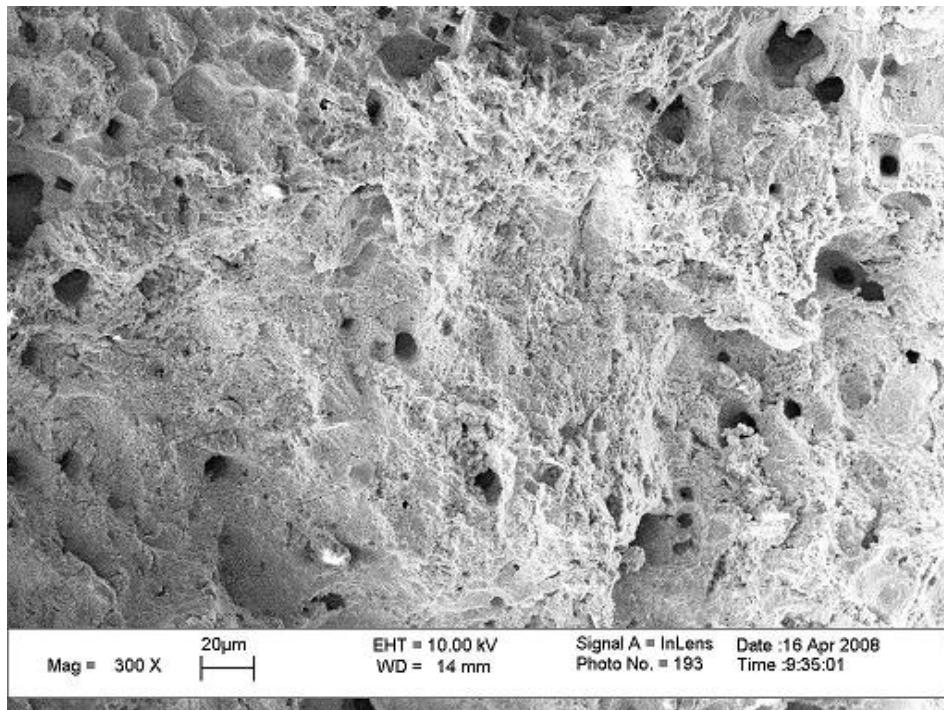


Figure 7.13: Surface of bolt in Figure 7.2 at 300 x magnification. Ridges in the surface were created during ductile failure of the bolt.

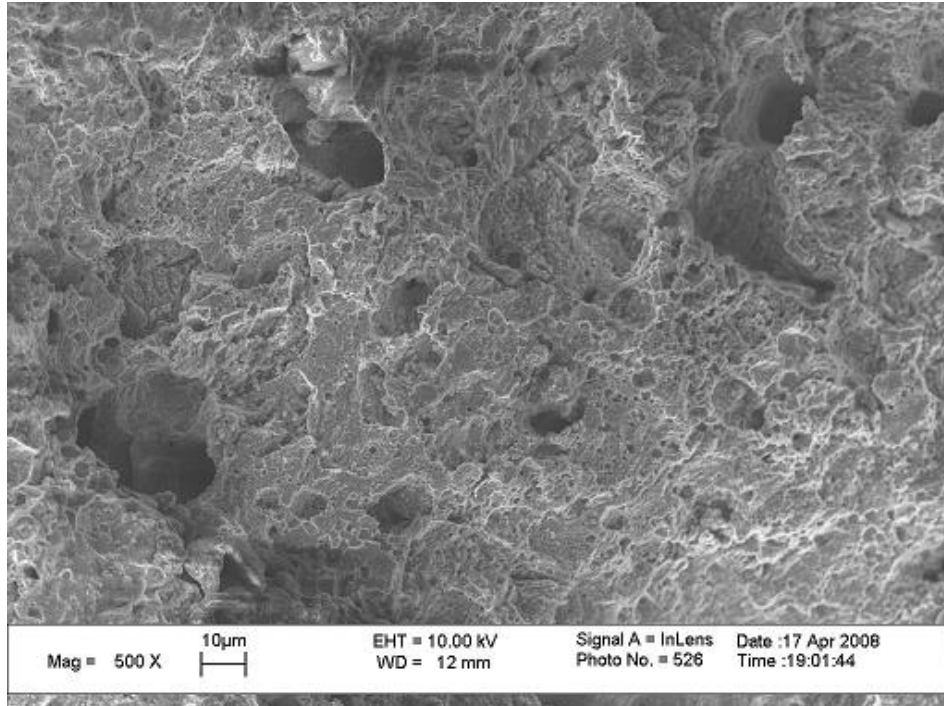


Figure 7.14: Surface of bolt in Figure 7.2 at 500 x magnification. Voids on surface, corresponding to dark spots in the image, were opened during ductile failure.

In Figures 7.12 through 7.14, the wavy surface indicates that general corrosion morphology is prominent for these specimens with a ductile fracture mode. Fracture surface showed a typical ductile fracture morphology with microvoids, which corresponds to the dark spots in the images.

7.3 Analysis of bolt scale

X-ray diffraction under $\text{CuK}\alpha$ radiation was used to analyze the chemical composition of the bolt scale from the bolts obtained in the field. The chemical composition of the scale provides insight into the corrosive environment surrounding the bolt. The peaks in the diffraction patterns correspond to peaks produced by known

chemical compounds. By matching up the peaks from the bolt scale to peaks of known compounds, the chemical composition of the scale can be deduced. Evidence of iron chloride products, for instance, would indicate the presence and participation of chlorides in the corrosion process. X-ray diffraction was performed on bolt scale from a sample in northern Georgia and southern Georgia to compare the different environments.

Figure 7.15 displays the diffraction pattern for the scale from the bolt in Figure 7.3.

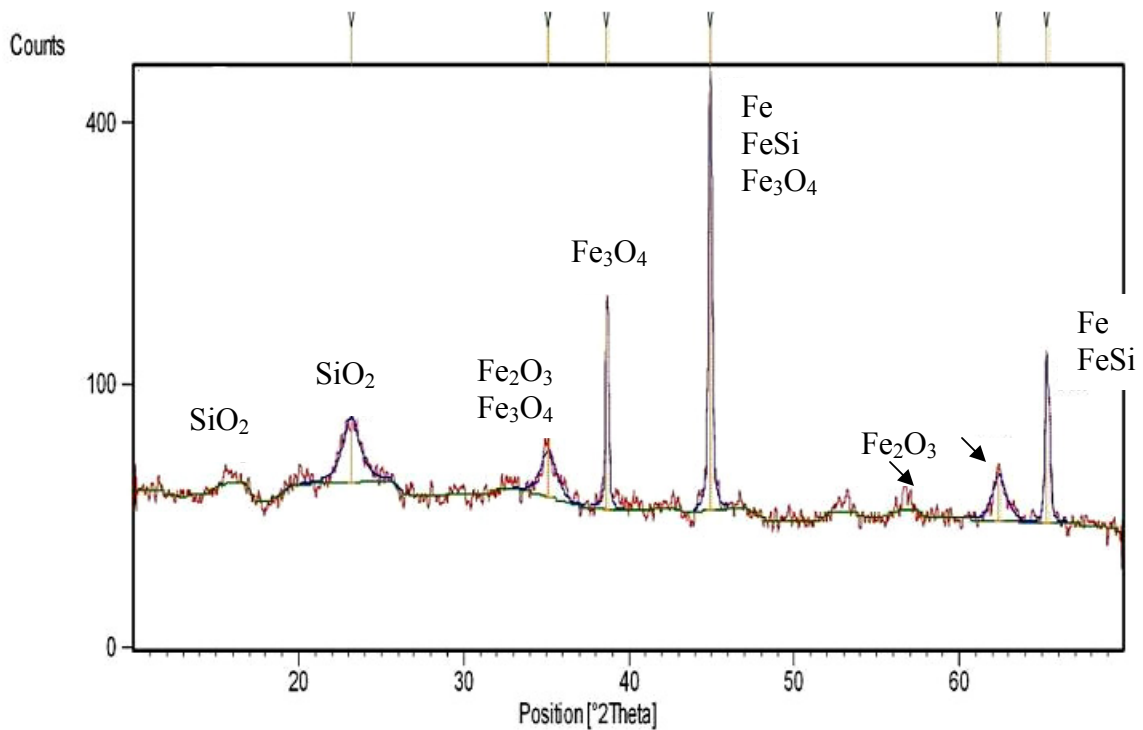


Figure 7.15: X-ray diffraction pattern for the bolt scale taken from the specimen shown in Figure 7.3. The peaks in the pattern correlate with iron, iron oxides, iron carbides, and iron silicates.

The diffraction pattern for the sample from southern Georgia correlates with iron, iron oxides, iron carbides, and iron silicates, as shown in Figure 7.15. For this specimen from southern Georgia, no correlations with corrosive ions existed. Similarly, the diffraction pattern for the specimen from northern Georgia does not show any chlorides or presence of other corrosive compounds in the surface scale as the scales were mostly oxides of iron. The role of this environment in the anchor bolt corrosion mechanism is unclear because the chemical composition of the bolt scale is indistinct. Thus, the mechanism for corrosion of anchor bolts in southern and northern Georgia is not positively associated with chlorides from deicing salts or any other corrosive ions in the environment, according to analysis by x-ray diffraction technique. As discussed in Chapter 9, the lack of chloride-containing compounds in the bolt scale, as determined by x-ray diffraction analysis, does not eliminate the possibility that chlorides aided in the initiation or acceleration of corrosion.

CHAPTER 8: LABORATORY EXPERIMENTAL TESTING

8.1 Experimental method

8.1.1 Laboratory tests conducted

Several laboratory experimental tests were conducted to determine the corrosion behavior of the anchor bolt materials currently in use and candidate alloy materials to be considered for future use in the State of Georgia.

In a long term test ASTM Grade 36 carbon steel and ASTM Type 304 stainless steel samples from new anchor bolts were exposed to simulated environmental conditions for approximately two months. Their corrosion potentials were regularly monitored to determine their corrosion behavior. Polarization resistance method and weight loss measurements on these samples provided their corrosion rates.

Additionally, electrochemical polarization curves were created for the same materials. The polarization curves provided insight into the corrosion behavior of the materials tested and served to isolate the specific environmental conditions of concern.

Cyclic polarization was performed on the Type 304 stainless steel samples from new anchor bolts and on commercially available coupons of other candidate alloy materials to compare the pitting corrosion potentials of these materials in the given environment.

Finally, potentials and corrosion rates were measured for several combinations of electrically coupled materials simulating galvanic or concentration cell conditions in the plate bearing assembly. These combinations included: (1) carbon steel coupled with

stainless steel, simulating carbon steel bearing plates in contact with stainless steel bolts; (2) carbon steel coupled with bronze, simulating carbon steel bearing plates in contact with the bronze lubrication plate; (3) stainless steel coupled with bronze, simulating the stainless steel bolt in contact with the bronze lubrication plate; (4) carbon steel, stainless steel, and bronze all coupled with each other simulating the bearing plates and bolt in contact with each other; (5) carbon steel in the alkaline environment coupled with carbon steel in the neutral environment, simulating the partial embedment of the bolt in concrete; and (6) stainless steel in the alkaline environment coupled with stainless steel in the neutral environment, simulating the partial embedment of the bolt in concrete.

8.1.2 Experimental testing environments

The testing environments chosen were based on existing conditions at bridge bearings. A solution simulating the environment found at the State Route 92 bridge over I-20 in GDOT District 7 was used in the experimental testing because this bridge displayed the worst case conditions. Of the bridges involved in the field investigations, the State Route 92 bridge had the most bearing corrosion damage. Age distribution data given in Chapter 5 suggest that bearing corrosion initiates and/or propagates faster in northern, metropolitan, and Interstate-related bridges; the State Route 92 bridge matches all of these classifications.

Soil samples were taken from debris found within the expansion bearings of the bridge. The soil samples were made into a solution of 10 grams of soil in 25 mL of de-ionized water, which was then analyzed for cations and anions. Table 8.1 shows the

results of the analysis which was used as the basis for the solutions used throughout the laboratory experimental testing.

Soil samples from several other existing bridges involved in the field investigation were taken to verify the validity of the environment chosen. The bearing environment for southern Georgia was determined from soil samples from bridges in Districts 4 and 5, and the environmental conditions for northern Georgia bridges was investigated through soil samples from bridges in Districts 1 and 6. These results can be seen in Appendix D. From these results, it was determined that the solution based on conditions in District 7 is representative for the state. Ionic concentrations in the District 7 solution were typically higher than those in southern Georgia, and with few exceptions, similar to those in northern Georgia.

Table 8.1: Soil solution analysis from S.R. 92 bridge over I-20 in District 7 used as basis for solutions in laboratory experimental testing.

Ion	Concentration (mg/L)
Na ⁺	59.5
Ca ²⁺	30.5
K ⁺	12.9
Cl ⁻	40.1
SO ₄ ²⁻	65.3
NO ₃ ⁻	1.71
CO ₃ ²⁻	56.7
pH	7.65

Experimental tests were conducted in four variations of the chosen solution. The first was a “normal solution” of ion concentrations matching that shown in Table 8.1. The normal solution simulated a wet bearing environment where abundant water could easily

mix with the bearing soil. The soil was damp at the time it was retrieved. A second testing solution, the “concentrated solution”, contained ion concentrations that were ten times higher than the normal solution. The concentrated solution simulated expected conditions at the bearing as ion concentrations build up over time and/or when less moisture would be available, such as after the area had dried. The concentrated solution also accounted for exceptions where normal ion concentrations were higher than those in the chosen solution, such as some northern bridges that are exposed to deicing salts more often.

Both the normal and concentrated solutions were used at two different pH values, pH 7.5 and pH 13. The solutions at pH 7.5 replicated the pH found at the bearing in atmospheric conditions, while the solutions at pH 13 represented the typical pH within new concrete. In addition to the normal and concentrated ionic solutions at pH 7 and pH 13, a concrete pore solution was the fifth testing environment used. The pore solution did not contain the ions found at the bearings, but rather represented the solution typically found in clean concrete.

8.2 Experimental set-up

8.2.1 Sample preparation

New anchor bolts were ordered from Highway Materials, a contractor supply company located in Forest Park, Georgia, and which commonly supplies anchor bolts to bridge constructors. Both galvanized Grade 36 carbon steel and Type 304 stainless steel 1 ¼-inch diameter bolts were supplied conforming to the GDOT previous and current

material specifications, respectively. Thus, the materials tested were the same as those used in bridge bearing applications.

To conduct the laboratory experiments, the bolts were cut into coupons. The corrosion coupons were a $\frac{3}{8}$ -inch thick slice of the 1 $\frac{1}{4}$ -inch diameter bolt. The carbon steel coupons cut from the galvanized bolt retained the zinc coating along the $\frac{3}{8}$ -inch edge. The cut faces of the coupons were polished on the grinding wheel with 120 grit paper. For crevice corrosion and waterline corrosion tests, as a part of the long term experiment, 9.6 mm holes were drilled through the center of the sample, to allow the building of the racks as described in Section 8.2.3.

For the galvanic corrosion series of tests, a new cast bronze plate conforming to ASTM B 22 Alloy 911 was cut into square samples that were 2 $\frac{1}{2}$ -inches by 2 $\frac{1}{2}$ -inches and $\frac{3}{8}$ -inch thick. The cast bronze was donated by Lubrite Technologies, the company that manufactures and supplies the bronze lubrication plates to Georgia bearing manufacturers.

8.2.2 Solution preparation

Solid chemicals were dissolved in de-ionized water in proportion to create the concentrations of ions described in Section 8.1.2. To reach the desired pH value for the solutions, trace amounts of sulfuric acid were added to decrease the pH, and sodium hydroxide was added to increase the pH.

The simulated concrete pore solution was based on a recommended pore solution in ACI 440R-96. The solution was a saturated calcium hydroxide solution containing trace amounts of potassium hydroxide and sodium hydroxide. The pore solution was

created by dissolving the prescribed sodium hydroxide and potassium hydroxide in de-ionized water, followed by the addition of calcium hydroxide to saturation.

8.2.3 Equipment set-up

Each test conducted required a special set-up, as described in the following sections. Common to all the tests, however, was the saturated calomel reference electrode and salt bridge, shown in Figure 8.1. On the left side of the picture, where the salt bridge is held by a clamp, the reference electrode is securely inserted into the salt bridge with a stopper. The solution in the salt bridge and around the electrode is a highly conductive potassium chloride solution. The tip of the salt bridge, which is placed near the corrosion coupon for measurements, is on the right in the figure entering a beaker of potassium chloride solution. .

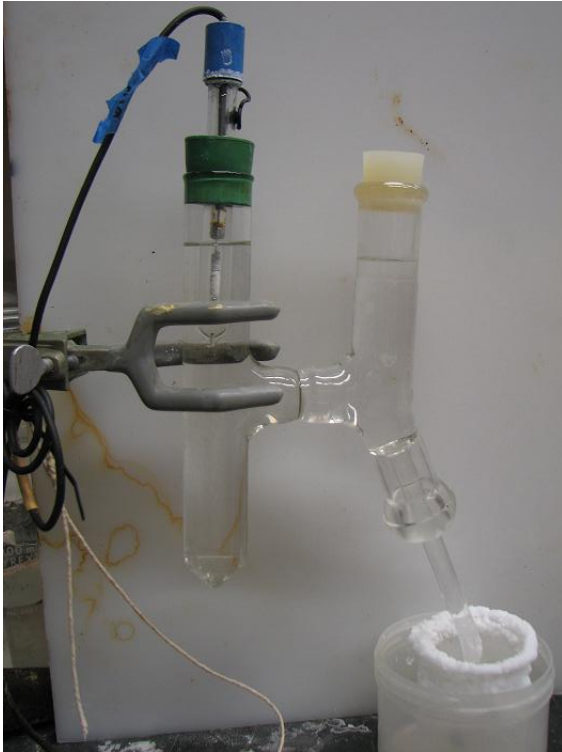


Figure 8.1: Saturated calomel reference electrode and salt bridge used in all experimental laboratory tests.

8.2.3.1 Long term tests

For the long term experimental testing, carbon steel and stainless steel corrosion coupons were placed directly in the solution. One five-liter capacity container was used for each solution type for a total of five containers. Three different corrosion coupons of each steel type were monitored in each solution. Figure 8.2 shows the complete set-up of one solution container, with the general, crevice, and waterline coupons



Figure 8.2: Example of long term test set-up. One solution container with carbon steel and stainless steel general, crevice, and waterline corrosion coupons.

The general corrosion coupons were completely submerged in the solution, resting on the bottom of the container on a $\frac{3}{8}$ -inch thick side, so that both polished faces of 1 $\frac{1}{4}$ -inch diameter were exposed to solution. Crevice corrosion and waterline corrosion coupons were placed in the solution as part of a rack assembly. A close-up view of a waterline rack assembly is shown in Figure 8.3.

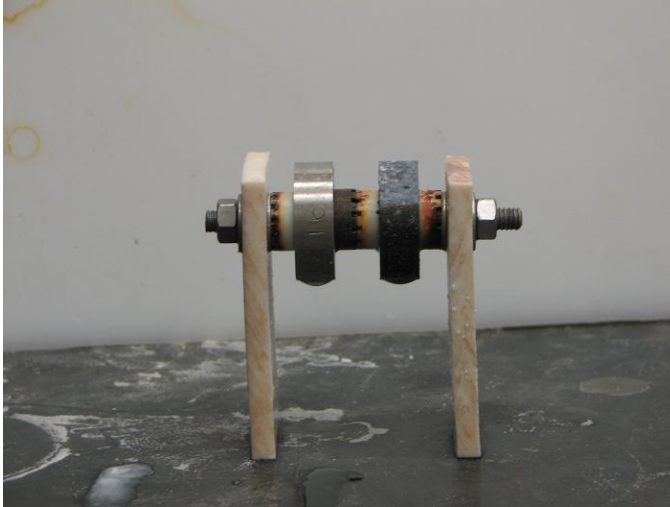


Figure 8.3: A waterline rack assembly with plastic washers electrically separating the stainless steel (left) and carbon steel (right) corrosion coupons.

The racks were composed of threaded rod supported by plastic end stands through which the rod passed. Stiff plastic tubing with an outside diameter of 916 mm was placed around the rod to prevent electrical contact between the corrosion coupons and the rod; the rod and tubing was fit through the holes drilled in the center of the coupons. Plastic washers, either crevice or flat, were placed in between the coupons to create a desired exposure surface on the coupon and for electrical separation between the carbon and stainless steel coupons. Nuts on the outside of the plastic end stands were used to tighten the assembly and hold it together. A torque wrench was used to consistently tighten the racks at a torque of 75 in-lb in accordance with ASTM G78: Standard Guide for Crevice Corrosion Testing of Iron-Base and Nickel-Base Stainless Alloys in Seawater and Other Chloride-Containing Aqueous Environments (ASTM 2001).

For the crevice corrosion coupons, crevice washers were positioned on both sides of the steel coupons. The uneven surface of the plastic crevice washers created a surface on the coupon in which the solution was in contact with the metal at small regular

locations where the washer material was cut away. The crevice corrosion coupons and racks were completely submerged in the solution.

For the waterline corrosion coupons, a flat washer surface in contact with the coupon was used to avoid crevice effects. The rack was placed in the solution such that the bottom half of the coupons were submerged while the top half remained outside of the solution. .

Three additional corrosion coupons were set up in the container of concentrated solution at pH 7.5 – carbon steel coupons of each type with the no zinc edge were included to provide a comparison to the coupons with the galvanized edge.

8.2.3.2 Electrochemical polarization tests

The equipment set-up used for the electrochemical polarization of the carbon steel and stainless steel was also used for the cyclic polarization of the stainless steel. The general set-up of the electrochemical polarization cell can be seen in Figure 8.4. The electrochemical polarization cell was a custom designed. As seen in Figure 8.4 the main component of the cell is a beaker of approximately 300 mL capacity with a spout to the side. The corrosion coupon was clamped at the opening of the spout, with a rubber O-ring sealing the contact of the specimen and the glass.

As the solution filled the beaker and came into contact with the face of the coupon, the O-ring formed a slight crevice on the polished metal surface. The possibility of crevice corrosion during the polarizations was recognized as it had an effect on the polarization results. In real life application, however, the bolt is also subjected to

significant crevice effects in the bearing assembly, and thus the conditions at the surface of the material during the polarizations simulated the anchor bolt environment.

Other components of the electrochemical polarization cell included the reference and counter electrodes. The reference electrode salt bridge entered the cell through the top opening and was clamped to a stand to secure the tip position next to the corrosion coupon. A platinum foil was introduced into the cell as a counter electrode, or cathode, during the polarization. The reference electrode, counter electrode, and corrosion coupon, or working electrode, were all electrically connected to the potentiostat and data were collected by the computer, as shown in Figure 8.5.

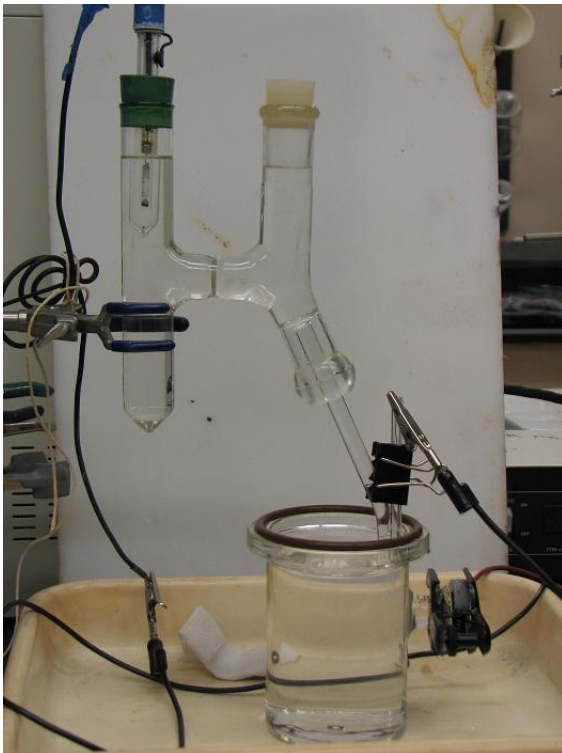


Figure 8.4: Experimental set-up for electrochemical polarization and cyclic polarization. The coupon that is being tested is clamped to the spout of the beaker.



Figure 8.5: Computer software collects data from the potentiostat, which is electrically connected to the electrodes in the electrochemical polarization cell.

8.2.3.3 *Galvanic and concentration coupling tests*

Several combinations of galvanically coupled metals exist in plate bearings. In newer bridges, carbon steel plates and flanges are in contact with stainless steel anchor bolts, and both carbon steel plates and stainless steel anchor bolts are in contact with bronze plates. In this series of experiments, all these combinations are reproduced in both normal and concentrated solution at a pH of 7.5.

Additionally, a concentration cell exists along the bolt itself. As part of the bolt is protected within high pH concrete, the rest is actively corroding outside of the concrete. To model this environment, concentration cells were also set-up experimentally between the pH 7.5 solutions and pH 13 solutions.

The corrosion coupons that were coupled had stainless steel wire spot welded to them. The face of the coupon to which the wire was welded and the wire itself were lacquered to prevent them from affecting the corrosion potentials. Wires from two

specimens were connected to provide the necessary electrical connection for corrosion. In all carbon steel and stainless steel connections, lacquer was used to set the anode and cathode areas equal. Similarly, the cast bronze plate had stainless steel wire spot welded to it, was lacquered, and was connected to either carbon steel, stainless steel, or both.

The same containers of solution as the long term tests were used for galvanic couples within the same solution. For concentration cell couples across two different solutions, the solution from the original containers was transferred to smaller containers so that a salt bridge could be placed in between the two to provide the necessary electrolytic connection, as shown in Figure 8.6.



Figure 8.6: Concentration cell coupling of similar metals in solutions with differing pH values. Stainless steel in solution with pH 13 is coupled with stainless steel in solution with pH 7.5, and carbon steel in solution with pH 13 is coupled with carbon steel in solution with pH 7.5.

8.3 Experimental procedures

8.3.1 Potential readings

Corrosion potential of exposed steel samples versus the saturated calomel reference electrode was measured using the salt bridge described in Section 8.2.3, a stainless steel wire probe, and a voltmeter. The voltmeter leads were connected to the reference electrode and the stainless steel wire probe. The salt bridge tip was placed within a centimeter of the corrosion coupon for which the reading was taken. When the wire probe firmly touched the coupon, an electrical potential difference reading between the coupon and the reference electrode was recorded. Care was taken to isolate all but the tip of the stainless steel wire probe to avoid creating a mixed potential reading of the corrosion coupon and the wire probe.

8.3.2 Electrochemical polarization tests

As described in Section 8.2.3, the reference electrode, counter electrode, and working electrode in the polarization cell were all connected electrically to a potentiostat. In the electrochemical polarization tests potentiodynamic potentials were applied to the specimen and the corresponding currents were recorded. As explained in Chapter 3, a plot of the voltages and corresponding current densities on log scale generates the polarization curve, which can be used to provide insight to the material corrosion behavior.

8.3.3 Cyclic polarization

Cyclic polarization applies the same concepts as electrochemical polarization described in Chapter 3 and the experimental procedure as described in Section 8.3.2. The test receives its name, however, from a cycling of the applied voltage. After the applied voltage has reached a set peak, it is subsequently decreased and the corresponding behavior of the current density is examined for evidence of localized corrosion.

8.3.4 Polarization resistance

The polarization resistance method as described in Chapter 3 was used for determining active corrosion rates on samples in both the long term test and the galvanic and concentration cell coupling tests. To measure the polarization resistance, the potentiostat was electrically connected to the reference electrode, platinum counter electrode, and working electrode. The polarization resistance curve was generated by plotting the overvoltages, within a few millivolts of the corrosion coupons' stable corrosion potential, versus the current. From these curves, the corrosion rates of the corrosion coupons were extracted according to the equations presented in Chapter 3, and using assumed Tafel constants equal to 0.12 volts..

8.4 Results

8.4.1 Long term tests

8.4.1.1 Corrosion potential readings

The following graphs, Figures 8.7 through 8.11, are representative of the long term corrosion potential measurements. The graphs shown are for the steel samples exposed to the concentrated test solution with pH 7.5 and pH 13. No significant difference in the corrosion potential readings was observed between steel samples exposed to the normal and concentrated solutions. A complete set of graphs for the normal solution and pore solution environments is given in Appendix D. In these graphs more negative potential difference values in the range of -0.9 to -0.6 volts indicates active corrosion, while more positive potential difference values in the range of -0.4 to 0.0 volts indicate passive behavior of the material.

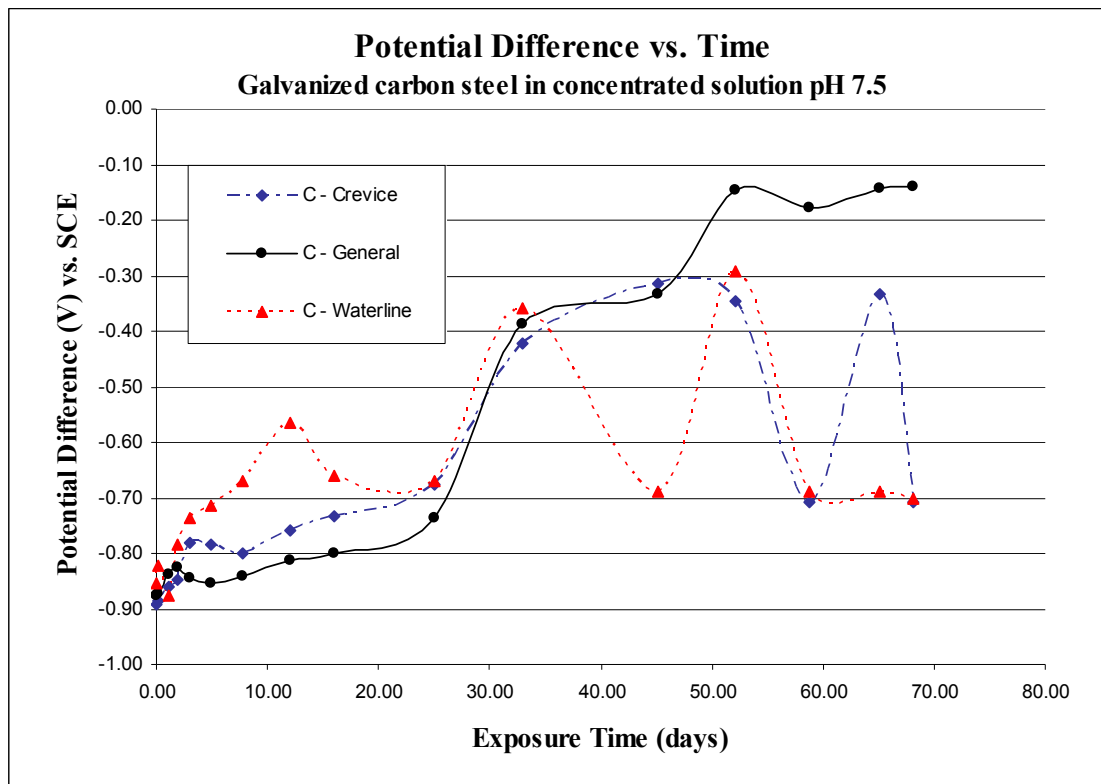


Figure 8.7: Long term corrosion potential readings of galvanized carbon steel corrosion coupons in the concentrated solution at pH 7.5. The galvanized carbon steel displays unstable passivity with potentials undulating between active and passive values.

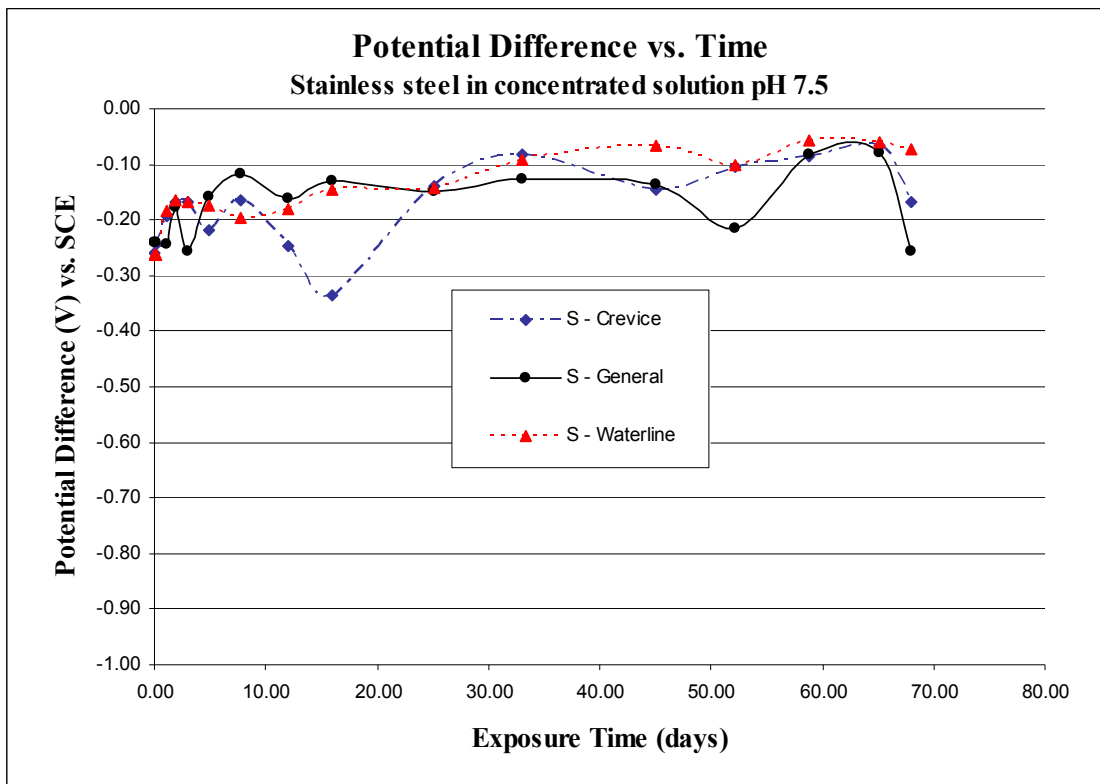


Figure 8.8: Long term corrosion potential readings of stainless steel corrosion coupons in the concentrated solution at pH 7.5. The stainless steel coupons have passive corrosion potentials.

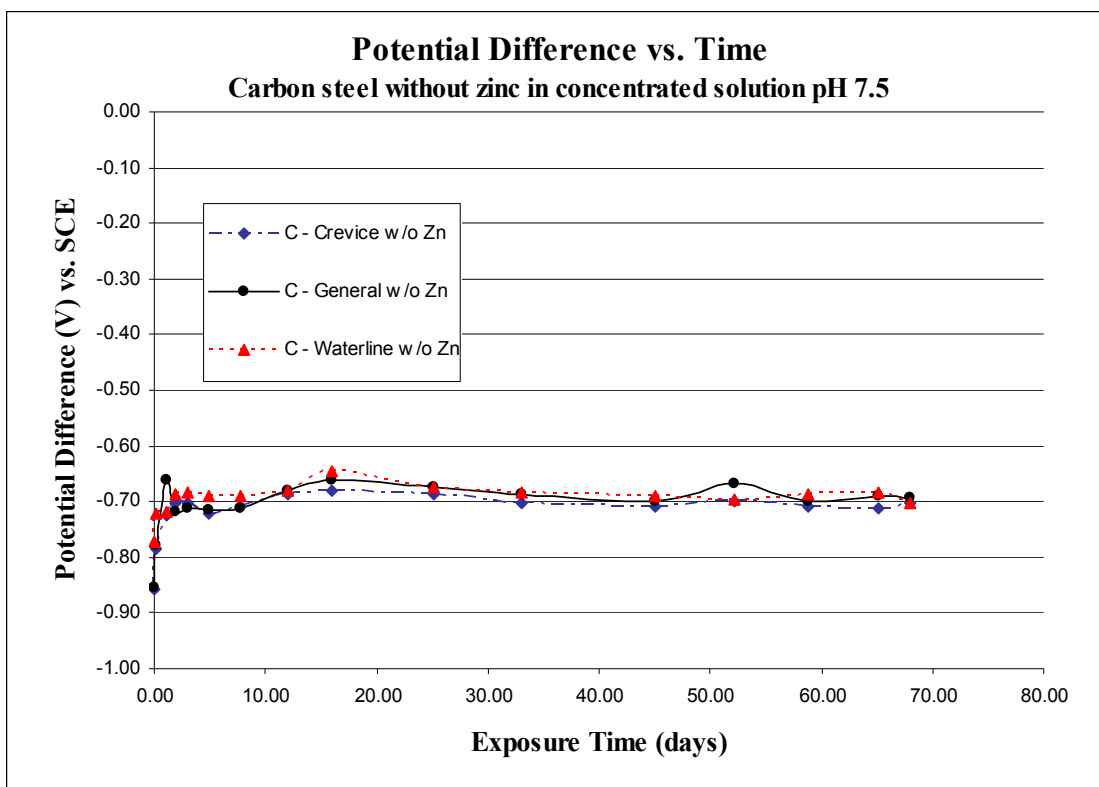


Figure 8.9: Long term corrosion potential readings of carbon steel corrosion coupons without zinc in the concentrated solution at pH 7.5. The carbon steel coupons without zinc have active corrosion potentials.

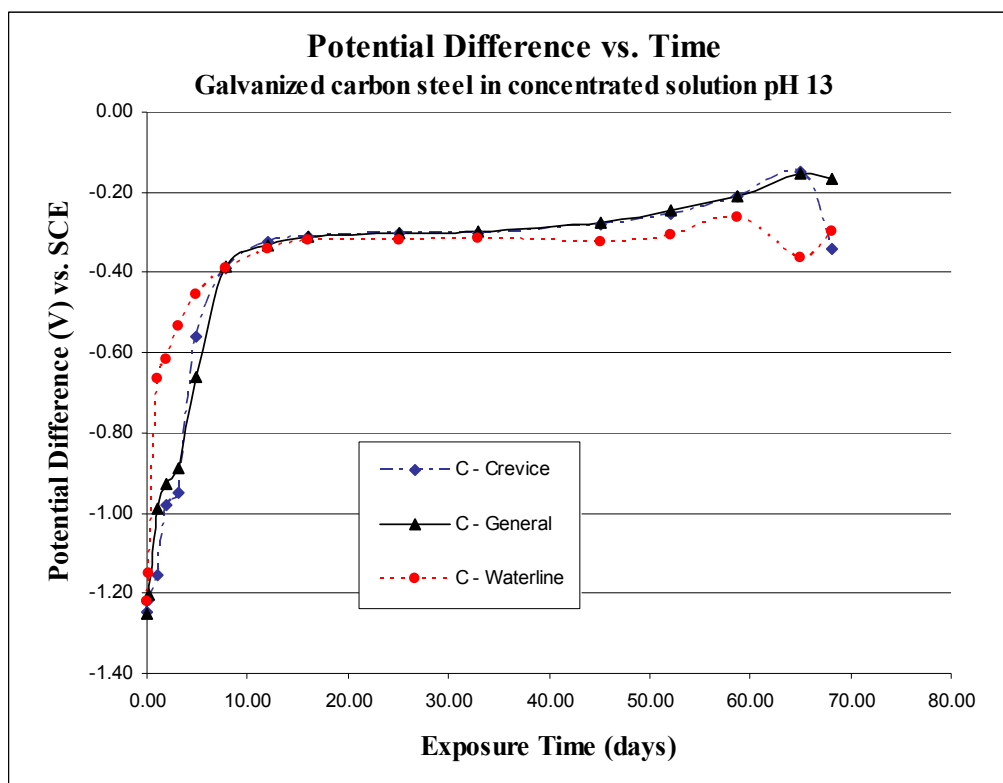


Figure 8.10: Long term corrosion potential readings of galvanized carbon steel corrosion coupons in the concentrated solution at pH 13. The carbon steel coupons achieve passive potentials.

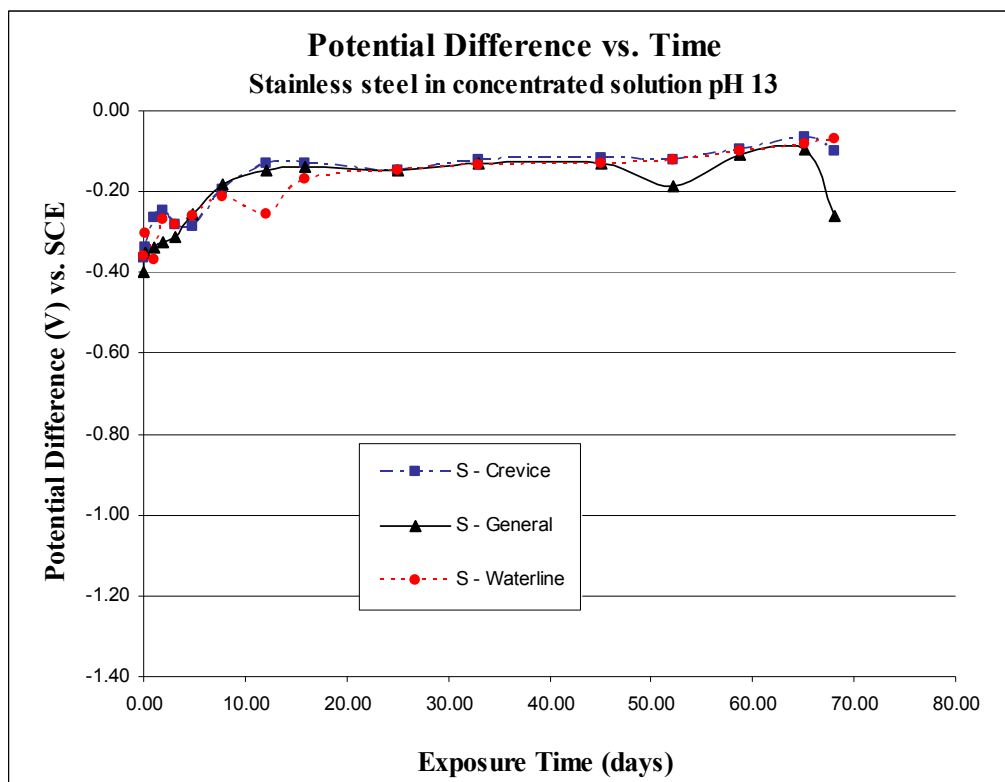


Figure 8.11: Long term corrosion potential readings of stainless steel corrosion coupons in the concentrated solution at pH 13. The stainless steel coupons have passive potentials.

From these graphs several key observations are revealed. The first is that in solutions of both pH 7.5 and pH 13, and likewise in all solution types, the stainless steel demonstrated passive behavior with corrosion potential values in the range of -0.1 to -0.2 volts versus the saturated calomel reference electrode. Similarly, the carbon steel coupons displayed passive behavior in the range of -0.2 to -0.4 volts in solutions with high pH values. However, at the lower pH value, the carbon steel did not exhibit stable passivity. In fact, the corrosion potentials of the carbon steel coupons without the zinc edge remained constantly active with no indication of passivity.

In both the normal and concentrated solutions at pH 7.5 the galvanized carbon steel coupons sustained active corrosion potentials for the first 20 to 30 days. As shown

in Figures 8.7 and 8.9, the galvanized coupons were initially more active than the coupons with no zinc, with potentials in the range of -0.9 to -0.8 compared to -0.7. The zinc had effectively lowered the corrosion potential difference by preferentially corroding at a lower potential than the carbon steel. The corrosion potentials of the galvanized coupons universally increased at 30 days, which can be interpreted as the time when the zinc coating became ineffective. As the zinc protection dissolved, the corrosion potentials of the galvanized coupons undulated between active and passive values, signifying unstable passive behavior of the carbon steel. The dissolution of the zinc layer and the unstable passivity of the carbon steel proved that the zinc protection on galvanized carbon steel bolts can not be effectively sustained for the entire bridge service life.

8.4.1.2 Corrosion rates

After the final corrosion potential readings, the corrosion rates of the general and crevice coupons were found using two methods, polarization resistance and gravimetric calculation. Table 8.2 provides the corrosion rates found by both methods for select coupons. The complete table of results is included in Appendix D.

Table 8.2: Corrosion rates calculated by polarization resistance and gravimetric methods for select corrosion coupons.

ID	Time exposed (days)	Coupon type	Exposure solution/pH	Initial weight (grams)	Final weight (grams)	Final - Initial (mg)	Corrosion Rate	
							wt. loss (mpy)	Polar. resistance (mpy)
C5	68	general	conc / 13	65.5903	65.5764	13.90	0.147	0.043
C7	68	general (no zinc)	conc / 7.5	65.0630	64.8046	258.40	6.470	3.129
C10	69	crevice	norm / 7.5	60.4340	60.3313	102.70	1.197	1.926
C12	68	crevice	conc / 7.5	59.4293	59.3004	128.90	1.525	2.307
C21	68	crevice (no zinc)	conc / 7.5	58.8939	58.6487	245.20	6.139	4.574
S3	68	general	conc / 7.5	65.6472	65.6464	0.80	0.008	0.015
S7	69	crevice	norm / 7.5	57.9295	57.9278	1.70	0.020	0.001

In general, the corrosion rates by gravimetric method were found to correspond to measurements by the polarization resistant method, and the corrosion rates correlated with the corrosion behavior predicted by the corrosion potential measurements. The stainless steel coupons and carbon steel coupons in high pH solution, in which stable passive potential values were measured as shown in Figures 8.8, 8.10 and 8.11, were found to have corrosion rates of less than one mil per year (mpy); corrosion rates less than one mpy, or 0.001 inch penetration per year, are considered negligible. In contrast, the carbon steel coupons with no zinc, in which constant active potential values were measured as shown in Figure 8.9, were found to have the highest corrosion rates. The galvanized carbon steel crevice corrosion coupons in solutions of pH 7.5 were found to have corrosion rates greater than one mpy, and are expected to have higher corrosion rates similar to the carbon steel samples without zinc, as the passivity of the samples breaks down following the dissolution of zinc.

8.4.2 Electrochemical polarization curves

Electrochemical polarization curves for each tested material in each solution type further characterize material corrosion patterns. The following polarization curves of potential versus the log of current density, shown in Figures 8.12 through 8.15, are representative of the polarization behaviors of carbon steel and stainless steel in solutions of pH 7.5 and pH 13. For each experimental polarization curve, three tests were conducted on polished coupons to ensure reproducible and accurate results.

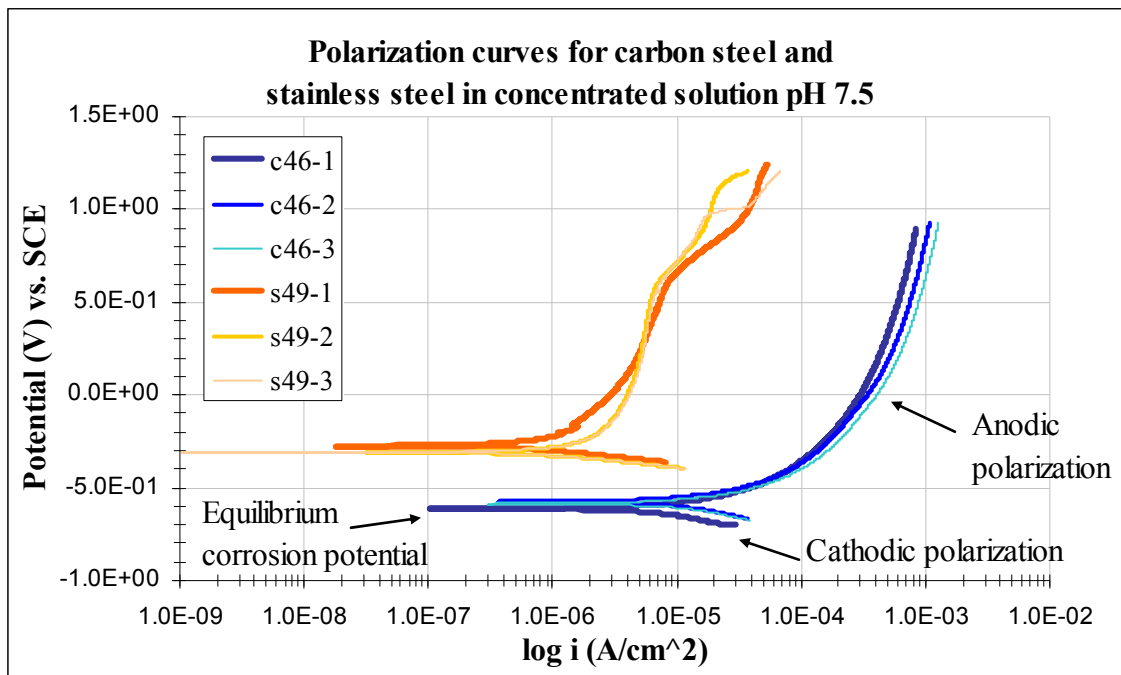


Figure 8.12: Electrochemical polarization curves for stainless steel and carbon steel in concentrated solution with pH 7.5. The stainless steel displayed passivity, while the carbon steel actively corroded at significantly higher current densities.

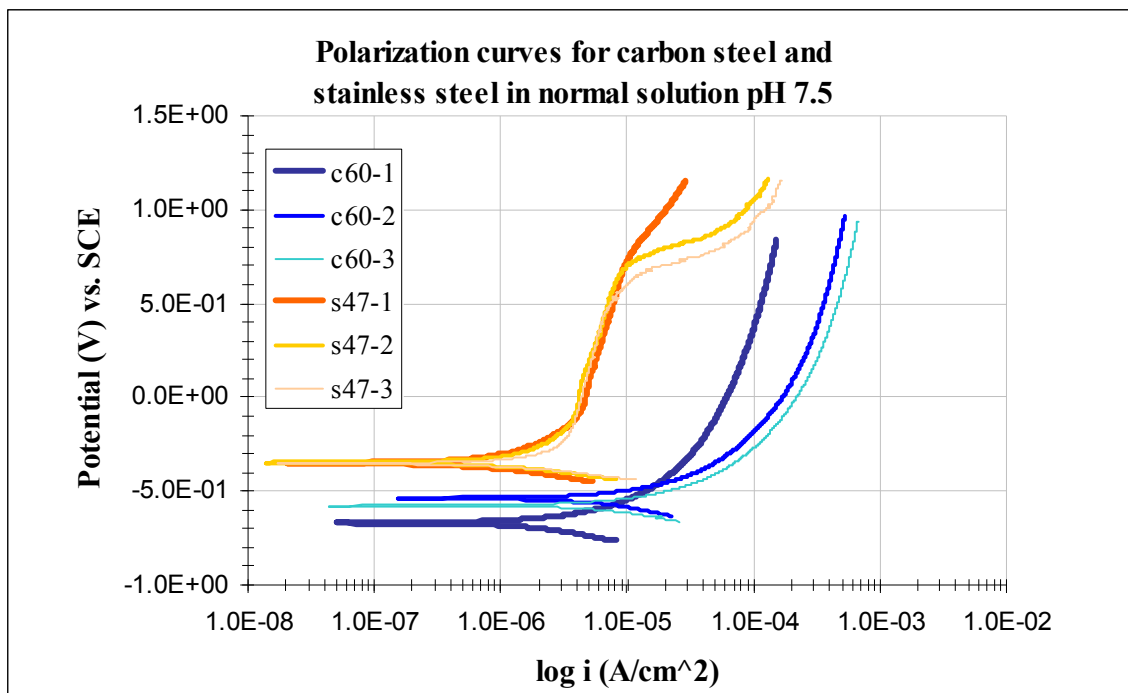


Figure 8.13: Electrochemical polarization curves for stainless steel and carbon steel in normal solution with pH 7.5. The stainless steel displayed passivity similar to stainless steel in concentrated solution, while the carbon steel actively corroded at current densities lower than current densities for carbon steel in concentrated solution.

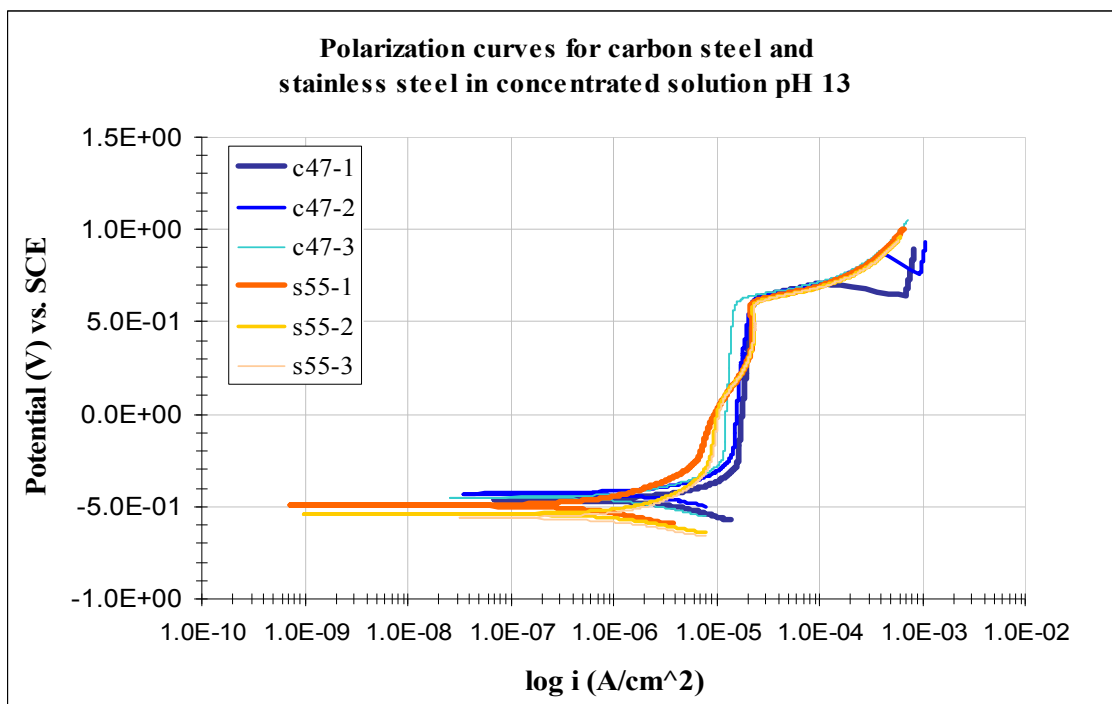


Figure 8.14: Electrochemical polarization curves for stainless steel and carbon steel in concentrated solution with pH 13. The stainless steel and carbon steel displayed similar passive behavior.

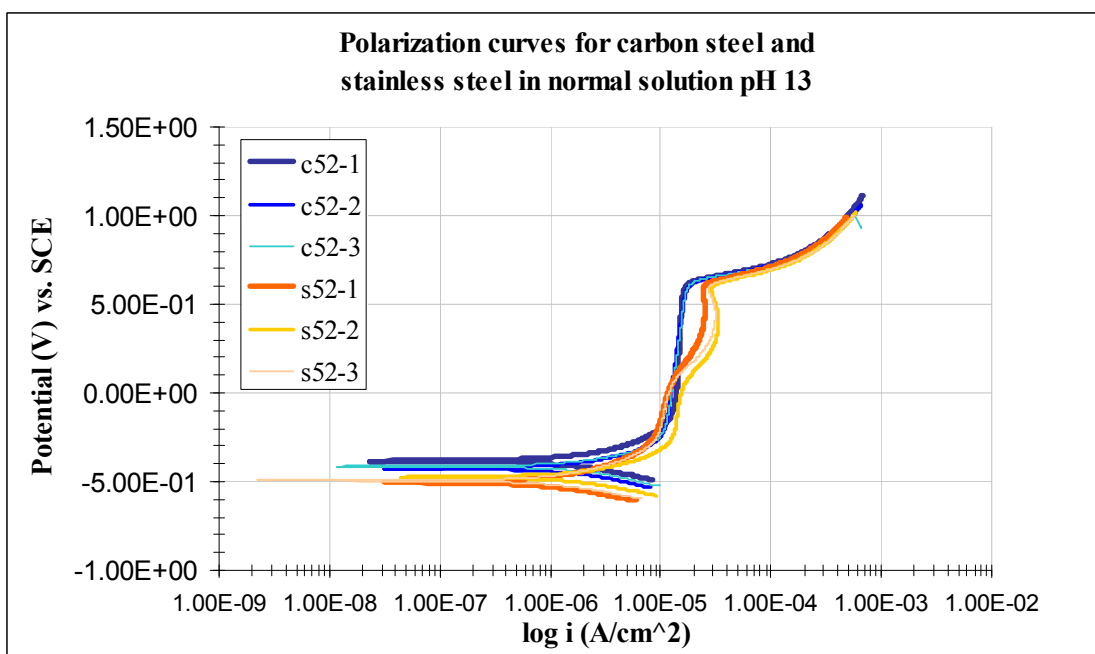


Figure 8.15: Electrochemical polarization curves for stainless steel and carbon steel in normal solution with pH 13. The stainless steel and carbon steel displayed similar passive behavior to each other and to the steels in concentrated solution at pH 13.

The horizontal portion of the curve corresponds to the open circuit, or equilibrium, corrosion potential of the coupon; the portion of the curve below the horizontal curve is the cathodic polarization of the sample and the portion above the horizontal curve is the anodic polarization, as labeled in Figure 8.12. The corrosion behavior of the material is interpreted from the anodic portion of the curve. In the curves shown in Figures 8.12 through 8.15, a nearly vertical slope in the curve indicates passive behavior of metal in that solution. Due to the fast potential scan rate used in these tests, 2 mV/s, a lower current density does not correspond to the passive region because the steel specimen did not come to a steady state at each point along the curve before the voltage was increased. If the steel sample had come to a steady state at each point before the voltage was increased, a decrease in the current density would have been observed along the vertical slope.

From the polarization curves, previous observations from the long term test were confirmed and new observations were made. First, the polarization curves verified the long term corrosion potential readings in high pH solutions. The stainless steel and carbon steel exhibited nearly the same stable passivity in both the solutions with pH 13. Second, in the solutions with pH 7.5, the polarization curves for stainless steel contained a region with a vertical slope, confirming that the stainless steel passivated, while the polarization curves for carbon steel did not, indicating active corrosion with no tendency for the carbon steel to passivate under these conditions.

In addition to insight on the active or passive behavior of the material, the polarization curves offer perspective on the material's corrosion rate. As shown in Figure 8.12, the current densities of the carbon steel are several orders of magnitude higher than

those for stainless steel at the same potential. This difference could translate into corrosion rates that are up to 100 times higher for carbon steel than stainless steel under environmental conditions representing that potential. Furthermore, the current densities as a function of the potential are nearly the same for stainless steel in concentrated solution compared to stainless steel in normal solution, as shown by comparing Figures 8.12 and 8.13, but the current densities versus potential for carbon steel vary with respect to the solution concentration. Although less than one order of magnitude, the current densities versus potential of carbon steel are higher in the concentrated solution in Figure 8.12 compared to the carbon steel polarization curve in normal solution in Figure 8.13, indicating that corrosion rates for carbon steel will be up to 10 times higher in the concentrated solution.

8.4.3 Cyclic polarization curves

Cyclic polarization curves are used to evaluate a material's resistance to localized corrosion attack. As the applied voltages are decreased, the response of the current densities indicates whether localized corrosion can occur during the process of the polarization. If the plot of the current density as a function of the voltage during the reverse scan of potential follows the same curve that was created during the forward scan of voltage polarization, then no localized corrosion is expected to occur. However, if the current densities are higher during the reverse scan than they were during forward scan at the same voltages, then the curve forms a hysteresis. This hysteretic curve is an indication that localized corrosion has occurred, because it shows that the passive layer has been broken and cannot be reformed. The area contained by the hysteretic loop correlates to

the voltages at which localized corrosion occurs, and the passive layer cannot repair itself.

Therefore the point at which the hysteretic curve crosses over the curve of the initial polarization is of special interest. If the hysteresis crosses the polarization curve within the passive region above the open circuit potential, then a margin of applied voltage exists in which localized corrosion will not occur. This point is called the protection potential. For example, in Figure 8.16 the hysteretic curve for sample s30-1 crosses the original polarization curve at 0.0 volts. Since the open circuit potential of that material was found to be -0.3 volts, localized corrosion will not be induced when that sample is at its equilibrium potential, and a range of 0.3 volts exists in which the material can be polarized without inducing localized corrosion. However, if the material is polarized beyond the protection potential of 0.0 volts, or more than the 0.3 volt range, then localized corrosion will occur.

The cyclic polarization curves shown in Figures 8.16, 8.19, and 8.20 were created in concentrated solution at pH 7.5 with the Type 304 stainless steel anchor bolt material and other candidate alloys that may be considered for anchor bolt use. The cyclic polarization of steel samples exposed to concentrated solutions at pH 7.5 is more critical than cyclic polarization of steel samples in normal solution at pH 7.5 because protection potentials are lower in concentrated solutions. Cyclic polarization curves for candidate steel alloys in normal solution can be found in Appendix D.

The curves in Figure 8.16 were produced using a corrosion coupon from the Type 304 stainless steel anchor bolt and the same equipment set-up as described in Section 8.2.3 for the polarization tests. As can be seen in Figure 8.16, the 304 stainless steel is

susceptible to localized corrosion at high potentials and has a relatively low protection potential. Figures 8.17 and 8.18 show images at 32 x magnification of the crevices and pits formed on the surface of the coupon during the test, respectively. However, all the potential measurements of the 304 stainless steel at equilibrium in the long term test fell below the protection potential, indicating that for typical conditions at a bridge bearing the Type 304 stainless steel anchor bolt will be protected from localized corrosion.

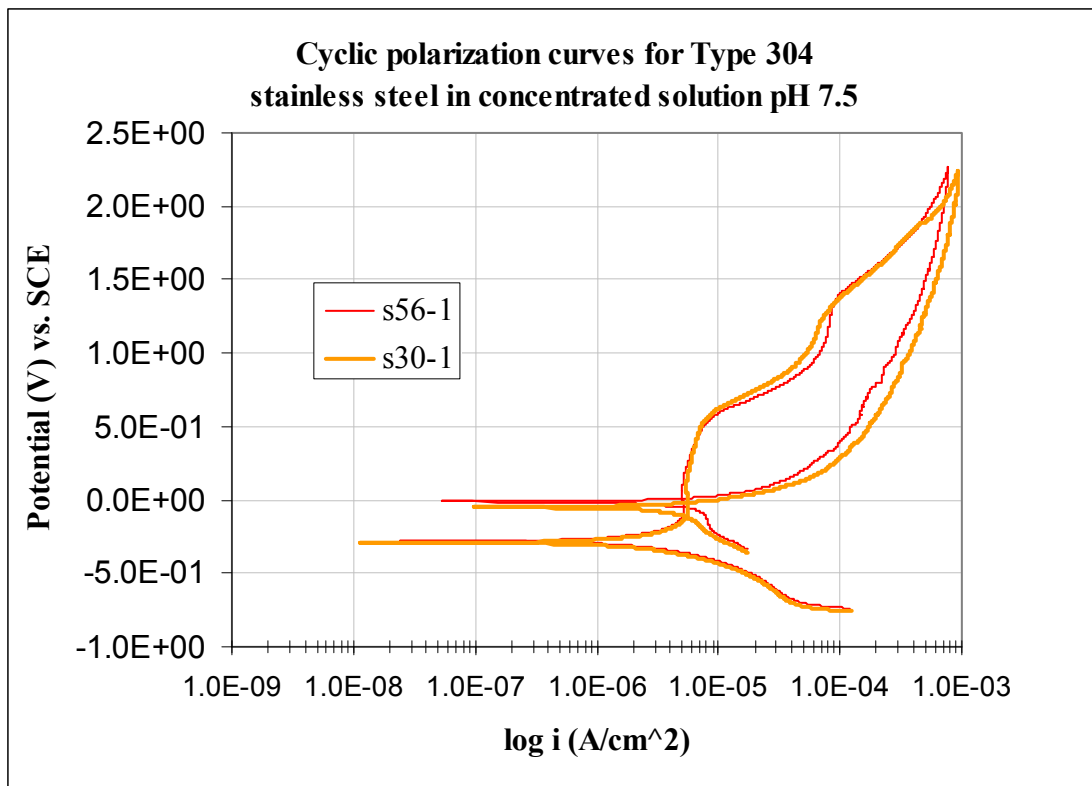


Figure 8.16: Cyclic polarization curves for Type 304 stainless steel subjected to localized corrosion. The protection potential is higher than the potential readings taken during the long term test of the same material, indicating that this material is protected from localized corrosion in this environment.

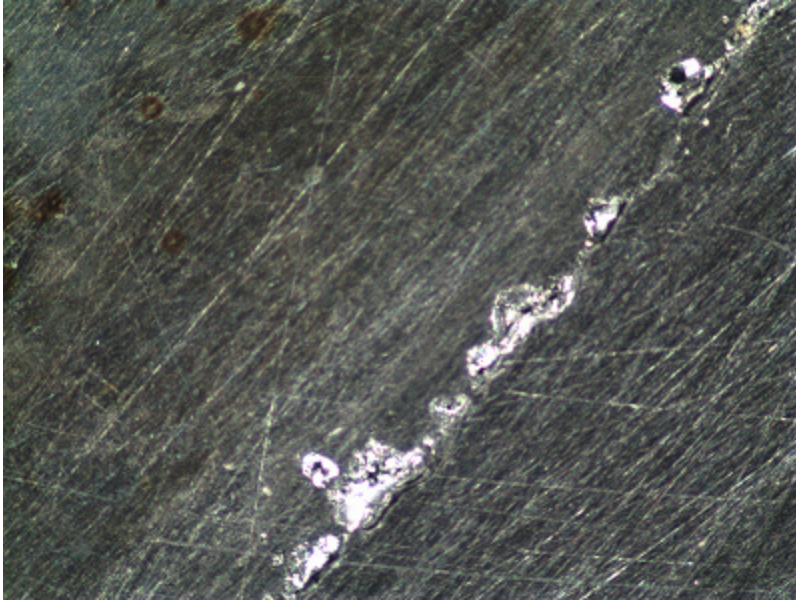


Figure 8.17: Crevice formed on stainless steel corrosion coupon during cyclic polarization at 32 x magnification. The O-ring sealing the coupon to the glass opening in the polarization set-up created the crevice. Anchor bolts are also exposed to crevice conditions in the bearing.

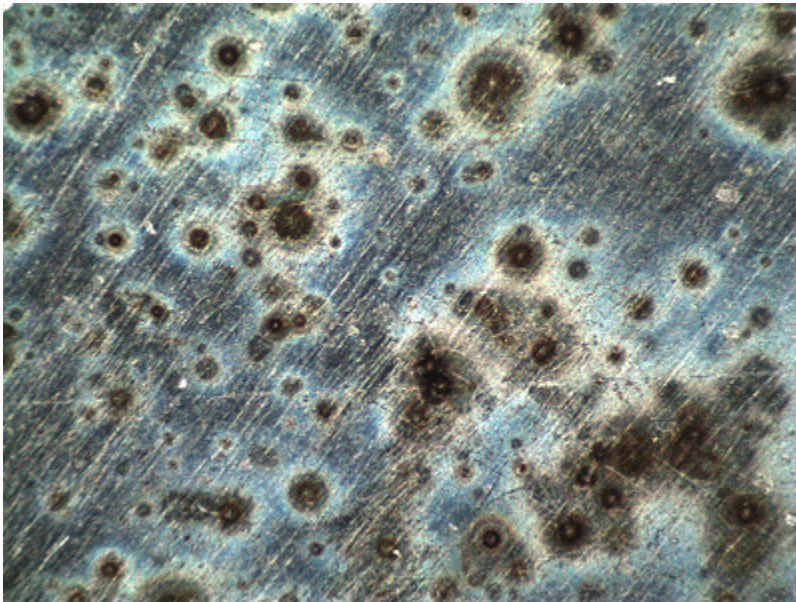


Figure 8.18: Pitting on the surface of the stainless steel corrosion coupon during cyclic polarization at 32 x magnification. The typical environment at a bridge bearing will not induce pitting corrosion in Type 304 stainless steel anchor bolts.

The cyclic polarization curves in Figures 8.19 and 8.20 were created from manufactured corrosion coupons of candidate alloys which may be considered for anchor bolt use. These alloys were Type 304 stainless steel, Type 316 stainless steel, and the duplex stainless steel alloys 2101 and 2205. The equipment set up for these tests required that the coupons be dipped into the solution, rather than clamped to the spout on the beaker. The specimens used to create the curves in Figure 8.19 were not subjected to crevice conditions, and the figure presents cyclic polarization data in which the samples were only susceptible to pitting corrosion. The samples used to create the curves in Figure 8.20 were lacquered to control the exposed surface area. By lacquering the samples, crevices were created at holidays in the seal, and Figure 8.20 presents cyclic polarization data in which the samples were susceptible to pitting and crevice corrosion.

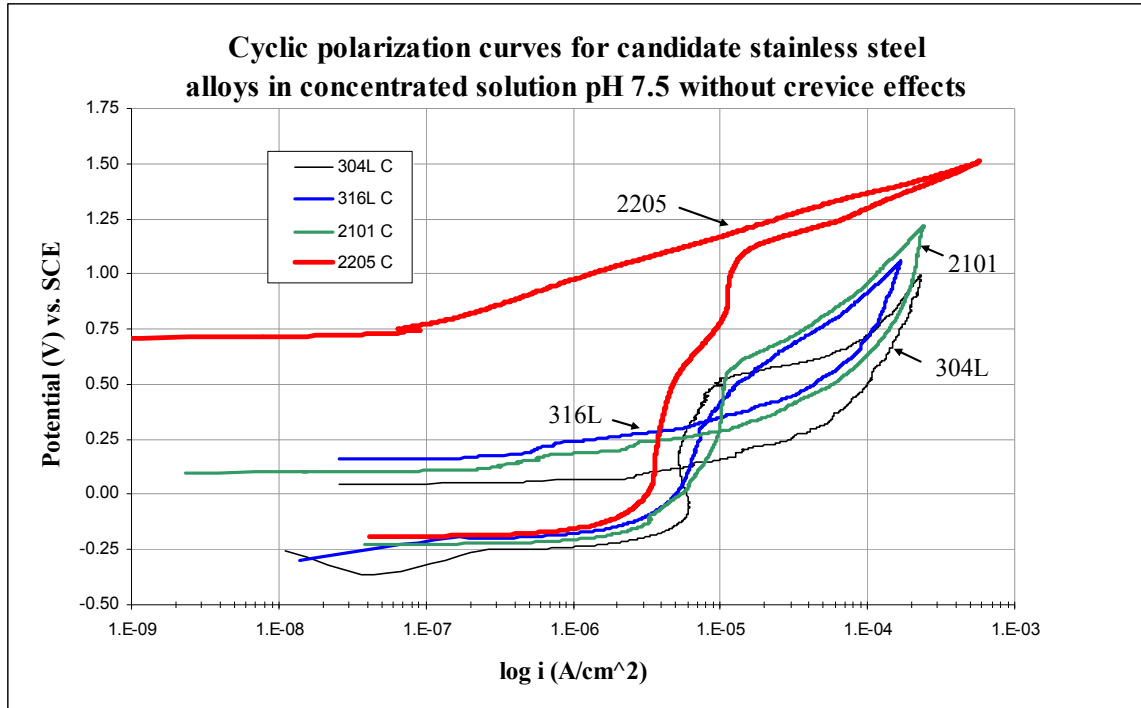


Figure 8.19: Cyclic polarization of candidate alloys which may be considered for anchor bolt use. Type 316, Type 2101, and 2205 stainless steel alloys are considered acceptable alternative materials to Type 304 stainless steel.

The results shown in Figure 8.19 clearly indicate that duplex stainless steel 2205 did not show any susceptibility to pitting corrosion in concentrated solution at pH 7.5. In contrast, the other tested steel grades showed a hysteresis in their cyclic polarization curves, indicating their susceptibility to pitting under the same oxidizing conditions. Regardless, the protection potentials indicated in Figures 8.19 are sufficiently high that localized corrosion will not be induced in Type 304, 316, 2102, or 2205 stainless steel alloys in concentrated solution at pH 7.5.

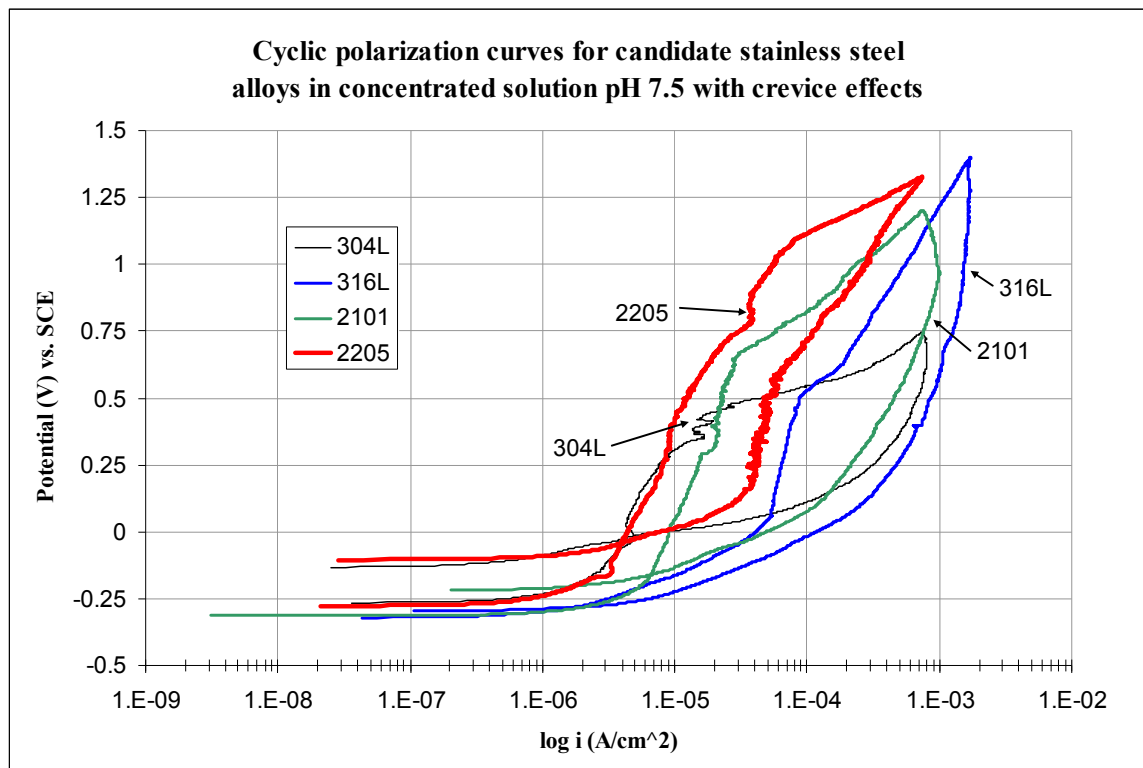


Figure 8.20: Cyclic polarization of candidate alloys which may be considered for anchor bolt use. The materials in this test were subjected to crevice effects resulting in a decrease in the protection potentials.

As shown by comparing the results shown in Figure 8.19 to the results in Figure 8.20 the protection potentials of all the materials significantly decrease with the introduction of crevice effects. A crevice condition on the surface of the stainless steel alloys causes the material to be more susceptible to localized corrosion. As discussed in Chapter 3, protection potentials for crevice corrosion cannot be predicted because the geometry and exposure of the crevice, which is specific to individual applications, affects the corrosion behavior. The best protection from crevice corrosion is the elimination of crevice conditions.

8.4.4 Galvanic and concentration cell coupling

8.4.4.1 Galvanic coupling between dissimilar metals

Galvanic corrosion cells between dissimilar metals that exist within a typical plate bearing were simulated in the laboratory in both the normal and concentrated solutions of pH 7.5. These galvanic couples are electrical connections of: (1) stainless steel and carbon steel, (2) stainless steel and bronze, (3) carbon steel and bronze, and (4) stainless steel and carbon steel and bronze.

Once the mixed corrosion potential reached equilibrium for the couple, the corrosion rate of the anode was measured using the polarization resistance method described in Section 8.3.4. Table 8.3 compares the equilibrium corrosion potential of the couple to the corrosion potential of the individual materials in the same solution.

Table 8.3: Comparison of equilibrium corrosion potentials of galvanically coupled coupons to corrosion potentials of non-coupled coupons in the same solution. When coupled, the materials polarized each other.

Galvanic couple		Anodic metal	Equilibrium potential (V)	Uncoupled coupon	Corrosion potential (V)	Notes
Normal Solution pH 7.5	cs to ss	cs	-0.670	C1	-0.163	cs corrosion potential is more active
	cs to bronze	cs	-0.615	C1	-0.163	cs corrosion potential is more active
	ss to bronze	ss	-0.085	S1	-0.120	potential change for ss is negligible
	ss to cs to bronze	cs	-0.543	C1	-0.163	cs corrosion potential is more active
Conc. Solution pH 7.5	cs to ss	cs	-0.714	C3	-0.141	cs corrosion potential is more active
	cs to bronze	cs	-0.640	C3	-0.141	cs corrosion potential is more active
	ss to bronze	ss	-0.104	S3	-0.079	potential change for ss is negligible
	ss to cs to bronze	cs	-0.601	C3	-0.141	cs corrosion potential is more active

The differences in the equilibrium potentials of the coupled specimens compared to the corrosion potentials of the individual specimens shows that the materials polarize each other when electrically connected, and the equilibrium potential for the anodic material becomes more active. Table 8.4 qualitatively compares the corrosion rates of the anodic specimen in the couple to the corresponding corrosion rate measured gravimetrically in the long term test for a coupon of the same material in the same solution that was not galvanically coupled. For the comparison the corrosion rates based on an equal cathode to anode ratio was calculated.

Table 8.4: Qualitative comparison of corrosion rates of galvanically coupled coupons to corrosion rates of non-coupled coupons in the same solution. Corrosion rates increased for the carbon steel when coupled with the more noble stainless steel or bronze.

Galvanic couple		Anodic metal	Corrosion rate (mpy)	Uncoupled coupon	Corrosion rate (mpy)	Notes
Normal Solution pH 7.5	cs to ss	cs	10.27	C1	1.074	carbon steel corrosion rate increased ~10 times
	cs to bronze	cs	6.07	C1	1.074	carbon steel corrosion rate increased ~ 5 times
	ss to bronze	ss	0.06	S1	0.013	Corrosion rates are negligible
	ss to cs to bronze	cs	2.01	C1	1.074	carbon steel corrosion rate increased ~ 2 times
Conc. Solution pH 7.5	cs to ss	cs	7.66	C3	0.678	carbon steel corrosion rate increased ~ 10 times
	cs to bronze	cs	5.42	C3	0.678	carbon steel corrosion rate increased ~ 5 times
	ss to bronze	ss	0.07	S3	0.008	Corrosion rates are negligible
	ss to cs to bronze	cs	2.50	C3	0.678	carbon steel corrosion rate increased ~ 2 times

For an equal cathode to anode ratio, the corrosion rates of carbon steel increased by approximately two to ten times when galvanically coupled to more noble metals, as compared to the already high corrosion rate of carbon steel alone.

8.4.4.2 Concentration cell coupling on same metal

Concentration cells between two different environments to which anchor bolts are simultaneously exposed were simulated in the laboratory. The part of an anchor bolt embedded in the concrete support is exposed to a high pH solution, while the part protruding from the concrete is exposed to a solution closer to a neutral pH, like the solution presented in Table 8.1. Samples of carbon steel and stainless steel were electrically connected such that: (1) carbon steel in normal solution at pH 7.5 was connected to carbon steel in normal solution at pH 13, (2) stainless steel in normal solution at pH 7.5 was connected to stainless steel in normal solution at pH 13, (3) carbon steel in concentrated solution at pH 7.5 was connected to carbon steel in concentrated solution at pH 13, and (4) stainless steel in concentrated solution at pH 7.5 was connected to stainless steel in concentrated solution at pH 13.

Once the mixed corrosion potential reached equilibrium for the couple, the corrosion rate of the anode was measured using the polarization resistance method described in Section 8.3.4. Table 8.5 compares the equilibrium corrosion potential of the couple to the corrosion potential of the individual materials in the same solution.

Table 8.5: Comparison of equilibrium corrosion potentials of coupons coupled in concentration cells to corrosion potentials of non-coupled coupons in the same solution. When coupled, the materials polarized each other.

Concentration cell couple		Anodic metal	Equilibrium potential (V)	Uncoupled coupon	Corrosion potential (V)	Notes
Normal Solution	cs pH 7.5 to cs pH 13	cs pH 7.5	-0.542*	C1	-0.163	the coupled material has a more active potential
	ss pH 7.5 to ss pH 13	ss pH 7.5	-0.418*	S1	-0.089	the coupled material has a more active potential
Conc. Solution	cs pH 7.5 to cs pH 13	cs pH 7.5	-0.627	C3	-0.141	the coupled material has a more active potential
	ss pH 7.5 to ss pH 13	ss pH 7.5	-0.359	S3	-0.079	the coupled material has a more active potential

*Note: Corrosion potentials for couples in normal solution were not at equilibrium at the time of corrosion measurements.

The differences in the equilibrium potentials of the coupled specimens compared to the corrosion potentials of the individual specimens proves that the materials polarize each other when electrically connected. Even though the couples in the normal solution had not completely polarized each other to the point of equilibrium after six weeks of electrical connection, the effects of the connection were apparent in the difference in corrosion potential and corrosion rate compared to uncoupled coupons, nonetheless. The anodic material is polarized to a more active equilibrium potential.

Table 8.6 qualitatively compares the corrosion rates of the anodic specimen in the couple to the corresponding corrosion rate measured gravimetrically in the long term test for a coupon of the same material in the same solution that was not coupled in a concentration cell. For the comparison the corrosion rates based on an equal cathode to anode ratio was calculated.

Table 8.6: Qualitative comparison of corrosion rates of coupons coupled in concentration cells to corrosion rates of non-coupled coupons in the same solution. Corrosion rates increased for the carbon steel coupled coupons.

Concentration cell couple		Anodic metal	Corrosion rate (mpy)	Uncoupled coupon	Corrosion rate (mpy)	Notes
Normal Solution	cs pH 7.5 to cs pH 13	cs pH 7.5	4.677	C1	1.074	carbon steel corrosion rate increased ~4 times
	ss pH 7.5 to ss pH 13	ss pH 7.5	1.146	S1	0.013	Corrosion rates are negligible
Conc. Solution	cs pH 7.5 to cs pH 13	cs pH 7.5	4.226	C3	0.678	carbon steel corrosion rate increased ~6 times
	ss pH 7.5 to ss pH 13	ss pH 7.5	330.2×10^{-3}	S3	0.008	Corrosion rates are negligible

For an equal cathode to anode ratio, the corrosion rates of carbon steel in pH 7.5 solution increased by approximately four to six times, as compared to the already high corrosion rate of carbon steel alone, when coupled in a concentration cell to passive carbon steel in pH 13 solution. On the other hand, the corrosion rates of the stainless steel were not affected by the concentration cell coupling, because the stainless steel was passive in both environments.

CHAPTER 9: DISCUSSION

9.1 Causes of anchor bolt corrosion

Corrosion of bridge bearings and anchor bolts was observed throughout the state of Georgia; corrosion affected the bolt shaft, nuts, washers, and bearing plates. By comparing what was observed in the field with laboratory test results and corrosion theory, several corrosion mechanisms were identified as the main contributing factors of anchor bolt corrosion in Georgia.

The first form of corrosion identified was concentration cell corrosion which affects the anchor bolt shaft and can be attributed to the fact that the bolts are partially embedded in concrete. The corrosion of the bolts' nuts and washers and the corrosion of the bearing plates are independent of concentration cell corrosion and are caused by the environmental conditions at the bearing. Both the corrosion of the materials in the bearing environment and the effects of partial embedment are relevant to anchor bolt corrosion in Georgia.

The three corrosion mechanisms presented in this section were determined to influence the corrosion behavior of the bearing assembly the most. However, anchor bolt and bearing corrosion is not exclusively defined by these three corrosion mechanisms.

9.1.1 Concentration cell corrosion

As first discussed in Chapter 3, high pH is known to aid the passivation of steel; the typical solution inside concrete is approximately pH 13. Therefore, the part of the anchor bolt embedded in the concrete pier cap is presumably passive and is protected

from corrosion. On the other hand, the typical bearing environment on top of the concrete support is pH 7.5. Theoretically, the difference in the environments creates a differing corrosion potential for the carbon steel in each environment.

Laboratory testing in simulated the field environments, presented in Chapter 8, verified that the equilibrium potential for carbon steel in the pH 13 environment is more noble than the equilibrium potential for carbon steel in the pH 7.5 environment. Corrosion potentials measured in the laboratory also proved that galvanized carbon steel is not sufficiently protected throughout the anchor bolts' expected service life. Thus, concentration cell corrosion is thermodynamically favorable in the carbon steel bolt in the presence of electrolyte. Laboratory tests also revealed that the corrosion rate of carbon steel electrochemically connected in a concentration cell is higher than the corrosion rate of uncoupled carbon steel.

Analysis of carbon steel bolts from the field confirmed the presence of concentration cell corrosion. The corrosion that was visually observed on carbon steel anchor bolt shafts, described in Chapters 6 and 7, indicated that general corrosion was accelerated near the interface of the bolt and the concrete. The accelerated corrosion caused a neck in the bolt shaft in the areas near the concrete, and the corrosion in the areas of the bolt farther from this interface was not as severe. The cone shape of the corroded carbon steel bolts indicated that a concentration cell had formed between the steel embedded in the concrete and the steel exposed to the environment.

Failure analysis of the carbon steel bolts gave further evidence supporting concentration cell corrosion. Microscopy of the necked surface of the bolts revealed that the corrosion had a uniform morphology – the failure surface did not indicate any

localized pitting, crevice, or corrosion cracking. From the nature of the corrosion mechanisms, it is suggested that galvanic and concentration cell corrosion morphology is the same as general corrosion, but accelerated in a specific area. Therefore, the microscopic images showing uniform corrosion of the carbon steel bolt in the necked area confirms that corrosion was accelerated in the part of the bolt that was not embedded in concrete.

Alternatively, laboratory testing in simulated field environments for the Type 304 stainless steel bolt material revealed that the equilibrium potential for the stainless steel was the same for the pH 7.5 and pH 13 solutions. Therefore, concentration cell corrosion would not initiate on stainless steel anchor bolts, according to corrosion thermodynamics. Corrosion rate measurements of stainless steels from each environment that were electrochemically coupled were found to be negligible.

9.1.2 Galvanic corrosion

Laboratory testing in solutions simulating the bearing environment proved that an electrochemical couple between carbon steel and a more noble alloy, such as stainless steel or bronze, increases the corrosion rate of the carbon steel, as predicted by theory presented in Chapter 3. Dissimilar metals in bearings should be electrochemically separated. Dissimilar metals may be electrochemically separated by encasing the anchor bolt in a non-conducting material and using a non-conducting washer to eliminate contact between the stainless steel anchor bolt and carbon steel bearing plates and flange.

9.1.3 Localized corrosion effects

Localized corrosion, such as pitting or crevice corrosion, must be considered when using active-passive stainless steel alloys. Localized attack is not a concern for carbon steel, because in the pH 7.5 solution the equilibrium potential of carbon steel indicated active, general corrosion. Passive films are susceptible to local breakdown by chloride attack, depending on the chloride concentration in the environment. Soil samples from the bearing environment were used to determine ion concentrations at a typical bearing in Georgia, and the chemical composition of corrosion scale was analyzed by x-ray diffraction to determine the effect of the ions in the environment on the corrosion behavior of the bolt. From the soil analysis it was determined that chlorides, carbides, and sulfates were present in the bearing environment, but the chemical composition of the bolt scale revealed that these corrosive ions were not present in the corrosion products. Thus, the role of the ions in the environment on the corrosion behavior of the material could not be positively identified by x-ray diffraction technique.

Cyclic polarization tests in solutions simulating the bearing environment were used to determine the protection potential of the Type 304 stainless steel along with other candidate alloys. It was found that the protection potential of the Type 304 alloy was more noble than the equilibrium potential of the stainless steel in solution. This implies that Type 304 stainless steel passivates and remains protected from corrosion in the typical bearing environment. Other candidate alloys for which the protection potential was higher than the equilibrium potential are Type 316, Type 2101, and Type 2205 stainless steels. When crevice effects were included, however, cyclic polarization showed a decrease in the protection potentials for all the alloys, confirming the theory presented

in Chapter 3 that the protection potential for pitting corrosion is higher than that for crevice corrosion. The introduction of crevice conditions on any of the alloys makes the material more susceptible to localized corrosion.

Currently, the most expensive alloying element in stainless steel is nickel. Since the composition of Type 2101 duplex stainless steel has significantly less nickel, the present day cost of this alloy is comparable to the cost of Type 304 austenitic stainless steel. The superior corrosion resistance of Type 2101 stainless steel makes it an attractive alternative to the current design. Yet, the corrosion resistance of Type 2205 stainless steel is even better. While the cost of this 2205 alloy is still considerably higher than the other two, it may also be accepted as a suitable design alternative. Further testing should be completed to verify the cyclic polarization data presented in Chapter 8.

9.2 Role of bearing design in corrosion

The current design for steel girder bridge bearings in the state of Georgia advances bearing corrosion. In the current design, stainless steel anchor bolts and bronze lube plates are in direct contact with carbon steel bearing plates and flanges; this contact promotes galvanic corrosion of the carbon steel components. The mechanism for movement of Georgia's bronze plate bearing design corresponds to the sliding bearing design described in Lee's book, *Bridge Bearings and Expansion Joints*, and is not a recommended type of bearing (Lee 1994). Sliding plates have a high coefficient of friction that only increases throughout the design life of the bearing as debris, moisture, and corrosion products are trapped in the crevices between the plates.

As corrosion products and debris build up inside the sliding plates, the bearing is at risk of becoming frozen. Frozen bearings restrict movements that the bearings are designed to accommodate, and forces are induced for which the original bridge is not designed. The effects of corrosion build up were demonstrated in Chapter 7, where corrosion products had essentially fused the anchor bolts to the bearing plates in fixed and expansion bearing holes.

Given that the inspection quality and regularity is the same for all types of bridges, it was reported in Chapter 5 that the rate at which corrosion initiates and propagates in bearings is higher for metropolitan and Interstate-related bridges, compared to rural and non-Interstate bridges. Based on this finding, it may be hypothesized that bearing corrosion is related to the loading conditions of the bridge. To some extent, bridge movements are dependent on the loading conditions, with greater movement occurring in the bridges with higher loads. As bridges are repetitively loaded in high traffic areas, the bearings may become subject to fretting corrosion in addition to the major corrosion mechanisms proposed in the previous section, leading to the acceleration of the overall corrosion of the bearing.

9.3 Role of maintenance procedures in corrosion

Proper bearing maintenance is key to reducing bearing corrosion. The build up of debris at the bearings traps moisture and corrosive agents at the bearing surface. Since electrolyte is necessary for all corrosion processes, this build up of moisture enables all the corrosion mechanisms described previously.

In the retrofit of existing bearings by “sleeving”, steel angles are bolted to the sides of the bearings to provide the lateral restraint that was lost when the anchor bolt corroded. The bolts used for the retrofit are subjected to the same environment that corroded the original carbon steel anchor bolt. Use of stainless steel bolts in the retrofit would protect against the same corrosion failure.

9.4 Correlation to inspection report data

Inspection report data enabled a statewide assessment of bearing corrosion in Georgia, which was presented in Chapter 5. The distribution of bearing corrosion incidences was found to be uniform across the state, but the mean ages at which corrosion was reported implied that corrosion initiated and propagated faster in northern and coastal regions, metropolitan areas, and Interstate-related bridges.

Bearing corrosion reported at an earlier mean age for bridges in the northern and coastal geographic regions of the state may be attributed to a more corrosive bearing environment in these regions compared to southern Georgia. Soil analysis from bearings in southern and northern Georgia did reveal that chloride concentrations in northern Georgia are higher than the concentrations in southern Georgia. Despite the lack of chloride-containing compounds in the bolt scale as determined by x-ray diffraction analysis, chlorides may still be responsible for accelerated corrosion rates and accelerated corrosion initiation by functioning to break down local passivity of the bolt.

The report of bearing corrosion in metropolitan and Interstate-related bridges at an earlier age than their rural and non-Interstate counterparts may also be attributed to the environmental conditions specific to these classifications. As discussed in Section 9.2,

fretting corrosion may be caused by the heavier traffic loading for these areas. Bridges that fall into the metropolitan and Interstate-related categories are also possibly exposed to higher amounts of pollutants, or collect more debris than bridges in other categories, both of which increase the rate of corrosion initiation and propagation.

Regardless of the bearing environment and apparent rate of corrosion initiation and propagation based on the age of bridges when anchor bolt corrosion was first reported, the occurrence of anchor bolt corrosion was found to be ubiquitous to all regions in Georgia. Concentration cell corrosion of the anchor bolts is not dependent on the geographic, demographic, or span type classifications of bridges, because it will occur anywhere that carbon steel is partially embedded in concrete. While the bearing environment may affect the rate of corrosion, the critical mechanism responsible for corrosion of carbon steel bolts is the concentration cell. Hence, the number of bearing corrosion occurrences is uniform for all bridge classifications.

The author notes that the inspection of anchor bolts within the plate bearing assembly is difficult, which leads to unknown variability in the inspection report data that are presented.

CHAPTER 10: CONCLUSIONS AND RECOMMENDATIONS

10.1 Summary

The research objectives for this project were to explicitly define the anchor bolt corrosion problem in the state of Georgia, research solutions to the problem, and recommend action to the Georgia Department of Transportation. As a first step, the researcher interviewed key personnel within the state Department of Transportation to understand the steel girder bearing design, maintenance procedures, and the history of both. The main bearing assemblies of concern in Georgia are the plate bearing assembly, in which carbon steel base and sole plates slide on a bronze lubrication plate at the expansion end of the girder, and the plate bearing assembly, in which carbon steel base and sole plate support the girder at the fixed end of the girder. The bolts used to anchor the girder and the bearing to the concrete support were ASTM Grade 36 carbon steel bolts if the bridge was constructed prior to 1990, and Type 304 stainless steel bolts if constructed after 1990. Existing bearings in which the anchor bolts had corroded were retrofitted by “sleeving”, in which steel angles were bolted to both sides of the bearing to provide lateral restraint.

To define the extent of anchor bolt corrosion in Georgia, inspection data from throughout the state was compiled and interpreted. The inspection report files were complete and reliable; the inspectors and the inspection process are commended. The occurrence of anchor bolt corrosion was found to be ubiquitous for all regional and demographic environments in Georgia, with 411 of 1500, or 27%, of steel girder bridges throughout the state reported to experience anchor bolt corrosion. Field investigations at

eight key bridges representing anchor bolt corrosion throughout the state confirmed the inspection report data that anchor bolt corrosion is universal in older steel girder bridges. Based on the bridge ages when anchor bolt corrosion was first reported, the rate of initiation and/or propagation of anchor bolt corrosion was higher for bridges in northern, coastal, and metropolitan environments as well as for Interstate-related bridges. Bearing corrosion for bridges in these categories was reported at a median age in the range of 34 to 37 years, while the median age of bridges in southern, rural, and non-Interstate categories when anchor bolt corrosion was reported was in the range of 40 to 45 years.

To define the causes of corrosion specific to anchor bolts in Georgia, failure analyses on bolt specimens obtained from the field investigations were conducted and laboratory testing on anchor bolt materials in simulated environments were performed. Visual analysis of the field specimens indicated that concentration cell corrosion was prevalent, and surface analysis revealed general corrosion morphology in the necked regions of the bolts. Laboratory testing proved that corrosion potentials were favorable for concentration cell corrosion for carbon steel partially embedded in concrete, but not for stainless steel materials. Corrosion potentials of carbon steel and stainless steel also indicated that when galvanically coupled, the carbon steel preferentially corrodes. Carbon steel electrically coupled with stainless steel in a galvanic cell or passive carbon steel in a concentration cell corroded two to ten times faster than uncoupled carbon steel. Data from cyclic polarization tests confirmed that Type 304 and other candidate stainless steels were protected from localized corrosion in the simulated bearing environment.

To research solutions to abate anchor bolt corrosion in Georgia, literature addressing the corrosion of steel alloys and bridge bearing design was explored. A review

of literature in this field revealed that extensive research has been conducted on the corrosion of reinforcing steels completely embedded in concrete, but in general, there is a need for research on the corrosion of anchorages in concrete. Regarding bearing design, the bearing type and material must be selected to accommodate for the loads, movements, and environment specific to the bridge.

10.2 Conclusions

Based on a synthesis of the results of the field investigations, bolt failure analyses, laboratory experimental testing, and inspection report survey, the corrosion of carbon steel anchor bolts is caused universally by concentration cell corrosion that is created by the partial embedment of the bolt. Inside the concrete, the anchor bolt develops a noble corrosion potential due to the alkaline environment, but outside of the concrete the bolt has an active potential in the neutral electrolytic solution at the bearing. Corrosion protection of the carbon steel bolt provided through zinc galvanization cannot sufficiently protect the carbon steel bolt for its entire service life.

Other corrosion mechanisms affecting steel girder bridge bearings are galvanic and crevice corrosion, which are both enhanced by the current bearing design. Carbon steel that is in contact with the more noble bronze plate or a stainless steel bolt is preferentially corroded in the galvanic cell. Meanwhile, the sliding plates of the bearing form crevices that trap moisture and corrosive agents. Additional factors that contribute to the initiation and propagation of corrosion are the debris found at the bearings, the ion concentrations in the solution at the bearings, and bridge loading that causes repetitive movements in the bearings.

The use of stainless steel anchor bolts instead of carbon steel eliminates the concentration cell effect on the bolt and, thus, eliminates the predominant cause of anchor bolt corrosion. However, stainless steel is susceptible to crevice corrosion and the risk of galvanic corrosion is heightened where carbon steel is in contact with the stainless steel.

Most of the bridges included in this study were designed for a 50 year lifespan. The survey of the inspection reports revealed that bearing corrosion was first reported to occur approximately 30 to 40 years after the bridge was built for over 40% of steel girder bridges in Georgia. From this statistic, it is apparent that an improved bearing design is necessary. New construction is expected to have a service life of 100 years, and the new bearing design must be resistant to all forms of corrosion to accommodate this lengthy service life.

10.3 Recommendations

10.3.1 Recommendations for design

The ASTM 276 Type 304 stainless steel anchor bolt that is specified in the current GDOT design manual is an acceptable anchor bolt material. The stainless steel is resistant to concentration cell effects because it is passive both inside and outside of the concrete. This alloy is also resistant to localized corrosion because the protection potential of Type 304 stainless steel is more noble than the equilibrium potential in the typical bearing environment. ASTM 276 Type 316, Type 2101, and Type 2205 stainless steels are acceptable alternatives to the Type 304. Due to the cost of nickel, these duplex stainless

steels may be economically similar to Type 304 stainless steel. Further cyclic polarization tests should be conducted to confirm the results of this investigation.

The stainless steel anchor bolt should be electrically separated from all dissimilar metals. To prevent preferential corrosion of carbon steel, the carbon steel flanges and bearing plates should be separated from the stainless steel anchor bolts and from the bronze lubrication plate. The bolt should be electrochemically separated by a non-conducting encasement and a non-conducting washer.

Short descriptions of several types of special non-conducting washers can be obtained from a supplier, Superior Washer and Gasket, Corp, with a plant in South Carolina (www.superiorwasher.com). The author recommends a polytetrafluoroethylene (Teflon) washer to replace the current stainless steel washer, because the low coefficient of friction of the Teflon material is desirable for expansion bearing applications. A local supplier, Metro Bolt & Supply Co, Inc., only supplies round nylon non-conducting washers with inside diameters of up to ½ inch (<http://metrobolt.com>). Superior Washer and Gasket Corp supplies round Teflon washers with inside diameters of up to 1 ⅛ inch (www.superiorwasher.com).

In the current design, the carbon steel plates are electrically separated from the bronze bearing plate by the mastic lubricant, but for the most corrosion resistant bearing design, the bronze lube plate should be eliminated entirely.

The recommended bearing type is the reinforced elastomeric bearing. Reinforced elastomeric bearings should be designed with appropriate thickness to account for the effect of holes for anchor bolts, and electrical separation must be kept between the reinforcing plates and the stainless steel anchor bolts.

10.3.2 Maintenance recommendations

The regular bearing maintenance program should be continued. Sliding plate bearings should be regularly cleaned by brushing away dirt and debris from the bearing surfaces so that moisture and corrosive agents will not collect in the bearing. Chemical cleaning agents should not be used under any circumstances. Additionally, the paint on the bearings should be maintained to prevent general atmospheric corrosion of the carbon steel components.

Existing bridges with carbon steel anchor bolts should be “sleeved” to provide lateral restraint, according to current maintenance procedures. Carbon steel bolts are known to be subjected to accelerated corrosion due to concentration cell effects, even though it may be hard to observe the anchor bolt corrosion within the bearing and near the concrete surface. Sleeving should be performed with stainless steel bolts.

APPENDIX A

BRIDGES FROM QUERY OF INSPECTION REPORT DATA

Access to the inspection reports for all state owned steel girder bridges were provided to the researcher by the Georgia Department of Transportation. Pertinent information queried from the inspection report database included the bridge serial and location code numbers, superstructure evaluation notes, year constructed, and superstructure condition code. In the following tables, only the bridge serial and location code numbers are given for reference, due to space limitations in this document.

Table A.1 is a list of all the state owned steel girder bridges in Georgia. However, only the inspection reports of bridges with a superstructure maintenance item request number, #830, were reviewed by the researcher, since corrosion of bearings falls under this maintenance category. Table A.2 provides a list of all the bridges with maintenance item request number 830.

Table A.1: State owned steel girder bridges in Georgia

Record Number	Bridge Serial Number	Location ID
1	001-0011-0	001-00004D-021.18N
2	001-0014-0	001-00015D-016.01N
3	003-0005-0	003-00031D-008.00N
4	003-0012-0	003-00064D-017.10E
5	003-0021-0	003-00135D-007.48N
6	005-0026-0	005-00032D-003.16E
7	007-0002-0	007-00037D-015.01E
8	007-0003-0	007-00091D-002.87N
9	007-0006-0	007-00200D-009.53E
10	009-0001-0	009-00022D-002.00E
11	009-0002-0	009-00022D-004.02E
12	009-0003-0	009-00022D-007.18E
13	009-0004-0	009-00022D-009.28E
14	009-0005-0	009-00022D-011.05E
15	009-0006-0	009-00022D-011.09E
16	009-0007-0	009-00022D-012.46E

Table A.1 (continued)

Record Number	Bridge Serial Number	Location ID
17	009-0014-0	009-00243D-009.89N
18	009-0015-0	009-00049D-009.90N
19	009-0016-0	009-00112D-005.10N
20	009-0017-0	009-00112D-007.81N
21	011-0002-0	011-00015D-000.85N
22	011-0008-0	011-00051D-013.02E
23	011-0009-0	011-00059D-002.56N
24	011-0012-0	011-00098D-003.71E
25	011-0013-0	011-00098D-002.83E
26	011-0029-0	011-00403D-150.43N
27	011-0030-0	011-00403D-150.44N
28	011-0031-0	011-00403D-152.66N
29	011-0032-0	011-00403D-152.67N
30	013-0010-0	013-00082D-010.70E
31	013-0012-0	013-00211D-022.60N
32	013-0014-0	013-00211D-018.86N
33	013-0018-0	013-00324D-000.66E
34	013-0022-0	013-00403D-127.19N
35	013-0023-0	013-00403D-127.20N
36	015-0001-0	015-00003D-001.06N
37	015-0002-0	015-00003D-001.07N
38	015-0003-0	015-00003D-002.65N
39	015-0004-0	015-00003D-002.66N
40	015-0005-0	015-00003D-003.48N
41	015-0006-0	015-00003D-003.49N
42	015-0007-0	015-00003D-006.81N
43	015-0011-0	015-00003D-011.66N
44	015-0012-0	015-00003D-011.67N
45	015-0016-0	015-00003D-014.82N
46	015-0017-0	015-00003D-014.83N
47	015-0021-0	015-00003D-022.62N
48	015-0024-0	015-00020D-003.94E
49	015-0025-0	015-00020D-003.95E
50	015-0026-0	015-00020D-011.30E
51	015-0029-0	
52	015-0030-0	
53	015-0031-0	015-00061D-003.93N

Table A.1 (continued)

Record Number	Bridge Serial Number	Location ID
54	015-0032-0	015-00061D-004.24N
55	015-0033-0	015-00061D-004.39N
56	015-0034-0	015-00061D-005.30N
57	015-0043-0	015-00113D-005.96N
58	015-0044-0	015-00113D-007.04N
59	015-0046-0	015-00113D-014.79N
60	015-0047-0	015-00113D-014.80N
61	015-0050-0	015-00140D-005.75E
62	015-0057-0	015-00155X-005.12N
63	015-0077-0	015-00401D-280.69N
64	015-0078-0	015-00401D-280.70N
65	015-0079-0	015-00401D-281.51N
66	015-0080-0	015-00401D-281.52N
67	015-0081-0	015-00401D-283.69N
68	015-0082-0	015-00401D-283.70N
69	015-0083-0	015-00401D-286.75N
70	015-0084-0	015-00401D-286.76N
71	015-0087-0	015-00401D-287.16N
72	015-0088-0	015-00401D-287.17N
73	015-0089-0	015-00401D-289.20N
74	015-0090-0	015-00401D-289.21N
75	015-0091-0	015-00401D-290.40N
76	015-0092-0	015-00401D-290.41N
77	015-0093-0	015-00401D-293.87N
78	015-0094-0	015-00401D-293.88N
79	015-0095-0	015-00401D-293.98N
80	015-0096-0	015-00401D-293.99N
81	015-0101-0	015-00401D-299.66N
82	015-0103-0	015-00401D-304.19N
83	015-0104-0	015-00401D-304.22N
84	015-0105-0	015-00401R-294.00N
85	015-0124-0	015-01665F-006.24N
86	017-0003-0	017-00011D-014.68N
87	019-0027-0	019-00125D-012.92N
88	019-0028-0	019-00125D-013.22N
89	021-0010-0	021-00011D-015.38N
90	021-0011-0	021-00019D-000.02N

Table A.1 (continued)

Record Number	Bridge Serial Number	Location ID
91	021-0017-0	021-00019D-010.64N
92	021-0026-0	021-00022D-012.71E
93	021-0028-0	021-00022D-015.86E
94	021-0030-0	021-03206M-000.99E
95	021-0031-0	021-00011D-003.90N
96	021-0032-0	021-00011D-005.29N
97	021-0034-0	021-00011D-006.15N
98	021-0035-0	021-00049D-015.26N
99	021-0038-0	021-00074D-001.41E
100	021-0040-0	021-00074D-008.80E
101	021-0042-0	021-03207M-001.50E
102	021-0046-0	021-00087D-003.75N
103	021-0047-0	021-00087D-003.76N
104	021-0048-0	021-00087D-010.54N
105	021-0054-0	021-00091X-000.23S
106	021-0057-0	021-00247D-004.44N
107	021-0058-0	021-00247D-004.45N
108	021-0066-0	021-00940F-010.20N
109	021-0070-0	021-00940F-015.85N
110	021-0081-0	021-00401D-160.08N
111	021-0083-0	021-00401D-160.30N
112	021-0085-0	021-00401D-161.27N
113	021-0088-0	021-00401D-162.48N
114	021-0090-0	021-00401D-163.80N
115	021-0095-0	021-00401D-164.98N
116	021-0096-0	021-00401D-164.99N
117	021-0097-0	021-00401D-165.59N
118	021-0098-0	021-00401D-165.60N
119	021-0101-0	021-00401D-166.63N
120	021-0102-0	021-00401D-166.64N
121	021-0106-0	021-00401D-169.07N
122	021-0107-0	021-00401D-169.08N
123	021-0109-0	021-00401D-170.82N
124	021-0110-0	021-00401D-170.83N
125	021-0111-0	021-00401D-171.44N
126	021-0112-0	021-00401D-171.45N
127	021-0114-0	021-00401D-164.95N

Table A.1 (continued)

Record Number	Bridge Serial Number	Location ID
128	021-0115-0	021-00401R-164.96N
129	021-0116-0	021-00401R-164.97N
130	021-0119-0	021-00404D-000.70E
131	021-0120-0	021-00404D-000.71E
132	021-0121-0	021-00404D-001.39E
133	021-0122-0	021-00404D-001.40E
134	021-0125-0	021-00404D-003.01E
135	021-0126-0	021-00404D-003.02E
136	021-0131-0	021-00404D-005.48E
137	021-0132-0	021-00404D-005.49E
138	021-0136-0	021-00408D-000.00N
139	021-0141-0	021-00408D-003.39N
140	021-0143-0	021-00408D-007.24N
141	021-0148-0	021-00665F-002.05E
142	021-0152-0	021-00730X-000.73E
143	021-0160-0	021-00581X-000.31E
144	021-0174-0	021-00074D-013.15E
145	021-0176-0	021-03209M-002.72E
146	021-0181-0	021-03217M-001.20E
147	021-0188-0	021-03245M-000.35E
148	021-0191-0	021-03262M-000.04N
149	023-0001-0	023-00026D-011.63E
150	023-0012-0	023-00112D-022.28N
151	025-0008-0	025-00023D-016.23N
152	025-0009-0	025-00023D-017.49N
153	025-0025-0	025-00520D-019.87E
154	025-0026-0	025-00520D-020.67E
155	027-0003-0	027-00076D-010.34E
156	027-0031-0	027-00122D-002.00E
157	027-0033-0	027-00122D-007.91E
158	027-0034-0	027-00122D-008.29E
159	027-0036-0	027-00122D-017.28E
160	029-0001-0	029-00011X-000.49W
161	029-0002-0	029-00012X-002.34N
162	029-0005-0	029-00025D-009.04N
163	029-0006-0	029-00026D-005.79E
164	029-0013-0	029-00030D-020.22E

Table A.1 (continued)

Record Number	Bridge Serial Number	Location ID
165	029-0014-0	029-00030D-020.23E
166	029-0015-0	029-02768F-003.34E
167	029-0029-0	029-00404D-146.29E
168	029-0030-0	029-00404D-146.30E
169	029-0037-0	029-00405D-085.92N
170	029-0039-0	029-00405D-086.78N
171	029-0041-0	029-00405D-086.99N
172	029-0043-0	029-00405D-089.18N
173	029-0047-0	029-00405D-090.94N
174	029-0048-0	029-00405D-090.95N
175	031-0005-0	031-00024D-015.61N
176	031-0022-0	031-00067D-006.04N
177	031-0036-0	031-00073D-003.01N
178	031-0037-0	031-00073D-003.02N
179	031-0047-0	031-00119D-001.29N
180	031-0050-0	031-00119D-011.23N
181	031-0061-0	031-00404D-124.01E
182	031-0062-0	031-00404D-124.02E
183	031-0088-0	031-01603F-004.97N
184	031-0106-0	031-00024D-003.61N
185	033-0004-0	033-00017D-005.46N
186	033-0038-0	033-00305D-026.32N
187	033-0053-0	033-00088D-000.58E
188	035-0001-0	035-00016D-000.88E
189	035-0004-0	035-00016D-017.33E
190	035-0007-0	035-00036D-010.34E
191	035-0008-0	035-00036D-016.31E
192	035-0009-0	035-00036D-018.44E
193	035-0014-0	035-00299X-000.60N
194	039-0011-0	039-00025D-031.89N
195	039-0012-0	039-00025P-002.57E
196	039-0019-0	039-00061X-007.45E
197	039-0020-0	039-02936F-001.70E
198	039-0021-0	039-00094X-002.63W
199	039-0026-0	039-00138X-005.73E
200	039-0029-0	039-00405D-000.01N
201	039-0030-0	039-00405D-003.23N

Table A.1 (continued)

Record Number	Bridge Serial Number	Location ID
202	039-0031-0	039-00405D-003.24N
203	039-0038-0	039-00405D-014.65N
204	039-0039-0	039-00405D-014.66N
205	039-0044-0	039-00405D-027.74N
206	039-0045-0	039-00405D-027.75N
207	039-0046-0	039-01276F-001.67E
208	039-0052-0	039-02711F-001.89E
209	039-0053-0	039-27759X-002.50E
210	043-0004-0	043-00023D-006.43N
211	043-0014-0	043-00129D-004.65N
212	043-0015-0	043-00129D-004.83N
213	043-0017-0	043-00404D-097.92E
214	043-0018-0	043-00404D-097.93E
215	045-0001-0	045-00001D-010.48N
216	045-0002-0	045-00001D-010.49N
217	045-0004-0	045-00001D-013.30N
218	045-0014-0	045-00005D-018.88N
219	045-0026-0	045-00016D-011.00E
220	045-0027-0	045-00016D-014.95E
221	045-0028-0	045-00016D-014.96E
222	045-0030-0	045-00016D-027.34E
223	045-0032-0	045-00849X-000.65N
224	045-0033-0	045-00061D-008.60N
225	045-0034-0	045-00061D-008.61N
226	045-0036-0	045-00100D-011.04N
227	045-0040-0	045-00113D-009.27N
228	045-0049-0	045-00219X-004.20N
229	045-0050-0	045-00244X-004.41N
230	045-0052-0	045-00291X-005.97N
231	045-0054-0	045-00356X-000.60N
232	045-0055-0	045-00399X-001.36N
233	045-0057-0	045-00402D-011.26E
234	045-0058-0	045-00402D-011.28E
235	045-0070-0	045-00808M-002.07N
236	045-0072-0	045-00812M-001.70E
237	045-0082-0	045-01809F-007.17N
238	045-0088-0	045-02815F-005.69N

Table A.1 (continued)

Record Number	Bridge Serial Number	Location ID
239	045-0096-0	045-00001D-011.88N
240	047-0003-0	047-00002D-002.51E
241	047-0004-0	047-00002D-002.52E
242	047-0005-0	047-00002D-002.79E
243	047-0006-0	047-00002D-002.80E
244	047-0007-0	047-00002D-005.23E
245	047-0008-0	047-00002D-005.24E
246	047-0009-0	047-00002D-008.46E
247	047-0014-0	047-00003D-011.84N
248	047-0021-0	047-00151D-010.40N
249	047-0022-0	047-00151D-010.41N
250	047-0023-0	047-00151D-010.80N
251	047-0024-0	047-00209X-002.42S
252	047-0025-0	047-00401D-342.54N
253	047-0029-0	047-00401D-345.21N
254	047-0033-0	047-00401D-350.06N
255	047-0035-0	047-00401D-351.38N
256	047-0036-0	047-00401D-351.39N
257	047-0039-0	047-00401D-353.13N
258	047-0041-0	047-00401D-353.69N
259	047-0043-0	047-00401D-354.34N
260	047-0045-0	047-00401D-354.64N
261	047-0047-0	047-01110M-007.18E
262	049-0009-0	049-00004D-006.95N
263	049-0010-0	049-00004D-007.20N
264	049-0011-0	049-00004D-006.99N
265	049-0012-0	049-00023D-000.00N
266	049-0038-0	049-00252D-011.48E
267	051-0002-0	051-00017D-000.23N
268	051-0005-0	051-00421D-001.60N
269	051-0006-0	051-00421D-003.37N
270	051-0007-0	051-00421D-003.38N
271	051-0008-0	051-00421D-004.29N
272	051-0009-0	051-00421D-004.30N
273	051-0010-0	051-00421D-005.27N
274	051-0011-0	051-00421D-005.29N
275	051-0012-0	051-00421D-005.42N

Table A.1 (continued)

Record Number	Bridge Serial Number	Location ID
276	051-0013-0	051-00421D-005.43N
277	051-0014-0	051-00421D-005.57N
278	051-0015-0	051-00421D-005.58N
279	051-0016-0	051-00421D-005.96N
280	051-0017-0	051-00421D-005.97N
281	051-0019-0	051-00421D-006.10N
282	051-0020-0	051-00421D-006.20N
283	051-0022-0	051-00421D-006.35N
284	051-0023-0	051-00421D-006.36N
285	051-0024-0	051-00421D-006.90N
286	051-0025-0	051-00421D-006.91N
287	051-0026-0	051-00421D-007.00N
288	051-0027-0	051-00421D-007.01N
289	051-0028-0	051-00421D-007.21N
290	051-0029-0	051-00421D-007.22N
291	051-0038-0	051-00421R-006.10N
292	051-0041-0	051-04068M-005.82E
293	051-0047-0	051-00026D-016.67E
294	051-0049-0	051-00026D-016.99E
295	051-0054-0	051-00025D-019.86N
296	051-0060-0	051-00026D-011.20E
297	051-0066-0	051-00026D-032.43E
298	051-0069-0	051-00030D-002.04E
299	051-0070-0	051-02773F-003.00N
300	051-0074-0	051-00204D-011.88E
301	051-0075-0	051-00204D-012.49E
302	051-0076-0	051-00204D-014.90E
303	051-0078-0	051-00204D-025.61E
304	051-0079-0	051-00307D-002.41N
305	051-0087-0	051-00404D-163.30E
306	051-0089-0	051-00404D-163.59E
307	051-0090-0	051-00404D-163.60E
308	051-0092-0	051-00404D-163.95E
309	051-0093-0	051-00404D-163.97E
310	051-0095-0	051-00404D-165.03E
311	051-0096-0	051-00404D-165.02E
312	051-0097-0	051-00404D-165.69E

Table A.1 (continued)

Record Number	Bridge Serial Number	Location ID
313	051-0098-0	051-00404D-165.70E
314	051-0101-0	051-00404D-166.09E
315	051-0105-0	051-00405D-093.87N
316	051-0109-0	051-00405D-099.28N
317	051-0111-0	051-00405D-101.30N
318	051-0112-0	051-00405D-101.31N
319	051-0120-0	051-00405D-107.05N
320	051-0121-0	051-00405D-107.13N
321	051-0122-0	051-00405D-107.14N
322	051-0123-0	051-00405D-107.23N
323	051-0124-0	051-00405D-107.24N
324	051-0125-0	051-00405D-108.52N
325	051-0126-0	051-00405D-108.53N
326	051-0135-0	051-04067M-002.59N
327	051-0138-0	051-04070M-003.00E
328	051-0147-0	051-00204P-006.08E
329	051-0149-0	051-04024M-001.14N
330	051-0154-0	051-00021D-008.58N
331	053-0009-0	053-00026D-006.75E
332	055-0007-0	055-00048D-000.66E
333	055-0011-0	055-00048D-009.46E
334	055-0052-0	055-00100D-012.55N
335	057-0010-0	057-00020D-005.91E
336	057-0013-0	057-00020D-012.43E
337	057-0015-0	057-00092D-000.08N
338	057-0020-0	057-00108D-003.46N
339	057-0029-0	057-00140D-026.78E
340	057-0032-0	057-00341X-000.65S
341	057-0034-0	057-00369D-003.74E
342	057-0036-0	057-00372D-011.65N
343	057-0046-0	057-00417D-017.34N
344	057-0047-0	057-00417D-017.35N
345	057-0048-0	057-00417D-017.43N
346	057-0049-0	057-00417D-017.44N
347	057-0070-0	057-01375F-000.10N
348	057-0071-0	057-01375F-014.20N
349	059-0001-0	059-00010L-005.45E

Table A.1 (continued)

Record Number	Bridge Serial Number	Location ID
350	059-0002-0	059-00010L-005.44E
351	059-0003-0	059-00010L-004.68E
352	059-0004-0	059-00010L-004.67E
353	059-0005-0	059-00010L-002.97E
354	059-0006-0	059-00010L-002.96E
355	059-0007-0	059-00010L-002.44E
356	059-0008-0	059-00010L-002.43E
357	059-0009-0	059-00010L-002.21E
358	059-0010-0	059-00010L-002.20E
359	059-0011-0	059-00010L-001.88E
360	059-0012-0	059-00010L-001.87E
361	059-0013-0	059-00010L-001.77E
362	059-0014-0	059-00010L-001.76E
363	059-0015-0	059-00010L-001.56E
364	059-0016-0	059-00010L-001.55E
365	059-0017-0	059-00010L-000.05E
366	059-0018-0	059-00010L-000.04E
367	059-0020-0	059-00010D-003.13E
368	059-0021-0	059-00010D-003.14E
369	059-0023-0	059-00010D-005.36E
370	059-0029-0	059-00015A-004.33N
371	059-0035-0	059-00032X-000.55N
372	059-0036-0	059-00008D-001.97E
373	059-0037-0	059-00008D-001.98E
374	059-0040-0	059-00008D-003.40E
375	059-0041-0	059-00008D-003.41E
376	059-0044-0	059-00008D-004.21E
377	059-0045-0	059-00008D-004.22E
378	059-0047-0	059-00008D-006.00E
379	059-0048-0	059-00008D-006.01E
380	059-0049-0	059-00008R-001.99E
381	059-0050-0	059-00008R-002.00E
382	059-0051-0	059-00600X-001.55N
383	059-0052-0	059-00600X-001.56N
384	059-0053-0	059-00343M-001.87W
385	059-0059-0	059-00320M-000.56E
386	059-5032-0	059-00316D-001.63E

Table A.1 (continued)

Record Number	Bridge Serial Number	Location ID
387	061-0002-0	061-00037D-000.01E
388	061-0007-0	061-00039D-019.74N
389	061-0008-0	061-00039D-021.98N
390	063-0003-0	063-00003D-011.80N
391	063-0004-0	063-00003D-014.77N
392	063-0011-0	063-00042D-006.88N
393	063-0013-0	063-00054D-007.73E
394	063-0023-0	063-00139D-005.51N
395	063-0031-0	063-00401D-230.01N
396	063-0033-0	063-00401D-231.65N
397	063-0037-0	063-00401D-233.92N
398	063-0040-0	063-00401R-237.00N
399	063-0045-0	063-00407R-057.44C
400	063-0048-0	063-00407R-057.63C
401	063-0117-0	063-01516X-000.61W
402	065-0014-0	065-00089D-003.49N
403	065-0015-0	065-00089D-003.70N
404	067-0002-0	067-09003M-002.27N
405	067-0007-0	067-00003D-014.77N
406	067-0008-0	067-00003D-014.78N
407	067-0010-0	067-00003D-020.97N
408	067-0013-0	067-00003D-005.21N
409	067-0014-0	067-00003R-005.22N
410	067-0019-0	067-09004M-000.59N
411	067-0020-0	067-09004M-001.25N
412	067-0022-0	067-00005D-014.97N
413	067-0023-0	067-00005D-014.98N
414	067-0025-0	067-00005P-000.36N
415	067-0026-0	067-00005P-000.37N
416	067-0031-0	067-00005D-001.35N
417	067-0034-0	067-00008D-008.12E
418	067-0036-0	067-00092D-004.98N
419	067-0042-0	067-00120D-021.40E
420	067-0047-0	067-00120L-003.13C
421	067-0052-0	067-00280D-000.60N
422	067-0057-0	067-00280D-013.66N
423	067-0066-0	067-00401D-258.79N

Table A.1 (continued)

Record Number	Bridge Serial Number	Location ID
424	067-0068-0	067-00401D-260.69N
425	067-0069-0	067-00401D-260.70N
426	067-0072-0	067-00401D-263.72N
427	067-0073-0	067-00401D-264.21N
428	067-0074-0	067-00401D-265.02N
429	067-0076-0	067-00401D-267.51N
430	067-0078-0	067-00401D-267.79N
431	067-0081-0	067-00401D-269.45N
432	067-0082-0	067-00401D-269.46N
433	067-0083-0	067-00401D-270.25N
434	067-0084-0	067-00401D-270.32N
435	067-0085-0	067-00401D-271.97N
436	067-0086-0	067-00401D-271.98N
437	067-0089-0	067-00402D-047.10E
438	067-0090-0	067-00402D-047.83E
439	067-0091-0	067-00407D-014.60C
440	067-0093-0	067-00407D-014.67C
441	067-0095-0	067-00407D-015.60C
442	067-0097-0	067-00407D-016.24C
443	067-0099-0	067-00407D-019.51C
444	067-0100-0	067-00407D-020.04C
445	067-0101-0	067-00407D-020.17C
446	067-0102-0	067-00407R-020.18C
447	067-0103-0	067-00407D-020.26C
448	067-0104-0	067-00407R-020.27C
449	067-0106-0	067-00407D-020.41C
450	067-0109-0	067-00407D-021.43C
451	067-0110-0	067-00417D-000.06N
452	067-0115-0	067-00417D-002.28N
453	067-0116-0	067-00417D-002.29N
454	067-0122-0	067-09359M-002.65N
455	067-0129-0	067-09016M-000.26E
456	067-0130-0	067-09360M-000.49E
457	067-0140-0	067-04399X-001.72E
458	067-0143-0	067-09001M-008.03E
459	067-0162-0	067-09032M-002.90N
460	067-0184-0	067-00005D-014.33N

Table A.1 (continued)

Record Number	Bridge Serial Number	Location ID
461	067-0185-0	067-00005D-014.95N
462	069-0009-0	069-00032D-001.24E
463	069-0010-0	069-00032D-004.23E
464	069-0011-0	069-00032D-007.40E
465	069-0013-0	069-00032D-019.60E
466	069-0014-0	069-00032D-020.12E
467	069-0017-0	069-00032D-025.11E
468	069-0018-0	069-00032D-025.83E
469	069-0031-0	069-00135D-016.62N
470	069-0044-0	069-00158D-024.47E
471	069-0057-0	069-00206D-013.63E
472	071-0018-0	071-00037D-012.41E
473	071-0088-0	071-00037D-000.44E
474	071-0089-0	071-00037D-004.61E
475	073-0003-0	073-00047D-016.20E
476	073-0015-0	073-00047D-004.29E
477	073-0016-0	073-00223D-002.47E
478	073-0018-0	073-00223D-010.12E
479	073-0022-0	073-00232D-008.15E
480	073-0025-0	073-00238X-001.78N
481	073-0026-0	073-00253X-001.18S
482	073-0027-0	073-00047D-009.95E
483	073-0035-0	073-00383D-000.04N
484	073-0040-0	073-02122F-004.91N
485	073-0043-0	073-00388D-002.80N
486	075-0001-0	075-00007D-008.91N
487	075-0018-0	075-00216X-003.60N
488	075-0019-0	075-00240X-001.84N
489	075-0021-0	075-00401D-038.33N
490	075-0029-0	075-01211F-001.60N
491	075-0036-0	075-04211M-000.90E
492	077-0005-0	077-00016D-013.57E
493	077-0016-0	077-00054D-002.07E
494	077-0017-0	077-00054D-004.80E
495	077-0018-0	077-00054D-010.58E
496	077-0024-0	077-00070D-006.77N
497	077-0028-0	077-00074D-001.95E

Table A.1 (continued)

Record Number	Bridge Serial Number	Location ID
498	077-0030-0	077-00074D-000.00E
499	077-0037-0	077-00403D-038.84N
500	077-0040-0	077-00403D-041.18N
501	077-0043-0	077-00403D-043.47N
502	077-0044-0	077-00403D-043.48N
503	077-0045-0	077-00403D-043.65N
504	077-0047-0	077-00403D-046.88N
505	077-0048-0	077-00403D-046.89N
506	077-0049-0	077-00403D-050.02N
507	077-0052-0	077-03500M-002.75E
508	077-0069-0	077-01599F-007.01N
509	077-0076-0	077-02081F-002.01E
510	077-5136-0	077-00403D-050.03N
511	079-0006-0	079-00007D-018.71N
512	079-0014-0	079-00096D-001.22E
513	081-0002-0	081-00007D-013.83N
514	081-0013-0	081-00033C-001.50N
515	081-0017-0	081-00117X-001.80N
516	081-0021-0	081-00257D-000.08N
517	081-0023-0	081-00355X-001.67E
518	081-0028-0	081-00401D-100.54N
519	081-0030-0	081-00401D-100.75N
520	081-0034-0	081-00401D-101.12N
521	081-0045-0	081-01632F-012.36E
522	081-0056-0	081-01818F-002.20E
523	083-0008-0	083-00058D-019.81N
524	083-0009-0	083-00104X-000.14W
525	083-0010-0	083-00119X-000.18W
526	083-0012-0	083-00136D-005.16E
527	083-0013-0	083-00136D-005.76E
528	083-0014-0	083-00136D-006.33E
529	083-0016-0	083-00146X-001.94N
530	083-0017-0	083-00178X-000.11E
531	083-0018-0	083-00186X-002.38E
532	083-0020-0	083-00299D-002.62E
533	083-0021-0	083-00406D-004.66N
534	083-0022-0	083-00406D-004.67N

Table A.1 (continued)

Record Number	Bridge Serial Number	Location ID
535	083-0023-0	083-00406D-007.09N
536	083-0024-0	083-00406D-007.10N
537	083-0044-0	083-00409D-003.91E
538	083-0045-0	083-00409D-003.92E
539	085-0001-0	085-00009D-001.73N
540	085-0002-0	085-00009D-001.93N
541	085-0010-0	085-00053D-007.61E
542	085-0018-0	085-00136D-023.00E
543	085-0019-0	085-00136D-025.95E
544	085-0020-0	085-00136D-026.96E
545	085-0021-0	085-00183D-004.86N
546	087-0004-0	087-00001D-020.40N
547	087-0005-0	087-00001D-020.41N
548	087-0006-0	087-00001D-020.97N
549	087-0007-0	087-00001D-020.98N
550	087-0008-0	087-00001D-021.10N
551	087-0009-0	087-00001D-021.11N
552	087-0012-0	087-00001D-022.58N
553	087-0013-0	087-00001D-022.59N
554	087-0014-0	087-00001B-001.93N
555	087-0016-0	087-00038D-013.47E
556	087-0017-0	087-00038D-013.48E
557	087-0022-0	087-00097D-002.34N
558	087-0037-0	087-00412M-000.77N
559	087-0046-0	087-00262D-012.29E
560	089-0004-0	089-00008D-005.48E
561	089-0005-0	089-00008D-007.35E
562	089-0012-0	089-00010D-011.98E
563	089-0020-0	089-00013D-000.46N
564	089-0022-0	089-00042D-001.53N
565	089-0027-0	089-00042D-011.10N
566	089-0031-0	089-00042D-013.95N
567	089-0048-0	089-00236D-006.77E
568	089-0075-0	089-00407D-030.50C
569	089-0076-0	089-00407D-031.50C
570	089-0077-0	089-00407D-032.70C
571	089-0079-0	089-00407D-033.80C

Table A.1 (continued)

Record Number	Bridge Serial Number	Location ID
572	089-0080-0	089-00407D-034.30C
573	089-0082-0	089-00407D-035.05C
574	089-0085-0	089-00407D-038.50C
575	089-0091-0	089-00407D-041.80C
576	089-0092-0	089-00407D-044.65C
577	089-0097-0	089-00407R-046.25C
578	089-0098-0	089-00407D-047.81C
579	089-0111-0	089-00410D-008.06E
580	089-0118-0	089-00848X-000.61W
581	089-0165-0	089-09332M-002.35E
582	089-0180-0	089-09223M-002.42N
583	089-0199-0	089-09265M-003.53E
584	089-0293-0	089-00413R-010.60N
585	091-0005-0	091-00030D-007.51E
586	093-0006-0	093-00027D-010.90E
587	093-0007-0	093-00027D-015.64E
588	093-0017-0	093-00157X-001.00N
589	093-0021-0	093-00215X-009.10N
590	093-0022-0	093-00230D-000.20E
591	093-0028-0	093-00230D-021.38E
592	093-0037-0	093-00401D-120.35N
593	093-0039-0	093-00401D-120.54N
594	093-0042-0	093-00440X-004.00E
595	093-0046-0	093-00679F-010.25E
596	093-0048-0	093-01175F-002.67N
597	095-0004-0	095-00520D-002.36E
598	095-0005-0	095-00520D-002.37E
599	095-0008-0	095-00520D-002.72E
600	095-0009-0	095-00520D-002.73E
601	095-0010-0	095-00520D-004.08E
602	095-0011-0	095-00520D-004.09E
603	095-0012-0	095-00520D-004.33E
604	095-0014-0	095-00520D-004.72E
605	095-0015-0	095-00520D-004.73E
606	095-0016-0	095-00520D-004.97E
607	095-0017-0	095-00520D-004.98E
608	095-0018-0	095-00520D-005.21E

Table A.1 (continued)

Record Number	Bridge Serial Number	Location ID
609	095-0019-0	095-00520D-005.22E
610	095-0020-0	095-00520D-006.96E
611	095-0021-0	095-00520D-006.97E
612	095-0022-0	095-00520D-007.14E
613	095-0024-0	095-00003D-009.49N
614	095-0025-0	095-00003D-009.48N
615	095-0027-0	095-00003D-009.27N
616	095-0028-0	095-00003D-008.96N
617	095-0030-0	095-00520B-011.31E
618	095-0033-0	095-00520B-006.20E
619	095-0041-0	095-00091D-014.12N
620	095-0045-0	095-00128M-000.90N
621	095-0048-0	095-00133D-009.14N
622	095-0049-0	095-00133D-009.15N
623	095-0050-0	095-00133D-009.70N
624	095-0053-0	095-00144M-000.92N
625	095-0058-0	095-00234D-020.77E
626	097-0004-0	097-00005D-013.29N
627	097-0005-0	097-00006D-003.45E
628	097-0006-0	097-00006D-000.96E
629	097-0009-0	097-00092D-009.31N
630	097-0010-0	097-09040M-000.60E
631	097-0011-0	097-00142X-000.55E
632	097-0013-0	097-00166D-009.55E
633	097-0017-0	097-00247X-000.50N
634	097-0018-0	097-00247X-000.56N
635	097-0025-0	097-00402D-043.44E
636	097-0027-0	097-09370M-003.10N
637	097-0031-0	097-09397M-001.95N
638	097-0032-0	097-09403M-000.75N
639	097-0034-0	097-02278F-004.04E
640	097-0041-0	097-02876F-008.94N
641	097-0043-0	097-09040M-002.36E
642	099-0002-0	099-00001D-007.82N
643	099-0019-0	099-00200D-013.00E
644	101-0002-0	101-00011D-014.78N
645	101-0016-0	101-00094D-036.10E

Table A.1 (continued)

Record Number	Bridge Serial Number	Location ID
646	103-0025-0	103-00405D-112.30N
647	103-0026-0	103-00405D-112.31N
648	103-0034-0	103-01868F-001.42N
649	105-0002-0	105-00017D-013.17N
650	105-0006-0	105-00072D-024.83E
651	105-0007-0	105-00077D-000.13N
652	105-0008-0	105-00077D-001.81N
653	105-0015-0	105-00172D-006.13N
654	105-0018-0	105-00368D-009.35N
655	107-0026-0	107-00046D-003.55E
656	107-0058-0	107-00466X-000.17S
657	107-0060-0	107-00297D-005.00N
658	107-0069-0	107-00404D-089.40E
659	107-0070-0	107-00404D-089.41E
660	109-0030-0	109-00030D-012.75E
661	111-0012-0	111-00515D-013.66N
662	111-0013-0	111-00515D-013.67N
663	111-0016-0	111-00515D-002.37N
664	111-0019-0	
665	111-0024-0	111-00060D-024.11N
666	113-0009-0	113-00085D-001.17N
667	113-0011-0	113-00085D-014.22N
668	113-0013-0	113-00085D-015.84N
669	115-0004-0	115-00001D-008.99N
670	115-0005-0	115-00001D-009.00N
671	115-0010-0	115-00001D-010.17N
672	115-0011-0	115-00001D-010.18N
673	115-0015-0	115-00001D-011.73N
674	115-0016-0	115-00001D-012.10N
675	115-0018-0	115-00001D-012.80N
676	115-0020-0	115-00001D-016.16N
677	115-0021-0	115-00001D-021.27N
678	115-0032-0	115-00020D-020.60E
679	115-0046-0	115-00100D-013.52N
680	115-0047-0	115-00101D-009.86N
681	115-0048-0	115-00101D-009.90N
682	115-0053-0	115-00140D-003.18E

Table A.1 (continued)

Record Number	Bridge Serial Number	Location ID
683	115-0055-0	115-00140D-007.24E
684	115-0063-0	115-03745M-000.55E
685	117-0004-0	117-00009D-018.41N
686	117-0006-0	117-00017X-000.18E
687	117-0007-0	117-00019X-001.66W
688	117-0008-0	117-00020D-010.14E
689	117-0010-0	117-00053D-004.89E
690	117-0012-0	117-00087X-000.37E
691	117-0013-0	117-00141D-006.95N
692	117-0019-0	117-00369D-013.65E
693	117-0021-0	117-00369D-016.83E
694	117-0022-0	117-00369D-019.32E
695	117-0027-0	117-00400D-011.55N
696	117-0028-0	117-00400D-011.56N
697	117-0031-0	117-00456X-006.87S
698	117-0032-0	117-01285F-006.75N
699	117-0035-0	117-02347F-000.28E
700	117-0039-0	117-02704F-000.96E
701	117-0040-0	117-02704F-000.97E
702	117-0042-0	117-02883F-000.95N
703	117-0044-0	117-02884F-002.52E
704	119-0002-0	119-00017D-013.65N
705	119-0006-0	119-00051D-014.66E
706	119-0007-0	119-00051D-017.42E
707	119-0016-0	119-00084X-001.32E
708	119-0017-0	119-00097X-000.45N
709	119-0018-0	119-00106D-002.11N
710	119-0021-0	119-00145D-001.00N
711	119-0024-0	119-00198D-006.46E
712	119-0025-0	119-00258X-000.51W
713	119-0032-0	119-00328D-000.73N
714	119-0033-0	119-00328D-003.20N
715	119-0034-0	119-00383X-002.52W
716	119-0035-0	119-00387X-002.69E
717	119-0038-0	119-00403D-158.51N
718	119-0039-0	119-00403D-158.52N
719	119-0040-0	119-00403D-161.55N

Table A.1 (continued)

Record Number	Bridge Serial Number	Location ID
720	119-0041-0	119-00403D-161.56N
721	119-0050-0	119-00403D-173.24N
722	121-0001-0	121-00003D-000.45N
723	121-0011-0	121-00003D-009.94N
724	121-0013-0	121-00003D-012.85N
725	121-0015-0	121-00003D-017.91N
726	121-0019-0	121-00008D-001.11E
727	121-0022-0	121-00008D-007.70E
728	121-0030-0	121-00009D-007.21N
729	121-0031-0	121-00009D-010.44N
730	121-0041-0	121-00014D-006.25N
731	121-0042-0	121-00014D-011.89N
732	121-0043-0	121-00014D-012.82N
733	121-0044-0	121-00014D-017.24N
734	121-0049-0	121-00014D-025.70N
735	121-0065-0	121-00070D-024.26N
736	121-0066-0	121-00070D-028.49N
737	121-0069-0	121-00074D-001.59E
738	121-0073-0	121-00092D-013.06N
739	121-0075-0	121-00120D-009.76E
740	121-0079-0	121-00120D-017.51E
741	121-0080-0	121-00138D-003.59E
742	121-0083-0	121-00139D-013.01N
743	121-0084-0	121-00139D-015.86N
744	121-0085-0	121-00140D-007.61E
745	121-0086-0	121-00140D-008.03E
746	121-0093-0	121-00154D-021.12N
747	121-0094-0	121-00154D-022.22N
748	121-0095-0	121-00154D-022.24N
749	121-0103-0	121-00166D-014.61E
750	121-0104-0	121-00166D-014.78E
751	121-0105-0	121-00154R-022.14N
752	121-0106-0	121-00154R-022.25N
753	121-0110-0	121-00237D-000.19N
754	121-0111-0	121-00237D-000.36N
755	121-0112-0	121-00279D-005.00N
756	121-0115-0	121-00280D-004.00N

Table A.1 (continued)

Record Number	Bridge Serial Number	Location ID
757	121-0119-0	121-00400D-006.80N
758	121-0120-0	121-00400D-006.90N
759	121-0121-0	121-00400D-008.43N
760	121-0123-0	121-00400D-013.55N
761	121-0125-0	121-00400D-013.96N
762	121-0127-0	121-00400D-015.92N
763	121-0148-0	121-00401D-251.40N
764	121-0149-0	121-00401D-252.50N
765	121-0150-0	121-00401D-253.55N
766	121-0153-0	121-00401D-255.57N
767	121-0164-0	121-00402D-047.95E
768	121-0165-0	121-00402D-048.57E
769	121-0170-0	121-00402D-052.13E
770	121-0172-0	121-00402D-052.57E
771	121-0173-0	121-00402D-053.58E
772	121-0178-0	121-00402D-055.38E
773	121-0202-0	121-00403R-076.33N
774	121-0208-0	121-00013D-002.53N
775	121-0209-0	121-00013D-002.67N
776	121-0215-0	121-00403R-068.75N
777	121-0222-0	121-00407D-000.58C
778	121-0227-0	121-00407D-004.82C
779	121-0234-0	121-00407D-007.70C
780	121-0237-0	121-00407D-010.00C
781	121-0238-0	121-00407D-010.81C
782	121-0239-0	121-00407D-010.82C
783	121-0242-0	121-00407D-013.78C
784	121-0244-0	121-00407D-024.05C
785	121-0245-0	121-00407D-024.35C
786	121-0246-0	121-00407D-025.80C
787	121-0247-0	121-00407D-026.10C
788	121-0248-0	121-00407D-026.40C
789	121-0252-0	121-00407R-010.00C
790	121-0255-0	121-00407R-010.61C
791	121-0256-0	121-00407R-013.05C
792	121-0257-0	121-00407R-026.07C
793	121-0270-0	121-09260M-005.23N

Table A.1 (continued)

Record Number	Bridge Serial Number	Location ID
794	121-0285-0	121-02564F-001.91E
795	121-0297-0	121-01702X-000.20E
796	121-0299-0	121-09411M-004.10E
797	121-0303-0	121-09409M-002.80N
798	121-0307-0	121-09407M-002.46E
799	121-0311-0	121-01002X-001.99N
800	121-0316-0	121-00139X-001.50N
801	121-0326-0	121-09013M-007.75N
802	121-0327-0	121-09022M-000.50E
803	121-0346-0	121-09054M-009.75N
804	121-0380-0	121-09095M-000.91E
805	121-0389-0	121-09133M-000.20E
806	121-0429-0	121-09190M-000.68N
807	121-0444-0	121-09212M-007.19N
808	121-0445-0	121-09212M-009.84N
809	121-0452-0	121-09248M-000.60N
810	121-0455-0	121-09248M-006.08E
811	121-0459-0	121-09255M-001.25E
812	121-0466-0	121-09329M-003.04N
813	121-0472-0	121-00140D-013.74E
814	121-0475-0	121-00085X-000.80E
815	121-0477-0	121-00288X-000.65S
816	121-0489-0	121-00407D-005.26C
817	121-0504-0	121-00154D-026.54N
818	121-0543-0	121-00013D-004.11N
819	121-0557-0	121-00403R-086.28N
820	123-0025-0	123-00282D-008.29E
821	123-0027-0	123-00282D-012.06E
822	125-0004-0	125-00171D-008.54N
823	125-0005-0	125-00171D-008.96N
824	125-0007-0	125-00102D-006.20E
825	125-0008-0	125-00123D-002.58N
826	127-0013-0	127-00025P-004.33N
827	127-0014-0	127-00025P-004.34N
828	127-0024-0	127-00027D-018.40E
829	127-0025-0	127-00623M-000.14S
830	127-0026-0	127-00027X-000.75N

Table A.1 (continued)

Record Number	Bridge Serial Number	Location ID
831	127-0039-0	127-00099D-015.59N
832	127-0041-0	127-00303D-001.16N
833	127-0042-0	127-00303D-004.42N
834	127-0043-0	127-00405D-029.37N
835	127-0044-0	127-00405D-029.38N
836	127-0045-0	127-00405D-029.61N
837	127-0046-0	127-00405D-029.62N
838	127-0049-0	127-00405D-031.44N
839	127-0050-0	127-00405D-031.45N
840	127-0051-0	127-00405D-033.21N
841	127-0052-0	127-00405D-033.22N
842	127-0055-0	127-00405D-035.58N
843	127-0056-0	127-00405D-035.59N
844	127-0057-0	127-00405D-036.21N
845	127-0058-0	127-00405D-036.22N
846	129-0008-0	129-00003D-010.05N
847	129-0012-0	129-00053D-007.92E
848	129-0013-0	129-00053D-009.92E
849	129-0019-0	129-00053D-023.31E
850	129-0022-0	129-00053P-001.93N
851	129-0029-0	129-05607M-000.95E
852	129-0030-0	129-00071X-003.35S
853	129-0031-0	129-00136D-007.32E
854	129-0032-0	129-00136D-007.53E
855	129-0033-0	129-00136D-009.18E
856	129-0037-0	129-00136D-018.82E
857	129-0042-0	129-00136C-008.92E
858	129-0044-0	129-00156D-007.00E
859	129-0048-0	129-00156D-020.28E
860	129-0050-0	129-00156D-027.64E
861	129-0051-0	129-00225D-002.44N
862	129-0052-0	129-00225D-002.62N
863	129-0060-0	129-00401D-317.34N
864	129-0062-0	129-00401D-318.18N
865	129-0064-0	129-00401D-318.70N
866	129-0066-0	129-00401D-319.84N
867	129-0073-0	129-05608M-002.23E

Table A.1 (continued)

Record Number	Bridge Serial Number	Location ID
868	131-0008-0	131-00038D-015.40E
869	131-0010-0	131-00038D-019.04E
870	131-0014-0	131-00093D-014.83N
871	131-0028-0	131-00112D-003.59N
872	131-0035-0	131-00188D-001.72E
873	133-0003-0	133-00012D-011.10E
874	133-0013-0	133-00038X-001.81W
875	133-0017-0	133-00044D-026.17E
876	133-0019-0	133-00077D-000.51N
877	133-0020-0	133-00094X-000.36S
878	133-0021-0	133-00178X-003.97N
879	133-0022-0	133-00196X-002.42E
880	133-0023-0	133-00402D-129.22E
881	133-0024-0	133-00402D-129.23E
882	133-0028-0	133-00402D-136.62E
883	133-0029-0	133-00402D-136.63E
884	133-0033-0	133-00925F-012.64N
885	135-0004-0	135-00008D-011.43N
886	135-0008-0	135-00010D-002.33E
887	135-0018-0	135-00020D-004.34E
888	135-0028-0	135-00120D-011.66E
889	135-0034-0	135-00141D-006.47N
890	135-0046-0	135-00365D-000.35N
891	135-0047-0	135-00365D-000.34N
892	135-0054-0	135-00403D-112.88N
893	135-0073-0	135-02343F-000.87N
894	135-0110-0	135-00141D-001.88N
895	135-0112-0	135-00141D-000.01N
896	137-0002-0	137-00015D-000.68N
897	137-0005-0	137-00015D-002.36N
898	137-0011-0	137-00017D-008.64N
899	137-0019-0	137-00197D-004.84N
900	137-0022-0	137-00197D-013.03N
901	137-0028-0	137-00365D-043.11N
902	137-0029-0	137-00365D-043.12N
903	137-0032-0	137-00384D-004.22N
904	139-0002-0	139-00011D-008.15N

Table A.1 (continued)

Record Number	Bridge Serial Number	Location ID
905	139-0003-0	139-00011D-008.16N
906	139-0004-0	139-00011D-008.90N
907	139-0005-0	139-00011D-013.58N
908	139-0006-0	139-00011D-015.69N
909	139-0009-0	139-00013D-005.95N
910	139-0010-0	139-00013D-010.10N
911	139-0013-0	139-00051D-000.40E
912	139-0014-0	139-00052D-023.90E
913	139-0016-0	139-00052D-013.65E
914	139-0020-0	139-00053D-004.92E
915	139-0025-0	139-00053C-001.23N
916	139-0026-0	139-00060D-013.54N
917	139-0033-0	139-00283D-001.42E
918	139-0036-0	139-00284D-001.72N
919	139-0037-0	139-00284D-012.77N
920	139-0038-0	139-00323D-005.24N
921	139-0039-0	139-00323D-005.35N
922	139-0040-0	139-00332D-006.24E
923	139-0043-0	139-00419D-011.64N
924	139-0044-0	139-00419D-011.65N
925	139-0045-0	139-00419D-015.93N
926	139-0046-0	139-00419D-015.94N
927	139-0047-0	139-00419D-020.13N
928	139-0048-0	139-00419D-020.14N
929	139-0049-0	139-00419D-020.25N
930	139-0050-0	139-00419D-020.26N
931	139-0051-0	139-00419D-024.01N
932	139-0055-0	139-00472X-000.68N
933	139-0056-0	139-00524X-000.17W
934	139-0057-0	139-00621X-001.01E
935	139-0058-0	139-00751X-000.84W
936	139-0059-0	139-00013A-004.19N
937	139-0062-0	139-02423M-000.54N
938	139-0075-0	139-00060D-013.55N
939	139-0076-0	139-00053D-004.91E
940	141-0001-0	141-00015D-010.08N
941	141-0010-0	141-00016D-024.82E

Table A.1 (continued)

Record Number	Bridge Serial Number	Location ID
942	143-0004-0	143-00008D-001.18E
943	143-0005-0	143-00008D-008.43E
944	143-0007-0	143-00100D-003.63N
945	143-0008-0	143-00100D-008.98N
946	143-0010-0	143-00110X-001.76N
947	143-0018-0	143-00402D-004.72E
948	143-0019-0	143-00402D-004.73E
949	143-0029-0	143-01605F-000.25N
950	145-0005-0	145-00001D-018.29N
951	145-0006-0	145-00018D-004.19E
952	145-0007-0	145-00018D-004.20E
953	145-0008-0	145-00085D-006.07N
954	145-0010-0	145-00085A-003.85N
955	145-0017-0	145-00103D-010.87N
956	145-0028-0	145-00219D-014.82N
957	145-0031-0	145-00315D-004.40N
958	145-0036-0	145-00403D-000.00N
959	145-0037-0	145-00403D-000.01N
960	145-0038-0	145-00411D-016.93N
961	145-0039-0	145-00411D-016.94N
962	145-0041-0	145-00411D-021.01N
963	145-0042-0	145-00411D-021.02N
964	145-0045-0	145-00411D-025.40N
965	145-0046-0	145-00411D-025.41N
966	145-0050-0	145-01427F-000.30E
967	147-0013-0	147-00077P-006.66N
968	147-0015-0	147-00172D-003.46N
969	149-0003-0	149-00001D-008.53N
970	149-0012-0	149-00100D-002.92N
971	151-0009-0	151-00042D-006.66N
972	151-0015-0	151-00081D-024.20N
973	151-0018-0	151-00155D-007.00N
974	151-0024-0	151-00199X-003.25W
975	151-0025-0	151-00312X-000.78W
976	151-0028-0	151-01415F-004.66E
977	151-0031-0	151-00401D-211.83N
978	151-0033-0	151-00401D-216.36N

Table A.1 (continued)

Record Number	Bridge Serial Number	Location ID
979	151-0042-0	151-00401D-225.22N
980	151-0046-0	151-00401D-228.15N
981	151-0048-0	151-00755F-001.19N
982	151-0063-0	151-09321M-001.81E
983	153-0010-0	153-00011D-006.40N
984	153-0028-0	153-00096D-011.18E
985	153-0037-0	153-00247D-022.82N
986	153-0041-0	153-00401D-124.43N
987	153-0042-0	153-00401D-124.44N
988	153-0052-0	153-00401D-136.37N
989	153-0056-0	153-00543X-001.27E
990	157-0014-0	157-00060D-000.81N
991	157-0015-0	157-00060D-002.00N
992	157-0017-0	157-00082P-001.56N
993	157-0020-0	157-00177X-000.74W
994	157-0021-0	157-00229X-002.04N
995	157-0022-0	157-00250X-000.25N
996	157-0027-0	157-00332D-006.10E
997	157-0030-0	157-00334D-001.26N
998	157-0037-0	157-00346D-003.62E
999	157-0041-0	157-00403D-135.98N
1000	157-0042-0	157-00403D-135.99N
1001	157-0043-0	157-00403D-136.17N
1002	157-0044-0	157-00403D-136.18N
1003	157-0045-0	157-00403D-144.34N
1004	157-0046-0	157-00403D-144.35N
1005	157-0057-0	157-00330D-003.34E
1006	159-0001-0	159-00011D-007.43N
1007	159-0006-0	159-00016D-017.49E
1008	161-0008-0	161-00019D-018.22N
1009	161-0020-0	161-00135D-024.38N
1010	163-0002-0	163-00004D-003.34N
1011	163-0004-0	163-00004D-010.67N
1012	163-0023-0	163-00078D-004.92N
1013	165-0018-0	165-00017Y-001.36N
1014	165-0019-0	165-00023D-024.77N
1015	167-0007-0	167-00026D-006.33E

Table A.1 (continued)

Record Number	Bridge Serial Number	Location ID
1016	169-0015-0	169-00044D-014.33E
1017	169-0016-0	169-00049D-001.48N
1018	171-0001-0	171-00007D-010.66N
1019	171-0002-0	171-00007D-010.67N
1020	171-0006-0	171-00007D-015.20N
1021	171-0007-0	171-00007D-015.21N
1022	171-0012-0	171-00018D-001.15E
1023	171-0017-0	171-00036D-017.59E
1024	171-0021-0	171-00401D-199.10N
1025	175-0002-0	175-00019D-003.34N
1026	175-0004-0	175-00019D-007.98N
1027	175-0008-0	175-00019D-016.77N
1028	175-0017-0	175-00026D-018.58E
1029	175-0018-0	175-00026D-018.80E
1030	175-0031-0	175-00031D-021.42N
1031	175-0042-0	175-00096X-001.20N
1032	175-0046-0	175-00124X-003.00N
1033	175-0061-0	175-00278D-001.83E
1034	175-0068-0	175-00338D-013.20E
1035	175-0089-0	175-00531X-002.20N
1036	177-0001-0	177-00003D-000.21N
1037	177-0004-0	177-00032D-012.26E
1038	177-0005-0	177-00032D-018.29E
1039	177-0006-0	177-00032D-018.64E
1040	177-0010-0	177-00195D-003.65N
1041	179-0001-0	179-00021X-002.97N
1042	179-0004-0	179-00025D-006.91N
1043	179-0021-0	179-00038D-021.76E
1044	179-0022-0	179-00050X-007.60E
1045	179-0032-0	179-00405D-067.18N
1046	179-0033-0	179-00405D-067.19N
1047	181-0002-0	181-00043D-015.51N
1048	181-0003-0	181-00043D-018.27N
1049	181-0010-0	181-00079D-018.97N
1050	181-0014-0	181-00220D-017.70E
1051	181-0017-0	181-00047D-016.50E
1052	185-0007-0	185-00007D-023.78N

Table A.1 (continued)

Record Number	Bridge Serial Number	Location ID
1053	185-0008-0	185-00007D-023.79N
1054	185-0009-0	185-00007D-024.60N
1055	185-0010-0	185-00031D-000.00N
1056	185-0012-0	185-00031D-008.98N
1057	185-0013-0	185-00031D-008.99N
1058	185-0016-0	185-00038D-023.21E
1059	185-0020-0	185-00133D-002.24N
1060	185-0024-0	185-00122D-000.41E
1061	185-0026-0	185-00122D-004.22E
1062	185-0032-0	185-00274X-001.28N
1063	185-0034-0	185-00376D-005.74E
1064	185-0036-0	185-00401D-007.10N
1065	185-0041-0	185-00401D-012.27N
1066	185-0045-0	185-00401D-015.61N
1067	185-0073-0	185-02509F-004.60N
1068	187-0001-0	187-00009D-005.86N
1069	187-0002-0	187-00009D-009.58N
1070	187-0003-0	187-00060B-003.32N
1071	187-0009-0	187-00052D-007.98E
1072	187-0010-0	187-00052D-014.85E
1073	187-0011-0	187-00052D-017.70E
1074	187-0014-0	187-00060D-005.44N
1075	187-0015-0	187-00060D-006.24N
1076	187-0016-0	187-00400D-003.56N
1077	189-0001-0	189-00010D-004.15E
1078	189-0002-0	189-00010D-005.74E
1079	189-0007-0	189-00021X-000.60N
1080	189-0008-0	189-00024X-001.29N
1081	189-0009-0	189-00043D-007.61N
1082	189-0013-0	189-00150D-004.60E
1083	189-0015-0	189-00223D-001.94E
1084	189-0022-0	189-00797F-000.59N
1085	189-0026-0	189-02150F-000.01N
1086	191-0002-0	191-00017X-002.50E
1087	191-0004-0	191-00024X-003.76E
1088	191-0007-0	191-00025D-002.72N
1089	191-0014-0	191-00057D-008.49E

Table A.1 (continued)

Record Number	Bridge Serial Number	Location ID
1090	191-0015-0	191-00057D-008.29E
1091	191-0016-0	191-00057D-005.55E
1092	191-0018-0	191-00129X-010.39E
1093	191-0021-0	191-00251D-012.20E
1094	191-0045-0	191-32021X-003.00E
1095	193-0012-0	193-00049D-009.27N
1096	193-0014-0	193-00049D-009.91N
1097	193-0019-0	193-00090D-014.60N
1098	193-0025-0	193-00128D-005.90N
1099	193-5042-0	193-00090D-005.54N
1100	195-0009-0	195-00072D-009.05E
1101	195-0016-0	195-00106D-016.12N
1102	195-0017-0	
1103	195-0018-0	195-00172D-010.75N
1104	195-0019-0	195-00191D-003.67N
1105	195-0021-0	195-00281D-004.11N
1106	197-0008-0	
1107	197-0009-0	197-00137D-014.87N
1108	197-0010-0	197-00137D-015.44N
1109	199-0002-0	199-00017X-001.20N
1110	199-0007-0	199-00018D-006.03E
1111	199-0015-0	199-00041D-001.27N
1112	199-0017-0	199-00041D-003.91N
1113	199-0026-0	199-00074D-016.02E
1114	199-0027-0	199-00074D-012.72E
1115	199-0030-0	199-00074D-002.90E
1116	199-0031-0	199-00085D-000.13N
1117	199-0032-0	199-00085D-000.28N
1118	199-0033-0	199-00085D-002.05N
1119	199-0034-0	199-00085D-008.73N
1120	199-0041-0	199-00085A-011.05N
1121	199-0047-0	199-00109D-009.60E
1122	199-0055-0	199-00362D-016.54E
1123	201-0007-0	201-00091D-001.72N
1124	207-0002-0	207-00015X-001.65N
1125	207-0007-0	207-00018D-020.22E
1126	207-0008-0	207-02784F-000.66E

Table A.1 (continued)

Record Number	Bridge Serial Number	Location ID
1127	207-0014-0	207-00042D-011.26N
1128	207-0015-0	207-00042D-020.75N
1129	207-0021-0	207-00083D-008.36N
1130	207-0022-0	207-00083D-010.68N
1131	207-0027-0	207-00083D-024.57N
1132	207-0035-0	207-00087D-018.66N
1133	207-0038-0	207-00401D-176.37N
1134	207-0045-0	207-00401D-188.07N
1135	207-0053-0	207-00408D-014.72N
1136	207-0054-0	207-00408D-014.73N
1137	207-0055-0	207-00408D-014.95N
1138	207-0060-0	207-01431F-002.25E
1139	207-0063-0	207-01698F-000.05E
1140	207-0069-0	207-00018D-008.61E
1141	209-0004-0	209-00030D-000.58E
1142	209-0005-0	209-00030D-000.84E
1143	211-0001-0	211-00012D-014.15E
1144	211-0008-0	211-00046X-000.77N
1145	211-0010-0	211-00083D-003.17N
1146	211-0016-0	211-00083D-018.93N
1147	211-0017-0	211-00083D-020.61N
1148	211-0018-0	211-00146X-003.27N
1149	211-0019-0	211-00246X-006.32E
1150	211-0020-0	211-00256X-001.63N
1151	211-0021-0	211-00249X-001.49N
1152	211-0022-0	211-00252X-004.44N
1153	211-0029-0	211-00402D-113.37E
1154	211-0030-0	211-00402D-113.38E
1155	211-0037-0	211-00402D-126.46E
1156	211-0038-0	211-00402D-126.47E
1157	211-0063-0	211-02425F-007.27N
1158	213-0001-0	213-00002D-000.24E
1159	213-0008-0	213-00061D-001.40N
1160	213-0018-0	213-00002D-008.30E
1161	213-0021-0	213-00061D-028.20N
1162	213-0023-0	213-00136D-001.87E
1163	213-0026-0	213-00225D-005.32N

Table A.1 (continued)

Record Number	Bridge Serial Number	Location ID
1164	213-0031-0	213-00225D-021.33N
1165	215-0003-0	215-00520D-005.84E
1166	215-0005-0	215-00520D-003.27E
1167	215-0008-0	215-00001D-013.29N
1168	215-0009-0	215-00520D-000.00E
1169	215-0028-0	215-00085D-007.60N
1170	215-0029-0	215-00085D-007.61N
1171	215-0030-0	215-00085D-008.60N
1172	215-0031-0	215-00085D-008.61N
1173	215-0037-0	215-00219D-002.13N
1174	215-0047-0	215-08042M-002.45N
1175	215-0050-0	215-00411D-001.35N
1176	215-0051-0	215-00411D-001.36N
1177	215-0055-0	215-00411D-004.26N
1178	215-0057-0	215-00411D-004.47N
1179	215-0063-0	215-00411D-006.02N
1180	215-0065-0	215-00411D-006.49N
1181	215-0067-0	215-00411D-007.13N
1182	215-0070-0	215-00411D-008.09N
1183	215-0072-0	215-00411D-008.25N
1184	215-0074-0	215-00411D-009.60N
1185	215-0075-0	215-00411D-009.61N
1186	215-0076-0	215-00411D-009.75N
1187	215-0084-0	215-00411R-008.09N
1188	215-0092-0	215-08016M-002.84E
1189	215-0149-0	215-00001D-014.20N
1190	215-0161-0	215-00411D-005.46N
1191	217-0008-0	217-00036D-001.31E
1192	217-0010-0	217-00057X-000.02N
1193	217-0011-0	217-00081D-000.48N
1194	217-0015-0	217-00081D-011.92N
1195	217-0016-0	217-00114X-000.25N
1196	217-0018-0	217-00142D-011.34N
1197	217-0019-0	217-00142D-011.87N
1198	217-0020-0	217-00212D-011.19E
1199	217-0021-0	217-00212D-006.95E
1200	217-0022-0	217-00212D-006.38E

Table A.1 (continued)

Record Number	Bridge Serial Number	Location ID
1201	217-0023-0	217-00301X-000.25N
1202	217-0024-0	217-00402D-087.96E
1203	217-0026-0	217-00402D-090.33E
1204	217-0028-0	217-00402D-090.43E
1205	217-0031-0	217-00402D-092.24E
1206	217-0032-0	217-00402D-092.25E
1207	217-0034-0	217-00402D-092.89E
1208	217-0035-0	217-00402D-094.50E
1209	217-0036-0	217-00402D-094.51E
1210	217-0037-0	217-00402D-094.63E
1211	217-0038-0	217-00402D-094.64E
1212	217-0041-0	217-00516X-002.45E
1213	217-0063-0	217-00212D-016.62E
1214	217-0064-0	217-00012D-004.77E
1215	221-0010-0	221-00022D-028.37E
1216	221-0014-0	221-00077D-033.75N
1217	223-0004-0	223-00061D-010.31N
1218	223-0012-0	223-00092D-006.36N
1219	223-0013-0	223-00092D-006.98N
1220	223-0020-0	223-00120D-013.32E
1221	225-0006-0	225-00049D-015.88N
1222	225-0009-0	225-00247C-000.06E
1223	225-0010-0	225-00247C-003.00E
1224	225-0016-0	225-01508F-001.04E
1225	227-0019-0	227-00136D-002.18E
1226	227-0037-0	227-00108D-003.77N
1227	229-0007-0	229-00015D-019.71N
1228	229-0008-0	229-00015D-021.57N
1229	229-0009-0	
1230	231-0001-0	231-00003D-008.90N
1231	231-0003-0	231-00018D-014.71E
1232	231-0005-0	231-00109D-003.62E
1233	233-0015-0	233-00006B-001.57E
1234	233-0023-0	233-00006D-008.31E
1235	233-0025-0	233-00101D-005.92N
1236	233-0028-0	233-00101D-008.69N
1237	233-0033-0	233-00006D-023.08E

Table A.1 (continued)

Record Number	Bridge Serial Number	Location ID
1238	235-0003-0	235-00011D-007.39N
1239	235-0008-0	235-00026D-008.86E
1240	235-0009-0	235-00026W-000.52W
1241	235-0023-0	235-00257D-008.00N
1242	237-0003-0	237-00016D-010.16E
1243	237-0005-0	237-00016D-024.12E
1244	237-0006-0	237-00024D-000.48N
1245	237-0008-0	237-00044D-002.34E
1246	237-0009-0	237-00044D-005.76E
1247	237-0011-0	237-00044D-020.39E
1248	237-0012-0	237-00044D-022.85E
1249	239-0002-0	239-00039D-004.97N
1250	241-0001-0	241-00002D-007.55E
1251	241-0008-0	241-00015D-000.32N
1252	241-0009-0	241-00015D-001.85N
1253	241-0010-0	241-00015D-002.10N
1254	241-0017-0	241-00028D-000.00N
1255	241-0022-0	241-00246D-000.08E
1256	243-0002-0	243-00001D-009.00N
1257	243-0012-0	243-00216D-005.87N
1258	243-0013-0	243-00266D-011.35E
1259	245-0004-0	245-00004D-011.18N
1260	245-0005-0	245-00004D-012.48N
1261	245-0007-0	245-00004D-016.73N
1262	245-0008-0	245-00004D-020.88N
1263	245-0009-0	245-00004D-025.46N
1264	245-0011-0	245-00010D-009.72E
1265	245-0013-0	245-00010D-014.90E
1266	245-0015-0	245-00010D-016.12E
1267	245-0016-0	245-00010D-017.34E
1268	245-0017-0	245-00010D-018.08E
1269	245-0018-0	245-00010D-018.17E
1270	245-0019-0	245-00010D-018.25E
1271	245-0020-0	245-00010D-018.35E
1272	245-0021-0	245-00010D-018.46E
1273	245-0022-0	245-00010R-018.24E
1274	245-0023-0	245-00010R-018.26E

Table A.1 (continued)

Record Number	Bridge Serial Number	Location ID
1275	245-0038-0	245-00105X-000.43W
1276	245-0045-0	245-00402D-196.49E
1277	245-0046-0	245-00402D-196.50E
1278	245-0047-0	245-00402D-199.21E
1279	245-0048-0	245-00402D-199.22E
1280	245-0049-0	245-00402D-200.18E
1281	245-0050-0	245-00402D-200.19E
1282	245-0051-0	245-00402D-201.07E
1283	245-0052-0	245-00402D-201.08E
1284	245-0053-0	245-00402D-201.38E
1285	245-0054-0	245-00402D-201.39E
1286	245-0055-0	245-00402R-199.20E
1287	245-0057-0	245-00415D-001.89E
1288	245-0059-0	245-00415D-002.76E
1289	245-0062-0	245-00415D-005.33E
1290	245-0063-0	245-00415D-007.40E
1291	245-0069-0	245-00842X-000.02N
1292	245-0073-0	245-02346X-000.92S
1293	245-0081-0	245-01056D-000.28W
1294	245-0085-0	245-00601X-003.37W
1295	245-0090-0	245-00145X-002.37W
1296	245-0095-0	245-00028D-007.12N
1297	245-0097-0	245-00028D-006.16N
1298	245-0098-0	245-00028D-006.00N
1299	245-0107-0	245-00028D-004.84N
1300	247-0003-0	247-00020D-007.28E
1301	247-0010-0	247-00020D-010.59E
1302	247-0015-0	247-00212D-004.97E
1303	251-0026-0	251-00073D-000.95N
1304	251-0027-0	251-00073D-007.08N
1305	251-0030-0	251-00073D-011.11N
1306	253-0006-0	253-00091D-000.00N
1307	255-0003-0	255-00092D-001.06N
1308	255-0004-0	255-00003D-005.74N
1309	255-0005-0	255-00003D-005.75N
1310	255-0006-0	255-00003D-003.03N
1311	255-0007-0	255-00003D-003.04N

Table A.1 (continued)

Record Number	Bridge Serial Number	Location ID
1312	255-0008-0	255-00003D-003.94N
1313	255-0009-0	255-00003D-003.95N
1314	255-0012-0	255-00016D-004.15E
1315	255-0015-0	255-00016D-012.27E
1316	255-0016-0	255-00016D-012.28E
1317	255-0017-0	255-00155D-007.03N
1318	255-0018-0	255-00036X-011.21E
1319	255-0021-0	255-00092D-008.52N
1320	255-0022-0	255-00115X-000.87S
1321	255-0027-0	255-00401D-207.87N
1322	257-0007-0	257-00017A-002.94N
1323	257-0011-0	257-00184D-014.53N
1324	259-0015-0	259-00027D-022.99E
1325	261-0002-0	261-00003D-004.31N
1326	261-0003-0	261-00003D-010.27N
1327	261-0007-0	261-00027D-012.93E
1328	261-0010-0	261-00027D-021.72E
1329	261-0011-0	261-00027D-029.16E
1330	261-0013-0	261-00030D-011.78E
1331	261-0037-0	261-00228D-003.51E
1332	263-0012-0	263-00036D-010.04E
1333	263-0014-0	263-00036D-022.02E
1334	263-0016-0	263-00041D-003.00N
1335	263-0022-0	263-00190D-000.95E
1336	265-0004-0	265-00022D-007.04E
1337	265-0008-0	265-00038X-002.74N
1338	265-0015-0	265-00402D-147.16E
1339	265-0016-0	265-00402D-147.17E
1340	265-0021-0	265-02179F-004.00N
1341	267-0020-0	267-00144D-008.01E
1342	267-0026-0	267-00178D-009.76E
1343	269-0003-0	269-00003D-005.19N
1344	269-0020-0	269-00128D-011.29N
1345	269-0024-0	269-00137D-006.59N
1346	269-0025-0	269-00137D-008.64N
1347	269-0028-0	269-00137D-022.90N
1348	271-0003-0	271-00027D-017.88E

Table A.1 (continued)

Record Number	Bridge Serial Number	Location ID
1349	275-0003-0	275-00003A-005.74N
1350	275-0010-0	275-00038D-000.06E
1351	275-0011-0	275-00038D-001.88E
1352	275-0013-0	275-00038D-009.41E
1353	275-0033-0	275-00188D-001.44E
1354	275-0046-0	275-00003D-011.85N
1355	275-0047-0	275-00003D-011.86N
1356	275-0071-0	275-00038D-001.89E
1357	277-0027-0	277-00401D-060.14N
1358	277-0029-0	277-00401D-060.53N
1359	277-0031-0	277-00401D-061.80N
1360	277-0032-0	277-00401D-061.87N
1361	277-0034-0	277-00401D-063.55N
1362	277-0036-0	277-00401D-063.90N
1363	277-0078-0	277-00035D-010.11N
1364	281-0008-0	281-00002D-017.97E
1365	283-0019-0	283-00056D-009.82N
1366	283-0026-0	283-00086D-009.31E
1367	283-0029-0	283-00167X-003.98N
1368	283-0036-0	283-00404D-066.74E
1369	283-0041-0	283-00404D-073.50E
1370	283-0042-0	283-00404D-073.51E
1371	283-0056-0	283-00199D-007.70N
1372	285-0003-0	285-00001D-009.09N
1373	285-0006-0	285-00001D-013.22N
1374	285-0013-0	285-00014D-000.40N
1375	285-0020-0	285-00014P-003.68N
1376	285-0021-0	285-00014P-004.58N
1377	285-0025-0	285-00018D-005.90E
1378	285-0027-0	285-00029C-000.65N
1379	285-0029-0	285-00054D-010.35E
1380	285-0030-0	285-00100D-004.07N
1381	285-0032-0	285-00109D-003.53E
1382	285-0035-0	285-00109D-016.77E
1383	285-0036-0	285-00109D-016.78E
1384	285-0038-0	285-00177X-001.43E
1385	285-0048-0	285-00219D-019.98N

Table A.1 (continued)

Record Number	Bridge Serial Number	Location ID
1386	285-0051-0	285-00403D-002.26N
1387	285-0052-0	285-00403D-002.27N
1388	285-0054-0	285-00403D-005.17N
1389	285-0057-0	285-00403D-009.28N
1390	285-0061-0	285-00403D-014.27N
1391	285-0063-0	285-00403D-016.39N
1392	285-0078-0	285-00411D-039.85N
1393	285-0079-0	285-00411D-039.86N
1394	285-0082-0	285-00411D-046.16N
1395	285-0091-0	285-01429F-000.49E
1396	285-0092-0	285-01429F-000.50E
1397	285-0093-0	285-01429F-013.50E
1398	285-0097-0	285-02031F-001.40N
1399	285-0114-0	285-00109D-012.10E
1400	285-0115-0	285-00109D-014.26E
1401	287-0008-0	287-00032D-012.90E
1402	287-0021-0	287-00112D-015.17N
1403	289-0003-0	289-00019D-019.72N
1404	289-0019-0	289-00096D-013.20E
1405	289-0020-0	289-00243X-002.25E
1406	289-0021-0	289-00358D-003.75E
1407	289-0035-0	289-01282F-003.69N
1408	289-0037-0	289-01471F-003.34E
1409	289-0038-0	289-01617F-001.09N
1410	291-0016-0	291-00060D-005.09N
1411	291-0017-0	291-00180D-005.00N
1412	291-0027-0	291-02899F-001.79S
1413	293-0001-0	293-00003D-007.23N
1414	295-0004-0	295-00001D-020.72N
1415	295-0010-0	295-00136D-007.78E
1416	295-0020-0	295-00151D-002.48N
1417	295-0021-0	295-00157D-025.70N
1418	295-0031-0	295-00341D-004.97N
1419	295-0051-0	295-00002D-002.11E
1420	297-0002-0	297-00010D-009.51E
1421	297-0003-0	297-00010B-000.09E
1422	297-0006-0	297-00010D-022.21E

Table A.1 (continued)

Record Number	Bridge Serial Number	Location ID
1423	297-0009-0	297-00010D-010.57E
1424	297-0010-0	297-00010D-010.58E
1425	297-0011-0	297-00010D-012.23E
1426	297-0012-0	297-00010D-012.24E
1427	297-0013-0	297-00010D-012.96E
1428	297-0014-0	297-00010D-012.97E
1429	297-0015-0	297-00011D-000.98N
1430	297-0017-0	297-00011D-012.74N
1431	297-0019-0	297-00011D-019.70N
1432	297-0022-0	297-00081D-017.30N
1433	297-0023-0	297-00081D-021.07N
1434	297-0024-0	297-00083D-005.05N
1435	297-0026-0	297-00138D-005.78E
1436	299-0004-0	299-00004D-030.32N
1437	299-0022-0	299-00158D-006.40E
1438	299-0023-0	299-00158D-006.20E
1439	299-0024-0	299-00158D-005.90E
1440	299-0030-0	299-00520D-022.31E
1441	299-0031-0	299-00520D-022.45E
1442	301-0004-0	301-00016D-004.65E
1443	301-0006-0	301-00016D-008.84E
1444	301-0012-0	301-00021X-000.09S
1445	301-0016-0	301-00080D-015.35N
1446	301-0021-0	301-00402D-154.29E
1447	301-0022-0	301-00402D-154.30E
1448	301-0024-0	301-00402D-164.52E
1449	301-0025-0	301-00402D-164.53E
1450	301-0030-0	301-01272F-003.17E
1451	301-0031-0	301-01649F-003.25E
1452	303-0017-0	303-00102D-006.89N
1453	305-0002-0	305-00023D-017.83N
1454	305-0003-0	305-00023D-017.84N
1455	305-0006-0	305-00023D-019.63N
1456	305-0007-0	305-00023D-019.64N
1457	305-0008-0	305-00023D-023.63N
1458	305-0019-0	305-00038D-017.31E
1459	305-0024-0	305-00169D-004.02N

Table A.1 (continued)

Record Number	Bridge Serial Number	Location ID
1460	305-0045-0	305-00023D-023.62N
1461	307-0008-0	
1462	307-0010-0	307-00041D-011.12N
1463	307-0011-0	307-00045D-001.85N
1464	307-0012-0	307-00045D-002.01N
1465	309-0014-0	309-00030D-017.42E
1466	309-0015-0	309-00031D-000.81N
1467	309-0018-0	309-00126D-008.22E
1468	311-0001-0	311-00011D-007.91N
1469	311-0007-0	311-00017D-004.62N
1470	311-0015-0	311-00075D-013.32N
1471	311-0030-0	311-00255D-014.70N
1472	313-0001-0	313-00002D-003.32E
1473	313-0003-0	313-00002D-006.43E
1474	313-0004-0	313-00002D-011.56E
1475	313-0017-0	313-00010X-001.08E
1476	313-0018-0	313-00052D-000.06E
1477	313-0019-0	313-00052D-002.10E
1478	313-0020-0	313-00052D-005.66E
1479	313-0021-0	313-00052D-006.79E
1480	313-0022-0	313-00052D-006.80E
1481	313-0024-0	313-00052D-008.11E
1482	313-0037-0	313-00286D-004.73E
1483	313-0038-0	313-00286D-005.05E
1484	313-0039-0	313-00401D-326.89N
1485	313-0041-0	313-00401D-327.03N
1486	313-0043-0	313-00401D-335.89N
1487	313-0045-0	313-00401D-336.09N
1488	313-0047-0	313-00401D-336.25N
1489	313-0050-0	313-00401D-341.07N
1490	313-0054-0	313-00691F-002.98N
1491	313-0066-0	313-01515M-000.33N
1492	313-5072-0	313-00003D-010.39N
1493	313-5073-0	313-00003D-010.40N
1494	313-5075-0	313-00003D-014.21N
1495	313-5076-0	313-00003D-014.22N
1496	315-0017-0	

Table A.1 (continued)

Record Number	Bridge Serial Number	Location ID
1497	317-0003-0	317-00010D-027.02E
1498	317-0009-0	317-00017D-028.72N
1499	319-0018-0	319-00057D-028.91E
1500	319-0022-0	319-00112D-024.30N

Table A.2: Steel girder bridges with superstructure maintenance item request number.

Record Number	Bridge Serial Number	Location ID
1	001-0011-0	001-00004D-021.18N
2	001-0014-0	001-00015D-016.01N
3	003-0012-0	003-00064D-017.10E
4	007-0002-0	007-00037D-015.01E
5	009-0002-0	009-00022D-004.02E
6	009-0005-0	009-00022D-011.05E
7	009-0006-0	009-00022D-011.09E
8	009-0007-0	009-00022D-012.46E
9	009-0015-0	009-00049D-009.90N
10	009-0016-0	009-00112D-005.10N
11	011-0002-0	011-00015D-000.85N
12	011-0008-0	011-00051D-013.02E
13	011-0009-0	011-00059D-002.56N
14	011-0012-0	011-00098D-003.71E
15	011-0013-0	011-00098D-002.83E
16	011-0029-0	011-00403D-150.43N
17	011-0030-0	011-00403D-150.44N
18	011-0031-0	011-00403D-152.66N
19	011-0032-0	011-00403D-152.67N
20	013-0010-0	013-00082D-010.70E
21	013-0012-0	013-00211D-022.60N
22	013-0014-0	013-00211D-018.86N
23	013-0018-0	013-00324D-000.66E
24	013-0022-0	013-00403D-127.19N
25	013-0023-0	013-00403D-127.20N
26	015-0004-0	015-00003D-002.66N
27	015-0005-0	015-00003D-003.48N
28	015-0006-0	015-00003D-003.49N

Table A.2 (continued)

Record Number	Bridge Serial Number	Location ID
29	015-0007-0	015-00003D-006.81N
30	015-0012-0	015-00003D-011.67N
31	015-0016-0	015-00003D-014.82N
32	015-0021-0	015-00003D-022.62N
33	015-0025-0	015-00020D-003.95E
34	015-0026-0	015-00020D-011.30E
35	015-0031-0	015-00061D-003.93N
36	015-0032-0	015-00061D-004.24N
37	015-0033-0	015-00061D-004.39N
38	015-0043-0	015-00061D-005.30N
39	015-0057-0	015-00155X-005.12N
40	015-0077-0	015-00401D-280.69N
41	015-0079-0	015-00401D-281.51N
42	015-0080-0	015-00401D-281.52N
43	015-0082-0	015-00401D-283.70N
44	015-0083-0	015-00401D-286.75N
45	015-0084-0	015-00401D-286.76N
46	015-0087-0	015-00401D-287.16N
47	015-0088-0	015-00401D-287.17N
48	015-0094-0	015-00401D-293.88N
49	015-0101-0	015-00401D-299.66N
50	015-0103-0	015-00401D-304.19N
51	015-0104-0	015-00401D-304.22N
52	017-0003-0	017-00011D-014.68N
53	019-0027-0	019-00125D-012.92N
54	021-0017-0	021-00019D-010.64N
55	021-0026-0	021-00022D-012.71E
56	021-0028-0	021-00022D-015.86E
57	021-0030-0	021-03206M-000.99E
58	021-0031-0	021-00011D-003.90N
59	021-0034-0	021-00011D-006.15N
60	021-0038-0	021-00074D-001.41E
61	021-0040-0	021-00074D-008.80E
62	021-0046-0	021-00087D-003.75N
63	021-0048-0	021-00087D-010.54N
64	021-0054-0	021-00091X-000.23S
65	021-0066-0	021-00940F-010.20N

Table A.2 (continued)

Record Number	Bridge Serial Number	Location ID
66	021-0070-0	021-00940F-015.85N
67	021-0081-0	021-00401D-160.08N
68	021-0083-0	021-00401D-160.30N
69	021-0085-0	021-00401D-161.27N
70	021-0088-0	021-00401D-162.48N
71	021-0090-0	021-00401D-163.80N
72	021-0095-0	021-00401D-164.98N
73	021-0096-0	021-00401D-164.99N
74	021-0097-0	021-00401D-165.59N
75	021-0098-0	021-00401D-165.60N
76	021-0101-0	021-00401D-166.63N
77	021-0106-0	021-00401D-169.07N
78	021-0107-0	021-00401D-169.08N
79	021-0109-0	021-00401D-170.82N
80	021-0110-0	021-00401D-170.83N
81	021-0115-0	021-00401R-164.96N
82	021-0116-0	021-00401R-164.97N
83	021-0119-0	021-00404D-000.70E
84	021-0120-0	021-00404D-000.71E
85	021-0122-0	021-00404D-001.40E
86	021-0125-0	021-00404D-003.01E
87	021-0126-0	021-00404D-003.02E
88	021-0131-0	021-00404D-005.48E
89	021-0136-0	021-00408D-000.00N
90	021-0143-0	021-00408D-007.24N
91	021-0148-0	021-00665F-002.05E
92	021-0160-0	021-00581X-000.31E
93	021-0174-0	021-00074D-013.15E
94	021-0176-0	021-03209M-002.72E
95	021-0181-0	021-03217M-001.20E
96	021-0188-0	021-03245M-000.35E
97	021-0191-0	021-03262M-000.04N
98	023-0001-0	023-00026D-011.63E
99	023-0012-0	023-00112D-022.28N
100	025-0025-0	025-00520D-019.87E
101	025-0026-0	025-00520D-020.67E
102	027-0003-0	027-00076D-010.34E

Table A.2 (continued)

Record Number	Bridge Serial Number	Location ID
103	027-0031-0	027-00122D-002.00E
104	027-0033-0	027-00122D-007.91E
105	027-0034-0	027-00122D-008.29E
106	029-0002-0	029-00012X-002.34N
107	029-0005-0	029-00025D-009.04N
108	029-0006-0	029-00026D-005.79E
109	029-0013-0	029-00030D-020.22E
110	029-0014-0	029-00030D-020.23E
111	029-0015-0	029-02768F-003.34E
112	029-0029-0	029-00404D-146.29E
113	029-0030-0	029-00404D-146.30E
114	029-0039-0	029-00405D-086.78N
115	029-0041-0	029-00405D-086.99N
116	029-0043-0	029-00405D-089.18N
117	029-0047-0	029-00405D-090.94N
118	031-0047-0	031-00119D-001.29N
119	031-0050-0	031-00119D-011.23N
120	033-0004-0	033-00017D-005.46N
121	033-0038-0	033-00305D-026.32N
122	033-0053-0	033-00088D-000.58E
123	035-0001-0	035-00016D-000.88E
124	039-0011-0	039-00025D-031.89N
125	039-0029-0	039-00405D-000.01N
126	039-0038-0	039-00405D-014.65N
127	039-0039-0	039-00405D-014.66N
128	039-0044-0	039-00405D-027.74N
129	039-0045-0	039-00405D-027.75N
130	043-0014-0	043-00129D-004.65N
131	043-0015-0	043-00129D-004.83N
132	045-0002-0	045-00001D-010.49N
133	045-0004-0	045-00001D-013.30N
134	047-0005-0	047-00002D-002.79E
135	047-0006-0	047-00002D-002.80E
136	047-0007-0	047-00002D-005.23E
137	047-0008-0	047-00002D-005.24E
138	047-0024-0	047-00209X-002.42S
139	047-0035-0	047-00401D-351.38N

Table A.2 (continued)

Record Number	Bridge Serial Number	Location ID
140	047-0036-0	047-00401D-351.39N
141	047-0039-0	047-00401D-353.13N
142	047-0043-0	047-00401D-354.34N
143	049-0012-0	049-00023D-000.00N
144	049-0038-0	049-00252D-011.48E
145	051-0005-0	051-00421D-001.60N
146	051-0007-0	051-00421D-003.38N
147	051-0008-0	051-00421D-004.29N
148	051-0009-0	051-00421D-004.30N
149	051-0012-0	051-00421D-005.42N
150	051-0015-0	051-00421D-005.58N
151	051-0016-0	051-00421D-005.96N
152	051-0017-0	051-00421D-005.97N
153	051-0019-0	051-00421D-006.10N
154	051-0020-0	051-00421D-006.20N
155	051-0029-0	051-00421D-007.22N
156	051-0038-0	051-00421R-006.10N
157	051-0047-0	051-00026D-016.67E
158	051-0054-0	051-00025D-019.86N
159	051-0060-0	051-00026D-011.20E
160	051-0066-0	051-00026D-032.43E
161	051-0069-0	051-00030D-002.04E
162	051-0074-0	051-00204D-011.88E
163	051-0076-0	051-00204D-014.90E
164	051-0078-0	051-00204D-025.61E
165	051-0089-0	051-00404D-163.59E
166	051-0090-0	051-00404D-163.60E
167	051-0092-0	051-00404D-163.95E
168	051-0093-0	051-00404D-163.97E
169	051-0095-0	051-00404D-165.03E
170	051-0096-0	051-00404D-165.02E
171	051-0097-0	051-00404D-165.69E
172	051-0098-0	051-00404D-165.70E
173	051-0101-0	051-00404D-166.09E
174	051-0105-0	051-00405D-093.87N
175	051-0109-0	051-00405D-099.28N
176	051-0124-0	051-00405D-107.24N

Table A.2 (continued)

Record Number	Bridge Serial Number	Location ID
177	051-0125-0	051-00405D-108.52N
178	051-0126-0	051-00405D-108.53N
179	051-0135-0	051-04067M-002.59N
180	051-0138-0	051-04070M-003.00E
181	051-0147-0	051-00204P-006.08E
182	057-0015-0	057-00092D-000.08N
183	057-0020-0	057-00108D-003.46N
184	057-0071-0	057-01375F-014.20N
185	059-0001-0	059-00010L-005.45E
186	059-0002-0	059-00010L-005.44E
187	059-0011-0	059-00010L-001.88E
188	059-0017-0	059-00010L-000.05E
189	059-0018-0	059-00010L-000.04E
190	059-0020-0	059-00010D-003.13E
191	059-0021-0	059-00010D-003.14E
192	059-0029-0	059-00015A-004.33N
193	059-0036-0	059-00008D-001.97E
194	059-0044-0	059-00008D-004.21E
195	059-0045-0	059-00008D-004.22E
196	059-0047-0	059-00008D-006.00E
197	059-0048-0	059-00008D-006.01E
198	059-0059-0	059-00320M-000.56E
199	061-0002-0	061-00037D-000.01E
200	063-0045-0	063-00407R-057.44C
201	063-0048-0	063-00407R-057.63C
202	067-0007-0	067-00003D-014.77N
203	067-0008-0	067-00003D-014.78N
204	067-0010-0	067-00003D-020.97N
205	067-0013-0	067-00003D-005.21N
206	067-0019-0	067-09004M-000.59N
207	067-0022-0	067-00005D-014.97N
208	067-0023-0	067-00005D-014.98N
209	067-0031-0	067-00005D-001.35N
210	067-0042-0	067-00120D-021.40E
211	067-0052-0	067-00280D-000.60N
212	067-0066-0	067-00401D-258.79N
213	067-0069-0	067-00401D-260.70N

Table A.2 (continued)

Record Number	Bridge Serial Number	Location ID
214	067-0073-0	067-00401D-264.21N
215	067-0074-0	067-00401D-265.02N
216	067-0076-0	067-00401D-267.51N
217	067-0084-0	067-00401D-270.32N
218	067-0090-0	067-00402D-047.83E
219	067-0095-0	067-00407D-015.60C
220	067-0099-0	067-00407D-019.51C
221	067-0106-0	067-00407D-020.41C
222	067-0184-0	067-00005D-014.33N
223	069-0009-0	069-00032D-001.24E
224	069-0010-0	069-00032D-004.23E
225	069-0013-0	069-00032D-019.60E
226	069-0014-0	069-00032D-020.12E
227	069-0017-0	069-00032D-025.11E
228	069-0018-0	069-00032D-025.83E
229	069-0031-0	069-00135D-016.62N
230	073-0016-0	073-00223D-002.47E
231	073-0018-0	073-00223D-010.12E
232	073-0022-0	073-00232D-008.15E
233	073-0040-0	073-02122F-004.91N
234	073-0043-0	073-00388D-002.80N
235	075-0019-0	075-00240X-001.84N
236	077-0005-0	077-00016D-013.57E
237	077-0016-0	077-00054D-002.07E
238	077-0017-0	077-00054D-004.80E
239	077-0018-0	077-00054D-010.58E
240	077-0043-0	077-00403D-043.47N
241	077-0044-0	077-00403D-043.48N
242	077-0047-0	077-00403D-046.88N
243	077-0048-0	077-00403D-046.89N
244	077-0049-0	077-00403D-050.02N
245	077-0069-0	077-01599F-007.01N
246	077-0076-0	077-02081F-002.01E
247	077-5136-0	077-00403D-050.03N
248	079-0006-0	079-00007D-018.71N
249	079-0014-0	079-00096D-001.22E
250	081-0002-0	081-00007D-013.83N

Table A.2 (continued)

Record Number	Bridge Serial Number	Location ID
251	081-0017-0	081-00117X-001.80N
252	081-0021-0	081-00257D-000.08N
253	081-0028-0	081-00401D-100.54N
254	083-0010-0	083-00119X-000.18W
255	083-0012-0	083-00136D-005.16E
256	083-0017-0	083-00178X-000.11E
257	083-0020-0	083-00299D-002.62E
258	083-0022-0	083-00406D-004.67N
259	083-0023-0	083-00406D-007.09N
260	083-0024-0	083-00406D-007.10N
261	085-0001-0	085-00009D-001.73N
262	085-0002-0	085-00009D-001.93N
263	085-0018-0	085-00136D-023.00E
264	085-0019-0	085-00136D-025.95E
265	085-0020-0	085-00136D-026.96E
266	085-0021-0	085-00183D-004.86N
267	087-0005-0	087-00001D-020.41N
268	087-0009-0	087-00001D-021.11N
269	087-0014-0	087-00001B-001.93N
270	087-0017-0	087-00038D-013.48E
271	087-0022-0	087-00097D-002.34N
272	087-0046-0	087-00262D-012.29E
273	089-0075-0	089-00407D-030.50C
274	089-0076-0	089-00407D-031.50C
275	089-0080-0	089-00407D-034.30C
276	089-0082-0	089-00407D-035.05C
277	089-0180-0	089-09223M-002.42N
278	091-0005-0	091-00030D-007.51E
279	093-0006-0	093-00027D-010.90E
280	093-0007-0	093-00027D-015.64E
281	093-0017-0	093-00157X-001.00N
282	093-0021-0	093-00215X-009.10N
283	093-0028-0	093-00230D-021.38E
284	093-0039-0	093-00401D-120.54N
285	093-0042-0	093-00440X-004.00E
286	093-0046-0	093-00679F-010.25E
287	093-0048-0	093-01175F-002.67N

Table A.2 (continued)

Record Number	Bridge Serial Number	Location ID
288	095-0014-0	095-00520D-004.72E
289	095-0049-0	095-00133D-009.15N
290	097-0004-0	097-00005D-013.29N
291	097-0010-0	097-09040M-000.60E
292	097-0025-0	097-00402D-043.44E
293	097-0027-0	097-09370M-003.10N
294	097-0041-0	097-02876F-008.94N
295	099-0002-0	099-00001D-007.82N
296	099-0019-0	099-00200D-013.00E
297	101-0002-0	101-00011D-014.78N
298	103-0025-0	103-00405D-112.30N
299	103-0026-0	103-00405D-112.31N
300	105-0002-0	105-00017D-013.17N
301	105-0006-0	105-00072D-024.83E
302	105-0007-0	105-00077D-000.13N
303	105-0008-0	105-00077D-001.81N
304	105-0018-0	105-00368D-009.35N
305	107-0058-0	107-00466X-000.17S
306	107-0069-0	107-00404D-089.40E
307	111-0016-0	111-00515D-002.37N
308	111-0019-0	
309	113-0011-0	113-00085D-014.22N
310	113-0013-0	113-00085D-015.84N
311	115-0005-0	115-00001D-009.00N
312	115-0010-0	115-00001D-010.17N
313	115-0021-0	115-00001D-021.27N
314	115-0047-0	115-00101D-009.86N
315	115-0063-0	115-03745M-000.55E
316	117-0006-0	117-00017X-000.18E
317	117-0007-0	117-00019X-001.66W
318	117-0008-0	117-00020D-010.14E
319	117-0010-0	117-00053D-004.89E
320	117-0012-0	117-00087X-000.37E
321	117-0013-0	117-00141D-006.95N
322	117-0019-0	117-00369D-013.65E
323	117-0021-0	117-00369D-016.83E
324	117-0022-0	117-00369D-019.32E

Table A.2 (continued)

Record Number	Bridge Serial Number	Location ID
325	117-0027-0	117-00400D-011.55N
326	117-0031-0	117-00456X-006.87S
327	117-0032-0	117-01285F-006.75N
328	117-0039-0	117-02704F-000.96E
329	117-0040-0	117-02704F-000.97E
330	117-0042-0	117-02883F-000.95N
331	117-0044-0	117-02884F-002.52E
332	119-0006-0	119-00051D-014.66E
333	119-0007-0	119-00051D-017.42E
334	119-0016-0	119-00084X-001.32E
335	119-0017-0	119-00097X-000.45N
336	119-0018-0	119-00106D-002.11N
337	119-0021-0	119-00145D-001.00N
338	119-0024-0	119-00198D-006.46E
339	119-0025-0	119-00258X-000.51W
340	119-0032-0	119-00328D-000.73N
341	119-0033-0	119-00328D-003.20N
342	119-0034-0	119-00383X-002.52W
343	119-0035-0	119-00387X-002.69E
344	119-0038-0	119-00403D-158.51N
345	119-0039-0	119-00403D-158.52N
346	119-0040-0	119-00403D-161.55N
347	119-0041-0	119-00403D-161.56N
348	119-0050-0	119-00403D-173.24N
349	121-0013-0	121-00003D-012.85N
350	121-0015-0	121-00003D-017.91N
351	121-0030-0	121-00009D-007.21N
352	121-0049-0	121-00014D-025.70N
353	121-0094-0	121-00154D-022.22N
354	121-0095-0	121-00154D-022.24N
355	121-0103-0	121-00166D-014.61E
356	121-0106-0	121-00154R-022.25N
357	121-0127-0	121-00400D-015.92N
358	121-0165-0	121-00402D-048.57E
359	121-0170-0	121-00402D-052.13E
360	121-0178-0	121-00402D-055.38E
361	121-0208-0	121-00013D-002.53N

Table A.2 (continued)

Record Number	Bridge Serial Number	Location ID
362	121-0227-0	121-00407D-004.82C
363	121-0237-0	121-00407D-010.00C
364	121-0238-0	121-00407D-010.81C
365	121-0239-0	121-00407D-010.82C
366	121-0244-0	121-00407D-024.05C
367	121-0311-0	121-01002X-001.99N
368	121-0316-0	121-00139X-001.50N
369	121-0326-0	121-09013M-007.75N
370	121-0380-0	121-09095M-000.91E
371	121-0389-0	121-09133M-000.20E
372	121-0444-0	121-09212M-007.19N
373	121-0455-0	121-09212M-009.84N
374	123-0027-0	123-00282D-012.06E
375	127-0014-0	127-00025P-004.34N
376	127-0041-0	127-00303D-001.16N
377	127-0042-0	127-00303D-004.42N
378	127-0044-0	127-00405D-029.38N
379	127-0049-0	127-00405D-031.44N
380	127-0050-0	127-00405D-031.45N
381	127-0051-0	127-00405D-033.21N
382	127-0052-0	127-00405D-033.22N
383	127-0055-0	127-00405D-035.58N
384	127-0056-0	127-00405D-035.59N
385	127-0057-0	127-00405D-036.21N
386	127-0058-0	127-00405D-036.22N
387	129-0008-0	129-00003D-010.05N
388	129-0022-0	129-00053P-001.93N
389	129-0029-0	129-05607M-000.95E
390	129-0032-0	129-00136D-007.53E
391	129-0037-0	129-00136D-018.82E
392	129-0048-0	129-00156D-020.28E
393	129-0050-0	129-00156D-027.64E
394	129-0052-0	129-00225D-002.62N
395	129-0062-0	129-00401D-318.18N
396	129-0064-0	129-00401D-318.70N
397	129-0066-0	129-00401D-319.84N
398	131-0008-0	131-00038D-015.40E

Table A.2 (continued)

Record Number	Bridge Serial Number	Location ID
399	131-0028-0	131-00112D-003.59N
400	131-0035-0	131-00188D-001.72E
401	133-0003-0	133-00012D-011.10E
402	133-0017-0	133-00044D-026.17E
403	133-0019-0	133-00077D-000.51N
404	133-0028-0	133-00402D-136.62E
405	133-0029-0	133-00402D-136.63E
406	135-0028-0	135-00120D-011.66E
407	135-0054-0	135-00403D-112.88N
408	137-0002-0	137-00015D-000.68N
409	137-0011-0	137-00017D-008.64N
410	137-0019-0	137-00197D-004.84N
411	137-0022-0	137-00197D-013.03N
412	137-0029-0	137-00365D-043.12N
413	137-0032-0	137-00384D-004.22N
414	139-0002-0	139-00011D-008.15N
415	139-0003-0	139-00011D-008.16N
416	139-0004-0	139-00011D-008.90N
417	139-0005-0	139-00011D-013.58N
418	139-0006-0	139-00011D-015.69N
419	139-0009-0	139-00013D-005.95N
420	139-0010-0	139-00013D-010.10N
421	139-0013-0	139-00051D-000.40E
422	139-0014-0	139-00052D-023.90E
423	139-0016-0	139-00052D-013.65E
424	139-0020-0	139-00053D-004.92E
425	139-0025-0	139-00053C-001.23N
426	139-0026-0	139-00060D-013.54N
427	139-0033-0	139-00283D-001.42E
428	139-0036-0	139-00284D-001.72N
429	139-0037-0	139-00284D-012.77N
430	139-0038-0	139-00323D-005.24N
431	139-0039-0	139-00323D-005.35N
432	139-0040-0	139-00332D-006.24E
433	139-0043-0	139-00419D-011.64N
434	139-0044-0	139-00419D-011.65N
435	139-0045-0	139-00419D-015.93N

Table A.2 (continued)

Record Number	Bridge Serial Number	Location ID
436	139-0046-0	139-00419D-015.94N
437	139-0047-0	139-00419D-020.13N
438	139-0048-0	139-00419D-020.14N
439	139-0049-0	139-00419D-020.25N
440	139-0050-0	139-00419D-020.26N
441	139-0051-0	139-00419D-024.01N
442	139-0055-0	139-00472X-000.68N
443	139-0056-0	139-00524X-000.17W
444	139-0057-0	139-00621X-001.01E
445	139-0058-0	139-00751X-000.84W
446	139-0075-0	139-00060D-013.55N
447	139-0076-0	139-00053D-004.91E
448	141-0010-0	141-00016D-024.82E
449	143-0008-0	143-00100D-008.98N
450	143-0029-0	143-01605F-000.25N
451	145-0008-0	145-00085D-006.07N
452	145-0028-0	145-00219D-014.82N
453	145-0031-0	145-00315D-004.40N
454	145-0038-0	145-00411D-016.93N
455	145-0039-0	145-00411D-016.94N
456	145-0041-0	145-00411D-021.01N
457	147-0015-0	147-00172D-003.46N
458	151-0048-0	151-00755F-001.19N
459	153-0028-0	153-00096D-011.18E
460	153-0037-0	153-00247D-022.82N
461	153-0041-0	153-00401D-124.43N
462	153-0042-0	153-00401D-124.44N
463	153-0052-0	153-00401D-136.37N
464	157-0015-0	157-00060D-002.00N
465	157-0017-0	157-00082P-001.56N
466	157-0021-0	157-00229X-002.04N
467	157-0022-0	157-00250X-000.25N
468	157-0027-0	157-00332D-006.10E
469	157-0041-0	157-00403D-135.98N
470	157-0042-0	157-00403D-135.99N
471	157-0044-0	157-00403D-136.18N
472	157-0045-0	157-00403D-144.34N

Table A.2 (continued)

Record Number	Bridge Serial Number	Location ID
473	157-0046-0	157-00403D-144.35N
474	157-0057-0	157-00330D-003.34E
475	161-0020-0	161-00135D-024.38N
476	163-0023-0	163-00078D-004.92N
477	167-0007-0	167-00026D-006.33E
478	169-0015-0	169-00044D-014.33E
479	171-0012-0	171-00018D-001.15E
480	171-0017-0	171-00036D-017.59E
481	175-0002-0	175-00019D-003.34N
482	175-0017-0	175-00026D-018.58E
483	175-0018-0	175-00026D-018.80E
484	175-0031-0	175-00031D-021.42N
485	175-0046-0	175-00124X-003.00N
486	175-0089-0	175-00531X-002.20N
487	177-0001-0	177-00003D-000.21N
488	177-0006-0	177-00032D-018.64E
489	179-0022-0	179-00050X-007.60E
490	181-0010-0	181-00079D-018.97N
491	181-0017-0	181-00047D-016.50E
492	185-0009-0	185-00007D-024.60N
493	185-0010-0	185-00031D-000.00N
494	185-0012-0	185-00031D-008.98N
495	185-0013-0	185-00031D-008.99N
496	185-0016-0	185-00038D-023.21E
497	185-0020-0	185-00133D-002.24N
498	185-0024-0	185-00122D-000.41E
499	187-0001-0	187-00009D-005.86N
500	187-0002-0	187-00009D-009.58N
501	187-0003-0	187-00060B-003.32N
502	187-0009-0	187-00052D-007.98E
503	187-0011-0	187-00052D-017.70E
504	187-0014-0	187-00060D-005.44N
505	187-0015-0	187-00060D-006.24N
506	187-0016-0	187-00400D-003.56N
507	189-0002-0	189-00010D-005.74E
508	189-0007-0	189-00021X-000.60N
509	189-0008-0	189-00024X-001.29N

Table A.2 (continued)

Record Number	Bridge Serial Number	Location ID
510	189-0015-0	189-00223D-001.94E
511	189-0022-0	189-00797F-000.59N
512	189-0026-0	189-02150F-000.01N
513	191-0002-0	191-00017X-002.50E
514	191-0007-0	191-00025D-002.72N
515	191-0014-0	191-00057D-008.49E
516	191-0015-0	191-00057D-008.29E
517	191-0016-0	191-00057D-005.55E
518	191-0018-0	191-00129X-010.39E
519	193-0014-0	193-00049D-009.91N
520	193-0019-0	193-00090D-014.60N
521	193-0025-0	193-00128D-005.90N
522	193-5042-0	193-00090D-005.54N
523	195-0009-0	195-00072D-009.05E
524	195-0016-0	195-00106D-016.12N
525	195-0017-0	
526	195-0018-0	195-00172D-010.75N
527	195-0019-0	195-00191D-003.67N
528	195-0021-0	195-00281D-004.11N
529	197-0010-0	197-00137D-015.44N
530	199-0007-0	199-00018D-006.03E
531	199-0015-0	199-00041D-001.27N
532	199-0027-0	199-00074D-012.72E
533	199-0031-0	199-00085D-000.13N
534	199-0032-0	199-00085D-000.28N
535	199-0033-0	199-00085D-002.05N
536	199-0034-0	199-00085D-008.73N
537	199-0047-0	199-00109D-009.60E
538	199-0055-0	199-00362D-016.54E
539	207-0002-0	207-00015X-001.65N
540	207-0008-0	207-02784F-000.66E
541	207-0021-0	207-00083D-008.36N
542	207-0035-0	207-00087D-018.66N
543	207-0038-0	207-00401D-176.37N
544	207-0053-0	207-00408D-014.72N
545	207-0054-0	207-00408D-014.73N
546	207-0069-0	207-00018D-008.61E

Table A.2 (continued)

Record Number	Bridge Serial Number	Location ID
547	209-0004-0	209-00030D-000.58E
548	209-0005-0	209-00030D-000.84E
549	211-0010-0	211-00083D-003.17N
550	211-0016-0	211-00083D-018.93N
551	211-0017-0	211-00083D-020.61N
552	211-0018-0	211-00146X-003.27N
553	211-0020-0	211-00256X-001.63N
554	211-0021-0	211-00249X-001.49N
555	211-0030-0	211-00402D-113.38E
556	211-0038-0	211-00402D-126.47E
557	211-0063-0	211-02425F-007.27N
558	213-0001-0	213-00002D-000.24E
559	213-0018-0	213-00002D-008.30E
560	213-0021-0	213-00061D-028.20N
561	213-0023-0	213-00136D-001.87E
562	215-0003-0	215-00520D-005.84E
563	215-0008-0	215-00001D-013.29N
564	215-0030-0	215-00085D-008.60N
565	215-0031-0	215-00085D-008.61N
566	215-0038-0	
567	215-0047-0	215-08042M-002.45N
568	215-0063-0	215-00411D-006.02N
569	215-0065-0	215-00411D-006.49N
570	215-0067-0	215-00411D-007.13N
571	215-0070-0	215-00411D-008.09N
572	215-0072-0	215-00411D-008.25N
573	215-0084-0	215-00411R-008.09N
574	215-0092-0	215-08016M-002.84E
575	215-0149-0	215-00001D-014.20N
576	215-0161-0	215-00411D-005.46N
577	217-0008-0	217-00036D-001.31E
578	217-0010-0	217-00057X-000.02N
579	217-0018-0	217-00142D-011.34N
580	217-0020-0	217-00212D-011.19E
581	217-0023-0	217-00301X-000.25N
582	217-0031-0	217-00402D-092.24E
583	217-0034-0	217-00402D-092.89E

Table A.2 (continued)

Record Number	Bridge Serial Number	Location ID
584	217-0035-0	217-00402D-094.50E
585	217-0036-0	217-00402D-094.51E
586	217-0037-0	217-00402D-094.63E
587	217-0038-0	217-00402D-094.64E
588	217-0041-0	217-00516X-002.45E
589	221-0014-0	221-00077D-033.75N
590	225-0010-0	225-00247C-003.00E
591	225-0016-0	225-01508F-001.04E
592	227-0037-0	227-00108D-003.77N
593	229-0007-0	229-00015D-019.71N
594	229-0008-0	229-00015D-021.57N
595	229-0009-0	
596	231-0003-0	231-00018D-014.71E
597	231-0005-0	231-00109D-003.62E
598	233-0015-0	233-00006B-001.57E
599	233-0023-0	233-00006D-008.31E
600	233-0033-0	233-00006D-023.08E
601	235-0003-0	235-00011D-007.39N
602	235-0008-0	235-00026D-008.86E
603	235-0009-0	235-00026W-000.52W
604	237-0005-0	237-00016D-024.12E
605	241-0001-0	241-00002D-007.55E
606	241-0008-0	241-00015D-000.32N
607	241-0009-0	241-00015D-001.85N
608	241-0010-0	241-00015D-002.10N
609	241-0017-0	241-00028D-000.00N
610	241-0022-0	241-00246D-000.08E
611	243-0002-0	243-00001D-009.00N
612	243-0012-0	243-00216D-005.87N
613	245-0013-0	243-00266D-011.35E
614	245-0017-0	245-00010D-018.08E
615	245-0018-0	245-00010D-018.17E
616	245-0019-0	245-00010D-018.25E
617	245-0020-0	245-00010D-018.35E
618	245-0021-0	245-00010D-018.46E
619	245-0022-0	245-00010R-018.24E
620	245-0023-0	245-00010R-018.26E

Table A.2 (continued)

Record Number	Bridge Serial Number	Location ID
621	245-0038-0	245-00105X-000.43W
622	245-0049-0	245-00402D-200.18E
623	245-0050-0	245-00402D-200.19E
624	245-0069-0	245-00842X-000.02N
625	251-0026-0	251-00073D-000.95N
626	251-0027-0	251-00073D-007.08N
627	251-0030-0	251-00073D-011.11N
628	255-0006-0	255-00003D-003.03N
629	255-0008-0	255-00003D-003.94N
630	255-0009-0	255-00003D-003.95N
631	255-0015-0	255-00016D-012.27E
632	255-0016-0	255-00016D-012.28E
633	255-0017-0	255-00155D-007.03N
634	255-0018-0	255-00036X-011.21E
635	255-0021-0	255-00092D-008.52N
636	255-0027-0	255-00401D-207.87N
637	257-0011-0	257-00184D-014.53N
638	261-0002-0	261-00003D-004.31N
639	261-0007-0	261-00027D-012.93E
640	261-0010-0	261-00027D-021.72E
641	261-0011-0	261-00027D-029.16E
642	261-0013-0	261-00030D-011.78E
643	263-0014-0	263-00036D-022.02E
644	267-0026-0	267-00178D-009.76E
645	269-0003-0	269-00003D-005.19N
646	269-0024-0	269-00137D-006.59N
647	269-0025-0	269-00137D-008.64N
648	269-0028-0	269-00137D-022.90N
649	271-0003-0	271-00027D-017.88E
650	275-0013-0	275-00038D-009.41E
651	275-0033-0	275-00188D-001.44E
652	277-0027-0	277-00401D-060.14N
653	281-0008-0	281-00002D-017.97E
654	283-0036-0	283-00404D-066.74E
655	285-0006-0	285-00001D-013.22N
656	285-0027-0	285-00029C-000.65N
657	285-0030-0	285-00100D-004.07N

Table A.2 (continued)

Record Number	Bridge Serial Number	Location ID
658	285-0032-0	285-00109D-003.53E
659	285-0035-0	285-00109D-016.77E
660	285-0048-0	285-00219D-019.98N
661	285-0051-0	285-00403D-002.26N
662	285-0052-0	285-00403D-002.27N
663	285-0078-0	285-00411D-039.85N
664	285-0082-0	285-00411D-046.16N
665	285-0115-0	285-00109D-014.26E
666	287-0021-0	287-00112D-015.17N
667	289-0003-0	289-00019D-019.72N
668	291-0017-0	291-00180D-005.00N
669	291-0027-0	291-02899F-001.79S
670	295-0004-0	295-00001D-020.72N
671	295-0010-0	295-00136D-007.78E
672	295-0020-0	295-00151D-002.48N
673	297-0002-0	297-00010D-009.51E
674	297-0003-0	297-00010B-000.09E
675	297-0010-0	297-00010D-010.58E
676	297-0011-0	297-00010D-012.23E
677	297-0012-0	297-00010D-012.24E
678	297-0015-0	297-00011D-000.98N
679	297-0017-0	297-00011D-012.74N
680	297-0022-0	297-00081D-017.30N
681	297-0024-0	297-00083D-005.05N
682	297-0026-0	297-00138D-005.78E
683	299-0022-0	299-00158D-006.40E
684	299-0023-0	299-00158D-006.20E
685	299-0024-0	299-00158D-005.90E
686	301-0016-0	301-00080D-015.35N
687	301-0021-0	301-00402D-154.29E
688	301-0022-0	301-00402D-154.30E
689	301-0024-0	301-00402D-164.52E
690	301-0025-0	301-00402D-164.53E
691	305-0008-0	305-00023D-023.63N
692	305-0045-0	305-00023D-023.62N
693	307-0008-0	
694	307-0010-0	307-00041D-011.12N

Table A.2 (continued)

Record Number	Bridge Serial Number	Location ID
695	307-0011-0	307-00045D-001.85N
696	307-0012-0	307-00045D-002.01N
697	309-0014-0	309-00030D-017.42E
698	311-0001-0	311-00011D-007.91N
699	311-0007-0	311-00017D-004.62N
700	311-0015-0	311-00075D-013.32N
701	311-0030-0	311-00255D-014.70N
702	313-0001-0	313-00002D-003.32E
703	313-0003-0	313-00002D-006.43E
704	313-0004-0	313-00002D-011.56E
705	313-0017-0	313-00010X-001.08E
706	313-0018-0	313-00052D-000.06E
707	313-0024-0	313-00052D-008.11E
708	313-0039-0	313-00401D-326.89N
709	313-0041-0	313-00401D-327.03N
710	313-0043-0	313-00401D-335.89N
711	313-0050-0	313-00401D-341.07N
712	313-0054-0	313-00691F-002.98N
713	313-0066-0	313-01515M-000.33N
714	315-0017-0	
715	317-0003-0	317-00010D-027.02E
716	317-0009-0	317-00017D-028.72N

The researcher read the superstructure evaluation notes of the bridges listed in Table A.2 to find reports indicative of bearing and anchor bolt corrosion. In addition to specific reports of anchor bolt corrosion, reports of loose, pushed up, sheared off, or missing anchor bolts and reports of bearing corrosion implicitly denoted anchor bolt corrosion, as well. Table A.3 is a list of steel girder bridges in Georgia determined to be experiencing anchor bolt corrosion.

Table A.3: Steel girder bridges in Georgia experiencing anchor bolt corrosion

Record Number	Bridge Serial Number	Location ID
1	001-0011-0	001-00004D-021.18N
2	009-0002-0	009-00022D-004.02E
3	009-0007-0	009-00022D-012.46E
4	009-0016-0	009-00112D-005.10N
5	011-0002-0	011-00015D-000.85N
6	011-0029-0	011-00403D-150.43N
7	011-0030-0	011-00403D-150.44N
8	011-0031-0	011-00403D-152.66N
9	013-0012-0	013-00211D-022.60N
10	013-0014-0	013-00211D-018.86N
11	013-0018-0	013-00324D-000.66E
12	013-0022-0	013-00403D-127.19N
13	013-0023-0	013-00403D-127.20N
14	015-0005-0	015-00003D-003.48N
15	015-0006-0	015-00003D-003.49N
16	015-0021-0	015-00003D-022.62N
17	015-0031-0	015-00061D-003.93N
18	015-0033-0	015-00061D-004.39N
19	015-0057-0	015-00155X-005.12N
20	015-0079-0	015-00401D-281.51N
21	015-0082-0	015-00401D-283.70N
22	015-0083-0	015-00401D-286.75N
23	015-0084-0	015-00401D-286.76N
24	015-0087-0	015-00401D-287.16N
25	015-0088-0	015-00401D-287.17N
26	015-0101-0	015-00401D-299.66N
27	015-0103-0	015-00401D-304.19N
28	015-0104-0	015-00401D-304.22N
29	017-0003-0	017-00011D-014.68N
30	021-0030-0	021-03206M-000.99E
31	021-0031-0	021-00011D-003.90N
32	021-0034-0	021-00011D-006.15N
33	021-0038-0	021-00074D-001.41E
34	021-0048-0	021-00087D-010.54N
35	021-0054-0	021-00091X-000.23S
36	021-0070-0	021-00940F-015.85N
37	021-0083-0	021-00401D-160.30N
38	021-0085-0	021-00401D-161.27N
39	021-0088-0	021-00401D-162.48N

Table A.3 (continued)

Record Number	Bridge Serial Number	Location ID
40	021-0095-0	021-00401D-164.98N
41	021-0097-0	021-00401D-165.59N
42	021-0098-0	021-00401D-165.60N
43	021-0101-0	021-00401D-166.63N
44	021-0106-0	021-00401D-169.07N
45	021-0107-0	021-00401D-169.08N
46	021-0110-0	021-00401D-170.83N
47	021-0115-0	021-00401R-164.96N
48	021-0116-0	021-00401R-164.97N
49	021-0119-0	021-00404D-000.70E
50	021-0120-0	021-00404D-000.71E
51	021-0125-0	021-00404D-003.01E
52	021-0126-0	021-00404D-003.02E
53	021-0136-0	021-00408D-000.00N
54	021-0143-0	021-00408D-007.24N
55	021-0148-0	021-00665F-002.05E
56	021-0181-0	021-03217M-001.20E
57	021-0188-0	021-03245M-000.35E
58	021-0191-0	021-03262M-000.04N
59	023-0001-0	023-00026D-011.63E
60	023-0012-0	023-00112D-022.28N
61	025-0026-0	025-00520D-020.67E
62	027-0003-0	027-00076D-010.34E
63	027-0031-0	027-00122D-002.00E
64	027-0034-0	027-00122D-008.29E
65	029-0006-0	029-00026D-005.79E
66	029-0029-0	029-00404D-146.29E
67	029-0030-0	029-00404D-146.30E
68	031-0047-0	031-00119D-001.29N
69	033-0004-0	033-00017D-005.46N
70	035-0001-0	035-00016D-000.88E
71	039-0011-0	039-00025D-031.89N
72	047-0006-0	047-00002D-002.80E
73	047-0007-0	047-00002D-005.23E
74	047-0008-0	047-00002D-005.24E
75	047-0035-0	047-00401D-351.38N
76	047-0039-0	047-00401D-353.13N
77	047-0043-0	047-00401D-354.34N
78	049-0012-0	049-00023D-000.00N

Table A.3 (continued)

Record Number	Bridge Serial Number	Location ID
79	051-0005-0	051-00421D-001.60N
80	051-0007-0	051-00421D-003.38N
81	051-0008-0	051-00421D-004.29N
82	051-0009-0	051-00421D-004.30N
83	051-0012-0	051-00421D-005.42N
84	051-0016-0	051-00421D-005.96N
85	051-0019-0	051-00421D-006.10N
86	051-0060-0	051-00026D-011.20E
87	051-0066-0	051-00026D-032.43E
88	051-0078-0	051-00204D-025.61E
89	051-0090-0	051-00404D-163.60E
90	051-0092-0	051-00404D-163.95E
91	051-0093-0	051-00404D-163.97E
92	051-0095-0	051-00404D-165.03E
93	051-0096-0	051-00404D-165.02E
94	051-0097-0	051-00404D-165.69E
95	051-0098-0	051-00404D-165.70E
96	051-0101-0	051-00404D-166.09E
97	051-0105-0	051-00405D-093.87N
98	051-0109-0	051-00405D-099.28N
99	051-0124-0	051-00405D-107.24N
100	051-0125-0	051-00405D-108.52N
101	051-0126-0	051-00405D-108.53N
102	051-0138-0	051-04070M-003.00E
103	051-0147-0	051-00204P-006.08E
104	057-0015-0	057-00092D-000.08N
105	057-0071-0	057-01375F-014.20N
106	059-0001-0	059-00010L-005.45E
107	059-0002-0	059-00010L-005.44E
108	059-0011-0	059-00010L-001.88E
109	059-0018-0	059-00010L-000.04E
110	059-0020-0	059-00010D-003.13E
111	059-0021-0	059-00010D-003.14E
112	059-0029-0	059-00015A-004.33N
113	059-0036-0	059-00008D-001.97E
114	059-0044-0	059-00008D-004.21E
115	059-0045-0	059-00008D-004.22E
116	059-0047-0	059-00008D-006.00E
117	059-0048-0	059-00008D-006.01E

Table A.3 (continued)

Record Number	Bridge Serial Number	Location ID
118	059-0059-0	059-00320M-000.56E
119	061-0002-0	061-00037D-000.01E
120	067-0013-0	067-00003D-005.21N
121	067-0019-0	067-09004M-000.59N
122	067-0022-0	067-00005D-014.97N
123	067-0023-0	067-00005D-014.98N
124	067-0031-0	067-00005D-001.35N
125	067-0052-0	067-00280D-000.60N
126	067-0066-0	067-00401D-258.79N
127	067-0069-0	067-00401D-260.70N
128	067-0073-0	067-00401D-264.21N
129	067-0074-0	067-00401D-265.02N
130	067-0076-0	067-00401D-267.51N
131	067-0184-0	067-00005D-014.33N
132	069-0013-0	069-00032D-019.60E
133	069-0014-0	069-00032D-020.12E
134	069-0017-0	069-00032D-025.11E
135	069-0018-0	069-00032D-025.83E
136	069-0031-0	069-00135D-016.62N
137	073-0016-0	073-00223D-002.47E
138	073-0018-0	073-00223D-010.12E
139	073-0022-0	073-00232D-008.15E
140	073-0040-0	073-02122F-004.91N
141	073-0043-0	073-00388D-002.80N
142	075-0019-0	075-00240X-001.84N
143	077-0018-0	077-00054D-010.58E
144	077-0043-0	077-00403D-043.47N
145	077-0044-0	077-00403D-043.48N
146	077-0049-0	077-00403D-050.02N
147	077-0069-0	077-01599F-007.01N
148	077-0076-0	077-02081F-002.01E
149	077-5136-0	077-00403D-050.03N
150	079-0006-0	079-00007D-018.71N
151	081-0021-0	081-00257D-000.08N
152	083-0010-0	083-00119X-000.18W
153	083-0012-0	083-00136D-005.16E
154	083-0017-0	083-00178X-000.11E
155	083-0020-0	083-00299D-002.62E
156	083-0022-0	083-00406D-004.67N

Table A.3 (continued)

Record Number	Bridge Serial Number	Location ID
157	083-0023-0	083-00406D-007.09N
158	083-0024-0	083-00406D-007.10N
159	085-0001-0	085-00009D-001.73N
160	085-0002-0	085-00009D-001.93N
161	085-0018-0	085-00136D-023.00E
162	085-0019-0	085-00136D-025.95E
163	085-0020-0	085-00136D-026.96E
164	087-0005-0	087-00001D-020.41N
165	087-0009-0	087-00001D-021.11N
166	087-0014-0	087-00001B-001.93N
167	089-0075-0	089-00407D-030.50C
168	089-0076-0	089-00407D-031.50C
169	089-0080-0	089-00407D-034.30C
170	091-0005-0	091-00030D-007.51E
171	093-0006-0	093-00027D-010.90E
172	093-0007-0	093-00027D-015.64E
173	093-0017-0	093-00157X-001.00N
174	093-0021-0	093-00215X-009.10N
175	093-0028-0	093-00230D-021.38E
176	093-0039-0	093-00401D-120.54N
177	093-0042-0	093-00440X-004.00E
178	093-0048-0	093-01175F-002.67N
179	095-0014-0	095-00520D-004.72E
180	097-0004-0	097-00005D-013.29N
181	097-0027-0	097-09370M-003.10N
182	099-0002-0	099-00001D-007.82N
183	103-0026-0	103-00405D-112.31N
184	105-0002-0	105-00017D-013.17N
185	105-0018-0	105-00368D-009.35N
186	107-0058-0	107-00466X-000.17S
187	107-0069-0	107-00404D-089.40E
188	111-0016-0	111-00515D-002.37N
189	111-0019-0	
190	113-0013-0	113-00085D-015.84N
191	115-0010-0	115-00001D-010.17N
192	115-0047-0	115-00101D-009.86N
193	115-0063-0	115-03745M-000.55E
194	117-0006-0	117-00017X-000.18E
195	117-0007-0	117-00019X-001.66W

Table A.3 (continued)

Record Number	Bridge Serial Number	Location ID
196	117-0008-0	117-00020D-010.14E
197	117-0012-0	117-00087X-000.37E
198	117-0013-0	117-00141D-006.95N
199	117-0021-0	117-00369D-016.83E
200	117-0031-0	117-00456X-006.87S
201	117-0032-0	117-01285F-006.75N
202	117-0039-0	117-02704F-000.96E
203	117-0040-0	117-02704F-000.97E
204	117-0042-0	117-02883F-000.95N
205	117-0044-0	117-02884F-002.52E
206	119-0007-0	119-00051D-017.42E
207	119-0016-0	119-00084X-001.32E
208	119-0017-0	119-00097X-000.45N
209	119-0018-0	119-00106D-002.11N
210	119-0025-0	119-00258X-000.51W
211	119-0032-0	119-00328D-000.73N
212	119-0034-0	119-00383X-002.52W
213	119-0035-0	119-00387X-002.69E
214	119-0038-0	119-00403D-158.51N
215	119-0040-0	119-00403D-161.55N
216	119-0041-0	119-00403D-161.56N
217	121-0015-0	121-00003D-017.91N
218	121-0095-0	121-00154D-022.24N
219	121-0170-0	121-00402D-052.13E
220	121-0178-0	121-00402D-055.38E
221	121-0227-0	121-00407D-004.82C
222	121-0238-0	121-00407D-010.81C
223	121-0244-0	121-00407D-024.05C
224	121-0380-0	121-09095M-000.91E
225	121-0389-0	121-09133M-000.20E
226	123-0027-0	123-00282D-012.06E
227	127-0041-0	127-00303D-001.16N
228	127-0042-0	127-00303D-004.42N
229	127-0049-0	127-00405D-031.44N
230	127-0050-0	127-00405D-031.45N
231	127-0055-0	127-00405D-035.58N
232	127-0056-0	127-00405D-035.59N
233	127-0057-0	127-00405D-036.21N
234	127-0058-0	127-00405D-036.22N

Table A.3 (continued)

Record Number	Bridge Serial Number	Location ID
235	129-0029-0	129-05607M-000.95E
236	129-0032-0	129-00136D-007.53E
237	129-0048-0	129-00156D-020.28E
238	129-0062-0	129-00401D-318.18N
239	129-0064-0	129-00401D-318.70N
240	129-0066-0	129-00401D-319.84N
241	133-0003-0	133-00012D-011.10E
242	133-0019-0	133-00077D-000.51N
243	133-0028-0	133-00402D-136.62E
244	133-0029-0	133-00402D-136.63E
245	135-0028-0	135-00120D-011.66E
246	135-0054-0	135-00403D-112.88N
247	137-0002-0	137-00015D-000.68N
248	137-0011-0	137-00017D-008.64N
249	137-0029-0	137-00365D-043.12N
250	137-0032-0	137-00384D-004.22N
251	139-0006-0	139-00011D-015.69N
252	139-0010-0	139-00013D-010.10N
253	139-0013-0	139-00051D-000.40E
254	139-0014-0	139-00052D-023.90E
255	139-0025-0	139-00053C-001.23N
256	139-0033-0	139-00283D-001.42E
257	139-0039-0	139-00323D-005.35N
258	139-0043-0	139-00419D-011.64N
259	139-0045-0	139-00419D-015.93N
260	139-0046-0	139-00419D-015.94N
261	139-0049-0	139-00419D-020.25N
262	139-0051-0	139-00419D-024.01N
263	139-0056-0	139-00524X-000.17W
264	139-0057-0	139-00621X-001.01E
265	139-0058-0	139-00751X-000.84W
266	141-0010-0	141-00016D-024.82E
267	143-0029-0	143-01605F-000.25N
268	145-0008-0	145-00085D-006.07N
269	145-0031-0	145-00315D-004.40N
270	145-0039-0	145-00411D-016.94N
271	147-0015-0	147-00172D-003.46N
272	153-0028-0	153-00096D-011.18E
273	153-0041-0	153-00401D-124.43N

Table A.3 (continued)

Record Number	Bridge Serial Number	Location ID
274	153-0042-0	153-00401D-124.44N
275	153-0052-0	153-00401D-136.37N
276	157-0017-0	157-00082P-001.56N
277	157-0021-0	157-00229X-002.04N
278	157-0022-0	157-00250X-000.25N
279	157-0027-0	157-00332D-006.10E
280	161-0020-0	161-00135D-024.38N
281	163-0023-0	163-00078D-004.92N
282	167-0007-0	167-00026D-006.33E
283	175-0017-0	175-00026D-018.58E
284	175-0018-0	175-00026D-018.80E
285	175-0031-0	175-00031D-021.42N
286	175-0046-0	175-00124X-003.00N
287	175-0089-0	175-00531X-002.20N
288	181-0010-0	181-00079D-018.97N
289	181-0017-0	181-00047D-016.50E
290	185-0010-0	185-00031D-000.00N
291	185-0020-0	185-00133D-002.24N
292	185-0024-0	185-00122D-000.41E
293	187-0002-0	187-00009D-009.58N
294	187-0003-0	187-00060B-003.32N
295	189-0002-0	189-00010D-005.74E
296	189-0007-0	189-00021X-000.60N
297	189-0008-0	189-00024X-001.29N
298	189-0015-0	189-00223D-001.94E
299	189-0022-0	189-00797F-000.59N
300	189-0026-0	189-02150F-000.01N
301	191-0014-0	191-00057D-008.49E
302	193-0014-0	193-00049D-009.91N
303	193-0019-0	193-00090D-014.60N
304	195-0009-0	195-00072D-009.05E
305	195-0016-0	195-00106D-016.12N
306	195-0021-0	195-00281D-004.11N
307	197-0010-0	197-00137D-015.44N
308	199-0007-0	199-00018D-006.03E
309	199-0033-0	199-00085D-002.05N
310	199-0034-0	199-00085D-008.73N
311	199-0047-0	199-00109D-009.60E
312	207-0008-0	207-02784F-000.66E

Table A.3 (continued)

Record Number	Bridge Serial Number	Location ID
313	207-0021-0	207-00083D-008.36N
314	207-0038-0	207-00401D-176.37N
315	207-0053-0	207-00408D-014.72N
316	207-0054-0	207-00408D-014.73N
317	207-0069-0	207-00018D-008.61E
318	209-0004-0	209-00030D-000.58E
319	209-0005-0	209-00030D-000.84E
320	211-0017-0	211-00083D-020.61N
321	211-0018-0	211-00146X-003.27N
322	211-0021-0	211-00249X-001.49N
323	211-0030-0	211-00402D-113.38E
324	211-0038-0	211-00402D-126.47E
325	211-0063-0	211-02425F-007.27N
326	213-0018-0	213-00002D-008.30E
327	213-0021-0	213-00061D-028.20N
328	215-0003-0	215-00520D-005.84E
329	215-0008-0	215-00001D-013.29N
330	215-0063-0	215-00411D-006.02N
331	215-0065-0	215-00411D-006.49N
332	215-0067-0	215-00411D-007.13N
333	215-0070-0	215-00411D-008.09N
334	215-0072-0	215-00411D-008.25N
335	215-0084-0	215-00411R-008.09N
336	215-0092-0	215-08016M-002.84E
337	215-0149-0	215-00001D-014.20N
338	215-0161-0	215-00411D-005.46N
339	217-0008-0	217-00036D-001.31E
340	217-0010-0	217-00057X-000.02N
341	217-0018-0	217-00142D-011.34N
342	217-0031-0	217-00402D-092.24E
343	217-0035-0	217-00402D-094.50E
344	217-0036-0	217-00402D-094.51E
345	217-0037-0	217-00402D-094.63E
346	217-0038-0	217-00402D-094.64E
347	217-0041-0	217-00516X-002.45E
348	225-0010-0	225-00247C-003.00E
349	225-0016-0	225-01508F-001.04E
350	229-0007-0	229-00015D-019.71N
351	229-0008-0	229-00015D-021.57N

Table A.3 (continued)

Record Number	Bridge Serial Number	Location ID
352	235-0003-0	235-00011D-007.39N
353	235-0008-0	235-00026D-008.86E
354	235-0009-0	235-00026W-000.52W
355	237-0005-0	237-00016D-024.12E
356	241-0001-0	241-00002D-007.55E
357	241-0009-0	241-00015D-001.85N
358	241-0010-0	241-00015D-002.10N
359	241-0022-0	241-00246D-000.08E
360	245-0018-0	245-00010D-018.17E
361	245-0020-0	245-00010D-018.35E
362	245-0021-0	245-00010D-018.46E
363	245-0069-0	245-00842X-000.02N
364	251-0026-0	251-00073D-000.95N
365	255-0006-0	255-00003D-003.03N
366	257-0011-0	257-00184D-014.53N
367	261-0007-0	261-00027D-012.93E
368	261-0011-0	261-00027D-029.16E
369	263-0014-0	263-00036D-022.02E
370	269-0003-0	269-00003D-005.19N
371	269-0024-0	269-00137D-006.59N
372	269-0025-0	269-00137D-008.64N
373	269-0028-0	269-00137D-022.90N
374	271-0003-0	271-00027D-017.88E
375	275-0013-0	275-00038D-009.41E
376	281-0008-0	281-00002D-017.97E
377	283-0036-0	283-00404D-066.74E
378	285-0035-0	285-00109D-016.77E
379	285-0051-0	285-00403D-002.26N
380	285-0052-0	285-00403D-002.27N
381	289-0003-0	289-00019D-019.72N
382	291-0027-0	291-02899F-001.79S
383	295-0010-0	295-00136D-007.78E
384	295-0020-0	295-00151D-002.48N
385	297-0010-0	297-00010D-010.58E
386	297-0011-0	297-00010D-012.23E
387	297-0012-0	297-00010D-012.24E
388	297-0015-0	297-00011D-000.98N
389	297-0017-0	297-00011D-012.74N
390	297-0022-0	297-00081D-017.30N

Table A.3 (continued)

Record Number	Bridge Serial Number	Location ID
391	297-0024-0	297-00083D-005.05N
392	297-0026-0	297-00138D-005.78E
393	299-0022-0	299-00158D-006.40E
394	299-0024-0	299-00158D-005.90E
395	301-0016-0	301-00080D-015.35N
396	301-0021-0	301-00402D-154.29E
397	301-0022-0	301-00402D-154.30E
398	301-0024-0	301-00402D-164.52E
399	301-0025-0	301-00402D-164.53E
400	307-0010-0	307-00041D-011.12N
401	307-0011-0	307-00045D-001.85N
402	307-0012-0	307-00045D-002.01N
403	309-0014-0	309-00030D-017.42E
404	311-0007-0	311-00017D-004.62N
405	313-0001-0	313-00002D-003.32E
406	313-0003-0	313-00002D-006.43E
407	313-0024-0	313-00052D-008.11E
408	313-0043-0	313-00401D-335.89N
409	313-0054-0	313-00691F-002.98N
410	313-0066-0	313-01515M-000.33N
411	317-0003-0	317-00010D-027.02E

Possible trends relating anchor bolt corrosion to environmental conditions were examined by grouping bridges with anchor bolt corrosion by region and by span type.

Tables A.4 through A.11 catalog the bridges with anchor bolt corrosion in their regional and span classifications.

Table A.4: Steel girder bridges with anchor bolt corrosion in northern Georgia

Record Number	Bridge Serial Number	Location ID
1	011-0002-0	011-00015D-000.85N
2	011-0029-0	011-00403D-150.43N
3	011-0030-0	011-00403D-150.44N
4	011-0031-0	011-00403D-152.66N
5	013-0012-0	013-00211D-022.60N
6	013-0014-0	013-00211D-018.86N
7	013-0018-0	013-00324D-000.66E
8	013-0022-0	013-00403D-127.19N
9	013-0023-0	013-00403D-127.20N
10	015-0005-0	015-00003D-003.48N
11	015-0006-0	015-00003D-003.49N
12	015-0021-0	015-00003D-022.62N
13	015-0031-0	015-00061D-003.93N
14	015-0033-0	015-00061D-004.39N
15	015-0057-0	015-00155X-005.12N
16	015-0079-0	015-00401D-281.51N
17	015-0082-0	015-00401D-283.70N
18	015-0083-0	015-00401D-286.75N
19	015-0084-0	015-00401D-286.76N
20	015-0087-0	015-00401D-287.16N
21	015-0088-0	015-00401D-287.17N
22	015-0101-0	015-00401D-299.66N
23	015-0103-0	015-00401D-304.19N
24	015-0104-0	015-00401D-304.22N
25	047-0006-0	047-00002D-002.80E
26	047-0007-0	047-00002D-005.23E
27	047-0008-0	047-00002D-005.24E
28	047-0035-0	047-00401D-351.38N
29	047-0039-0	047-00401D-353.13N
30	047-0043-0	047-00401D-354.34N
31	057-0015-0	057-00092D-000.08N
32	057-0071-0	057-01375F-014.20N
33	059-0001-0	059-00010L-005.45E
34	059-0002-0	059-00010L-005.44E
35	059-0011-0	059-00010L-001.88E
36	059-0018-0	059-00010L-000.04E
37	059-0020-0	059-00010D-003.13E

Table A.4 (continued)

Record Number	Bridge Serial Number	Location ID
38	059-0021-0	059-00010D-003.14E
39	059-0029-0	059-00015A-004.33N
40	059-0036-0	059-00008D-001.97E
41	059-0044-0	059-00008D-004.21E
42	059-0045-0	059-00008D-004.22E
43	059-0047-0	059-00008D-006.00E
44	059-0048-0	059-00008D-006.01E
45	059-0059-0	059-00320M-000.56E
46	067-0013-0	067-00003D-005.21N
47	067-0019-0	067-09004M-000.59N
48	067-0022-0	067-00005D-014.97N
49	067-0023-0	067-00005D-014.98N
50	067-0031-0	067-00005D-001.35N
51	067-0052-0	067-00280D-000.60N
52	067-0066-0	067-00401D-258.79N
53	067-0069-0	067-00401D-260.70N
54	067-0073-0	067-00401D-264.21N
55	067-0074-0	067-00401D-265.02N
56	067-0076-0	067-00401D-267.51N
57	067-0184-0	067-00005D-014.33N
58	073-0016-0	073-00223D-002.47E
59	073-0018-0	073-00223D-010.12E
60	073-0022-0	073-00232D-008.15E
61	073-0040-0	073-02122F-004.91N
62	073-0043-0	073-00388D-002.80N
63	083-0010-0	083-00119X-000.18W
64	083-0012-0	083-00136D-005.16E
65	083-0017-0	083-00178X-000.11E
66	083-0020-0	083-00299D-002.62E
67	083-0022-0	083-00406D-004.67N
68	083-0023-0	083-00406D-007.09N
69	083-0024-0	083-00406D-007.10N
70	085-0001-0	085-00009D-001.73N
71	085-0002-0	085-00009D-001.93N
72	085-0018-0	085-00136D-023.00E
73	085-0019-0	085-00136D-025.95E
74	085-0020-0	085-00136D-026.96E

Table A.4 (continued)

Record Number	Bridge Serial Number	Location ID
75	089-0075-0	089-00407D-030.50C
76	089-0076-0	089-00407D-031.50C
77	089-0080-0	089-00407D-034.30C
78	097-0004-0	097-00005D-013.29N
79	097-0027-0	097-09370M-003.10N
80	105-0002-0	105-00017D-013.17N
81	105-0018-0	105-00368D-009.35N
82	111-0016-0	111-00515D-002.37N
83	111-0019-0	
84	115-0010-0	115-00001D-010.17N
85	115-0047-0	115-00101D-009.86N
86	115-0063-0	115-03745M-000.55E
87	117-0006-0	117-00017X-000.18E
88	117-0007-0	117-00019X-001.66W
89	117-0008-0	117-00020D-010.14E
90	117-0012-0	117-00087X-000.37E
91	117-0013-0	117-00141D-006.95N
92	117-0021-0	117-00369D-016.83E
93	117-0031-0	117-00456X-006.87S
94	117-0032-0	117-01285F-006.75N
95	117-0039-0	117-02704F-000.96E
96	117-0040-0	117-02704F-000.97E
97	117-0042-0	117-02883F-000.95N
98	117-0044-0	117-02884F-002.52E
99	119-0007-0	119-00051D-017.42E
100	119-0016-0	119-00084X-001.32E
101	119-0017-0	119-00097X-000.45N
102	119-0018-0	119-00106D-002.11N
103	119-0025-0	119-00258X-000.51W
104	119-0032-0	119-00328D-000.73N
105	119-0034-0	119-00383X-002.52W
106	119-0035-0	119-00387X-002.69E
107	119-0038-0	119-00403D-158.51N
108	119-0040-0	119-00403D-161.55N
109	119-0041-0	119-00403D-161.56N
110	121-0015-0	121-00003D-017.91N
111	121-0095-0	121-00154D-022.24N

Table A.4 (continued)

Record Number	Bridge Serial Number	Location ID
112	121-0170-0	121-00402D-052.13E
113	121-0178-0	121-00402D-055.38E
114	121-0227-0	121-00407D-004.82C
115	121-0238-0	121-00407D-010.81C
116	121-0244-0	121-00407D-024.05C
117	121-0380-0	121-09095M-000.91E
118	121-0389-0	121-09133M-000.20E
119	123-0027-0	123-00282D-012.06E
120	129-0029-0	129-05607M-000.95E
121	129-0032-0	129-00136D-007.53E
122	129-0048-0	129-00156D-020.28E
123	129-0062-0	129-00401D-318.18N
124	129-0064-0	129-00401D-318.70N
125	129-0066-0	129-00401D-319.84N
126	133-0003-0	133-00012D-011.10E
127	133-0019-0	133-00077D-000.51N
128	133-0028-0	133-00402D-136.62E
129	133-0029-0	133-00402D-136.63E
130	135-0028-0	135-00120D-011.66E
131	135-0054-0	135-00403D-112.88N
132	137-0002-0	137-00015D-000.68N
133	137-0011-0	137-00017D-008.64N
134	137-0029-0	137-00365D-043.12N
135	137-0032-0	137-00384D-004.22N
136	139-0006-0	139-00011D-015.69N
137	139-0010-0	139-00013D-010.10N
138	139-0013-0	139-00051D-000.40E
139	139-0014-0	139-00052D-023.90E
140	139-0025-0	139-00053C-001.23N
141	139-0033-0	139-00283D-001.42E
142	139-0039-0	139-00323D-005.35N
143	139-0043-0	139-00419D-011.64N
144	139-0045-0	139-00419D-015.93N
145	139-0046-0	139-00419D-015.94N
146	139-0049-0	139-00419D-020.25N
147	139-0051-0	139-00419D-024.01N
148	139-0056-0	139-00524X-000.17W

Table A.4 (continued)

Record Number	Bridge Serial Number	Location ID
149	139-0057-0	139-00621X-001.01E
150	139-0058-0	139-00751X-000.84W
151	141-0010-0	141-00016D-024.82E
152	143-0029-0	143-01605F-000.25N
153	147-0015-0	147-00172D-003.46N
154	157-0017-0	157-00082P-001.56N
155	157-0021-0	157-00229X-002.04N
156	157-0022-0	157-00250X-000.25N
157	157-0027-0	157-00332D-006.10E
158	181-0010-0	181-00079D-018.97N
159	181-0017-0	181-00047D-016.50E
160	187-0002-0	187-00009D-009.58N
161	187-0003-0	187-00060B-003.32N
162	189-0002-0	189-00010D-005.74E
163	189-0007-0	189-00021X-000.60N
164	189-0008-0	189-00024X-001.29N
165	189-0015-0	189-00223D-001.94E
166	189-0022-0	189-00797F-000.59N
167	189-0026-0	189-02150F-000.01N
168	195-0009-0	195-00072D-009.05E
169	195-0016-0	195-00106D-016.12N
170	195-0021-0	195-00281D-004.11N
171	211-0017-0	211-00083D-020.61N
172	211-0018-0	211-00146X-003.27N
173	211-0021-0	211-00249X-001.49N
174	211-0030-0	211-00402D-113.38E
175	211-0038-0	211-00402D-126.47E
176	211-0063-0	211-02425F-007.27N
177	213-0018-0	213-00002D-008.30E
178	213-0021-0	213-00061D-028.20N
179	217-0008-0	217-00036D-001.31E
180	217-0010-0	217-00057X-000.02N
181	217-0018-0	217-00142D-011.34N
182	217-0031-0	217-00402D-092.24E
183	217-0035-0	217-00402D-094.50E
184	217-0036-0	217-00402D-094.51E
185	217-0037-0	217-00402D-094.63E

Table A.4 (continued)

Record Number	Bridge Serial Number	Location ID
186	217-0038-0	217-00402D-094.64E
187	217-0041-0	217-00516X-002.45E
188	241-0001-0	241-00002D-007.55E
189	241-0009-0	241-00015D-001.85N
190	241-0010-0	241-00015D-002.10N
191	241-0022-0	241-00246D-000.08E
192	245-0018-0	245-00010D-018.17E
193	245-0020-0	245-00010D-018.35E
194	245-0021-0	245-00010D-018.46E
195	245-0069-0	245-00842X-000.02N
196	257-0011-0	257-00184D-014.53N
197	281-0008-0	281-00002D-017.97E
198	283-0036-0	283-00404D-066.74E
199	291-0027-0	291-02899F-001.79S
200	295-0010-0	295-00136D-007.78E
201	295-0020-0	295-00151D-002.48N
202	297-0010-0	297-00010D-010.58E
203	297-0011-0	297-00010D-012.23E
204	297-0012-0	297-00010D-012.24E
205	297-0015-0	297-00011D-000.98N
206	297-0017-0	297-00011D-012.74N
207	297-0022-0	297-00081D-017.30N
208	297-0024-0	297-00083D-005.05N
209	297-0026-0	297-00138D-005.78E
210	301-0016-0	301-00080D-015.35N
211	301-0021-0	301-00402D-154.29E
212	301-0022-0	301-00402D-154.30E
213	301-0024-0	301-00402D-164.52E
214	301-0025-0	301-00402D-164.53E
215	311-0007-0	311-00017D-004.62N
216	313-0001-0	313-00002D-003.32E
217	313-0003-0	313-00002D-006.43E
218	313-0024-0	313-00052D-008.11E
219	313-0043-0	313-00401D-335.89N
220	313-0054-0	313-00691F-002.98N
221	313-0066-0	313-01515M-000.33N
222	317-0003-0	317-00010D-027.02E

Table A.5: Steel girder bridges with anchor bolt corrosion in southern Georgia

Record Number	Bridge Serial Number	Location ID
1	001-0011-0	001-00004D-021.18N
2	009-0002-0	009-00022D-004.02E
3	009-0007-0	009-00022D-012.46E
4	009-0016-0	009-00112D-005.10N
5	017-0003-0	017-00011D-014.68N
6	021-0030-0	021-03206M-000.99E
7	021-0031-0	021-00011D-003.90N
8	021-0034-0	021-00011D-006.15N
9	021-0038-0	021-00074D-001.41E
10	021-0048-0	021-00087D-010.54N
11	021-0054-0	021-00091X-000.23S
12	021-0070-0	021-00940F-015.85N
13	021-0083-0	021-00401D-160.30N
14	021-0085-0	021-00401D-161.27N
15	021-0088-0	021-00401D-162.48N
16	021-0095-0	021-00401D-164.98N
17	021-0097-0	021-00401D-165.59N
18	021-0098-0	021-00401D-165.60N
19	021-0101-0	021-00401D-166.63N
20	021-0106-0	021-00401D-169.07N
21	021-0107-0	021-00401D-169.08N
22	021-0110-0	021-00401D-170.83N
23	021-0115-0	021-00401R-164.96N
24	021-0116-0	021-00401R-164.97N
25	021-0119-0	021-00404D-000.70E
26	021-0120-0	021-00404D-000.71E
27	021-0125-0	021-00404D-003.01E
28	021-0126-0	021-00404D-003.02E
29	021-0136-0	021-00408D-000.00N
30	021-0143-0	021-00408D-007.24N
31	021-0148-0	021-00665F-002.05E
32	021-0181-0	021-03217M-001.20E
33	021-0188-0	021-03245M-000.35E
34	021-0191-0	021-03262M-000.04N
35	023-0001-0	023-00026D-011.63E
36	023-0012-0	023-00112D-022.28N
37	025-0026-0	025-00520D-020.67E

Table A.5 (continued)

Record Number	Bridge Serial Number	Location ID
38	027-0003-0	027-00076D-010.34E
39	027-0031-0	027-00122D-002.00E
40	027-0034-0	027-00122D-008.29E
41	029-0006-0	029-00026D-005.79E
42	029-0029-0	029-00404D-146.29E
43	029-0030-0	029-00404D-146.30E
44	031-0047-0	031-00119D-001.29N
45	033-0004-0	033-00017D-005.46N
46	035-0001-0	035-00016D-000.88E
47	049-0012-0	049-00023D-000.00N
48	061-0002-0	061-00037D-000.01E
49	069-0013-0	069-00032D-019.60E
50	069-0014-0	069-00032D-020.12E
51	069-0017-0	069-00032D-025.11E
52	069-0018-0	069-00032D-025.83E
53	069-0031-0	069-00135D-016.62N
54	075-0019-0	075-00240X-001.84N
55	077-0018-0	077-00054D-010.58E
56	077-0043-0	077-00403D-043.47N
57	077-0044-0	077-00403D-043.48N
58	077-0049-0	077-00403D-050.02N
59	077-0069-0	077-01599F-007.01N
60	077-0076-0	077-02081F-002.01E
61	077-5136-0	077-00403D-050.03N
62	079-0006-0	079-00007D-018.71N
63	081-0021-0	081-00257D-000.08N
64	087-0005-0	087-00001D-020.41N
65	087-0009-0	087-00001D-021.11N
66	087-0014-0	087-00001B-001.93N
67	091-0005-0	091-00030D-007.51E
68	093-0006-0	093-00027D-010.90E
69	093-0007-0	093-00027D-015.64E
70	093-0017-0	093-00157X-001.00N
71	093-0021-0	093-00215X-009.10N
72	093-0028-0	093-00230D-021.38E
73	093-0039-0	093-00401D-120.54N
74	093-0042-0	093-00440X-004.00E

Table A.5 (continued)

Record Number	Bridge Serial Number	Location ID
75	093-0048-0	093-01175F-002.67N
76	095-0014-0	095-00520D-004.72E
77	099-0002-0	099-00001D-007.82N
78	107-0058-0	107-00466X-000.17S
79	107-0069-0	107-00404D-089.40E
80	113-0013-0	113-00085D-015.84N
81	145-0008-0	145-00085D-006.07N
82	145-0031-0	145-00315D-004.40N
83	145-0039-0	145-00411D-016.94N
84	153-0028-0	153-00096D-011.18E
85	153-0041-0	153-00401D-124.43N
86	153-0042-0	153-00401D-124.44N
87	153-0052-0	153-00401D-136.37N
88	161-0020-0	161-00135D-024.38N
89	163-0023-0	163-00078D-004.92N
90	167-0007-0	167-00026D-006.33E
91	175-0017-0	175-00026D-018.58E
92	175-0018-0	175-00026D-018.80E
93	175-0031-0	175-00031D-021.42N
94	175-0046-0	175-00124X-003.00N
95	175-0089-0	175-00531X-002.20N
96	185-0010-0	185-00031D-000.00N
97	185-0020-0	185-00133D-002.24N
98	185-0024-0	185-00122D-000.41E
99	193-0014-0	193-00049D-009.91N
100	193-0019-0	193-00090D-014.60N
101	197-0010-0	197-00137D-015.44N
102	199-0007-0	199-00018D-006.03E
103	199-0033-0	199-00085D-002.05N
104	199-0034-0	199-00085D-008.73N
105	199-0047-0	199-00109D-009.60E
106	207-0008-0	207-02784F-000.66E
107	207-0021-0	207-00083D-008.36N
108	207-0038-0	207-00401D-176.37N
109	207-0053-0	207-00408D-014.72N
110	207-0054-0	207-00408D-014.73N
111	207-0069-0	207-00018D-008.61E

Table A.5 (continued)

Record Number	Bridge Serial Number	Location ID
112	209-0004-0	209-00030D-000.58E
113	209-0005-0	209-00030D-000.84E
114	215-0003-0	215-00520D-005.84E
115	215-0008-0	215-00001D-013.29N
116	215-0063-0	215-00411D-006.02N
117	215-0065-0	215-00411D-006.49N
118	215-0067-0	215-00411D-007.13N
119	215-0070-0	215-00411D-008.09N
120	215-0072-0	215-00411D-008.25N
121	215-0084-0	215-00411R-008.09N
122	215-0092-0	215-08016M-002.84E
123	215-0149-0	215-00001D-014.20N
124	215-0161-0	215-00411D-005.46N
125	225-0010-0	225-00247C-003.00E
126	225-0016-0	225-01508F-001.04E
127	229-0007-0	229-00015D-019.71N
128	229-0008-0	229-00015D-021.57N
129	235-0003-0	235-00011D-007.39N
130	235-0008-0	235-00026D-008.86E
131	235-0009-0	235-00026W-000.52W
132	237-0005-0	237-00016D-024.12E
133	251-0026-0	251-00073D-000.95N
134	255-0006-0	255-00003D-003.03N
135	261-0007-0	261-00027D-012.93E
136	261-0011-0	261-00027D-029.16E
137	263-0014-0	263-00036D-022.02E
138	269-0003-0	269-00003D-005.19N
139	269-0024-0	269-00137D-006.59N
140	269-0025-0	269-00137D-008.64N
141	269-0028-0	269-00137D-022.90N
142	271-0003-0	271-00027D-017.88E
143	275-0013-0	275-00038D-009.41E
144	285-0035-0	285-00109D-016.77E
145	285-0051-0	285-00403D-002.26N
146	285-0052-0	285-00403D-002.27N
147	289-0003-0	289-00019D-019.72N
148	299-0022-0	299-00158D-006.40E

Table A.5 (continued)

Record Number	Bridge Serial Number	Location ID
149	299-0024-0	299-00158D-005.90E
150	307-0010-0	307-00041D-011.12N
151	307-0011-0	307-00045D-001.85N
152	307-0012-0	307-00045D-002.01N
153	309-0014-0	309-00030D-017.42E

Table A.6: Steel girder bridges with anchor bolt corrosion in coastal Georgia

Record Number	Bridge Serial Number	Location ID
1	039-0011-0	039-00025D-031.89N
2	051-0005-0	051-00421D-001.60N
3	051-0007-0	051-00421D-003.38N
4	051-0008-0	051-00421D-004.29N
5	051-0009-0	051-00421D-004.30N
6	051-0012-0	051-00421D-005.42N
7	051-0016-0	051-00421D-005.96N
8	051-0019-0	051-00421D-006.10N
9	051-0060-0	051-00026D-011.20E
10	051-0066-0	051-00026D-032.43E
11	051-0078-0	051-00204D-025.61E
12	051-0090-0	051-00404D-163.60E
13	051-0092-0	051-00404D-163.95E
14	051-0093-0	051-00404D-163.97E
15	051-0095-0	051-00404D-165.03E
16	051-0096-0	051-00404D-165.02E
17	051-0097-0	051-00404D-165.69E
18	051-0098-0	051-00404D-165.70E
19	051-0101-0	051-00404D-166.09E
20	051-0105-0	051-00405D-093.87N
21	051-0109-0	051-00405D-099.28N
22	051-0124-0	051-00405D-107.24N
23	051-0125-0	051-00405D-108.52N
24	051-0126-0	051-00405D-108.53N
25	051-0138-0	051-04070M-003.00E
26	051-0147-0	051-00204P-006.08E
27	103-0026-0	103-00405D-112.31N

Table A.6 (continued)

Record Number	Bridge Serial Number	Location ID
28	127-0041-0	127-00303D-001.16N
29	127-0042-0	127-00303D-004.42N
30	127-0049-0	127-00405D-031.44N
31	127-0050-0	127-00405D-031.45N
32	127-0055-0	127-00405D-035.58N
33	127-0056-0	127-00405D-035.59N
34	127-0057-0	127-00405D-036.21N
35	127-0058-0	127-00405D-036.22N
36	191-0014-0	191-00057D-008.49E

Table A.7: Steel girder bridges with anchor bolt corrosion in metropolitan areas

Record Number	Bridge Serial Number	Location ID
1	021-0030-0	021-03206M-000.99E
2	021-0031-0	021-00011D-003.90N
3	021-0034-0	021-00011D-006.15N
4	021-0048-0	021-00087D-010.54N
5	021-0054-0	021-00091X-000.23S
6	021-0070-0	021-00940F-015.85N
7	021-0083-0	021-00401D-160.30N
8	021-0085-0	021-00401D-161.27N
9	021-0088-0	021-00401D-162.48N
10	021-0095-0	021-00401D-164.98N
11	021-0097-0	021-00401D-165.59N
12	021-0098-0	021-00401D-165.60N
13	021-0101-0	021-00401D-166.63N
14	021-0106-0	021-00401D-169.07N
15	021-0107-0	021-00401D-169.08N
16	021-0110-0	021-00401D-170.83N
17	021-0115-0	021-00401R-164.96N
18	021-0116-0	021-00401R-164.97N
19	021-0119-0	021-00404D-000.70E
20	021-0120-0	021-00404D-000.71E
21	021-0125-0	021-00404D-003.01E
22	021-0126-0	021-00404D-003.02E
23	021-0136-0	021-00408D-000.00N

Table A.7 (continued)

Record Number	Bridge Serial Number	Location ID
24	021-0143-0	021-00408D-007.24N
25	021-0181-0	021-03217M-001.20E
26	021-0188-0	021-03245M-000.35E
27	021-0191-0	021-03262M-000.04N
28	051-0005-0	051-00421D-001.60N
29	051-0007-0	051-00421D-003.38N
30	051-0008-0	051-00421D-004.29N
31	051-0009-0	051-00421D-004.30N
32	051-0012-0	051-00421D-005.42N
33	051-0016-0	051-00421D-005.96N
34	051-0019-0	051-00421D-006.10N
35	051-0060-0	051-00026D-011.20E
36	051-0066-0	051-00026D-032.43E
37	051-0078-0	051-00204D-025.61E
38	051-0090-0	051-00404D-163.60E
39	051-0092-0	051-00404D-163.95E
40	051-0093-0	051-00404D-163.97E
41	051-0095-0	051-00404D-165.03E
42	051-0096-0	051-00404D-165.02E
43	051-0097-0	051-00404D-165.69E
44	051-0098-0	051-00404D-165.70E
45	051-0101-0	051-00404D-166.09E
46	051-0105-0	051-00405D-093.87N
47	051-0109-0	051-00405D-099.28N
48	051-0124-0	051-00405D-107.24N
49	051-0125-0	051-00405D-108.52N
50	051-0126-0	051-00405D-108.53N
51	051-0138-0	051-04070M-003.00E
52	051-0147-0	051-00204P-006.08E
53	059-0001-0	059-00010L-005.45E
54	059-0002-0	059-00010L-005.44E
55	059-0011-0	059-00010L-001.88E
56	059-0018-0	059-00010L-000.04E
57	059-0020-0	059-00010D-003.13E
58	059-0021-0	059-00010D-003.14E
59	059-0029-0	059-00015A-004.33N
60	059-0036-0	059-00008D-001.97E

Table A.7 (continued)

Record Number	Bridge Serial Number	Location ID
61	059-0044-0	059-00008D-004.21E
62	059-0045-0	059-00008D-004.22E
63	059-0047-0	059-00008D-006.00E
64	059-0048-0	059-00008D-006.01E
65	059-0059-0	059-00320M-000.56E
66	067-0013-0	067-00003D-005.21N
67	067-0019-0	067-09004M-000.59N
68	067-0022-0	067-00005D-014.97N
69	067-0023-0	067-00005D-014.98N
70	067-0031-0	067-00005D-001.35N
71	067-0052-0	067-00280D-000.60N
72	067-0066-0	067-00401D-258.79N
73	067-0069-0	067-00401D-260.70N
74	067-0073-0	067-00401D-264.21N
75	067-0074-0	067-00401D-265.02N
76	067-0076-0	067-00401D-267.51N
77	067-0184-0	067-00005D-014.33N
78	073-0018-0	073-00223D-010.12E
79	073-0022-0	073-00232D-008.15E
80	073-0040-0	073-02122F-004.91N
81	073-0043-0	073-00388D-002.80N
82	089-0075-0	089-00407D-030.50C
83	089-0076-0	089-00407D-031.50C
84	089-0080-0	089-00407D-034.30C
85	095-0014-0	095-00520D-004.72E
86	097-0004-0	097-00005D-013.29N
87	097-0027-0	097-09370M-003.10N
88	113-0013-0	113-00085D-015.84N
89	115-0010-0	115-00001D-010.17N
90	115-0047-0	115-00101D-009.86N
91	115-0063-0	115-03745M-000.55E
92	117-0006-0	117-00017X-000.18E
93	117-0007-0	117-00019X-001.66W
94	117-0008-0	117-00020D-010.14E
95	117-0012-0	117-00087X-000.37E
96	117-0013-0	117-00141D-006.95N
97	117-0031-0	117-00456X-006.87S

Table A.7 (continued)

Record Number	Bridge Serial Number	Location ID
98	117-0032-0	117-01285F-006.75N
99	117-0039-0	117-02704F-000.96E
100	117-0040-0	117-02704F-000.97E
101	117-0042-0	117-02883F-000.95N
102	117-0044-0	117-02884F-002.52E
103	121-0015-0	121-00003D-017.91N
104	121-0095-0	121-00154D-022.24N
105	121-0170-0	121-00402D-052.13E
106	121-0178-0	121-00402D-055.38E
107	121-0227-0	121-00407D-004.82C
108	121-0238-0	121-00407D-010.81C
109	121-0244-0	121-00407D-024.05C
110	121-0380-0	121-09095M-000.91E
111	121-0389-0	121-09133M-000.20E
112	135-0028-0	135-00120D-011.66E
113	135-0054-0	135-00403D-112.88N
114	139-0006-0	139-00011D-015.69N
115	139-0025-0	139-00053C-001.23N
116	139-0033-0	139-00283D-001.42E
117	139-0043-0	139-00419D-011.64N
118	139-0045-0	139-00419D-015.93N
119	139-0046-0	139-00419D-015.94N
120	139-0049-0	139-00419D-020.25N
121	139-0051-0	139-00419D-024.01N
122	139-0056-0	139-00524X-000.17W
123	139-0057-0	139-00621X-001.01E
124	139-0058-0	139-00751X-000.84W
125	145-0008-0	145-00085D-006.07N
126	145-0031-0	145-00315D-004.40N
127	145-0039-0	145-00411D-016.94N
128	185-0020-0	185-00133D-002.24N
129	207-0053-0	207-00408D-014.72N
130	207-0054-0	207-00408D-014.73N
131	215-0003-0	215-00520D-005.84E
132	215-0008-0	215-00001D-013.29N
133	215-0063-0	215-00411D-006.02N
134	215-0065-0	215-00411D-006.49N

Table A.7 (continued)

Record Number	Bridge Serial Number	Location ID
135	215-0067-0	215-00411D-007.13N
136	215-0070-0	215-00411D-008.09N
137	215-0072-0	215-00411D-008.25N
138	215-0084-0	215-00411R-008.09N
139	215-0092-0	215-08016M-002.84E
140	215-0149-0	215-00001D-014.20N
141	215-0161-0	215-00411D-005.46N
142	225-0010-0	225-00247C-003.00E
143	225-0016-0	225-01508F-001.04E
144	245-0018-0	245-00010D-018.17E
145	245-0020-0	245-00010D-018.35E
146	245-0021-0	245-00010D-018.46E
147	245-0069-0	245-00842X-000.02N
148	285-0035-0	285-00109D-016.77E
149	313-0043-0	313-00401D-335.89N
150	313-0066-0	313-01515M-000.33N

Table A.8: Steel girder bridges with anchor bolt corrosion in rural areas

Record Number	Bridge Serial Number	Location ID
1	001-0011-0	001-00004D-021.18N
2	009-0002-0	009-00022D-004.02E
3	009-0007-0	009-00022D-012.46E
4	009-0016-0	009-00112D-005.10N
5	011-0002-0	011-00015D-000.85N
6	011-0029-0	011-00403D-150.43N
7	011-0030-0	011-00403D-150.44N
8	011-0031-0	011-00403D-152.66N
9	013-0012-0	013-00211D-022.60N
10	013-0014-0	013-00211D-018.86N
11	013-0018-0	013-00324D-000.66E
12	013-0022-0	013-00403D-127.19N
13	013-0023-0	013-00403D-127.20N
14	015-0005-0	015-00003D-003.48N
15	015-0006-0	015-00003D-003.49N
16	015-0021-0	015-00003D-022.62N

Table A.8 (continued)

Record Number	Bridge Serial Number	Location ID
17	015-0031-0	015-00061D-003.93N
18	015-0033-0	015-00061D-004.39N
19	015-0057-0	015-00155X-005.12N
20	015-0079-0	015-00401D-281.51N
21	015-0082-0	015-00401D-283.70N
22	015-0083-0	015-00401D-286.75N
23	015-0084-0	015-00401D-286.76N
24	015-0087-0	015-00401D-287.16N
25	015-0088-0	015-00401D-287.17N
26	015-0101-0	015-00401D-299.66N
27	015-0103-0	015-00401D-304.19N
28	015-0104-0	015-00401D-304.22N
29	017-0003-0	017-00011D-014.68N
30	021-0038-0	021-00074D-001.41E
31	021-0148-0	021-00665F-002.05E
32	023-0001-0	023-00026D-011.63E
33	023-0012-0	023-00112D-022.28N
34	025-0026-0	025-00520D-020.67E
35	027-0003-0	027-00076D-010.34E
36	027-0031-0	027-00122D-002.00E
37	027-0034-0	027-00122D-008.29E
38	029-0006-0	029-00026D-005.79E
39	029-0029-0	029-00404D-146.29E
40	029-0030-0	029-00404D-146.30E
41	031-0047-0	031-00119D-001.29N
42	033-0004-0	033-00017D-005.46N
43	035-0001-0	035-00016D-000.88E
44	039-0011-0	039-00025D-031.89N
45	047-0006-0	047-00002D-002.80E
46	047-0007-0	047-00002D-005.23E
47	047-0008-0	047-00002D-005.24E
48	047-0035-0	047-00401D-351.38N
49	047-0039-0	047-00401D-353.13N
50	047-0043-0	047-00401D-354.34N
51	049-0012-0	049-00023D-000.00N
52	057-0015-0	057-00092D-000.08N
53	057-0071-0	057-01375F-014.20N

Table A.8 (continued)

Record Number	Bridge Serial Number	Location ID
54	061-0002-0	061-00037D-000.01E
55	069-0013-0	069-00032D-019.60E
56	069-0014-0	069-00032D-020.12E
57	069-0017-0	069-00032D-025.11E
58	069-0018-0	069-00032D-025.83E
59	069-0031-0	069-00135D-016.62N
60	073-0016-0	073-00223D-002.47E
61	075-0019-0	075-00240X-001.84N
62	077-0018-0	077-00054D-010.58E
63	077-0043-0	077-00403D-043.47N
64	077-0044-0	077-00403D-043.48N
65	077-0049-0	077-00403D-050.02N
66	077-0069-0	077-01599F-007.01N
67	077-0076-0	077-02081F-002.01E
68	077-5136-0	077-00403D-050.03N
69	079-0006-0	079-00007D-018.71N
70	081-0021-0	081-00257D-000.08N
71	083-0010-0	083-00119X-000.18W
72	083-0012-0	083-00136D-005.16E
73	083-0017-0	083-00178X-000.11E
74	083-0020-0	083-00299D-002.62E
75	083-0022-0	083-00406D-004.67N
76	083-0023-0	083-00406D-007.09N
77	083-0024-0	083-00406D-007.10N
78	085-0001-0	085-00009D-001.73N
79	085-0002-0	085-00009D-001.93N
80	085-0018-0	085-00136D-023.00E
81	085-0019-0	085-00136D-025.95E
82	085-0020-0	085-00136D-026.96E
83	087-0005-0	087-00001D-020.41N
84	087-0009-0	087-00001D-021.11N
85	087-0014-0	087-00001B-001.93N
86	091-0005-0	091-00030D-007.51E
87	093-0006-0	093-00027D-010.90E
88	093-0007-0	093-00027D-015.64E
89	093-0017-0	093-00157X-001.00N
90	093-0021-0	093-00215X-009.10N

Table A.8 (continued)

Record Number	Bridge Serial Number	Location ID
91	093-0028-0	093-00230D-021.38E
92	093-0039-0	093-00401D-120.54N
93	093-0042-0	093-00440X-004.00E
94	093-0048-0	093-01175F-002.67N
95	099-0002-0	099-00001D-007.82N
96	103-0026-0	103-00405D-112.31N
97	105-0002-0	105-00017D-013.17N
98	105-0018-0	105-00368D-009.35N
99	107-0058-0	107-00466X-000.17S
100	107-0069-0	107-00404D-089.40E
101	111-0016-0	111-00515D-002.37N
102	111-0019-0	
103	117-0021-0	117-00369D-016.83E
104	119-0007-0	119-00051D-017.42E
105	119-0016-0	119-00084X-001.32E
106	119-0017-0	119-00097X-000.45N
107	119-0018-0	119-00106D-002.11N
108	119-0025-0	119-00258X-000.51W
109	119-0032-0	119-00328D-000.73N
110	119-0034-0	119-00383X-002.52W
111	119-0035-0	119-00387X-002.69E
112	119-0038-0	119-00403D-158.51N
113	119-0040-0	119-00403D-161.55N
114	119-0041-0	119-00403D-161.56N
115	123-0027-0	123-00282D-012.06E
116	127-0041-0	127-00303D-001.16N
117	127-0042-0	127-00303D-004.42N
118	127-0049-0	127-00405D-031.44N
119	127-0050-0	127-00405D-031.45N
120	127-0055-0	127-00405D-035.58N
121	127-0056-0	127-00405D-035.59N
122	127-0057-0	127-00405D-036.21N
123	127-0058-0	127-00405D-036.22N
124	129-0029-0	129-05607M-000.95E
125	129-0032-0	129-00136D-007.53E
126	129-0048-0	129-00156D-020.28E
127	129-0062-0	129-00401D-318.18N

Table A.8 (continued)

Record Number	Bridge Serial Number	Location ID
128	129-0064-0	129-00401D-318.70N
129	129-0066-0	129-00401D-319.84N
130	133-0003-0	133-00012D-011.10E
131	133-0019-0	133-00077D-000.51N
132	133-0028-0	133-00402D-136.62E
133	133-0029-0	133-00402D-136.63E
134	137-0002-0	137-00015D-000.68N
135	137-0011-0	137-00017D-008.64N
136	137-0029-0	137-00365D-043.12N
137	137-0032-0	137-00384D-004.22N
138	139-0010-0	139-00013D-010.10N
139	139-0013-0	139-00051D-000.40E
140	139-0014-0	139-00052D-023.90E
141	139-0039-0	139-00323D-005.35N
142	141-0010-0	141-00016D-024.82E
143	143-0029-0	143-01605F-000.25N
144	147-0015-0	147-00172D-003.46N
145	153-0028-0	153-00096D-011.18E
146	153-0041-0	153-00401D-124.43N
147	153-0042-0	153-00401D-124.44N
148	153-0052-0	153-00401D-136.37N
149	157-0017-0	157-00082P-001.56N
150	157-0021-0	157-00229X-002.04N
151	157-0022-0	157-00250X-000.25N
152	157-0027-0	157-00332D-006.10E
153	161-0020-0	161-00135D-024.38N
154	163-0023-0	163-00078D-004.92N
155	167-0007-0	167-00026D-006.33E
156	175-0017-0	175-00026D-018.58E
157	175-0018-0	175-00026D-018.80E
158	175-0031-0	175-00031D-021.42N
159	175-0046-0	175-00124X-003.00N
160	175-0089-0	175-00531X-002.20N
161	181-0010-0	181-00079D-018.97N
162	181-0017-0	181-00047D-016.50E
163	185-0010-0	185-00031D-000.00N
164	185-0024-0	185-00122D-000.41E

Table A.8 (continued)

Record Number	Bridge Serial Number	Location ID
165	187-0002-0	187-00009D-009.58N
166	187-0003-0	187-00060B-003.32N
167	189-0002-0	189-00010D-005.74E
168	189-0007-0	189-00021X-000.60N
169	189-0008-0	189-00024X-001.29N
170	189-0015-0	189-00223D-001.94E
171	189-0022-0	189-00797F-000.59N
172	189-0026-0	189-02150F-000.01N
173	191-0014-0	191-00057D-008.49E
174	193-0014-0	193-00049D-009.91N
175	193-0019-0	193-00090D-014.60N
176	195-0009-0	195-00072D-009.05E
177	195-0016-0	195-00106D-016.12N
178	195-0021-0	195-00281D-004.11N
179	197-0010-0	197-00137D-015.44N
180	199-0007-0	199-00018D-006.03E
181	199-0033-0	199-00085D-002.05N
182	199-0034-0	199-00085D-008.73N
183	199-0047-0	199-00109D-009.60E
184	207-0008-0	207-02784F-000.66E
185	207-0021-0	207-00083D-008.36N
186	207-0038-0	207-00401D-176.37N
187	207-0069-0	207-00018D-008.61E
188	209-0004-0	209-00030D-000.58E
189	209-0005-0	209-00030D-000.84E
190	211-0017-0	211-00083D-020.61N
191	211-0018-0	211-00146X-003.27N
192	211-0021-0	211-00249X-001.49N
193	211-0030-0	211-00402D-113.38E
194	211-0038-0	211-00402D-126.47E
195	211-0063-0	211-02425F-007.27N
196	213-0018-0	213-00002D-008.30E
197	213-0021-0	213-00061D-028.20N
198	217-0008-0	217-00036D-001.31E
199	217-0010-0	217-00057X-000.02N
200	217-0018-0	217-00142D-011.34N
201	217-0031-0	217-00402D-092.24E

Table A.8 (continued)

Record Number	Bridge Serial Number	Location ID
202	217-0035-0	217-00402D-094.50E
203	217-0036-0	217-00402D-094.51E
204	217-0037-0	217-00402D-094.63E
205	217-0038-0	217-00402D-094.64E
206	217-0041-0	217-00516X-002.45E
207	229-0007-0	229-00015D-019.71N
208	229-0008-0	229-00015D-021.57N
209	235-0003-0	235-00011D-007.39N
210	235-0008-0	235-00026D-008.86E
211	235-0009-0	235-00026W-000.52W
212	237-0005-0	237-00016D-024.12E
213	241-0001-0	241-00002D-007.55E
214	241-0009-0	241-00015D-001.85N
215	241-0010-0	241-00015D-002.10N
216	241-0022-0	241-00246D-000.08E
217	251-0026-0	251-00073D-000.95N
218	255-0006-0	255-00003D-003.03N
219	257-0011-0	257-00184D-014.53N
220	261-0007-0	261-00027D-012.93E
221	261-0011-0	261-00027D-029.16E
222	263-0014-0	263-00036D-022.02E
223	269-0003-0	269-00003D-005.19N
224	269-0024-0	269-00137D-006.59N
225	269-0025-0	269-00137D-008.64N
226	269-0028-0	269-00137D-022.90N
227	271-0003-0	271-00027D-017.88E
228	275-0013-0	275-00038D-009.41E
229	281-0008-0	281-00002D-017.97E
230	283-0036-0	283-00404D-066.74E
231	285-0051-0	285-00403D-002.26N
232	285-0052-0	285-00403D-002.27N
233	289-0003-0	289-00019D-019.72N
234	291-0027-0	291-02899F-001.79S
235	295-0010-0	295-00136D-007.78E
236	295-0020-0	295-00151D-002.48N
237	297-0010-0	297-00010D-010.58E
238	297-0011-0	297-00010D-012.23E

Table A.8 (continued)

Record Number	Bridge Serial Number	Location ID
239	297-0012-0	297-00010D-012.24E
240	297-0015-0	297-00011D-000.98N
241	297-0017-0	297-00011D-012.74N
242	297-0022-0	297-00081D-017.30N
243	297-0024-0	297-00083D-005.05N
244	297-0026-0	297-00138D-005.78E
245	299-0022-0	299-00158D-006.40E
246	299-0024-0	299-00158D-005.90E
247	301-0016-0	301-00080D-015.35N
248	301-0021-0	301-00402D-154.29E
249	301-0022-0	301-00402D-154.30E
250	301-0024-0	301-00402D-164.52E
251	301-0025-0	301-00402D-164.53E
252	307-0010-0	307-00041D-011.12N
253	307-0011-0	307-00045D-001.85N
254	307-0012-0	307-00045D-002.01N
255	309-0014-0	309-00030D-017.42E
256	311-0007-0	311-00017D-004.62N
257	313-0001-0	313-00002D-003.32E
258	313-0003-0	313-00002D-006.43E
259	313-0024-0	313-00052D-008.11E
260	313-0054-0	313-00691F-002.98N
261	317-0003-0	317-00010D-027.02E

Table A.9: Steel girder bridges with anchor bolt corrosion in the Interstate system

Record Number	Bridge Serial Number	Location ID
1	011-0029-0	011-00403D-150.43N
2	011-0030-0	011-00403D-150.44N
3	011-0031-0	011-00403D-152.66N
4	013-0022-0	013-00403D-127.19N
5	013-0023-0	013-00403D-127.20N
6	015-0079-0	015-00401D-281.51N
7	015-0082-0	015-00401D-283.70N
8	015-0083-0	015-00401D-286.75N
9	015-0084-0	015-00401D-286.76N

Table A.9 (continued)

Record Number	Bridge Serial Number	Location ID
10	015-0087-0	015-00401D-287.16N
11	015-0088-0	015-00401D-287.17N
12	015-0101-0	015-00401D-299.66N
13	015-0103-0	015-00401D-304.19N
14	015-0104-0	015-00401D-304.22N
15	021-0083-0	021-00401D-160.30N
16	021-0085-0	021-00401D-161.27N
17	021-0088-0	021-00401D-162.48N
18	021-0095-0	021-00401D-164.98N
19	021-0097-0	021-00401D-165.59N
20	021-0098-0	021-00401D-165.60N
21	021-0101-0	021-00401D-166.63N
22	021-0106-0	021-00401D-169.07N
23	021-0107-0	021-00401D-169.08N
24	021-0110-0	021-00401D-170.83N
25	021-0115-0	021-00401R-164.96N
26	021-0116-0	021-00401R-164.97N
27	021-0119-0	021-00404D-000.70E
28	021-0120-0	021-00404D-000.71E
29	021-0125-0	021-00404D-003.01E
30	021-0126-0	021-00404D-003.02E
31	021-0136-0	021-00408D-000.00N
32	021-0143-0	021-00408D-007.24N
33	029-0029-0	029-00404D-146.29E
34	029-0030-0	029-00404D-146.30E
35	047-0035-0	047-00401D-351.38N
36	047-0039-0	047-00401D-353.13N
37	047-0043-0	047-00401D-354.34N
38	051-0005-0	051-00421D-001.60N
39	051-0007-0	051-00421D-003.38N
40	051-0008-0	051-00421D-004.29N
41	051-0009-0	051-00421D-004.30N
42	051-0012-0	051-00421D-005.42N
43	051-0016-0	051-00421D-005.96N
44	051-0019-0	051-00421D-006.10N
45	051-0090-0	051-00404D-163.60E
46	051-0092-0	051-00404D-163.95E

Table A.9 (continued)

Record Number	Bridge Serial Number	Location ID
47	051-0093-0	051-00404D-163.97E
48	051-0095-0	051-00404D-165.03E
49	051-0096-0	051-00404D-165.02E
50	051-0097-0	051-00404D-165.69E
51	051-0098-0	051-00404D-165.70E
52	051-0101-0	051-00404D-166.09E
53	051-0105-0	051-00405D-093.87N
54	051-0109-0	051-00405D-099.28N
55	051-0124-0	051-00405D-107.24N
56	051-0125-0	051-00405D-108.52N
57	051-0126-0	051-00405D-108.53N
58	067-0066-0	067-00401D-258.79N
59	067-0069-0	067-00401D-260.70N
60	067-0073-0	067-00401D-264.21N
61	067-0074-0	067-00401D-265.02N
62	067-0076-0	067-00401D-267.51N
63	077-0043-0	077-00403D-043.47N
64	077-0044-0	077-00403D-043.48N
65	077-0049-0	077-00403D-050.02N
66	077-5136-0	077-00403D-050.03N
67	083-0022-0	083-00406D-004.67N
68	083-0023-0	083-00406D-007.09N
69	083-0024-0	083-00406D-007.10N
70	089-0075-0	089-00407D-030.50C
71	089-0076-0	089-00407D-031.50C
72	089-0080-0	089-00407D-034.30C
73	093-0039-0	093-00401D-120.54N
74	103-0026-0	103-00405D-112.31N
75	107-0069-0	107-00404D-089.40E
76	111-0019-0	
77	119-0038-0	119-00403D-158.51N
78	119-0040-0	119-00403D-161.55N
79	119-0041-0	119-00403D-161.56N
80	121-0170-0	121-00402D-052.13E
81	121-0178-0	121-00402D-055.38E
82	121-0227-0	121-00407D-004.82C
83	121-0238-0	121-00407D-010.81C

Table A.9 (continued)

Record Number	Bridge Serial Number	Location ID
84	121-0244-0	121-00407D-024.05C
85	127-0049-0	127-00405D-031.44N
86	127-0050-0	127-00405D-031.45N
87	127-0055-0	127-00405D-035.58N
88	127-0056-0	127-00405D-035.59N
89	127-0057-0	127-00405D-036.21N
90	127-0058-0	127-00405D-036.22N
91	129-0062-0	129-00401D-318.18N
92	129-0064-0	129-00401D-318.70N
93	129-0066-0	129-00401D-319.84N
94	133-0028-0	133-00402D-136.62E
95	133-0029-0	133-00402D-136.63E
96	135-0054-0	135-00403D-112.88N
97	139-0043-0	139-00419D-011.64N
98	139-0045-0	139-00419D-015.93N
99	139-0046-0	139-00419D-015.94N
100	139-0049-0	139-00419D-020.25N
101	139-0051-0	139-00419D-024.01N
102	145-0039-0	145-00411D-016.94N
103	153-0041-0	153-00401D-124.43N
104	153-0042-0	153-00401D-124.44N
105	153-0052-0	153-00401D-136.37N
106	207-0038-0	207-00401D-176.37N
107	207-0053-0	207-00408D-014.72N
108	207-0054-0	207-00408D-014.73N
109	211-0030-0	211-00402D-113.38E
110	211-0038-0	211-00402D-126.47E
111	215-0063-0	215-00411D-006.02N
112	215-0065-0	215-00411D-006.49N
113	215-0067-0	215-00411D-007.13N
114	215-0070-0	215-00411D-008.09N
115	215-0072-0	215-00411D-008.25N
116	215-0084-0	215-00411R-008.09N
117	215-0161-0	215-00411D-005.46N
118	217-0031-0	217-00402D-092.24E
119	217-0035-0	217-00402D-094.50E
120	217-0036-0	217-00402D-094.51E

Table A.9 (continued)

Record Number	Bridge Serial Number	Location ID
121	217-0037-0	217-00402D-094.63E
122	217-0038-0	217-00402D-094.64E
123	283-0036-0	283-00404D-066.74E
124	285-0051-0	285-00403D-002.26N
125	285-0052-0	285-00403D-002.27N
126	301-0021-0	301-00402D-154.29E
127	301-0022-0	301-00402D-154.30E
128	301-0024-0	301-00402D-164.52E
129	301-0025-0	301-00402D-164.53E
130	313-0043-0	313-00401D-335.89N

Table A.10: Steel girder bridges with anchor bolt corrosion spanning an Interstate road

Record Number	Bridge Serial Number	Location ID
1	011-0002-0	011-00015D-000.85N
2	013-0012-0	013-00211D-022.60N
3	015-0057-0	015-00155X-005.12N
4	021-0030-0	021-03206M-000.99E
5	021-0048-0	021-00087D-010.54N
6	021-0054-0	021-00091X-000.23S
7	021-0070-0	021-00940F-015.85N
8	021-0148-0	021-00665F-002.05E
9	021-0181-0	021-03217M-001.20E
10	021-0188-0	021-03245M-000.35E
11	021-0191-0	021-03262M-000.04N
12	023-0012-0	023-00112D-022.28N
13	031-0047-0	031-00119D-001.29N
14	035-0001-0	035-00016D-000.88E
15	051-0078-0	051-00204D-025.61E
16	051-0138-0	051-04070M-003.00E
17	057-0015-0	057-00092D-000.08N
18	067-0022-0	067-00005D-014.97N
19	067-0023-0	067-00005D-014.98N
20	067-0052-0	067-00280D-000.60N
21	073-0040-0	073-02122F-004.91N
22	073-0043-0	073-00388D-002.80N

Table A.10 (continued)

Record Number	Bridge Serial Number	Location ID
23	075-0019-0	075-00240X-001.84N
24	077-0069-0	077-01599F-007.01N
25	077-0076-0	077-02081F-002.01E
26	081-0021-0	081-00257D-000.08N
27	083-0010-0	083-00119X-000.18W
28	083-0012-0	083-00136D-005.16E
29	083-0017-0	083-00178X-000.11E
30	083-0020-0	083-00299D-002.62E
31	093-0007-0	093-00027D-015.64E
32	093-0017-0	093-00157X-001.00N
33	093-0021-0	093-00215X-009.10N
34	093-0028-0	093-00230D-021.38E
35	093-0042-0	093-00440X-004.00E
36	093-0048-0	093-01175F-002.67N
37	097-0004-0	097-00005D-013.29N
38	097-0027-0	097-09370M-003.10N
39	107-0058-0	107-00466X-000.17S
40	119-0016-0	119-00084X-001.32E
41	119-0017-0	119-00097X-000.45N
42	119-0025-0	119-00258X-000.51W
43	119-0032-0	119-00328D-000.73N
44	119-0034-0	119-00383X-002.52W
45	119-0035-0	119-00387X-002.69E
46	121-0095-0	121-00154D-022.24N
47	121-0380-0	121-09095M-000.91E
48	121-0389-0	121-09133M-000.20E
49	129-0029-0	129-05607M-000.95E
50	129-0032-0	129-00136D-007.53E
51	133-0019-0	133-00077D-000.51N
52	139-0056-0	139-00524X-000.17W
53	139-0057-0	139-00621X-001.01E
54	139-0058-0	139-00751X-000.84W
55	143-0029-0	143-01605F-000.25N
56	145-0031-0	145-00315D-004.40N
57	157-0017-0	157-00082P-001.56N
58	157-0021-0	157-00229X-002.04N
59	157-0022-0	157-00250X-000.25N

Table A.10 (continued)

Record Number	Bridge Serial Number	Location ID
60	157-0027-0	157-00332D-006.10E
61	175-0031-0	175-00031D-021.42N
62	175-0046-0	175-00124X-003.00N
63	175-0089-0	175-00531X-002.20N
64	185-0020-0	185-00133D-002.24N
65	189-0007-0	189-00021X-000.60N
66	189-0008-0	189-00024X-001.29N
67	189-0015-0	189-00223D-001.94E
68	189-0022-0	189-00797F-000.59N
69	189-0026-0	189-02150F-000.01N
70	191-0014-0	191-00057D-008.49E
71	207-0008-0	207-02784F-000.66E
72	207-0069-0	207-00018D-008.61E
73	211-0018-0	211-00146X-003.27N
74	211-0021-0	211-00249X-001.49N
75	211-0063-0	211-02425F-007.27N
76	215-0003-0	215-00520D-005.84E
77	215-0008-0	215-00001D-013.29N
78	215-0092-0	215-08016M-002.84E
79	217-0010-0	217-00057X-000.02N
80	217-0018-0	217-00142D-011.34N
81	225-0010-0	225-00247C-003.00E
82	225-0016-0	225-01508F-001.04E
83	245-0069-0	245-00842X-000.02N
84	285-0035-0	285-00109D-016.77E
85	301-0016-0	301-00080D-015.35N
86	313-0054-0	313-00691F-002.98N
87	313-0066-0	313-01515M-000.33N

Table A.11: Steel girder bridges with anchor bolt corrosion not related to Interstates

Record Number	Bridge Serial Number	Location ID
1	001-0011-0	001-00004D-021.18N
2	009-0002-0	009-00022D-004.02E
3	009-0007-0	009-00022D-012.46E
4	009-0016-0	009-00112D-005.10N
5	013-0014-0	013-00211D-018.86N
6	013-0018-0	013-00324D-000.66E
7	015-0005-0	015-00003D-003.48N
8	015-0006-0	015-00003D-003.49N
9	015-0021-0	015-00003D-022.62N
10	015-0031-0	015-00061D-003.93N
11	015-0033-0	015-00061D-004.39N
12	017-0003-0	017-00011D-014.68N
13	021-0031-0	021-00011D-003.90N
14	021-0034-0	021-00011D-006.15N
15	021-0038-0	021-00074D-001.41E
16	023-0001-0	023-00026D-011.63E
17	025-0026-0	025-00520D-020.67E
18	027-0003-0	027-00076D-010.34E
19	027-0031-0	027-00122D-002.00E
20	027-0034-0	027-00122D-008.29E
21	029-0006-0	029-00026D-005.79E
22	033-0004-0	033-00017D-005.46N
23	039-0011-0	039-00025D-031.89N
24	047-0006-0	047-00002D-002.80E
25	047-0007-0	047-00002D-005.23E
26	047-0008-0	047-00002D-005.24E
27	049-0012-0	049-00023D-000.00N
28	051-0060-0	051-00026D-011.20E
29	051-0066-0	051-00026D-032.43E
30	051-0147-0	051-00204P-006.08E
31	057-0071-0	057-01375F-014.20N
32	059-0001-0	059-00010L-005.45E
33	059-0002-0	059-00010L-005.44E
34	059-0011-0	059-00010L-001.88E
35	059-0018-0	059-00010L-000.04E
36	059-0020-0	059-00010D-003.13E
37	059-0021-0	059-00010D-003.14E

Table A.11 (continued)

Record Number	Bridge Serial Number	Location ID
38	059-0029-0	059-00015A-004.33N
39	059-0036-0	059-00008D-001.97E
40	059-0044-0	059-00008D-004.21E
41	059-0045-0	059-00008D-004.22E
42	059-0047-0	059-00008D-006.00E
43	059-0048-0	059-00008D-006.01E
44	059-0059-0	059-00320M-000.56E
45	061-0002-0	061-00037D-000.01E
46	067-0013-0	067-00003D-005.21N
47	067-0019-0	067-09004M-000.59N
48	067-0031-0	067-00005D-001.35N
49	067-0184-0	067-00005D-014.33N
50	069-0013-0	069-00032D-019.60E
51	069-0014-0	069-00032D-020.12E
52	069-0017-0	069-00032D-025.11E
53	069-0018-0	069-00032D-025.83E
54	069-0031-0	069-00135D-016.62N
55	073-0016-0	073-00223D-002.47E
56	073-0018-0	073-00223D-010.12E
57	073-0022-0	073-00232D-008.15E
58	077-0018-0	077-00054D-010.58E
59	079-0006-0	079-00007D-018.71N
60	085-0001-0	085-00009D-001.73N
61	085-0002-0	085-00009D-001.93N
62	085-0018-0	085-00136D-023.00E
63	085-0019-0	085-00136D-025.95E
64	085-0020-0	085-00136D-026.96E
65	087-0005-0	087-00001D-020.41N
66	087-0009-0	087-00001D-021.11N
67	087-0014-0	087-00001B-001.93N
68	091-0005-0	091-00030D-007.51E
69	093-0006-0	093-00027D-010.90E
70	095-0014-0	095-00520D-004.72E
71	099-0002-0	099-00001D-007.82N
72	105-0002-0	105-00017D-013.17N
73	105-0018-0	105-00368D-009.35N
74	111-0016-0	111-00515D-002.37N

Table A.11 (continued)

Record Number	Bridge Serial Number	Location ID
75	113-0013-0	113-00085D-015.84N
76	115-0010-0	115-00001D-010.17N
77	115-0047-0	115-00101D-009.86N
78	115-0063-0	115-03745M-000.55E
79	117-0006-0	117-00017X-000.18E
80	117-0007-0	117-00019X-001.66W
81	117-0008-0	117-00020D-010.14E
82	117-0012-0	117-00087X-000.37E
83	117-0013-0	117-00141D-006.95N
84	117-0021-0	117-00369D-016.83E
85	117-0031-0	117-00456X-006.87S
86	117-0032-0	117-01285F-006.75N
87	117-0039-0	117-02704F-000.96E
88	117-0040-0	117-02704F-000.97E
89	117-0042-0	117-02883F-000.95N
90	117-0044-0	117-02884F-002.52E
91	119-0007-0	119-00051D-017.42E
92	119-0018-0	119-00106D-002.11N
93	121-0015-0	121-00003D-017.91N
94	123-0027-0	123-00282D-012.06E
95	127-0041-0	127-00303D-001.16N
96	127-0042-0	127-00303D-004.42N
97	129-0048-0	129-00156D-020.28E
98	133-0003-0	133-00012D-011.10E
99	135-0028-0	135-00120D-011.66E
100	137-0002-0	137-00015D-000.68N
101	137-0011-0	137-00017D-008.64N
102	137-0029-0	137-00365D-043.12N
103	137-0032-0	137-00384D-004.22N
104	139-0006-0	139-00011D-015.69N
105	139-0010-0	139-00013D-010.10N
106	139-0013-0	139-00051D-000.40E
107	139-0014-0	139-00052D-023.90E
108	139-0025-0	139-00053C-001.23N
109	139-0033-0	139-00283D-001.42E
110	139-0039-0	139-00323D-005.35N
111	141-0010-0	141-00016D-024.82E

Table A.11 (continued)

Record Number	Bridge Serial Number	Location ID
112	145-0008-0	145-00085D-006.07N
113	147-0015-0	147-00172D-003.46N
114	153-0028-0	153-00096D-011.18E
115	161-0020-0	161-00135D-024.38N
116	163-0023-0	163-00078D-004.92N
117	167-0007-0	167-00026D-006.33E
118	175-0017-0	175-00026D-018.58E
119	175-0018-0	175-00026D-018.80E
120	181-0010-0	181-00079D-018.97N
121	181-0017-0	181-00047D-016.50E
122	185-0010-0	185-00031D-000.00N
123	185-0024-0	185-00122D-000.41E
124	187-0002-0	187-00009D-009.58N
125	187-0003-0	187-00060B-003.32N
126	189-0002-0	189-00010D-005.74E
127	193-0014-0	193-00049D-009.91N
128	193-0019-0	193-00090D-014.60N
129	195-0009-0	195-00072D-009.05E
130	195-0016-0	195-00106D-016.12N
131	195-0021-0	195-00281D-004.11N
132	197-0010-0	197-00137D-015.44N
133	199-0007-0	199-00018D-006.03E
134	199-0033-0	199-00085D-002.05N
135	199-0034-0	199-00085D-008.73N
136	199-0047-0	199-00109D-009.60E
137	207-0021-0	207-00083D-008.36N
138	209-0004-0	209-00030D-000.58E
139	209-0005-0	209-00030D-000.84E
140	211-0017-0	211-00083D-020.61N
141	213-0018-0	213-00002D-008.30E
142	213-0021-0	213-00061D-028.20N
143	215-0149-0	215-00001D-014.20N
144	217-0008-0	217-00036D-001.31E
145	217-0041-0	217-00516X-002.45E
146	229-0007-0	229-00015D-019.71N
147	229-0008-0	229-00015D-021.57N
148	235-0003-0	235-00011D-007.39N

Table A.11 (continued)

Record Number	Bridge Serial Number	Location ID
149	235-0008-0	235-00026D-008.86E
150	235-0009-0	235-00026W-000.52W
151	237-0005-0	237-00016D-024.12E
152	241-0001-0	241-00002D-007.55E
153	241-0009-0	241-00015D-001.85N
154	241-0010-0	241-00015D-002.10N
155	241-0022-0	241-00246D-000.08E
156	245-0018-0	245-00010D-018.17E
157	245-0020-0	245-00010D-018.35E
158	245-0021-0	245-00010D-018.46E
159	251-0026-0	251-00073D-000.95N
160	255-0006-0	255-00003D-003.03N
161	257-0011-0	257-00184D-014.53N
162	261-0007-0	261-00027D-012.93E
163	261-0011-0	261-00027D-029.16E
164	263-0014-0	263-00036D-022.02E
165	269-0003-0	269-00003D-005.19N
166	269-0024-0	269-00137D-006.59N
167	269-0025-0	269-00137D-008.64N
168	269-0028-0	269-00137D-022.90N
169	271-0003-0	271-00027D-017.88E
170	275-0013-0	275-00038D-009.41E
171	281-0008-0	281-00002D-017.97E
172	289-0003-0	289-00019D-019.72N
173	291-0027-0	291-02899F-001.79S
174	295-0010-0	295-00136D-007.78E
175	295-0020-0	295-00151D-002.48N
176	297-0010-0	297-00010D-010.58E
177	297-0011-0	297-00010D-012.23E
178	297-0012-0	297-00010D-012.24E
179	297-0015-0	297-00011D-000.98N
180	297-0017-0	297-00011D-012.74N
181	297-0022-0	297-00081D-017.30N
182	297-0024-0	297-00083D-005.05N
183	297-0026-0	297-00138D-005.78E
184	299-0022-0	299-00158D-006.40E
185	299-0024-0	299-00158D-005.90E

Table A.11 (continued)

Record Number	Bridge Serial Number	Location ID
186	307-0010-0	307-00041D-011.12N
187	307-0011-0	307-00045D-001.85N
188	307-0012-0	307-00045D-002.01N
189	309-0014-0	309-00030D-017.42E
190	311-0007-0	311-00017D-004.62N
191	313-0001-0	313-00002D-003.32E
192	313-0003-0	313-00002D-006.43E
193	313-0024-0	313-00052D-008.11E
194	317-0003-0	317-00010D-027.02E

APPENDIX B

ADDITIONAL FIELD INVESTIGATION PICTURES

Several bridges throughout the state of Georgia were selected to be inspected specifically for anchor bolt corrosion by the researcher. Additional pictures from the bridges discussed in Chapter 6 are presented here.

B.1 Old Dixie Highway over Central of Georgia Railroad, District 7

Figures B.1 through B.33 correspond to the Old Dixie Highway bridge over Central of Georgia Railroad.



Figure B.1: Edge beam cover plate and bearing



Figure B.2: Typical bearing assembly at abutment



Figure B.3: Bearing at abutment



Figure B.4: Corrosion between bearing plate and flange



Figure B.5: Typical corrosion in flange (1)



Figure B.6: Typical corrosion in flange (2)



Figure B.7: Close up of crevice corrosion in flange (1)



Figure B.8: Close up of crevice corrosion in flange (2)



Figure B.9: Interior beams without crevice corrosion



Figure B.10: Corroded nut



Figure B.11: Close up of corroded nut



Figure B.12: View from above a typical bolt. Not a pure hexagonal shape.



Figure B.13: Edge beam bearing assemblies at interior Bent 2.



Figure B.14: Close up of bearing and bolt at Bent 2.



Figure B.15: Crevice corrosion in edge beam at Bent 2.



Figure B.16: Bearing assemblies of interior beams at Bent 2.



Figure B.17: Crevice corrosion in flange of interior beam at Bent 2.



Figure B.18: Interior Bent 3



Figure B.19: Spalling diaphragms at interior bent.



Figure B.20: Debris from diaphragms surrounding bearing



Figure B.21: Bearing assemblies of exterior beam at interior bent (1)



Figure B.22: Bearing assemblies of exterior beam at interior bent (2)



Figure B.23: Close-up of expansion slot



Figure B.24: Corroded bearing at interior Bent 3



Figure B.25: Accessing the joint at interior Bent 4



Figure B.26: Joint at Bent 4



Figure B.27: Bearing at southside of Bent 4



Figure B.28: Corrosion underneath flange at Bent 4 (1)



Figure B.29: Corrosion underneath flange at Bent 4 (2)

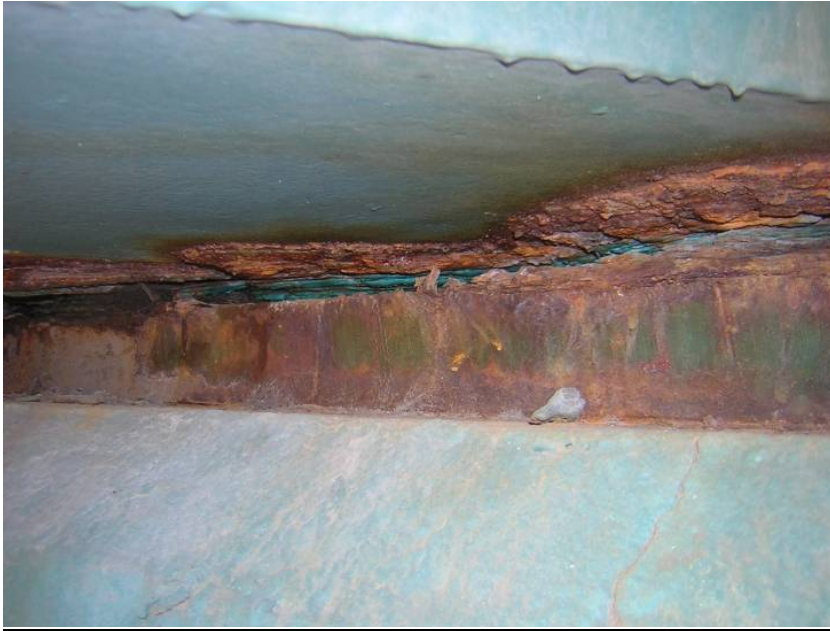


Figure B.30: Corrosion of the flange at Bent 4



Figure B.31: Corrosion around joint material at Bent 4



Figure B.32: Abutment backwall in between interior beams



Figure B.33: Oxides underneath chipped paint

B.2 Lawrenceville Highway over I-285, District 7

Figures B.34 through B.47 are from Lawrenceville Highway over I-285.



Figure B.34: Typical fixed bearing at abutment (1)



Figure B.35: Typical fixed bearing at abutment (2)



Figure B.36: Edge beam bearing at abutment (1)



Figure B.37: Edge beam bearing at abutment (2)



Figure B.38: Corrosion of edge beam bearing at abutment (1)



Figure B.39: Corrosion of edge beam bearing at abutment (2)



Figure B.40: Fixed bearing at interior bent



Figure B.41: Close-up of debris around anchor bolt at interior bent



Figure B.42: Expansion bearing at interior bent (1)



Figure B.43: Expansion bearing at interior bent (2)

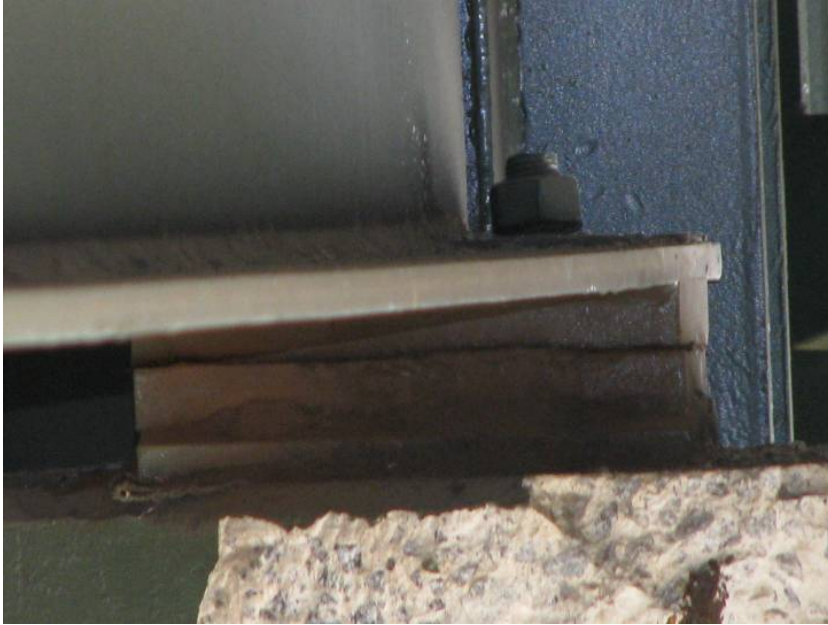


Figure B.44: Expansion bearing at interior bent (3)



Figure B.45: Edge beam bearing at opposite abutment. Corrosion on bearing plates.



Figure B.46: Fixed bearing at abutment



Figure B.47: Degradation of material behind fixed bearing

B.3 Memorial Drive over I-285, District 7

Figures B.48 through B.64 are from Memorial Drive over I-285.



Figure B.48: Typical rocker bearing at west abutment (1)



Figure B.49: Typical rocker bearing at west abutment (2)



Figure B.50: Side view of rocker bearing at west abutment (1)



Figure B.51: Side view of rocker bearing at west abutment (2)



Figure B.52: Interior bent



Figure B.53: Typical bearing at interior bent (1)



Figure B.54: Typical bearing at interior bent (2)



Figure B.55: Typical rocker bearing at east abutment



Figure B.56: Slight corrosion on bearing plate



Figure B.57: Bearing debris causing increased bearing corrosion (1)



Figure B.58: Bearing debris causing increased bearing corrosion (2)



Figure B.59: Bearing debris causing increased bearing corrosion (3)



Figure B.60: Bearing debris causing increased bearing corrosion (4)



Figure B.61: Corrosion between rocker and bearing plate (1)



Figure B.62: Corrosion between rocker and bearing plate (2)



Figure B.63: Corrosion between rocker and bearing plate (3)



Figure B.64: Corrosion between rocker and bearing plate (4)

B.4 State Route 92 over I-20, District 7

Figures B.65 through B.78 show further corrosion at State Route 92 over I-20.



Figure B.65: Joint at abutment (1)



Figure B.66: Joint at abutment (2)



Figure B.67: Example of anchor bolt corrosion (1)



Figure B.68: Example of anchor bolt corrosion (2)



Figure B.69: Example of anchor bolt corrosion (3)



Figure B.70: Example of anchor bolt and bearing corrosion



Figure B.71: Anchor bolt nut swelled with corrosion products (1)



Figure B.72: Anchor bolt nut swelled with corrosion products (2)



Figure B.73: Anchor bolt nut swelled with corrosion products (3)



Figure B.74: Bearing assembly missing anchor bolt (1)



Figure B.75: Bearing assembly missing anchor bolt (2)



Figure B.76: Corrosion of bearing and bearing retrofit angles (1)



Figure B.77: Corrosion of bearing and bearing retrofit angles (2)



Figure B.78: Corrosion of bearing and bearing retrofit angles (3)

B.5 State Route 122 over Little River, District 4

Figures B.79 through B.99 show State Route 122 over Little River.



Figure B.79: State Route 122 bridge over Little River



Figure B.80: Fixed bearing at interior bent in good condition



Figure B.81: Fixed bearing at interior bent with corrosion on bearing plate. Chipped paint only reveals orange primer paint underneath.



Figure B.82: Close up of corrosion on bearing plate and chipped paint



Figure B.83: Expansion bearing at interior bent with signs of corrosion between the bearing plate.



Figure B.84: Typical interior bent with fixed and expansion bearings (1)



Figure B.85: Typical interior bent with fixed and expansion bearings (2)



Figure B.86: Expansion bearing appearing in acceptable condition



Figure B.87: Closer inspection of expansion bearing reveals total anchor bolt corrosion.



Figure B.88: Investigation of anchor bolt shafts in the bearing slot, beneath the washer



Figure B.89: Anchor bolt corrosion inside the bearing, beneath the washer (1)



Figure B.90: Anchor bolt corrosion inside the bearing, beneath the washer (2)



Figure B.91: Anchor bolt corrosion inside the bearing, beneath the washer (3)



Figure B.92: Anchor bolt corrosion inside the bearing, beneath the washer (4)



Figure B.93: Anchor bolt corrosion inside the bearing, beneath the washer (5)



Figure B.94: Anchor bolt corrosion inside the bearing, beneath the washer (6)



Figure B.95: Anchor bolt corrosion inside the bearing, beneath the washer (7)



Figure B.96: Anchor bolt corrosion inside the bearing, beneath the washer (8)



Figure B.97: Anchor bolt corrosion inside the bearing, beneath the washer (9)



Figure B.98: Staining on the concrete piers from moisture from the deck joints



Figure B.99: Faulty deck joint

B.6 US 1 over Satilla River, District 5

Figures B.100 through B.107 show US 1 over Satilla River.



Figure B.100: Fixed bearing at steel girder end (1)



Figure B.101: Fixed bearing at steel girder end (2)



Figure B102: Expansion bearing



Figure B.103: Close up of an anchor bolt entering the expansion bearing base plate



Figure B.104: Fixed rocker



Figure B.105: Close up of corrosion between bearing plates in the fixed rocker



Figure B.106: Link cantilever bearing by river



Figure B.107: Close-up of corrosion at deck joint above link bearing

B.7 State Route 121 over Fishing Creek, District 5

Figures B.108 through B.120 are from State Route 121 over Fishing Creek.



Figure B.108: Fixed bearing at abutment



Figure B.109: Fixed bearing at interior bent



Figure B.110: Expansion and fixed bearings at expansion joint in the deck



Figure B.111: Bearing corrosion at deck joint



Figure B.112: Close-up of bearing corrosion at deck joint



Figure B.113: Investigation of anchor bolt shaft within the bearing by clearing away dirt



Figure B.114: Anchor bolt corrosion within the bearing (1)



Figure B.115: Anchor bolt corrosion within the bearing (2)



Figure B.116: Anchor bolt corrosion within the bearing (3)



Figure B.117: Anchor bolt corrosion within the bearing (4)



Figure B.118: Anchor bolt corrosion within the bearing (5)



Figure B.119: Anchor bolt corrosion within the bearing (6)



Figure B.120: Anchor bolt corrosion within the bearing (7)

B.8 State Route 144 over Watermelon Creek, District 5

Figures B.121 through B.____ are from State Route 144 over Watermelon Creek.



Figure B.121: Fixed bearing at abutment



Figure B.122: Expansion bearing at deck joint with visible corrosion on bearing plates



Figure B.123: Clearing away dirt to inspect anchor bolt shaft within the bearing

B.9 Northern Georgia bridges

Finally, the set of pictures in Figures B.124 through B.128 were obtained from the bridges in northern Georgia, from which no conclusions regarding bearing corrosion could be made.



Figure B.124: I-75 bridge over South Marietta Parkway, District 7



Figure B.125: US Route 76 over a creek in Blue Ridge, District 6



Figure B.126: State Route 515 over Georgia Northeast Railroad in Blue Ridge, District 6



Figure B.127: US Route 19 over US Route 76, District 1

APPENDIX C

SPECIMENS OBTAINED FROM BRIDGE DEMOLITION

Following the demolition of the Old Dixie Highway bridge over Central of Georgia Railroad, a variety of bearing plates and anchor bolts were acquired from fixed and expansion bearings at edge and interior girders. Anchor bolt corrosion within the bearing was apparent in these specimens that were not visible during previous inspection of the bridge.



Figure C.1: Fixed bearing with corroded anchor bolts



Figure C.2: Corrosion product build-up in the anchor bolt hole (1)



Figure C.3: Corrosion product build-up in the anchor bolt hole (2)



Figure C.4: Corrosion product build-up in the anchor bolt hole (3)



Figure C.5: Bolt and bearing plate from expansion bearing



Figure C.6: View of a fixed bearing with corroded anchor bolts from the top



Figure C.7: Anchor bolts protruding from fixed bearing plate



Figure C.8: Corrosion product on the anchor bolt protruding from the bearing plate (1)



Figure C.9: Corrosion product on the anchor bolt protruding from the bearing plate (2)



Figure C.10: Underside of a fixed bearing.



Figure C.11: Close-up of anchor bolt where it enters bearing plate from concrete (1)



Figure C.12: Close-up of anchor bolt where it enters bearing plate from concrete (2)



Figure C.13: Fixed bearing plate and anchor bolts



Figure C.14: Close-up of anchor bolts protruding from bearing plate



Figure C.15: Anchor bolt in bearing hole with severe necking



Figure C.16: Single anchor bolt showing necking



Figure C.17: Single anchor bolt, deformed during demolition, showing severe necking

APPENDIX D

ADDITIONAL DATA FROM EXPERIMENTAL TESTING

Soil analyses obtained from field investigations were used to create the simulated experimental testing environment, as presented in Chapter 8. In Table D.1 a complete listing of the results of the soil analyses from all the bridges is presented based on a solution of 10 grams of soil in 25 mL of water. The soil found in the Atlanta region was used for experimental testing.

Table D.1: Results of soil analyses from bridges in all regions

Ion	Conc (mg/L) at:							
	<i>Atlanta</i>	<i>South Georgia</i>			<i>North Georgia</i>			
	<u>S.R. 92</u>	<u>S.R. 121</u>	<u>US 1</u>	<u>SR 122</u>	<u>S.R. 515</u>	<u>US 19</u>	<u>US 76</u>	<u>I-75</u>
Na ⁺	58.97	20.10	4.33	5.29	25.35	1254.58	9.60	11.41
Ca ²⁺	30.23	311.46	35.61	39.42	26.86	36.26	118.02	29.90
K ⁺	12.78	16.56	18.61	14.91	14.79	1236.26	29.37	30.91
Fe	0.130	0.229	0.005	0.005	0.005	9.927	0.043	0.011
Cl ⁻	39.74	7.66	2.03	2.99	22.37	71.54	11.41	0.97
SO ₄ ²⁻	64.72	130.47	26.20	19.11	11.21	2259.05	404.54	18.05
NO ₃ ⁻	1.69	19.24	23.08	31.21	1.32	18.32	6.53	3.45
PO ₄ ⁻	-----	-----	-----	-----	0.50	18.32	6.53	0.51
CO ₃ ²⁻	56.19	154.17	14.97	21.16	-----	-----	-----	-----
pH	7.65	8.08	8.13	8.17	-----	-----	-----	-----

In Chapter 8, the long term potential readings for the steel samples in the concentrated solution were presented, as this was the critical environment. The long term potential readings for the steel samples in normal and pore solution are presented in Figures D.1 through D.6.

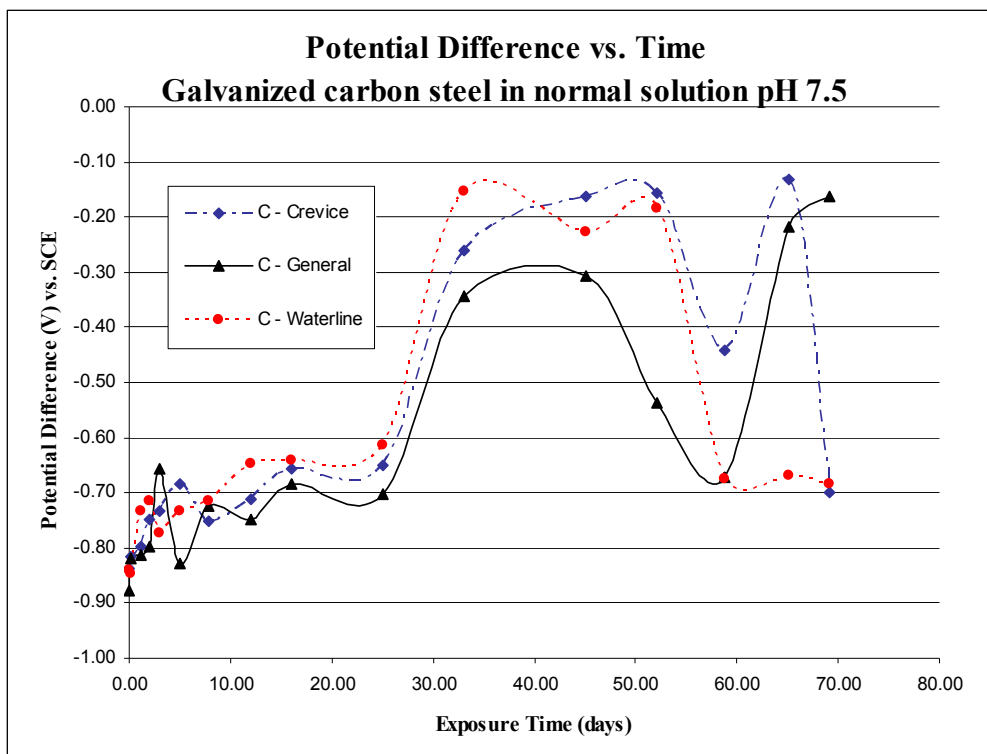


Figure D.1: Long term potential readings for carbon steel in normal solution pH 7.5

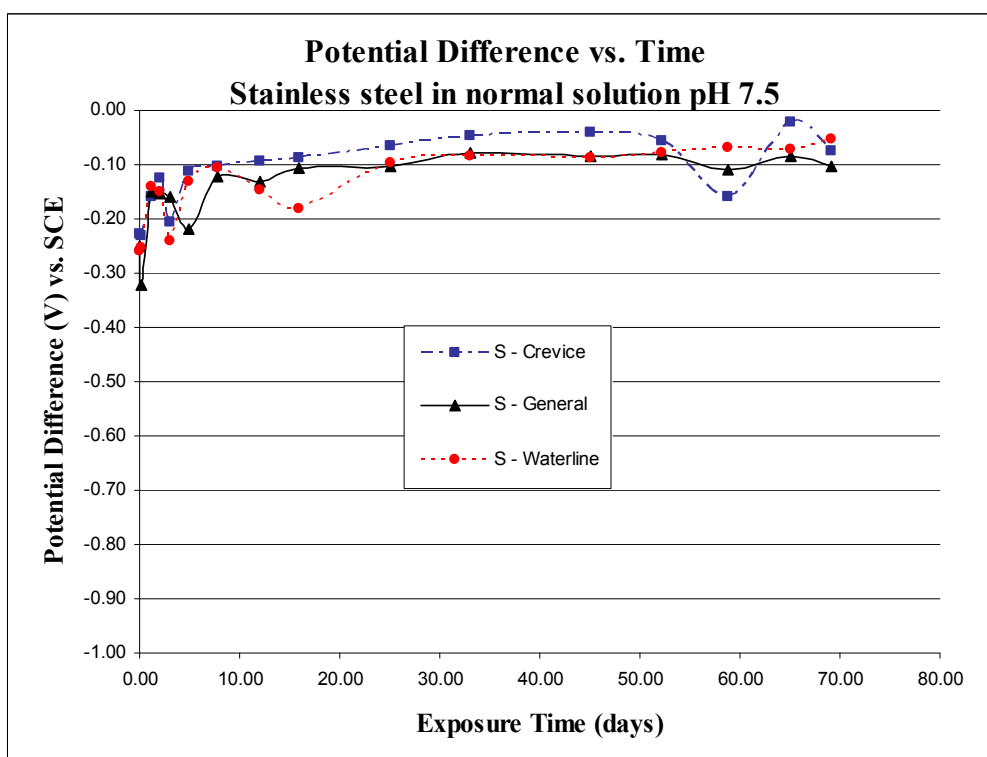


Figure D.2: Long term potential readings for stainless steel in normal solution at pH 7.5

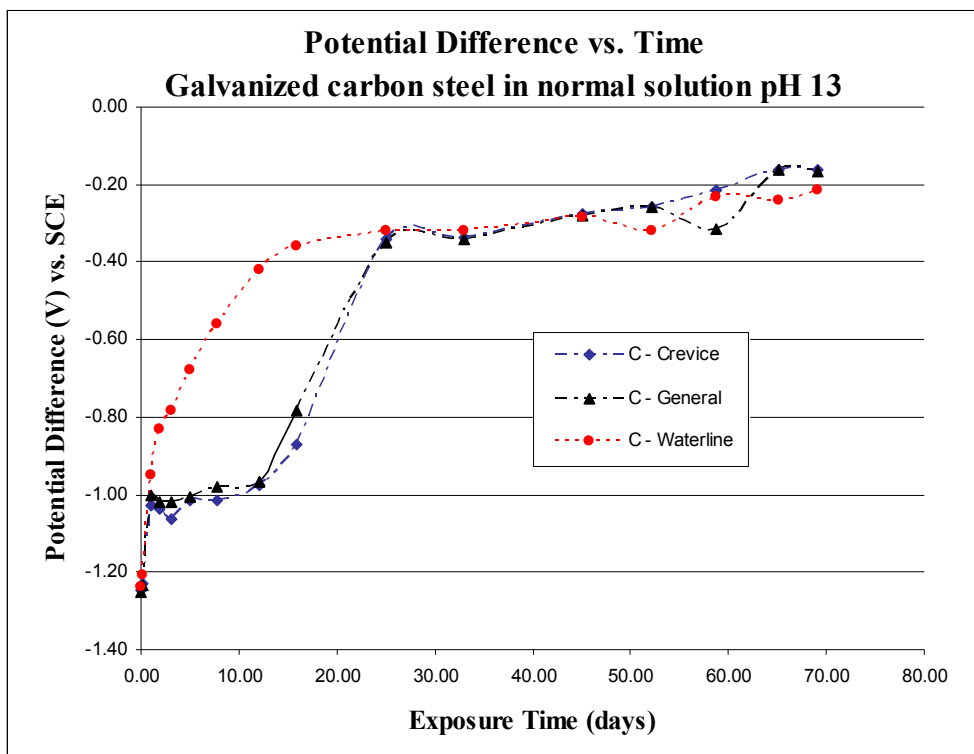


Figure D.3: Long term potential readings for carbon steel in normal solution at pH 13

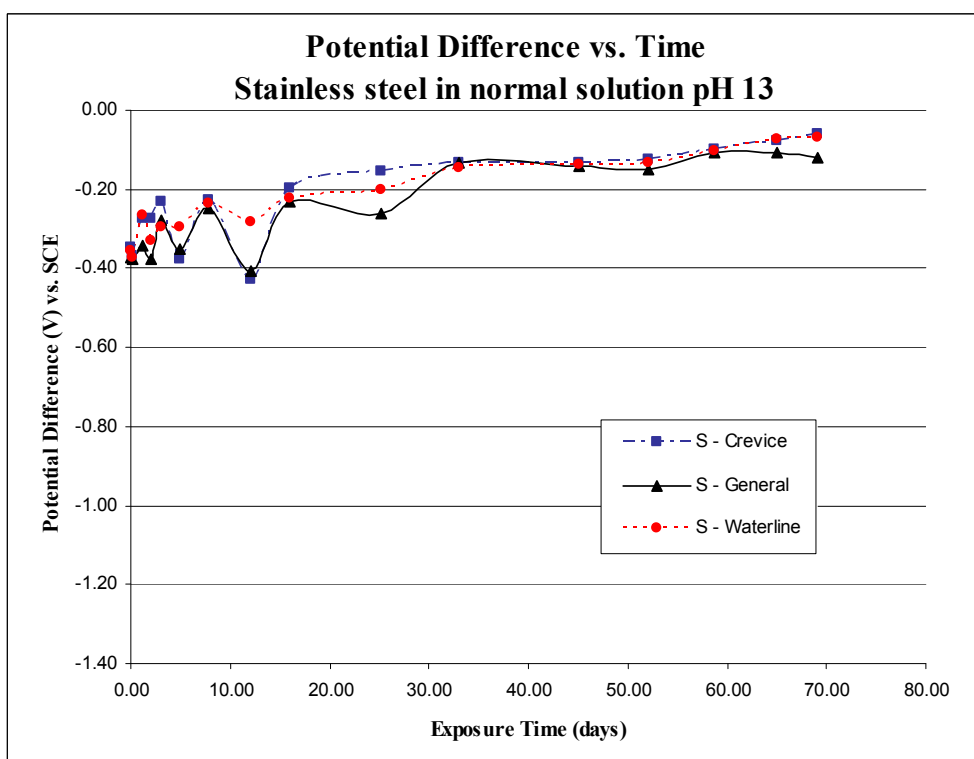


Figure D.4: Long term potential readings for stainless steel in normal solution at pH 13

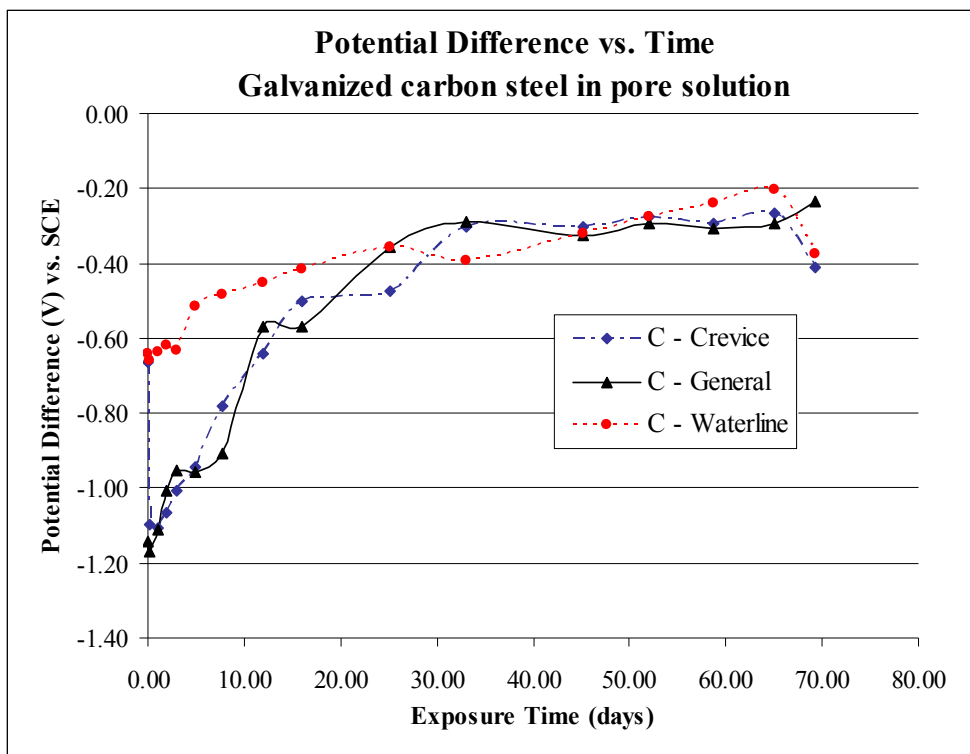


Figure D.5: Long term potential reading for carbon steel in pore solution

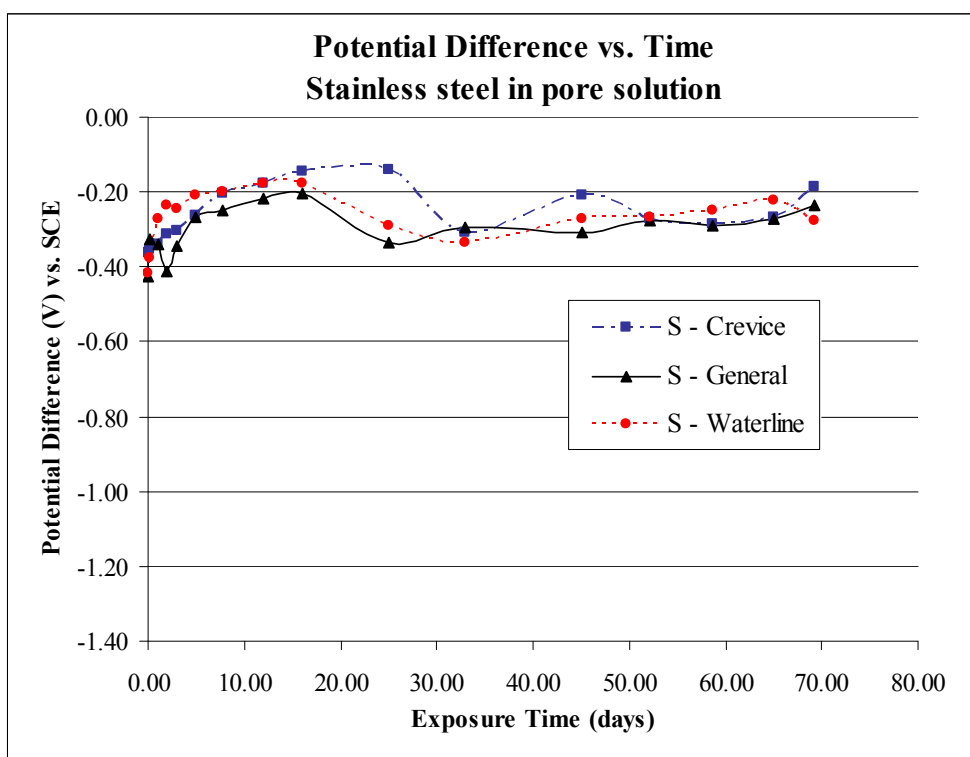


Figure D.6: Long term potential readings for stainless steel in pore solution

Table D.2 compares the corrosion rates of all the samples subjected to the long term test as determined by gravimetric and polarization resistance measurements.

Table D.2: Corrosion rates of long term samples determined by gravimetric and polarization resistance methods.

ID	Exposure Time (days)	Specimen type	Exposure solution / pH	Initial Weight (grams)	Final Weight (grams)	Final - Initial (mg)	Corrosion Rate	
							wt. loss (mpy)	polar. resistance (mpy)
C1	69.1	general	norm / 7.5	65.5902	65.4871	103.1	1.0740	6.27E-05
C2	69.19	general	norm / 13	63.1871	63.0387	148.4	1.5439	7.89E-05
C3	68.05	general	conc / 7.5	65.7445	65.6804	64.1	0.6780	1.67E-05
C5	68.07	general	conc / 13	65.5903	65.5764	13.9	0.1470	4.26E-02
C6	69.21	general	pore	64.5794	64.504	75.4	0.7842	1.01E-04
C7	68.05	general (no zinc)	conc / 7.5	65.063	64.8046	258.4	6.4699	3.129
C10	69.1	crevice	norm / 7.5	60.434	60.3313	102.7	1.1969	1.926
C11	69.19	crevice	norm / 13	57.8101	57.6209	189.2	2.2021	1.60E-04
C12	68.05	crevice	conc / 7.5	59.4293	59.3004	128.9	1.5254	2.307
C13	68.07	crevice	conc / 13	58.5302	58.5002	30	0.3549	5.68E-04
C14	69.21	crevice	pore	58.5797	58.4828	96.9	1.1275	3.26E-01
C21	68.05	crevice (no zinc)	conc / 7.5	58.8939	58.6487	245.2	6.1394	4.574
S1	69.1	general	norm / 7.5	65.6917	65.6905	1.2	0.0125	5.90E-04
S2	69.19	general	norm / 13	62.0451	62.0453	-0.2	-0.0021	5.84E-04
S3	68.05	general	conc / 7.5	65.6472	65.6464	0.8	0.0085	1.49E-02
S5	68.07	general	conc / 13	63.8604	63.8625	-2.1	-0.0222	3.04E-03
S6	69.21	general	pore	64.8002	64.7763	23.9	0.2486	9.79E-05
S7	69.1	crevice	norm / 7.5	57.9295	57.9278	1.7	0.0198	1.32E-03
S8	69.19	crevice	norm / 13	59.7853	59.7709	14.4	0.1676	1.20E-03
S9	68.05	crevice	conc / 7.5	59.7547	59.7493	5.4	0.0639	-2.18E-05
S10	68.07	crevice	conc / 13	59.4324	59.4172	15.2	0.1798	1.29E-03
S11	69.21	crevice	pore	57.3352	57.3198	15.4	0.1792	1.00E-04

In Chapter 8, the cyclic polarization curves were given for candidate alloys in concentrated solution, because the concentrated solution environment is the critical

environment compared to the normal solution. Figure D.7 presented the cyclic polarization curves for the candidate alloys in normal solution at pH 7.5

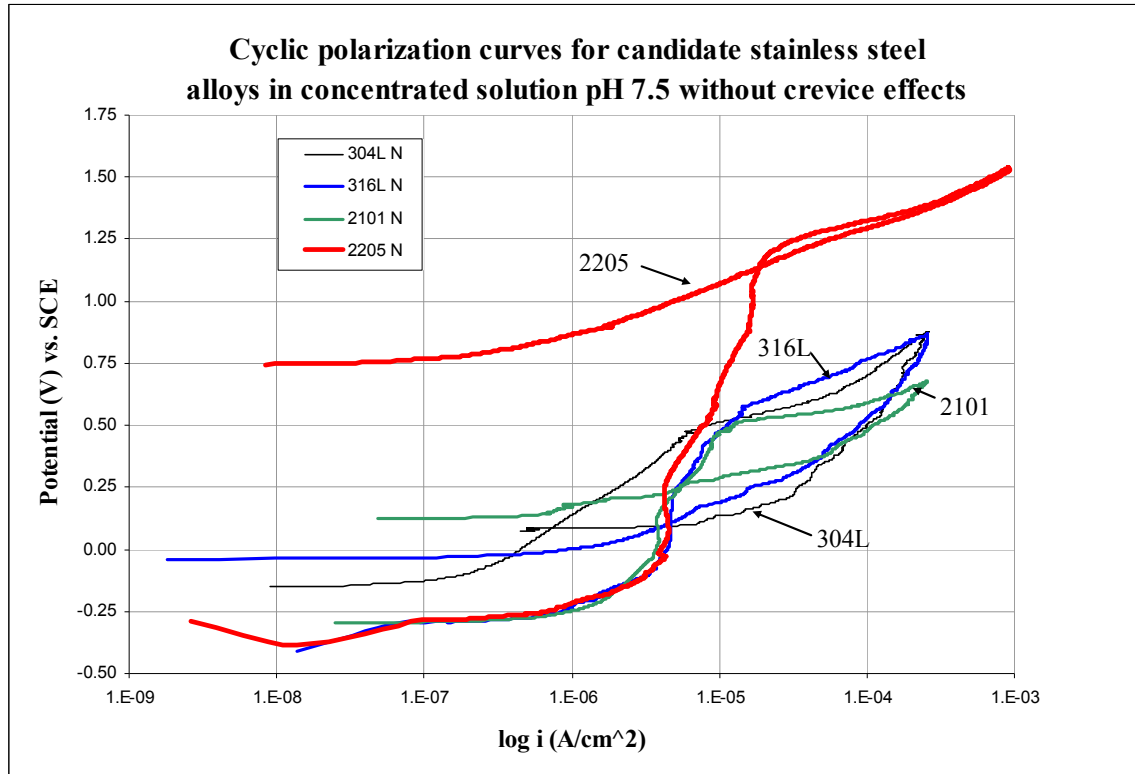


Figure D.7: Cyclic polarization curves for candidate alloys in normal solution at pH 7.5.

REFERENCES

- AASHTO. (2007). "AASHTO LRFD Bridge Design Specifications." American Association of State Highway and Transportation Officials, Washington DC.
- Abreu, C. M., Cristobal, M. J., Montemor, M. F., Novoa, X. R., Pena, G., and Perez, M. C. (2002). "Galvanic coupling between carbon steel and austenitic stainless steel in alkaline media." *Electrochimica Acta*, 47, 2271-2279.
- ACI, C., 222. (2001). "ACI 222R-01: Protection of Metals in Concrete Against Corrosion." American Concrete Institute.
- AISC. (2005). "Steel Construction Manual." American Institute of Steel Construction, Inc.
- Alonso, C., Andrade, C., Castellote, M., and Castro, P. (2000). "Chloride threshold values to depassivate reinforcing bars embedded in a standardized OPC mortar." *Cement and Concrete Research*, 30, 1047-1055.
- ASTM. (2001). "Standard Guide for Crevice Corrosion Testing of Iron-Base and Nickel-Base Stainless Alloys in Seawater and Other Chloride-Containing Aqueous Environments." American Society of Testing and Materials, West Conshohocken, PA.
- ASTM. (2002). "Standard Specification for Bronze Castings for Bridges and Turntables." American Society of Testing and Materials, West Conshohocken, PA.
- ASTM. (2003). "Standard Practice for Preparing, Cleaning, and Evaluating Corrosion Test Specimens" American Society of Testing and Materials, West Conshohocken, PA.
- ASTM. (2006). "Standard Specification for Stainless Steel Bars and Shapes." American Society of Testing and Materials, West Conshohocken, PA.
- ASTM. (2007). "Standard Specification for Structural Steel for Bridges." American Society of Testing and Materials, West Conshohocken, PA.
- Berke, N. S., Dallaire, M. P., Hicks, M. C., and Hoops, R. J. (1993). "Corrosion of Steel in Cracked Concrete." *Corrosion Engineering*, 49(11), 934-943.
- Bertolini, L., Bolzoni, F., and Pastore, T. (1996). "Behavior of stainless steel in simulated concrete pore solution." *British Corrosion Journal*, 31(3), 218-222.

- Bertolini, L., and Pedferri, P. (2002). "Laboratory and field experience on the use of stainless steel to improve durability of reinforced concrete." *Corrosion Reviews*, 20(1-2), 129-152.
- Bohni, H. (2005). "Corrosion in reinforced concrete structures." CRC Press, LLC, Boca Raton, FL.
- Broomfield, J. P. (2007). *Corrosion of Steel in Concrete*, Taylor and Francis Group.
- Castro, H., Rodriguez, C., Belzunce, F. J., and Canteli, A. F. (2003). "Mechanical properties and corrosion behavior of stainless steel reinforcing bars." *Journal of Materials Processing Technology*, 143-144, 134-137.
- Dabkowski, C. (2007). "Self-lubricating bearing plates." Personal telephone communication.
- Davis, J. R. (2000). "Corrosion: Understanding the Basics." ASM International, Materials Park, Ohio. 2-151.
- Duvall, W., Harper, M., and Clements, L. (2007). "Bearing design in Georgia." Personal communication, Atlanta, GA.
- Flint, G. N., and Cox, R. N. (1988). "The resistance of stainless steel partly embedded in concrete to corrosion by seawater." *Magazine of Concrete Research*, 40(142), 13-27.
- Fontana, M. G. (1986). *Corrosion Engineering*, McGraw-Hill, New York. 466.
- Frankel, G. S. (1998). "Pitting corrosion of metals: A Review of the critical factors." *Journal of the Electrochemical Society*, 145(6), 2186-2198.
- Garcia-Alonso, M. C., Escudero, M. L., Miranda, J. M., Vega, M. I., Capilla, F., Correia, M. J., Salta, M., Bennani, A., and Gonzalez, J. A. (2007). "Corrosion behaviour of new stainless steels reinforcing bars embedded in concrete." *Cement and Concrete Research*, 37, 1463-1471.
- GDOT. (2007). "Bridge and Structures Design Policy Manual." Georgia Department of Transportation, Atlanta, GA.
- Glass, G. K., and Buenfeld, N. R. (1997). "The presentation of the chloride threshold level for corrosion of steel in concrete." *Corrosion Science*, 39(5), 1001-1013.
- Gonzalez, J. A., and Andrade, C. (1982). "Effect of carbonation, chlorides and relative ambient humidity on the corrosion of galvanized rebars embedded in concrete." *British Corrosion Journal*, 17(1), 21-28.

- Gu, P., Elliott, S., Beaudoin, J. J., and Arsenault, B. (1996). "Corrosion resistance of stainless steel in chloride contaminated concrete." *Cement and Concrete Research*, 26(8), 1151-1156.
- Hartt, W. H., Powers, R. G., Lysogorski, D. K., Liroux, V., and Virmani, Y. P. (2007). "Corrosion Resistant Alloys for Reinforced Concrete." Office of Infrastructure Research and Development. Federal Highway Administration.
- Hausmann, D. A. (1967). "Steel corrosion in concrete: How does it occur?" *Materials Protection*, 6(11), 19-23.
- Johns, D. R., and Shemwell, K. (1997). "The crevice corrosion and stress corrosion cracking resistance of austenitic and duplex stainless steel fasteners." *Corrosion Science*, 39(3), 473-481.
- Jones, D. A. (1996). *Principles and Prevention of Corrosion*, Prentice Hall, Upper Saddle River, NJ. 1-286,350-351.
- Landolt, D. (unpublished work). "Corrosion and Surface Chemistry of Metals." 275-291.
- Leckie, H. P. (1970). "A contribution to the applicability of critical pitting potentials." *Journal of the Electrochemical Society: Electrochemical Science*, 117(9), 1152-1153.
- Leckie, H. P., and Uhlig, H. H. (1966). "Environmental factors affecting the critical potential for pitting in 18-8 stainless steel." *Journal of the Electrochemical Society*, 113(12), 1262-1267.
- Lee, D. J. (1994). *Bridge Bearings and Expansion Joints*, E & FN Spon, London.
- McCafferty, E. (1974). "Comparison of Pitting and Crevice Corrosion." *Report of NRL Progress*(February), 34-37.
- Mehta, P. K., and Monteiro, P. J. M. (2006). *Concrete: Microstructure, Properties, and Materials*, McGraw-Hill Companies, Ltd.
- Papadakis, V. G., Vayenas, C. G., and Fardis, M. N. (1991). "Fundamental modeling and experimental investigation of concrete carbonation." *ACI Materials Journal*, 88(4), 363-373.
- Qian, S., Qu, D., and Coates, G. (2006). "Galvanic coupling between carbon steel and stainless steel reinforcements." *Canadian Metallurgical Quarterly*, 45(4), 475-484.
- Revie, R. W. (2000). "Uhlig's Corrosion Handbook." Electrochemical Society Series, John Wiley & Sons, Inc., New York.165-204.

Singh, P. (2008). "MSE 8803L: Environmental Degradation of Materials Course notes."
School of Material Science and Engineering, Georgia Institute of Technology.
Atlanta, Georgia.

SSINA. (2005). "The Stainless Steel Information Center. Stainless steel overview:
Definition of terms." Specialty Steel Industry of North America.